

# ANNUAL REPORT 2018

National MagLab



Website: [nationalmaglab.org](http://nationalmaglab.org)

1800 E Paul Dirac Drive  
Tallahassee, FL 32310

NATIONAL  
**MAGLAB**

# 2018 ANNUAL REPORT

PRODUCED BY

**NATIONAL HIGH MAGNETIC FIELD LABORATORY**

DIRECTOR

*Gregory S. Boebinger*

DEPUTY LAB DIRECTOR

*Eric Palm*

CHIEF SCIENTIST

*Laura Greene*

USERS PROGRAM, CHIEF OF STAFF

*Anke Toth*

This document is available in alternate formats upon requests. Contact Anke Toth for assistance via [atoth@magnet.fsu.edu](mailto:atoth@magnet.fsu.edu)

# TABLE OF CONTENTS

Director's Executive Summary	1
1. Laboratory Management	5
2. User Facilities	19
3. Education and Outreach	51
4. In-house Research	61
5. Publications	83

## APPENDICES

I. User Facility Statistics	98
II. User Facilities Overview	124

## DIRECTOR'S EXECUTIVE SUMMARY

### THE USER PROGRAM

The National High Magnetic Field Laboratory continued to serve scientists from across the globe in 2018, advancing our understanding of new materials, energy solutions and the science that underlies life. More than 2,075 researchers, students and technicians were part of experiments across the lab in 2018 – a new record for annual user headcount!

The National MagLab's user community remains dynamic, with new members to report: Of the 696 principal investigators (PIs) in 2018, 18.7 percent are new PIs to the lab and 23.3 percent are new to the facility used to conduct research; 27 percent of the lab's users in 2018 performed experiments at our lab for the first time; and nearly half of the user community is comprised of students and postdocs. About 27 percent of the National MagLab's users who chose to identify were females and 8 percent identified as a minority.

National MagLab users are exceptionally positive about their experience. A user survey conducted every June continues to show overwhelming satisfaction:

- 95 percent of external users are satisfied with the performance of the facilities and equipment
- 94 percent of external users are satisfied with the assistance provided by technical staff
- 92 percent of external users are satisfied with the proposal process
- 96 percent of external users are satisfied with the availability of the equipment and facilities

Across the National MagLab's seven user facilities, enhancements and upgrades were made in 2018 that improved the user experience and experimental environment. These enhancements, arranged by facility, include:

- AMRIS recently purchased and installed an 800 MHz 4 channel console and magnet, ensuring that the high field NMR systems offer the latest in pulse sequence capabilities and multinuclear detection. User operation of the new 800 MHz system is expected to begin in early 2019.
- The installation of a <sup>13</sup>C-optimized 10 mm cryoprobe at 600 MHz in the AMRIS Facility, coupled with the Hypersense DNP polarizer, enables real-time metabolic measurements in functioning cardiac tissue.
- Four new 7 MW (2,000-ton) cooling power chillers installed in the DC Field Facility Plant greatly improved reliability for operating the water-cooled magnets while improving energy efficiency.
- Four 12.5 kV disconnects were installed as new energy isolation points for the primary side of the power supply transformers. This eliminates the hazard of pulling the power supply breakers off of the high voltage bus (racking out). These new disconnects are much faster to operate and to lock-out, providing an inherently safe visual verification of an open-circuit condition before servicing electrical equipment downstream.
- A 7T Magnetic Property Measurement System (SCM5) and 9T Physical Property Measurement System (SCM6) were added to the DC Field Facility User Program to broaden participation of users from smaller colleges and universities with limited research capabilities and to provide an important resource for the increasing number of users needing to perform low-field measurements to select the best samples onsite.
- Tremendous gains in the FIR measurement capabilities of the DC Field Facility improved signal to noise ratios by a factor of 20, dramatically reducing the amount of time needed to acquire spectra.
- Field-modulated Fourier-transform infrared measurements in the EMR Facility now allow users to probe much higher frequency magnetic excitations associated with crystal field splittings and first-order spin orbit coupling.
- Enhancements were made to the heterodyne pulsed EPR spectrometer: new local oscillators operating at 115 and 235 GHz allow for the generation of a phase stable Intermediate Frequency (IF) from the multiplied frequency difference between the source and detector.
- A separate layout was developed in the EMR Facility broadband homodyne spectrometer for pulsed EPR applications at 14.1T for  $g = 2$  spin species.
- A new helium exhaust system was installed above the High B/T Facility's magnet stations to safely and automatically evacuate helium gas in the event of a quench of one or more of the superconducting magnets to better protect users and staff.
- A solid state DNP system has been assembled in the NMR Facility around a new wide bore field swept 600 MHz magnet, a demo gyrotron, Bruker spectrometer and a quasi-optic table. This system is now the DNP instrument with the highest operational up-time anywhere nationwide.



- Major technology enhancements in the operation of the Series Connected Hybrid demonstrate significant enhancement in magnetic field stability of this unique magnet.
- The development of the Cascade Field Regulation (CFR) system in NMR results in a further reduction of resonance linewidths by a factor of two, largely due to the field stabilization in the frequency range of 1–60 Hz.
- Enhancements were made to the 1.4 GW motor-generator and pulsed power infrastructure of the Pulsed Field Facility. The 4 MJ capacitor bank that powers the PFF's four 65T magnet cells was upgraded to enable duplex magnet operation.
- A far infrared spectroscopy capability centered around time-domain THz spectroscopy and a 30T sub-millisecond rise time mini-magnet was developed at the Pulsed Field Facility, enabling a complete 200 GHz-to-THz spectrum to be recorded every 625 microseconds.

## USER RESEARCH

After conducting research at the MagLab, users submit brief summaries of their experimental results. In 2018, users generated 401 research reports across 21 categories in condensed matter physics, magnet science and technology, chemistry and life sciences. All research reports are available on our website at <https://nationalmaglab.org/research/publications-all/research-reports> and selected highlights will be released in the summer.

User research earned 380 publications in 2018, many in significant journals like Science, Nature, Physical Review Letters, Energy Fuels, Analytical Chemistry, and the Proceedings of the National Academy of Sciences. Important discoveries include:

- Novel properties of graphene, including switchable transmission of quantum Hall edge states in bilayer graphene using electrostatic gating.
- Pioneering lithographic techniques to realize a bilayer graphene device in which electrons can tunnel between two regions exhibiting Quantum Hall States, demonstrating gate-controlled transmission and pinch-off of quantum Hall edge states.
- A topological excitonic insulator ground state observed in a mesoscopic InAs/GaSb double-gate, bilayer quantum well device.
- The addition of a low concentration of the endohedral metallofullerene to DNP samples found that <sup>1</sup>H and <sup>13</sup>C enhancements increased by 40 percent and 50 percent, respectively, at 5T and 1.2K. This is the first time such increases have been observed at 5T, which may contribute to a significant reduction in toxicity of MRI for medical applications.
- Mass spectrum of an asphalt volcano sample after ion trap isolation at 21T represents the most peaks resolved and identified in a single spectrum (>125,000) of any kind and the highest broadband resolving power (>500,000 at 1000 Da) for any petroleum mass spectrum.
- Discovery of porphyrins from 1.1 billion-year-old marine black shales of the Taoudeni Basin in Mauritania that pushed back the geological record for photosynthesis by 600 million years.
- High-field NMR that provided unprecedented NMR resolution, enabling the creation of a new structural model of the fungal cell wall that will serve as the structural basis for designing better antifungal drugs to inhibit a broader spectrum of infectious fungi.
- An RF probe for dual <sup>19</sup>F/<sup>1</sup>H MRI was designed and built to realize sensitivity gains for <sup>19</sup>F MRI at 21.1T. This probe permitted the detection of inflamed regions of the mouse brain at 21.1T that were undetectable at 9.4T.
- Characterization of a structure for the Nitrogen Regulator protein (NR11) in native bacteria *E. coli* membranes, an exciting step forward in studying membrane proteins in their native environments.
- Measurement of polarized transmission spectra in pulsed fields to 65T, enabling the first measurement of the size and binding energy of the first four Rydberg states in monolayers of encapsulated WSe<sub>2</sub>, information that will guide the rational design and engineering of future optoelectronic devices based on this new class of 2D semiconductors.
- Discovery of a linear magnetoresistance in lanthanum strontium copper oxide (LSCO) up to 80T, providing further evidence of a quantum critical point in the vicinity of optimum doping in this high temperature superconductor.

Additional examples of exciting user research are featured on our website as monthly highlights <https://nationalmaglab.org/research/publications-all/science-highlights-all> and new articles <https://nationalmaglab.org/news-events/news>.

### NEW MAGNETS AHEAD

2018 saw the start of the National MagLab's next big magnet project: a 40T all superconducting magnet. Funded by NSF, the project is initially considering four different magnet conductor technologies: insulated Rare Earth Barium Copper Oxide (REBCO), no-insulation (NI-)REBCO, Bi-2212 and Bi-2223. Teams of magnet engineers are considering the advantages and disadvantages of each of these conductors, performing design calculations and creating test coils as the project continues through spiral one.

The MagLab's first duplex pulsed magnet was tested in 2018. Construction of large pulsed coils was moved from outside vendors to the MagLab, resulting in better quality control in the conductor-inspection and coil winding processes. The resistive magnet team witnessed the first full year of operations of the 36T Series Connected Hybrid, which provided a record 1,770 hours of magnet time to users without maintenance. The 41T magnet was modified and tested to 41.6T, the highest field available anywhere for DC resistive magnets.

Solidifying the MagLab's role as world leaders in magnet design, the Applied Superconductivity Center fabricated superconducting Nb<sub>3</sub>Sn wires with new in-house alloys to develop enhanced properties for use in accelerator magnets designed for the proposed Future Circular Collider (FCC).

### BROADENING PARTICIPATION & BUILDING THE STEM PIPELINE

In 2018, the National MagLab provided outreach to over 7,000 students from school districts in Florida and Georgia. Title I schools made up the bulk of these visits, accounting for 41 of the 59 school visits (72 percent). More than 100 middle-school aged students participated in one of the MagLab's summer camps and a record number of students were middle school mentors in 2018, nearly half of whom were female and 29 percent of whom were African-American. AMRIS and High B/T staff volunteered with the Women in Science and Engineering (WiSE) Girls spring break camp for middle school girls from Alachua County. Pulsed Field Facility researchers sponsored the Expanding Your Horizons conference in Santa Fe, a STEM program that fosters interest in science for middle school girls in Northern New Mexico. PFF scientist Scott Crooker also gave electricity and magnetism demonstrations at the Bradbury Science Museum as part of the Scientist Ambassador program.

At the 2018 MagLab Open House, science and sports teamed up to host more than 8,300 visitors. This year's event featured special demonstrations from the FSU Institute of Science and Sports Management, radar running and a look at MRI scans of sports injuries. In 2018, the lab hosted an epic public outreach in the form of a knock-down, drag-out science battle called the Subatomic Smackdown. Articles supporting the electron, neutron, photon or proton were published in *fields* magazine. A physical showdown was staged at both the MagLab Open House and the American Physical Society March Meeting before moving to the social sphere for the final battle in which more than 9 million people were engaged.

In 2018, MagLab staff gave more than 300 lectures, talks and presentations across 19 countries and nearly 30 states. AMRIS hosted an MRI pulse programming course, RF Coil building workshop and a NMR Metabolomics and 13C Fluxomics Workshop in 2018. The 2018 User Summer School attracted 32 graduate students and postdoc attendees, while the Winter Theory School, with its 60 participants, continued its own success this year with a focus on quantum information systems.

### CULTIVATING A SAFE LAB ENVIRONMENT

With strong support from our host institutions and the National Science Foundation, the National MagLab continues to focus on safety improvements for our users, staff, contractors and visitors. The lab makes key investments in safety and, in 2018, more than \$10M was devoted to major equipment and safety-related upgrades. This year, there were also a number of special safety initiatives, trainings and reviews conducted that offer opportunities to continue to improve the lab's safety toolkit:

- The lab had a three-site safety review by experts from Argonne National Laboratory, Cornell University, Georgia Institute of Technology and the University of Pennsylvania. The review team reported that MagLab leadership is fully supportive and capable of running a robust and sustainable safety program. The team also reported that all safety concerns raised in 2013 had been addressed, providing both positive feedback and identifying opportunities for additional improvement.
- A situational awareness training was held in 2018 to train staff who interface with the public on identifying and responding to potential threats or dangerous situations.

- A safety site assessment of the MagLab was conducted in 2018 to consider general safety improvements to our physical plant, including improved lighting and security. The MagLab is now working to implement the recommendations.
- The MagLab's emergency action plan was practiced during a tabletop exercise that included participation from state and county emergency management teams. A simulated scenario was facilitated to test the lab's preparedness, response and recovery capabilities in the event of a major hurricane directly impacting the area. This tabletop exercise became particularly useful when, only months later, the lab put its emergency action plan into action in response to Hurricane Michael.

## LOOKING AHEAD

The 32T All-Superconducting magnet system has been fully reassembled and installed in its permanent location in the new MilliKelvin building extension. Work will continue on control, protection and user-interface hardware and software as this magnet prepares to be integrated into the user program.

The first tests of the EMR Facility's 950 GHz source and mixer-detector in the Series Connected Hybrid Magnet (SCH) are anticipated in the year ahead.

The Pulsed Field Facility is planning a series of upgrades to its pulsed power capabilities and will continue the multiyear development of the optics cell with the addition of a horizontal-bore 65T short pulse magnet with optical access.

Work on the 40T superconducting magnet project will continue as we consolidate and validate technology through materials, analysis and small coils testing. Each test provides critical knowledge that will aid in the development of conceptual designs for the 40T superconducting magnet. Spiral one is designed to examine each technology path, reduce risks and facilitate down-selection decisions as soon as possible.

All MagLab user facilities and in-house research groups continue to advance the development of new instrumentation to serve our growing user community. Please explore the detailed information available in the individual chapters that follow and across our website at <https://nationalmaglab.org/>

## 1. LABORATORY MANAGEMENT

### a. Organization

The Florida State University (FSU), the University of Florida (UF) and Los Alamos National Laboratory (LANL) jointly operate the National High Magnetic Field Laboratory (NHMFL or MagLab) for the National Science Foundation (NSF) under a cooperative agreement that establishes the Lab's goals and objectives. FSU, as the signatory of the agreement, is responsible for establishing and maintaining administrative and financial oversight of the Lab and ensuring that the operations are in line with the objectives outlined in the cooperative agreement.

The structure of the MagLab is shown in the three figures below. **Figure 1.a.1** illustrates the external oversight and advisory committees, as well as the three internal committees that provide guidance to NHMFL leadership.

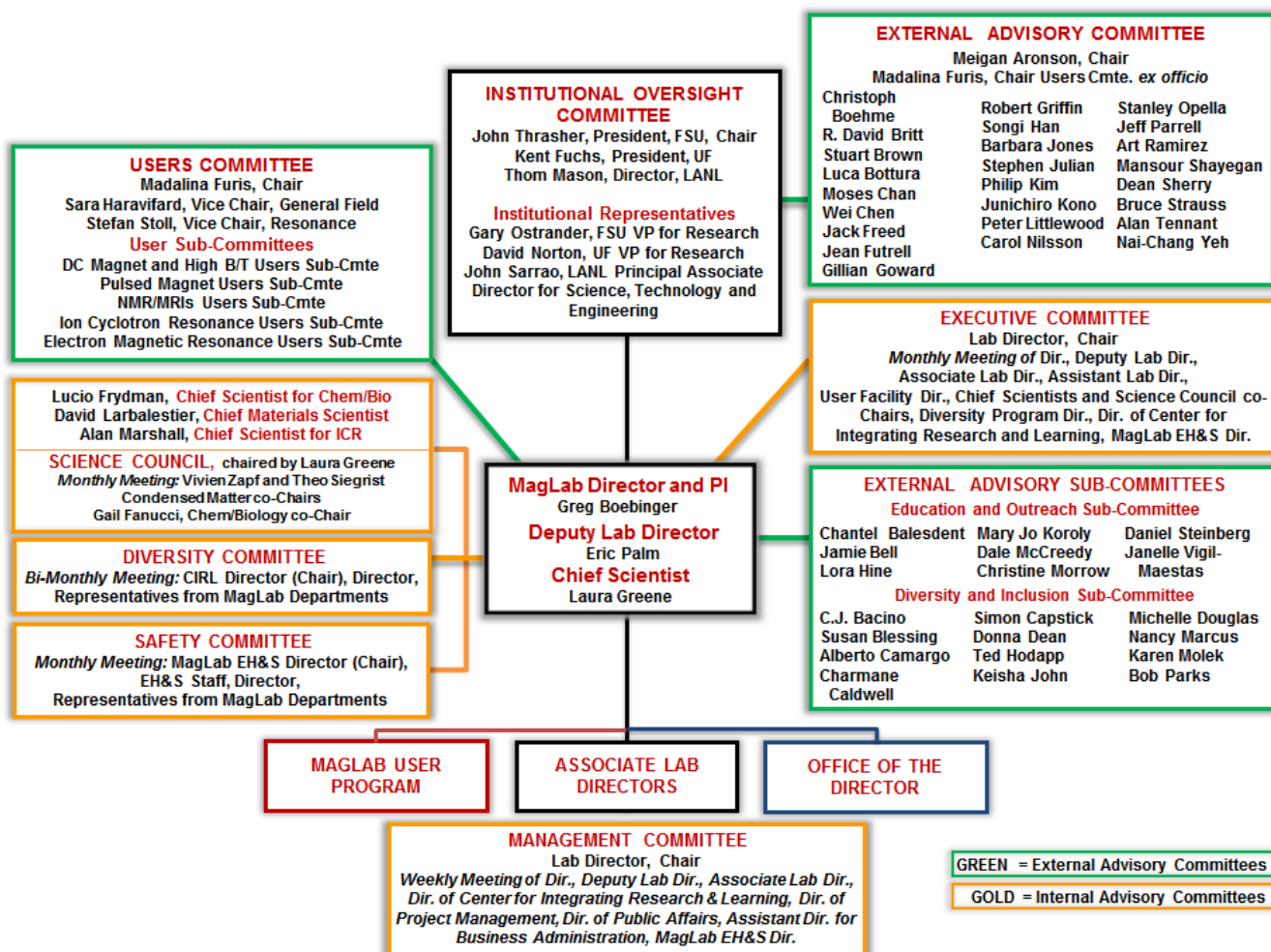


**Figure 1.a.1:** Advisory Committees of the MagLab, showing internal and external advisory committees (as of November 2018).

Greg Boebinger is the Director of the MagLab and PI of the cooperative agreement. Together, the Director, Deputy Laboratory Director, Eric Palm and Chief Scientist, Laura Greene, function as a team to provide management oversight for the Laboratory. **Lab Leadership** — consists of the MagLab Director, Deputy Lab Director, Chief Scientists, Associate Lab Directors and MagLab Facility Directors. Lance Cooley became the new Director for Applied Superconductivity Center. Cooley takes over for his long-time mentor David Larbalestier, who will remain the Chief Scientist for Materials at the MagLab and a professor in the FAMU-FSU College of Engineering. David Lunger joined the MagLab leadership as the Director of Project Management and Michael Rabin became the new Director for Pulsed Field Facility replacing Charles Mielke.

The **Executive Committee** meets on a monthly basis to discuss Lab-wide issues as well as program-specific issues. The Lab's scientific direction is overseen by the **Science Council**, a multidisciplinary "think tank" group of distinguished faculty from all three sites. The membership can be found at <https://nationalmaglab.org/about/organization/science-council>. Two external committees meet regularly to provide critical advice on important issues. The **External Advisory Committee**, made up of representatives from academia, government and industry, offers advice on matters critical to the successful management of the Lab. The **Users Committee**, which reflects the broad range of scientists who conduct research at the Lab, provides guidance on the development and use of facilities and services in support of the work of those scientists. These committees are further described below.

**Figure 1.a.2** shows the structure of the user program with its seven user facilities – DC Field Facility, Pulsed Field Facility, High B/T Facility, Electron Magnetic Resonance Facility, Nuclear Magnetic Resonance and Magnetic Resonance Imaging at Florida State University and at University of Florida and Ion Cyclotron Resonance.

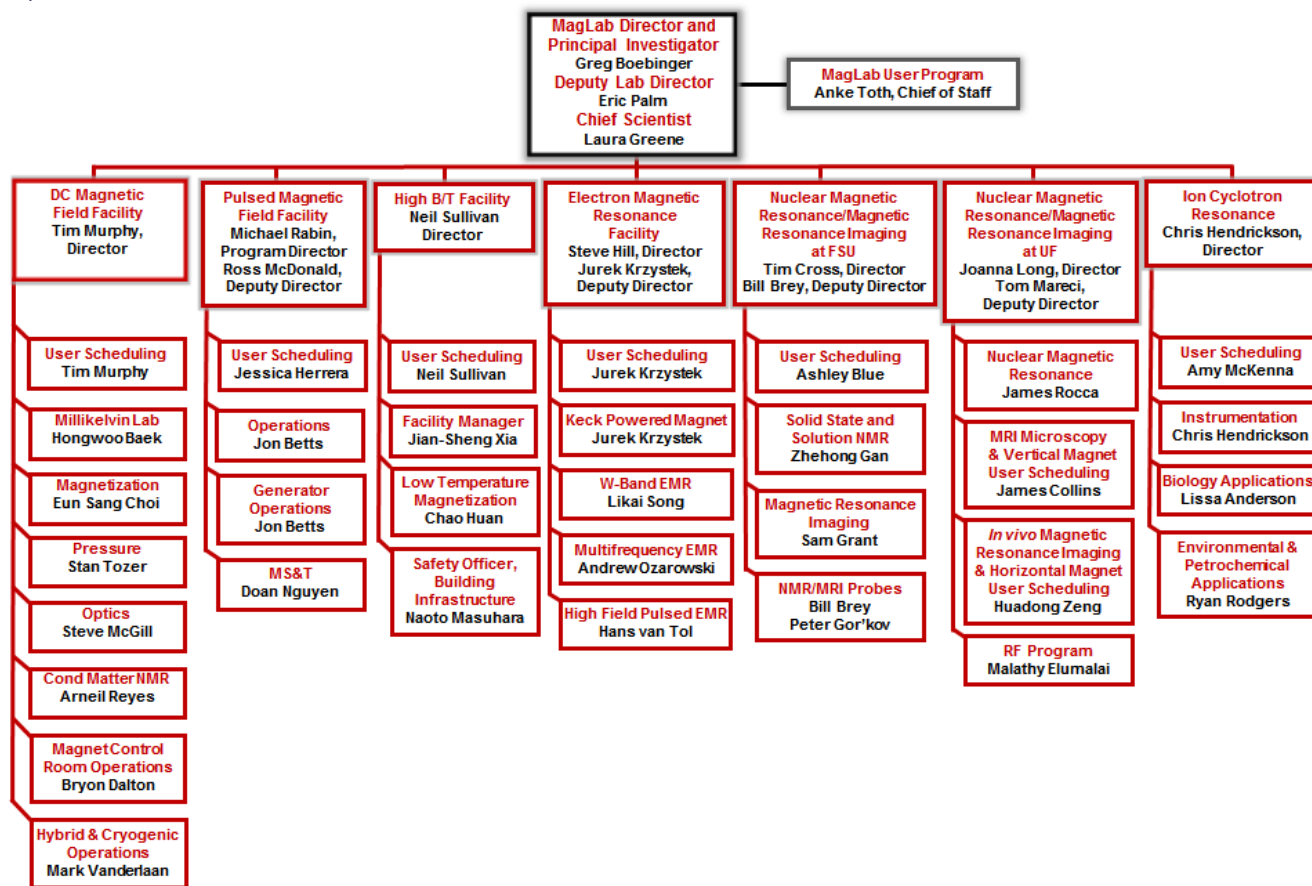


*Figure 1.a.2: NHMFL User Program (as of November 2018)*

**Figure 1.a.3** displays the internal, operational organization of the Laboratory. It includes the seven user facilities, all Associate Lab Directors as well as the Office of the Director structure.



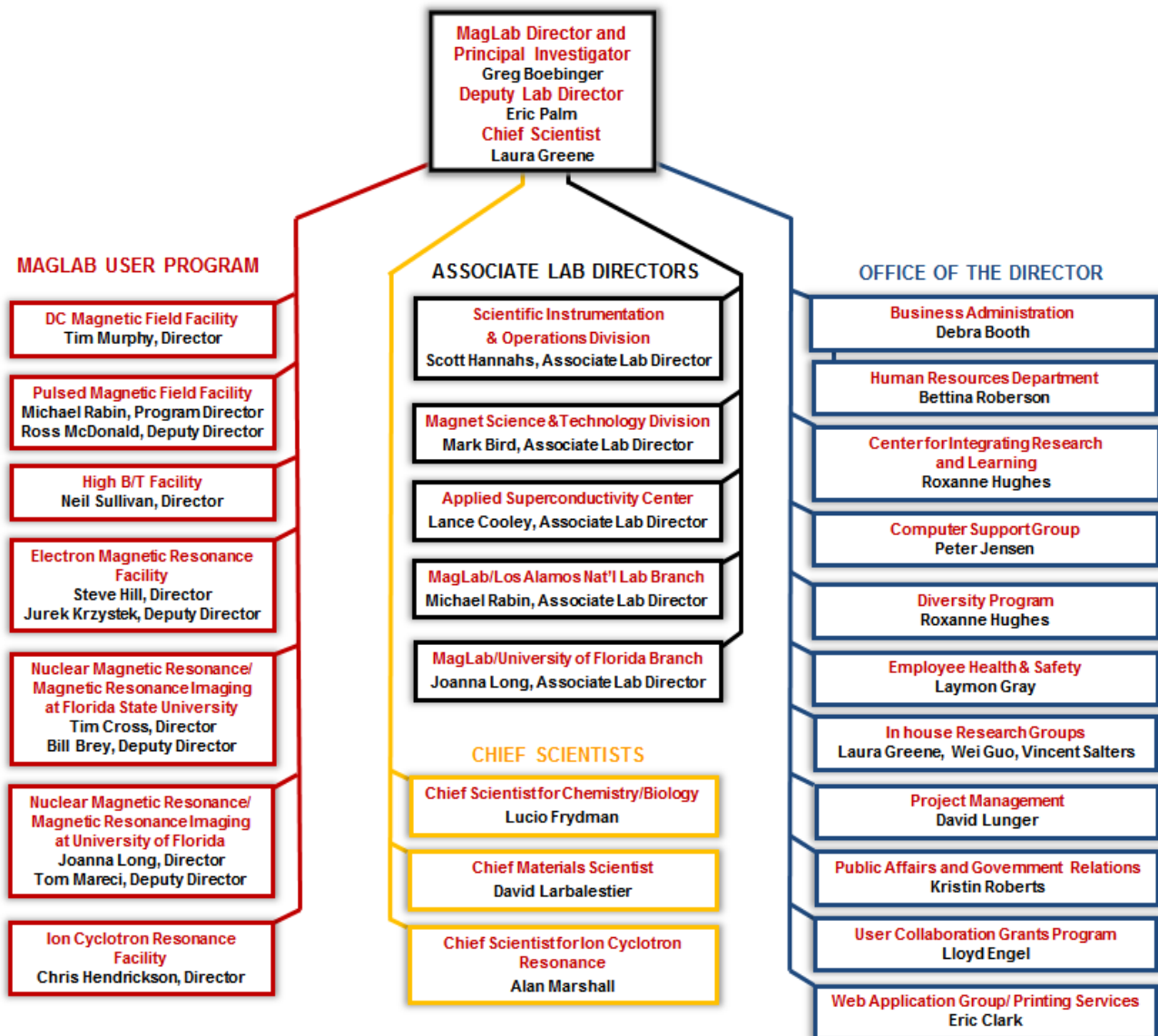


Figure 1.a.3: MagLab Organizational Chart (as of November 2018).

#### b. External Advisory Committee

Meigan Aronson—*External Advisory Committee Chair*—University of British Columbia

Madalina Furis (*ex officio* member of EAC)—University of Vermont

- **Biology and Chemistry Subcommittee**

R. David Britt—UC-Davis

Wei Chen—University of Minnesota

Jack Freed—Cornell University

Jean Futrell—Battelle

Gillian R. Goward—McMaster University

Robert Griffin - MIT

Songji Han—University of California, Santa Barbara

Carol Nilsson—Swedish National Infrastructure for Biological Mass Spectrometry

Stanley Opella—UC- San Diego

Dean Sherry—UT Southwestern

- **Condensed Matter Subcommittee**

Christoph Boehme—University of Utah

Stuart Brown—University of California, Los Angeles

Moses Chan—Penn State University

Barbara A. Jones—IBM Almaden Research Center

Stephen Julian—University of Toronto

Philip Kim—Harvard University

Junichiro Kono—Rice University

Peter Littlewood—University of Chicago

Art Ramirez—University of California, Santa Cruz

Mansour Shayegan—Princeton University

Nai-Chang Yeh—California Institute of Technology



- **Magnet Technology and Materials Subcommittee**

Luca Bottura—Magnets, Superconductors and Cryostat:

Jeff Parrell—Oxford Superconducting Technology

Bruce P. Strauss—US Department of Energy

Alan Tennant—Oak Ridge National Laboratory

**c. User Committee**

The MagLab's Users Committee represents the MagLab's broad, multidisciplinary user community and advises the Lab's leadership on all issues affecting users of our facilities. The Users Committee is elected from the user base of the NHMFL. Each facility has a subcommittee elected by its users to represent their interests to the NHMFL. DC Field and High B/T facilities have a single, combined subcommittee representing the two user facilities. Likewise, the NMR facilities at UF and FSU have a single, combined subcommittee. Pulsed Field, ICR and EMR facilities have their individual subcommittees. Each subcommittee then elects members to represent it on the Users Executive Committee. This Users Executive Committee elects a chair and two vice chairs. The DC Field/High B/T Advisory Committee, the Pulsed Field Advisory Subcommittee, the EMR Advisory Subcommittee, the NMR/MRI Advisory Committee and the representative from the ICR Advisory Committee met September 18–20 in Tallahassee, FL, to discuss the state of the Laboratory and provide feedback to the NSF and MagLab management. The 2018 User Advisory Committee Report can be found on our [website](#).

**Users Executive Committee**

**Representing the DC Field/High B/T Advisory Sub-Committee**

Madalina Furis, Chair—University of Vermont

Sara Haravifard, Vice Chair, General Field Facilities—Duke University

**Representing the EMR Advisory Sub-Committee**

Stefan Stoll, Vice Chair, Resonance Facilities—University of Washington

**Representing the ICR Advisory Sub-Committee**

Jonathan Amster—University of Georgia

**Representing the NMR/MRIs Advisory Sub-Committee**

Ed Chekmenev - Vanderbilt University

Len Mueller—UC Riverside

**Representing the PFF Advisory Sub-Committee**

Jamie Manson—Eastern Washington University

**DC Field/High B/T Advisory Sub-Committee**

Madalina Furis, Chair—University of Vermont

Elizabeth Green—Helmholtz-Zentrum Dresden-Rossendorf

Malte Grosche—Cambridge University, Cavendish Laboratory

Sara Haravifard\*—Duke University

Zhigang Jiang—Georgia Institute of Technology

Lu Li—University of Michigan

Philip Moll—Max Planck Institute for Chemical Physics of Solids

James Williams—University of Maryland

Haidong Zhou—University of Tennessee

**EMR Advisory Sub-Committee**

Erik Cizmar—P.J. Safarik University

Lloyd Lumata—University of Texas

Stergios Piligkos—University of Copenhagen

Hannah Shafaat—Ohio State University

Stefan Stoll—University of Washington

Joshua Telser—Roosevelt University

**ICR Advisory Sub-Committee**

Jonathan Amster—University of Georgia  
 Michael L. Easterling—Bruker Corporation  
 Ying Ge—University of Wisconsin  
 Kristina Hakansson—University of Michigan  
 Ljiljana Paša-Tolić—Pacific Northwest National Laboratory  
 Forest White—Massachusetts Institute of Technology

**NMR/MRI Advisory Sub-Committee**

David Bryce—University of Ottawa  
 Ed Chekmenev—Vanderbilt University  
 Paul Ellis—Doty Scientific, Inc.  
 Oc Hee Han—Korea Basic Science Institute  
 Doug Kojetin—Scripps Research Institute  
 Richard Magin—University of Illinois at Chicago  
 Doug Morris—National Institutes of Health  
 Len Mueller—UC Riverside  
 Aaron Rossini—Iowa State University

**Pulsed Field Advisory Sub-Committee**

Nicholas P. Butch—IST Center for Neutron Research  
 Krzysztof Gofryk—Idaho National Laboratory  
 Pei-Chun Ho—California State University, Fresno  
 Jamie Manson—Eastern Washington University  
 Zhiqiang Mao—Tulane University  
 Filip Ronning—Los Alamos National Laboratory

**d. Personnel**

The MagLab comprises of 788 people at its three sites, who are paid by NSF use grant, State of Florida funding, individual investigator awards, as well as home institutions and other sources. Of that number, senior personnel represent the largest group at 32 percent, followed by graduate students at 21 percent and other professionals at 11 percent. The total distribution appears in **Figure 1.d.1**.

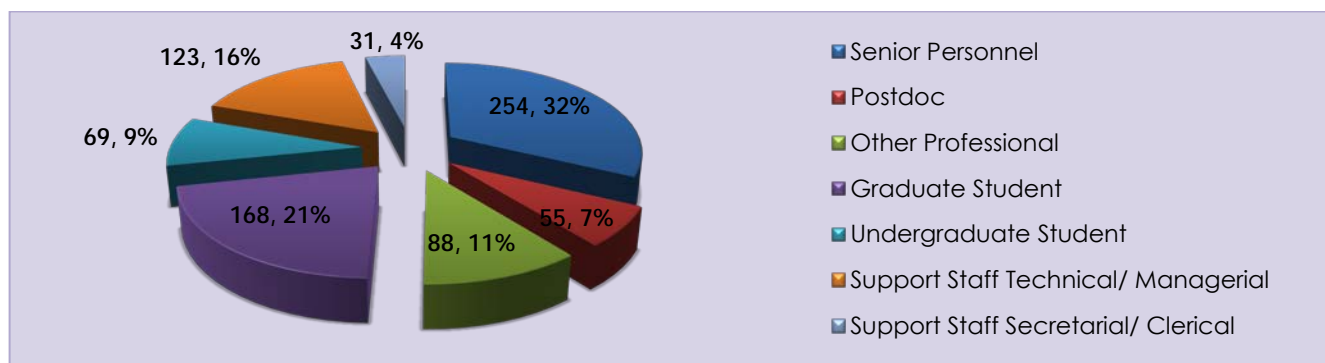


**Figure 1.d.1:** MagLab Position Distribution (as of January 7, 2019).

Overall distribution of diversity for all three sites of the MagLab includes: 47.2 percent white males, 23 percent Asian males and females, 18.3 percent white females, 7 percent black or African American, and 1% American Indian. The distribution by diversity appears in **Figure 1.d.2 and 1.d.3**.

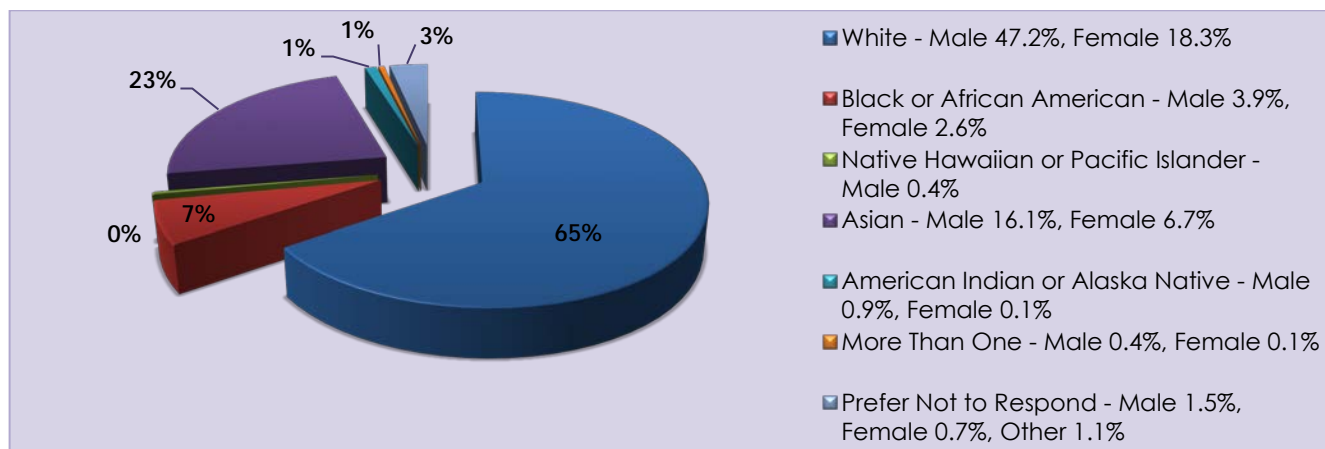


**Figure 1.d.2:** MagLab Distribution by Race (as of January 7, 2019).

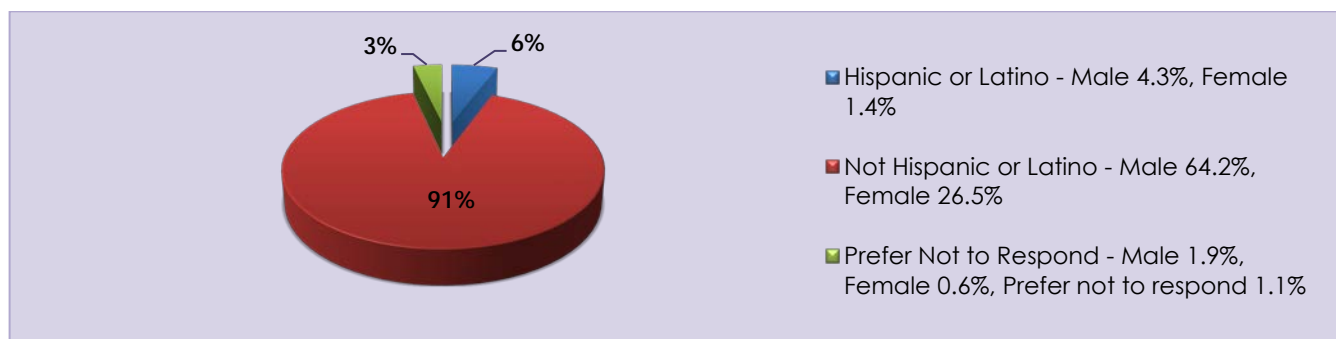


Figure 1.d.3: MagLab Distribution by Ethnicity (as of January 7, 2019).

Table 1.d.1 provides MagLab personnel funded by NSF core grant including FTE, counts for people, postdocs and students employed.

Table 1.d.1: MagLab s employed personnel funded by NSF as of February 11, 2019

	Number of FTEs employed	Number of people employed	Number of postdocs employed	Number of students employed
NHMFL/ FSU	85.79	115	3	8
NHMFL/ UF <sup>2</sup>	4.73 <sup>1</sup>	63	2	0
NHMFL/ LANL <sup>2</sup>	13.44	39	9	3

Note: <sup>1</sup>HBT 3.06 and AMRIS 1.67; <sup>2</sup>April-December 2018 and affiliated with NHMFL-FSU thru subcontract

#### e. Diversity Action Plan

The National High Magnetic Field Laboratory (MagLab) is committed to diversity and inclusion in the STEM workforce at the MagLab and throughout the nation. To accomplish this goal, [our efforts](#) are focused on: **outreach** to underrepresented and underserved populations in STEM from K-early career scientists; utilizing best practices in our **recruitment and hiring** strategies to improve the representation of underrepresented minority groups (including women) at the lab and in the STEM workforce; and creating a climate where all personnel feel that they have equal opportunities to career development and **mentoring** leading them to want to remain at the lab/within the STEM workforce (**retention**). As part of this strategic plan, the diversity committee structures its budget and subcommittees to align with these efforts.

The MagLab Diversity Committee meets every other month to discuss and review reports and issues facing the lab. The members of the NHMFL Diversity Committee in 2018 can be found in **Table 1.e.1**.

Table 1.e.1: 2018 NHMFL Diversity Committee Members (new members in bold)

Chair: Roxanne Hughes, FSU	<b>Jessica Herrera, LANL</b>	Kari Roberts, FSU
Shelby Anderson, FSU	Jason Kitchen, FSU	Kristin Roberts, FSU
Ryan Baumbach, FSU	You Lai, FSU Graduate Student	<b>Jose Sanchez, FSU</b>
Gregory Boebinger, NHMFL Director	Amy McKenna, FSU	<b>John Singleton, LANL</b>
<b>Kelly Deuerling, UF</b>	<b>Jennifer Neu, FSU Graduate Student</b>	Yasu Takano, UF
<b>Malathy Elumalai, UF</b>	<b>Martha L. Chacon Patino, FSU Postdoc</b>	Anke Toth, FSU
David Graf, FSU	Dragana Popovic, FSU	<b>Hans van Tol, FSU</b>
Laura Greene, NHMFL Chief Scientist	<b>Kirk Post, LANL</b>	Yan Xin, FSU
Eric Hellstrom, FSU	Bettina Roberson, FSU	

All of these members work diligently to reach our diversity mission in one and/or all three of the main areas of focus: outreach, recruitment and retention.

#### Outreach

The summary of outreach diversity initiatives and demographics can be found in Chapter X. In addition to the efforts mentioned there, the MagLab also held three additional events:

(1) *Event series for the UN International Day of Women and Girls (February 11)*

On February 7, 2018, the MagLab held a special Soda Fountain Science event for elementary school girls and their families at a local ice cream parlor. Dr. Amy McKenna and Kari Roberts focused on the language of math. Over 100 elementary school girls and some boys attended.

On February 8, 2018, the MagLab partnered with Tallahassee Community College (TCC) to sponsor a speed mentoring event for middle, high school and college women (**Fig.1.e.1**). Over 100 students participated and 17 mentors from FSU, FAMU, TCC and the MagLab.

(2) *Expanding your Horizons (LANL)*

For the third consecutive year, the MagLab helped to sponsor and provide role models for the annual Santa Fe, NM, Expanding Your Horizons Workshop on February 15, 2018. Over 250 middle school girls attended; of these, 61 percent were a member of an underrepresented minority group.

(3) *Host author and executive director of the Girl Scouts Sylvia Acevedo (September 8, 2018)*

In September, the MagLab partnered with the Girl Scouts and a local independently owned book store—Midtown Reader—in Tallahassee to host author and executive director of the Girl Scouts, Sylvia Acevedo (**Fig.1.e.2**). Over 150 girls and young women attended this event to meet an amazing role model and to learn about MagLab programs for girls.

### Recruitment and Hiring

The Diversity Committee has two subcommittees that are responsible for overseeing recruitment and hiring procedures. The first of these is the Compliance Subcommittee, chaired by Jason Kitchen. The purpose of the Compliance Subcommittee is to facilitate the overall goal of increasing MagLab faculty diversity by intervening at the critical point during the faculty position search. The committee meets with each faculty search committee chair at the outset of a potential search in order to review the search committee's plans to widely disseminate position advertising and specifically target underrepresented groups in STEM. Bettina Roberson, the Director of Human Resources for the MagLab, also serves on this subcommittee, and her participation is crucial to implementing the plans decided upon in this initial meeting for targeted advertising, all the way through to the extending of offer letters to final candidates. At the conclusion of a position search, the hiring search committee submits a summary of their actions to the Compliance Subcommittee, so that the process can be reviewed for compliance to the ideal of fair, wide and equitable searches and interviews. Finally, metrics such as number of overall and underrepresented-in-STEM applicants and final candidates are collected to measure the year-by-year effectiveness of the diverse search initiative.

In 2018, MagLab saw four faculty position searches, two of which were initiated in late 2017 and closed out with accepted offers in 2018. Neither of these two closed searches resulted in the hiring of an underrepresented-in-STEM candidate. The two remaining faculty searches began in November of 2018 and will extend into 2019.

The Recruitment Subcommittee, chaired by Kristin Roberts, continued to support recruitment efforts for the MagLab. In 2018, they supported four recruitment trips. Dr. Subramanian Ramakrishnan attended the National Organization for the Professional Advancement of Black Chemists and Chemical Engineers (NOBCCHE) Conference Recruiting Fair and reached about 50 graduate and undergraduate students. Dr. Huan Chen represented the MagLab at the Tuskegee University Grad School Fair on October 18, 2018, and interacted with 75 students. Dr. Thierry Dubroca recruited new users and potential staff at the International Conference on Nuclear Hyperpolarization on September 2–5, 2018, where he interacted with about 45 junior scientists (PhD students and postdocs) during the poster sessions to introduce them to the MagLab and the EMR and NMR user facilities. McKenna met with 40–60 undergraduate and graduate students and 10 faculty members in the Jackson State University Chemistry Department in April 2018. The Recruitment Subcommittee also promoted posted positions including six postdoc, two faculty and five staff positions across the lab's social media channels and on the MagLab website, which earned more than 4,000 unique page views, nearly 20 percent from females.



**Figure 1.e.1. above:** Speed Mentoring event at TCC on February 8, 2018.

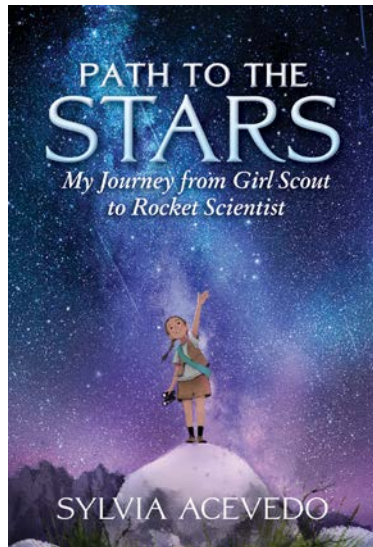


**Figure 1.e.2 above:** Sylvia Acevedo's memoir about her life.



### Retention, Advancement and Mentoring

In January 2018, Elizabeth Webb (UF), Kari Roberts (FSU) and Hughes and McKenna (FSU), attended the University of Michigan Making Strides Conference wherein the MagLab learned about the best practices being utilized at University of Michigan to recruit and retain faculty. Hughes utilized resources from the conference and the network of experts to update the MagLab's annual Faculty Recruitment and Retention workshop, which is mandatory for anyone serving on a research faculty hiring committee at the MagLab. FSU now has an online training for both faculty and staff hiring committee members, similar to UF and LANL's.

The MagLab conducted its fourth internal Climate Survey in 2018. The results indicated that the majority of respondents are satisfied with their supervisors. We saw an improvement in the percentage of postdocs and OPS employees receiving annual evaluations after we focused on this issue in quarterly meetings last year. In addition, we observed an improvement among all staff categories for their understanding of the promotion process, another issue we had focused on explaining during the year. The majority of respondents had positive perceptions of MagLab Leadership: 79 percent at FSU, 90 percent at UF, and 80 percent at LANL. The majority of respondents believed that they were held to an equal standard as their peer group: 78 percent at FSU, 80 percent at UF and 73 percent at LANL.

Trends over a 4-year period indicate that all categories have improved in their intention to stay at the lab for the next 5 years. This is evidence of an improved climate at the MagLab. However, there is still room for improvement. Based on recommendations from the 2018 National Academies of Sciences, Engineering, and Medicine Sexual Harassment Report we added the sexual questionnaire survey—a validated instrument. Results of this section indicated that some members of the MagLab are experiencing jokes or comments that make them uncomfortable.

In an effort to address the issue of gender harassment, in 2019 we will utilize our MagLab Women Faculty Affinity Group (Chaired by Laura Greene, Dragana Popovic and McKenna) and the newly formed FSU STEM Women Faculty group, led by McKenna to determine recommendations for how to proceed on improving this issue. Hughes will also utilize our Diversity External Advisory Committee for advice. We have already planned sessions in 2019 to address bystander awareness and unprofessional behavior. These choices were informed by the results of the 2018 Climate Survey.

In 2018, we held various sessions (**Tab. 1.e.2**).

**Table 1.e.2: 2018 Professional development opportunities**

Date	Title
1/26/18	FSU Greendot (Bystander Awareness)
2/9/18	Diversity and the GRE (Dr. Casey Miller)
3/30/18	FSU Greendot (Bystander Awareness)
5/15/18	Bystander Awareness (Dr. Mary Kite)
5/30/18	Faculty Recruitment Workshop (Drs. Greene, Hughes and Palm)
10/2/18	Conflict Communication Skills (Dr. Melissa Bolen, FSU)
10/25/18	Cross Cultural Dialogue (Dr. Elcin Haskollar, FSU)
11/30/18	Skits and Conversations about Implicit Bias in Hiring and Promotion for Researchers
11/30/18	FSU Online Sexual Misconduct Training

In order to facilitate professional development opportunities outside of the lab, the Retention, Advancement, and Mentoring Subcommittee accepts, reviews and votes on applications for Professional Development Travel Funding. In 2018, twenty-one MagLab undergraduates, graduate students, postdocs and faculty were granted funding to travel domestically and internationally to attend professional development opportunities. Of these twenty-one scientists, eleven used the funding to attend workshops or seminars on techniques directly related to their research, eight attended annual meetings of professional organizations, one continued a project started at the MagLab at Los Alamos National Lab and another used the funding to travel to receive one-on-one coaching to become a better mentor.

Bridge funding supports students and postdocs at the MagLab who are between funding sources and would otherwise not be paid during the transition time, thereby allowing the MagLab to retain students and postdocs who have already been trained in MagLab research techniques and procedures across multiple grant cycles rather than for only a single project. The 2018 Bridge funding supported five undergraduate students (one in DC Field, one in CMS, one in ASC and two in Geochemistry), three graduate students (one in MS&T, one in CMS and one in ASC), and one postdoc in Geochemistry. The

MagLab also offers a Dependent Care Travel Grant program. Please find more information in Chapter 2a.

### Diversity and Inclusion External Guidance and Advice

In addition to the internal Climate survey and other metrics (anonymous reporting through *diversemag*, confidential consultations with Hughes or other members of the Diversity Committee), members of the MagLab Diversity Committee serve on committees that allow them to benefit from others expertise and share the MagLab's successes. Popovic and Hughes serve on the FSU Diversity and Inclusion Committee. Hughes continues to be a part of the FSU National Coalition Building Institute (NCBI) Leadership team. NCBI is an international, nonprofit, leadership training organization that works to eliminate prejudice and discrimination. She co-facilitated two trainings in 2018 for FSU faculty, staff, and students. Hughes completed her term as a member of the American Physical Society's Committee on the Status of Women in Physics in 2018. During her tenure she was part of the Sexual Harassment subcommittee which drove the APS's updated statement of expectations for professional behaviors, which now includes sexual harassment as an example of unprofessional behavior.

The MagLab also utilizes an External Advisory Committee, which reviews our policies and procedures. In 2018, this committee reviewed an executive summary of our 2017 Climate Survey Report and our 2017 Annual Report Chapter. The members of our External Advisory Committee in 2018 were:

- C.J. Bacino, LANL Diversity Director
- Susan Blessing, FSU Physics Professor, Women in Math, Science, and Engineering Living and Learning (WIMSE) Director
- Alberto Camargo, Diversity Program Manager, Argonne National Laboratory
- Charmane Caldwell, Student Success Director for Florida Agricultural and Mechanical University—Florida State University College of Engineering
- Simon Capstick, FSU Physics Professor
- Donna Dean, Tulane University School of Science and Engineering retired, Research focuses on improving mentoring for women
- Ted Hodapp, American Physical Society Director of Education and Diversity
- Keisha John, Director of Diversity Programs, Graduate and Postdoctoral Affairs, University of Virginia
- Michelle Douglas, Florida State University Director of Equal Opportunity and Compliance
- Nancy Marcus, FSU Dean of Graduate School
- Karen Molek, University of West Florida, Chemistry Associate Professor
- Bob Parks, Director of University of Florida Training and Organizational Development

In addition to general recommendations, Hughes also asked for advice related to the following: (1) "We currently send our climate survey out each year. I learned that University of Michigan sends their climate survey out every three years. What is an adequate time between climate surveys?"

Overall, the members of the committee were impressed with what the MagLab is currently doing in terms of Outreach, Recruitment and Retention. Donna Dean specifically suggested that we create more workshops to address sexual harassment issues. As a result, we increased our Bystander Awareness and Sexual Harassment trainings in 2018.

For the specific question related to the regularity of using a climate survey, because of the length of the survey, two members advised giving the survey every two years. One recommended giving the survey every three years or rotating the issue of focus each year. And one recommended, based on responses related to the workplace equity section, that we send the survey every year. Based on this feedback and discussions with the Diversity Committee and MagLab Leadership, we shortened the 2018 Climate survey and decided to continue with an annual survey, but we cut some of the questions to make it less dense. We will give the survey anonymously rather than confidentially to increase the response rate.

### f. Safety

*A central focus of all activities conducted at National High Magnetic Field Laboratory (MagLab) is to ensure employees, users and visitors are provided with a safe and educational environment. The MagLab's Environmental, Health, and Safety team works collaboratively with management, researchers, staff and users, as well as with other public and private entities, to proactively mitigate hazards in our industrial, laboratory and office settings. The MagLab uses Integrated Safety*



Management (ISM) to integrate safety and health requirements and controls into daily work activities to ensure the protection of the MagLab Community.

The MagLab continues to foster a sustainable and strong Safety Culture. Examples of the activities that contribute to our commitment to a strong Safety Culture at the MagLab are listed below.

- Safety is viewed as an investment not a cost.
- Management drives and is actively involved with promoting our Safety Culture.
- Quarterly Safety Meetings are conducted by the Director of the MagLab to address lab-wide safety issues and initiatives.
- The Director of the MagLab and Director of Safety routinely walkthrough lab areas to engage researchers, staff and users and to observe ongoing work.
- New Employee Orientation is provided to all incoming employees with specific emphasis on our ISM System. New employees are taught that safety is the top priority at the MagLab, to have a questioning attitude about their safety and about our Stop Work Policy and No-Fault Self-Reporting Near Miss and Accident Policy.



**Safety Survey 2018**

In order to gauge the continued effectiveness of the safety program and the overall attitude toward safety, the MagLab conducted its Annual Safety Survey. The data from the survey provides reliable and measurable feedback. The results of the 2018 Safety Survey continue to indicate an improved climate for the ISM process and our EH&S program (Fig.1.f.1).

**Investments in Safety**

Our investments in safety equipment and materials along with management support and employee involvement demonstrates our strong commitment to sensibly utilize resources in a manner that protect all MagLab personnel, property and the environment.

In 2018, the MagLab strategically invested over \$70,000 for safety related equipment, supplies, training and processes. Some of the key investments included personal protective equipment, equipment used to lockout/tagout hazardous energy sources, installation of oxygen deficient monitoring systems and equipment testing.

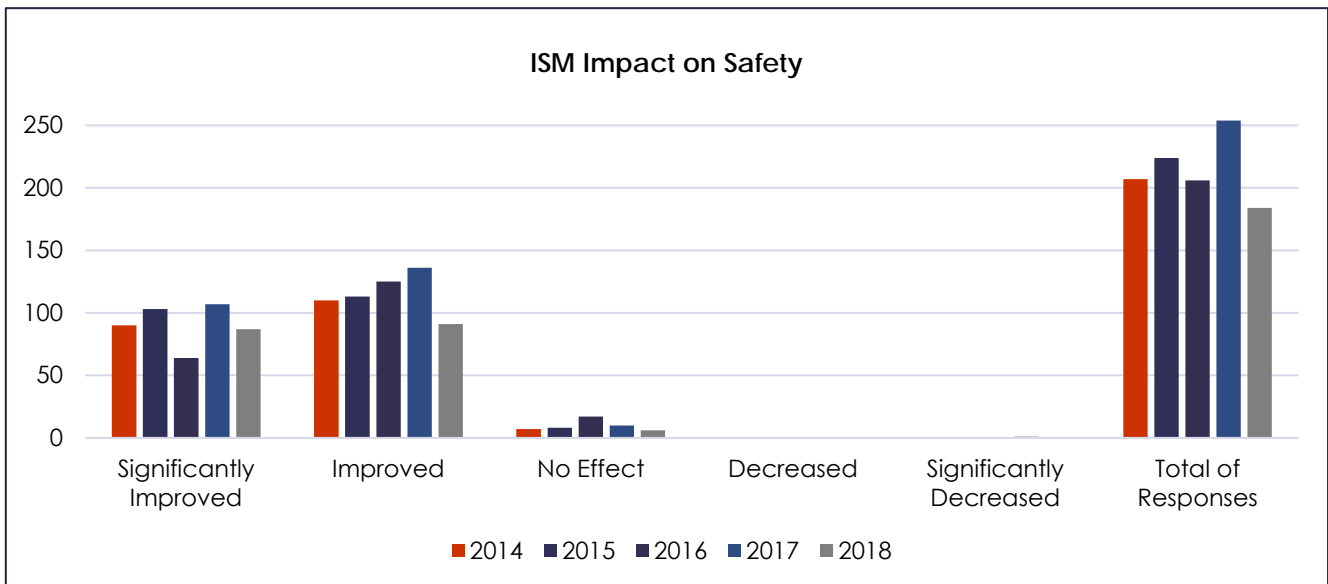


Figure 1.f.1: Results of the 2018 Safety Survey.

**Safety Support and Coordination with FSU Main Campus Safety Team**

Safety at the MagLab is supported by a dedicated on site team as well as support from the Florida State University (FSU) Environmental Health and Safety Department team. The two teams work together to provide a comprehensive integrated safety support to all activities at the MagLab. Machine Shop,

Biosafety, Laboratory, Safety Equipment and Radiation inspections were conducted and completed with team members from both groups. The two teams also work together to provide safety training. Both teams participated together in their annual 8-hour hazardous waste operations and emergency response refresher training at the MagLab.

### **Safety Committees**

Safety committees are an integral part of the MagLab's ISM. Committees meet to discuss and address safety concerns and provide program reviews. The following are a list of committees.

- Safety Committee (includes representative from UF and LANL Facilities)
- Lock/Tag Verification Committee
- Cryogen Safety Committee
- Laser Safety Committee

Members of these committees also form subcommittees as needed to address specific safety issues.

### **Safety Highlights**

#### ***5-Year Comprehensive Review of Safety Programs***

The MagLab coordinated an external safety review of the safety programs at its three Facilities (FSU, UF and LANL). The review team consisted of safety experts from Argonne National Laboratory, Cornell University, Georgia Institute of Technology and the University of Pennsylvania. The team reported that leadership has fully demonstrated their complete support of a robust and sustainable safety program and that leadership is wholly capable of running a sustainable safety program. The team found that all three sites had responded to safety concerns raised during the previous 5-year review conducted in 2013. The team provided both positive feedback and opportunities for continuous improvement. All three facilities are implementing the suggested improvements.

#### ***Situational Awareness Training & Security Assessment***

Situational awareness training was provided by the Florida State University Police Department (FSUPD). During the training employees learned techniques to improve their perception of what is going on around them at any time. This improved perception helps to identify potential threats and dangerous situations. The training also provided direction on how to respond to threats. Employees were taught the concepts of *run, hide, fight* in response to an active shooter situation. The MagLab Safety Team also worked with the FSUPD Crime Prevention division to conduct a site inspection of the MagLab. A report was provided that detailed recommendations to improve lighting and security at the MagLab. The MagLab is working to implement the recommendations provided in the assessment.

#### ***Table Top Exercise of Emergency Action Plan and Hurricane Michael***

On April 24, 2018 the MagLab conducted a Table Top Exercise. The exercise was sponsored by the Apalachee Local Emergency Planning Committee and the MagLab, and included participants from state and county emergency management representatives. The scenario for the exercise was a major hurricane that would directly impact the MagLab causing significant damage and power outages in the area limiting access to the lab and putting a halt to crucial operations. The exercise tested the MagLab's preparedness, response and recovery capabilities and included facilitated discussions with community partners. Although the MagLab had weathered two hurricanes during 2016 and 2017, the timing of the exercise turned out to be critical in preparation for the upcoming hurricane season.

In October the third most intense Atlantic hurricane to impact Florida made landfall just west of Tallahassee. The impacts of Hurricane Michael resulted in the MagLab losing power for multiple days. The University and MagLab remained closed for six days. The MagLab implemented its Emergency Action Plan and used lessons learned from prior years and the Table Top Exercise. The MagLab was able to efficiently prepare, respond and recover safely with minimal impacts.

#### ***Annual Maintenance Shutdown***

During November and December, the MagLab performed its annual maintenance shutdown and its first week-long power outage. Prior to shutdown several planning meetings were held to discuss work plans, safety equipment needs, organization of lockout/tagout boards and contractor coordination. The MagLab used its lock/tag/verify program to organize and coordinate lockouts to ensure all hazardous energy sources were safely controlled. In addition to the normal maintenance activities that occur annually during shutdown, existing chillers were replaced, significant upgrades to electrical

equipment were completed and the cooling tower basins were cleaned to reduce potential legionella growth. Disconnect switches were installed between the power supply breakers and the DC power supply transformers that simplify the lock-tag-verify process, greatly reduce worker's exposure to arc flash hazard, and provide easy visual verification when racking out 12.4 kV circuit breakers. The 4160 V switchgear breakers were replaced with more reliable systems that greatly reduce arc flash hazards to workers. These two projects represent over \$1.5 million dollars invested to provide more reliable and safer operations.

The greatest challenge during the shutdown was to carefully coordinate all work activities among many workgroups to ensure safety remained the top priority. To facilitate safe work, each morning, all workgroups including contractors met to review and discuss each group's planned work for the day. This facilitated communication among workgroups occurred prior to initiating tasks to ensure jobs were safely coordinated and all safety hazards were communicated. Also discussed were any difficulties or lessons learned from the previous workday. Although there were numerous inter-dependent work processes and workgroups involved with the shutdown, using ISM all employees and contractors safely completed their assigned work activities.

### User Facility Safety

The MagLab's user facilities (DC Field, Pulsed Field, High B/T, NMR, AMRIS, EMR and ICR) provide support to internal and external users. To facilitate their visit, users are assigned online training modules that are specific to the experiment they are conducting and the hazards associated with each facility they will be working in. These are generally coordinated several weeks prior to their arrival if they are an external user. Internal users complete the required training prior to receiving authorization to start work. When users arrive at the facility, they receive hands on training that is specific to each location and discuss any potential safety concerns with user support. While at each facility users are assigned an in-house scientist and support technician to ensure both technical and safety needs are met. Non-routine and any particularly hazardous activities are completed by trained and experienced facility technicians to minimize risks to users.

### g. Industrial Partners & Collaborators

The MagLab collaborated with more than 90 companies, national/international labs, universities or community groups in 2018.

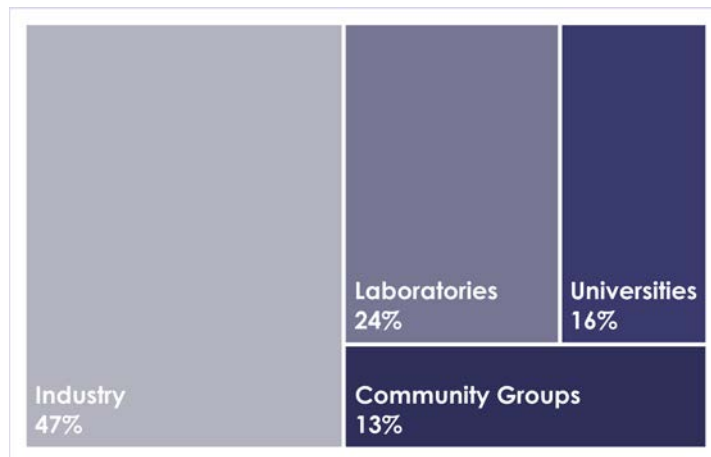


**Figure 1.g.1:** 2018 Partners and collaborators

support core research programs. Each of these corporate members will be asked to provide \$250,000/year for 4 years. The member may terminate the membership by giving the institute 30 days written notice prior to the membership renewal date. Current corporate members include Total and Reliance Industries. The institute also serves as a training center for fuel-related science and technology. (MagLab contact/ Director: Ryan Rodgers)

- **Omics LLC, FL**

Omics LLC is a spinoff company that serves the data analysis and interpretation needs of the high res mass spectrometry market. It was formed 8 years ago and has grown over the years to address a wider analytical community. (MagLab contact: Ryan Rodgers)

In addition, several spin off companies continued to operate in 2018, including:

- **Future Fuels Institute, FL**

The Future Fuels Institute (FFI) was established to enhance the existing Ion Cyclotron Resonance (ICR) Program at the NHMFL to deal specifically with bio- and fossil fuels, particularly for heavy oils and synthetic crudes. Supported by sponsoring companies and collaborative entities (instrument companies, universities, and research institutes), the FFI works to develop and advance novel techniques for research applications and problem solving. FFI is actively seeking up to 6 industrial collaborators as corporate members to

- **Magnetics Corporation (MagCorp), FL**

MagCorp is a new Tallahassee company that facilitates access to the world's leading magnetic experts to solve real world industrial problems. MagCorp was created to meet industry needs for feasibility studies, prototyping, and product development while eliminating the confusion that can come from partnering with academic institutions and research foundries. MagCorp is the world's one-stop shop for magnet science solutions and is the essential conduit between the private & government sectors and the National High Magnetic Field Lab. Leveraging completely new client & partner facing business models, MagCorp has already begun to attract industry to Tallahassee and put it on the map as the emerging magnetic capital of the world. (MagLab contact: Jeffrey Whalen)

#### h. Budget

The National High Magnetic Field Laboratory with its seven user facilities is primarily funded by the National Science Foundation. Other operating funds are provided through the participating institutions: Florida State University, University of Florida, and Los Alamos National Laboratory. Additionally, faculty and staff have been very successful in securing individual research funding for specific areas of research from a wide variety of sources, including federal, state, and private sectors.

The National Science Foundation Division/Directorate approved the MagLab's facilities award for 2018-2022 on March 23, 2018.

In 2018, the MagLab also receives three supplement awards:

- \$4,200,000 – Funding to launch a 40T Superconducting Magnet Project
- \$5,880,874 - Funding to replace and refurbish major equipment
- \$18,000 – Funding to support additional Research Experience for Undergraduates in the current program.

**Table 1.h.1** represents the budget allocation and percentage of the total budget to each department/division of the National High Magnetic Field Laboratory.

**Table 1.h.1: NHMFL NSF 2018 Calendar Year (CY) Budget with indirect cost distributed to programs**

Division/Program	CY 2018 Funding (\$)	Budget (%)
Operations/Safety	1,383,750	3.06
DC Field Facility	11,687,444	25.82
Magnet Science & Technology	9,233,670	20.40
Nuclear Magnetic Resonance & Magnetic Resonance Imaging/Spectroscopy	2,769,701	6.12
Ion Cyclotron Resonance	1,815,836	4.01
Electron Magnetic Resonance	1,144,472	2.53
Center for Integrated Learning and Research Experience for Undergraduates	574,769	1.27
Applied Superconductivity Center	2,474,194	5.47
Electricity & Cryogenics	4,226,981	9.34
Los Alamos National Laboratory/Pulsed Field Facility	8,038,831	17.76
University of Florida - High B/T	407,697	0.90
University of Florida - AMRIS	852,757	1.88
Diversity	82,549	0.18
User Collaboration Grants Program	576,128	1.27
<b>TOTAL NSF BUDGET FOR CY 2018</b>	<b>\$45,268,779</b>	<b>100%</b>

**Notes:**

CY 2018 included Funding in the amount of \$25,832,908 and \$9,337,000 under Cooperative Agreement DMR 1164779.

CY 2018 included award for the preliminary design of a 40T Magnet in the amount of \$4,200,000 under Cooperative Agreement DMR 1164779.

CY 2018 included award for major equipment purchases in the amount of \$5,888,874 under Cooperative Agreement DMR 1164779.

CY 2018 included supplement funding for the Research for Undergraduate Program in the amount of \$18,000 under Cooperative Agreement DMR 1164779.

The National Science Foundation approved \$184,050,000 which included front-funding under DMR 1157490 in the amount of \$8,937,095.

**Table 1.h. 2** summarizes the MagLab's budget position as of December 31, 2018. The report includes annual funding per our Cooperative Agreement plus the three supplement awards.

**Table 1.h.2: NSF Budget & Expenses Calendar Year 2018**

Expense Classification	Budget (\$)	Disbursed and Encumbered (\$)	Balance as of 12/31/2018 (\$)
Salaries and Fringe	12,668,597	10,497,786	2,170,811
Subawards	9,551,292	9,436,411	114,881
Equipment	7,052,325	3,340,294	3,712,031
Other Direct Costs	6,208,295	4,313,874	1,894,421
<b>Subtotal</b>	<b>35,480,509</b>	<b>27,588,365</b>	<b>7,892,144</b>
Indirect	9,788,270	5,012,335	4,775,935
<b>Total Direct and Indirect</b>	<b>45,268,779</b>	<b>32,600,700</b>	<b>12,668,079</b>

**Notes:**

Per Cooperative Agreement for DMR 11644779, the budget for CY 2018 is \$34,770,000.

A supplement in the amount of \$8,937,095 for CY 2018 Funds was funded in CY2017 under DMR 1157490.

Funding for CY 2018 also included three supplements: 40T, Major Equipment, and REU.

**i. Cost Recovery Report**

The NHMFL did not receive program income during CY 2018.

## 2. USER FACILITIES

### a. User Program

#### Proposal Review Process

Across all seven facilities, proposals for magnet time are submitted online: (<https://users.magnet.fsu.edu>) and reviewed in accordance with the [NHMFL User Proposal Policy](#). In brief, each user facility has a User Proposal Review Committee (UPRC) comprised of at least seven members, with more external members than internal. UPRC memberships are treated confidentially by the laboratory but are available for review by NSF and NHMFL advisory committees. Proposal reviews are conducted in strict confidence and are based on two criteria: (1) the scientific and/or technological merit of the proposed research and (2) the “broader impacts” of the proposed work. They are graded online according to a scale, ranging from “A”—Proposal is high quality and magnet time must be given a high priority; to “C”—Proposal is acceptable and magnet time should be granted at NHMFL discretion; to “F”—Proposal has little/no merit and magnet time should not be granted. The Facility Directors dovetail the UPRC recommendations with availability and scheduling of specific magnets, experimental instrumentation and user support scientists and make recommendations for magnet time assignments to the NHMFL Director. The NHMFL Director is responsible for final decisions on scheduling of magnet time based on these recommendations. A PDF of all 2018 User Proposals can be found at <https://nationalmaglab.org/research/publications-all/annual-reports>.

#### Research Report

At the end of each year, MagLab users and faculty at FSU, UF and LANL submit brief abstracts of their experiments, research and scholarly endeavors. Users generated 401 research reports in 2018 (**Table 2.a.1**). In 2018, 401 research reports were received in 21 categories, representing the life sciences, chemistry, magnet science and technology and condensed matter physics.

- 27 percent of the research activities (109 reports) were already published, many in prominent journals.
- 9 reports were accepted for publication; 34 were submitted for publication; and 166 have manuscripts in preparation.
- The majority of research projects were funded by the U.S. National Science Foundation, the U.S. Department of Energy and the U.S. National Institutes of Health. Other funding organizations included numerous universities. Research was also supported by science federations, ministries and universities in countries around the world including: Australia, Canada, China, Egypt, Germany, Ireland, Japan, Philippines, Poland, Russia, Slovakia, South Korea, Spain and the United Kingdom.

The MagLab User Collaboration Grants Program encourages collaborations between internal and external investigators, promotes bold but risky efforts and provides initial seed money for new faculty and research staff and facility enhancements. This program supported 12 of the 401 research activities. All reports will be released in summer 2019 on our website at <https://nationalmaglab.org/research/publications-all/annual-reports>.

**Table 2.a.1: 2018 Research Reports by Facility**

FACILITIES	Number of Reports
AMRIS Facility at UF	53
DC Field Facility	117
EMR Facility	43
High B/T Facility at UF	4
ICR Facility	42
NMR Facility	58
Pulsed Field Facility at LANL	62
<b>MAGLAB DEPARTMENTS &amp; RELATED GROUPS</b>	
Applied Superconductivity Center	5
Condensed Matter Theory/ Experiment (FSU)	6
Magnet Science & Technology	6
UF Physics	5
<b>TOTAL REPORTS</b>	<b>401</b>



## User Funding Opportunities

### 1. Dependent Care Travel Grant

The MagLab also offers a Dependent Care Travel Grant program which, provides up to \$800 for travel expenses for MagLab scientists traveling to conferences or MagLab users traveling to any of the three MagLab facilities. This money can be used to pay for dependent care costs. In 2018, three individuals utilized this funding opportunity: one MagLab Research faculty member and two MagLab users.

### 2. First Time User Support

The NHMFL is charged by the National Science Foundation with developing and maintaining facilities for magnet-related research that are open to all qualified scientists and engineers through a peer-reviewed proposal process. Facilities are generally available to users without cost. In an effort to encourage new research activities, first-time users are provided financial support for travel expenses. International users are provided \$1,000 of support and domestic users are provided \$500 of support for their travel costs. This funding is provided by the State of Florida and is available for Tallahassee user facilities only. In 2018, the MagLab spent \$15,000 supporting first time users.

### 3. User Collaboration Grants Program (UCGP)

The National Science Foundation charged the National High Magnetic Field Laboratory with developing an internal grants program that utilizes the NHMFL facilities to carry out high quality research at the forefront of science and engineering and advances the facilities and their scientific and technical capabilities. User Collaboration Grants Program (UCGP), established in 1996, stimulates magnet and facility development and provides intellectual leadership for research in magnetic materials and phenomena.

The Program strongly encourages collaboration between NHMFL scientists and external users of NHMFL facilities. Projects are also encouraged to drive new or unique research, i.e., serve as seed money to develop initial data leading to external funding of a larger program. In accord with NSF policies, the NHMFL cannot fund clinical studies.

Twenty one (21) UCGP solicitations have now been completed with a total of 564 pre-proposals being submitted for review. Of the 564 proposals, 292 were selected to advance to the second phase of review, and 130 were funded (23 percent of the total number of submissions).

#### 2018 Solicitation and Awards

The NHMFL UCGP has been highly successful as a mechanism for supporting outstanding projects in the various areas of research pursued at the laboratory. Its two-stage proposal review process is handled by means of a web-based system. Proposal review is done by a combination of internal and external reviewers. Details of the process and review criteria are available on the website <https://ucgp.magnet.fsu.edu/Guidance/ReviewCriteriaAndProcess>. The most recent solicitation, announced in March, 2018 is complete, and its awards will be issued approximately in March 2019.

Of the 18 pre-proposals received the committee recommended that 12 pre-proposals be moved to the full proposal state. Of the 12 full proposals, five were awarded. A breakdown of the review results is presented in **Tables 2.a.2 and 2.a.3**

**Table 2.a.2: UCGP Proposal Solicitation Results – 2018**

Research Area	Pre-Proposals Submitted	Pre-Proposals Proceeding to Full Proposal	Projects Funded
Condensed Matter Science	9	6	3
Biological & Chemical Sciences	7	4	2
Magnet & Magnet Materials Technology	2	2	0
<b>Total</b>	<b>18</b>	<b>12</b>	<b>5</b>

**Table 2.a.3: UCGP Funded Projects from 2017 Solicitation**

Principal Investigator	NHMFL Institution	Project Title	Funding
Komalavalli Thirunavukkuarasu	NHMFL/FAMU	High-Pressure High-Field Optical Magneto-Spectroscopy	\$214,179

Principal Investigator	NHMFL Institution	Project Title	Funding
Yasu Takano	UF	Development of Faraday force magnetometers for absolute magnetization measurements at temperatures below 100 mK in high magnetic fields	\$176,545
Fedor Balakirev	LANL	Pressure-Tuned Quantum Magneto-Transport in Topological Semimetals up to 100 T	\$190,000
Clifford Bowers	UF	Parahydrogen Enhanced MR Imaging and Spectroscopy at the NHMFL	\$188,232
Donald Smith	FSU	High Magnetic Field FT-ICR Mass Spectrometry Imaging	\$189,988

### Results Reporting

To assess the success of the UCGP, reports were requested in January 2019 on grants issued from the five solicitations, which had start dates from 2011 through 2018. At the time of the reporting, some of these grants were in progress, and some had been completed. For this “retrospective” reporting, principal investigators (PIs) were asked to include external grants, NHMFL facilities enhancements and publications that were generated by the UCGP. Since UCGP grants are intended to seed new research through high risk initial study or facility enhancements, PIs were allowed and encouraged to report results that their UCGP grant had made possible, even if these were obtained after the term of the UCGP grant was complete.

The PIs reported:

- Lab enhancements, which are listed in **Table 2.a.4** below.
- At least partial support for 16 undergraduate researchers, 46 grad students and 23 postdocs.
- 13 funded external grants, which were seeded by results from UCGP awards. The total dollar value of the external grants was \$24.2M, of which \$10.5 M was an Energy Frontier Research Center.
- 152 publications, many in high profile journals, including 2 in JACS, 2 in Nature, 12 in Nature Communications, 1 in PNAS and 8 in Phys. Rev. Lett.

**Table 2.a.4:** Facility Enhancements Reported from five UCGP Solicitations

Enhancement and Available Date	Users
Modified 1800 C tube furnace for molten metal flux growth of uranium compounds (1/15)	7
Development of capabilities for hazardous substance handling (1/15)	4
Arduino-controlled, NMR spectrometer-synchronized near-infrared high power laser tuning system	3
Three (3) cryogenic NMR probes, all with through-space optical access (9/12-8/15)	10
Ac susceptometers (12/13)	9
Improvement of high-field VSM (1/14)	6
Time-domain THz spectroscopy using TOPTICA Teraflash system	3
Variable temperature (VT) magic-angle spinning (MAS) probe for the 900 MHz NMR (6/14)	2
Coil winder for AC susceptibility (10/16)	4
Hybrid piston cylinder cell (10/16)	1
Relaxation-enhanced magnetic resonance spectroscopy set-up	4
Improved EMR high pressure facility (11/16)	2
High-temperature, high-resolution NMR (11/16)	9
High sensitivity pulsed NMR spectrometer and probe for ultralow temperature (6/18)	1
Fiber Bragg Grating based magnetostriction pulsed field and dc magnets (3/12)	23
Imaging and measurement of photocurrent and photoluminescence in high magnetic field (9/12)	1
mK (3He and dilution fridge) NMR probes (8/15)	9
1 kW, 1GHz NMR power amplifier (10/16)	3
Electrocrystallization facility for BEDT-TTF, or ET	9

Enhancement and Available Date	Users
Direct-optics setup for PL, reflectance, Raman magneto-spectroscopy at B<14.5T and T=4-300K (6/15)	10
Faraday magnetometer for the 20 T (6/13)	1
Expanded range of magnetic field sweep rates in the 60 T shaped-pulse magnet (8/12)	5

<sup>1</sup>Number of external users (PIs only) reported to have used the enhancement.

#### 4. Visiting Scientist Program

The National High Magnetic Field Laboratory provides researchers from academia, industry and national laboratories the opportunity to utilize the unique, world-class facilities of the laboratory to conduct magnet-related research. In 2018, the Visiting Scientist Program provided a total of \$38,387 financial support for ten research projects on a competitive basis. To apply for support from the Visiting Scientist Program, interested researchers are required to submit an application and a proposal that will be reviewed by appropriate facility directors and scientists at the NHMFL. All requests for support must be submitted online at <https://vsp.magnet.fsu.edu/> at any time throughout the year.

#### Annual User Program Survey

The MagLab conducted its eight annual user survey between June 4, 2018, and June 30, 2018. User input assisted all seven facilities to respond to user needs, improve facilities and services and guided the MagLab in setting priorities and planning for the future. This request was sent to all MagLab User Principal Investigators (PI) and to their collaborators who received magnet time between June 1, 2017, and May 31, 2018, including PIs who sent samples, where the experiment was performed by laboratory staff scientists. All user responses were treated anonymously. All presented figures exclude internal responders.

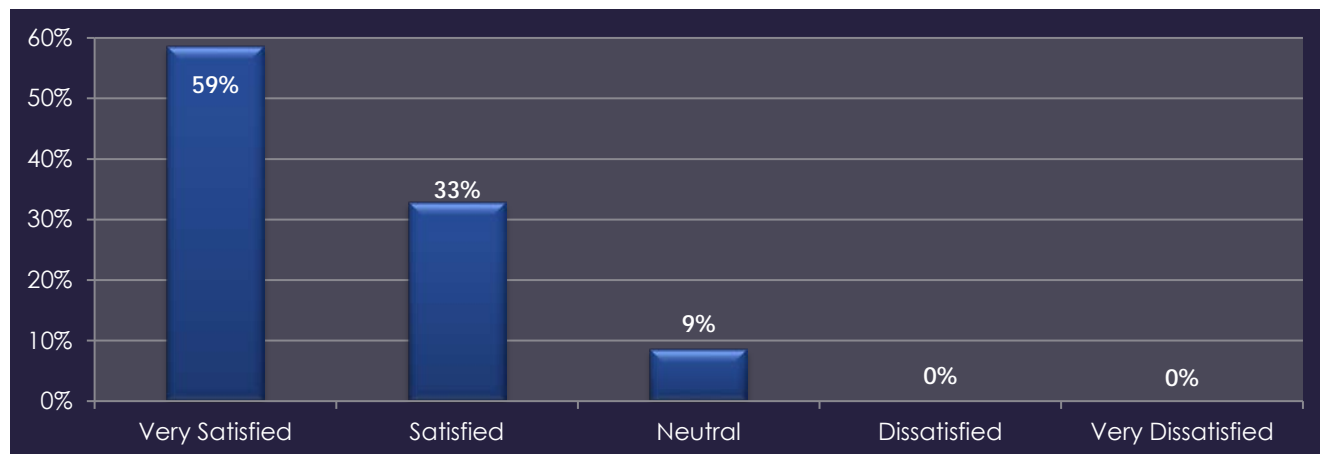


Figure 2.a.1: 92% of external users were satisfied or very satisfied with the proposal process (e.g., submission, review).

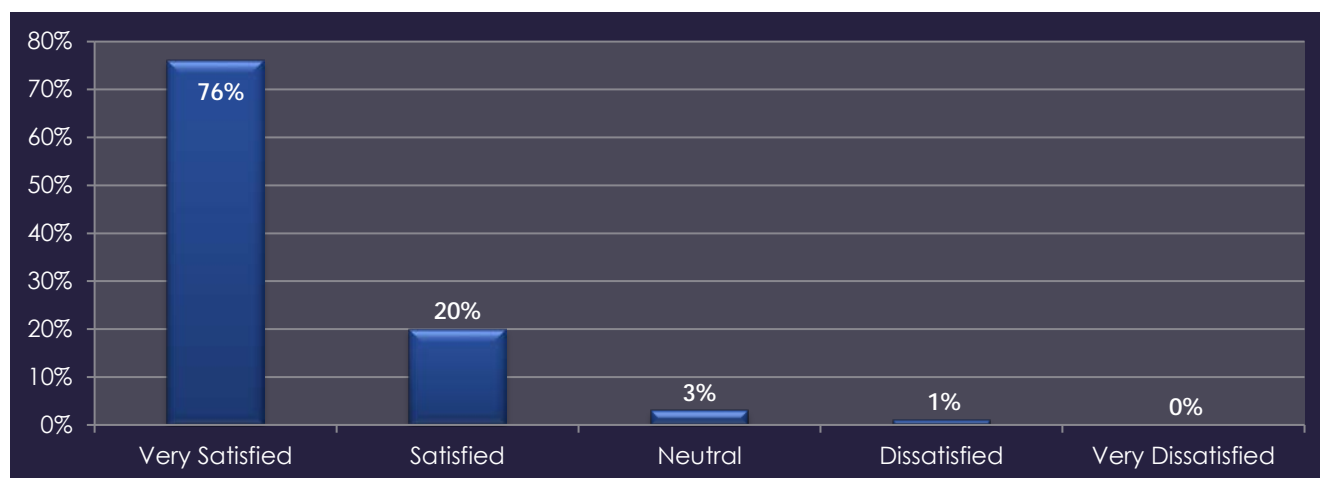
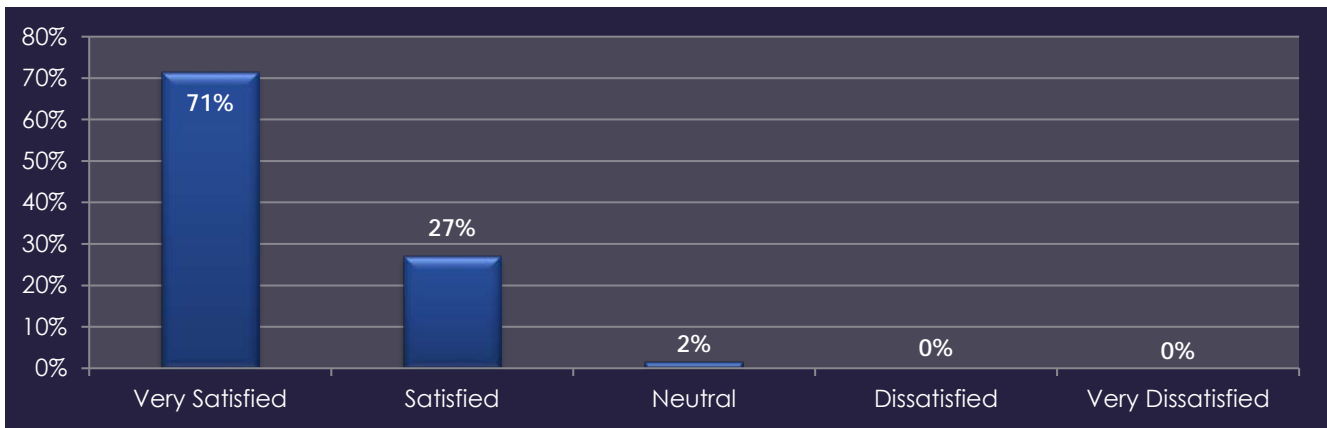
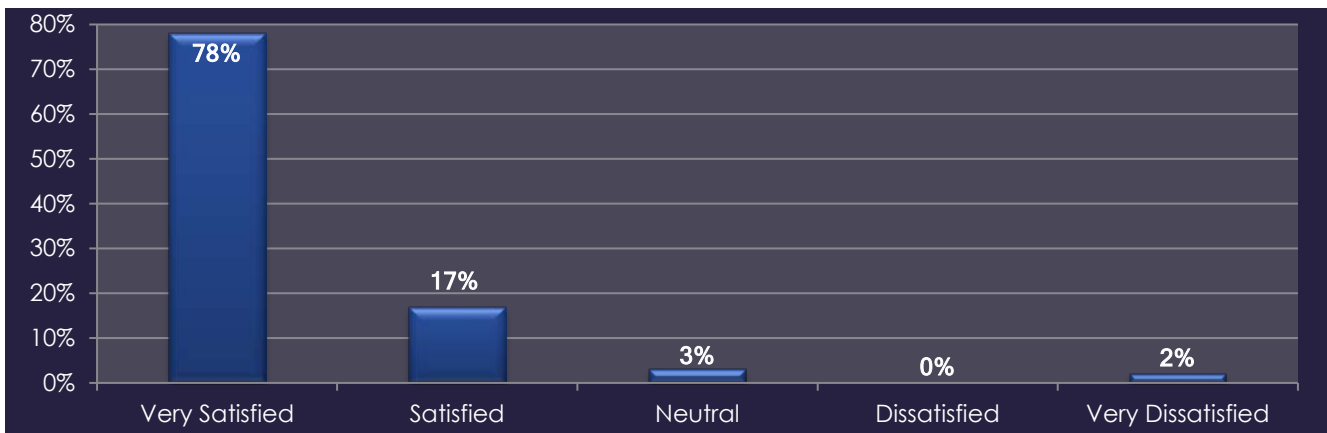


Figure 2.a.2: 96% of external users were satisfied or very satisfied with the availability of the facilities and equipment.



**Figure 2.a.3:** 98% of external users were satisfied or very satisfied with user friendliness of training and safety procedure.



**Figure 2.a.4:** 95% of external users were satisfied or very satisfied with the overall safety at the MagLab.

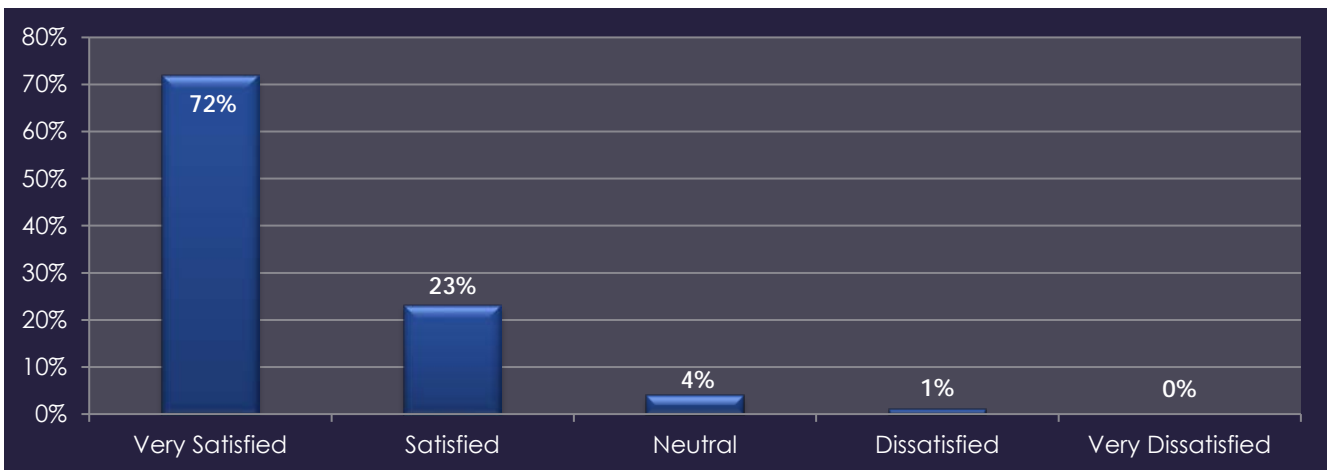


**Figure 2.a.5:** 95% of external users were satisfied or very satisfied with the performance of facilities and equipment (e.g., were they maintained to specifications for intended use, ready when scheduled, etc.).

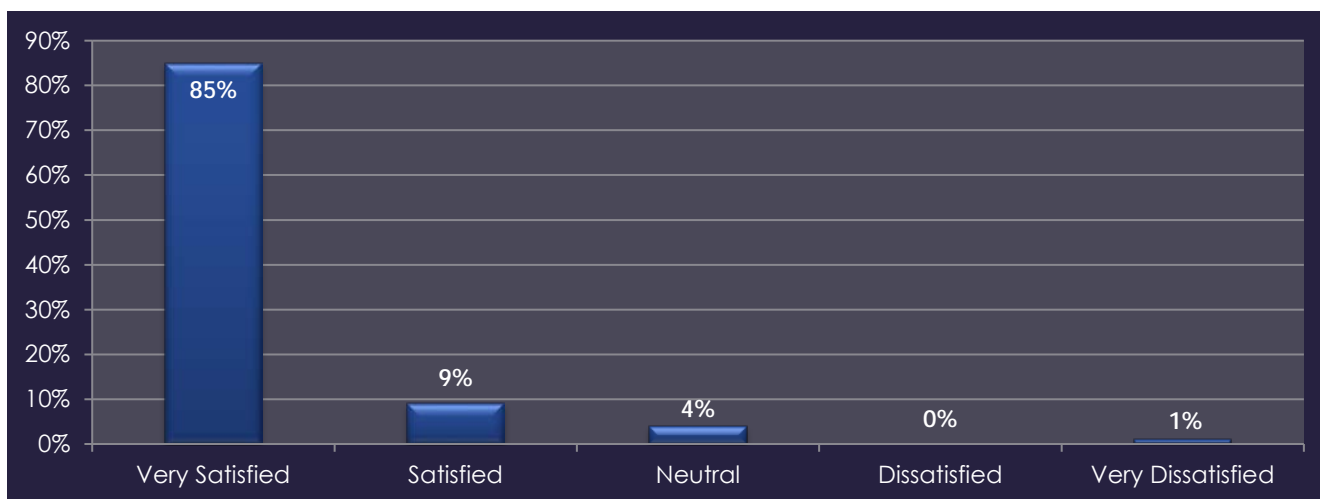


**Figure 2.a.5:** 94% of external users were satisfied or very satisfied with the assistance provided by MagLab facilities technical staff.

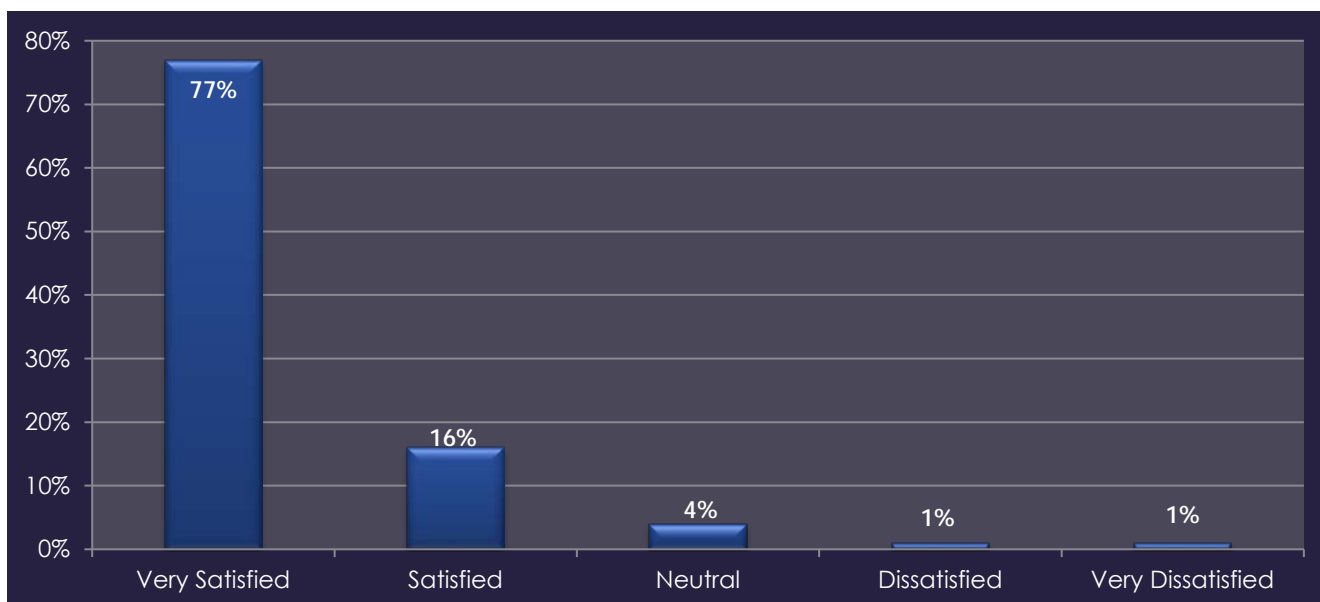


**Figure 2.a.6:** 93% of external users were satisfied or very satisfied with the assistance provided by MagLab facilities administrative staff.

#### b. User Facilities

The geographical distribution of our users' organizations can be found at <https://nationalmaglab.org/user-resources/user-community>.

#### AMRIS FACILITY

The AMRIS facility at the University of Florida supports nuclear magnetic resonance (NMR) and magnetic resonance imaging (MRI) studies of chemical compounds, biomolecular systems, tissues, small animals, large animals and humans. We currently offer twelve systems with different magnetic fields and configurations to users for magnetic resonance experiments. AMRIS has thirteen professional staff members to assist users, maintain instrumentation, build new coils and probes and help with administration.

#### Unique Aspects of Instrumentation Capability

Several of the AMRIS instruments offer users unique capabilities: the 750 MHz wide bore provides outstanding high-field imaging for excised tissues and small animals as well as diffusion measurements with gradient strengths up to 30T/m; the 11.1T horizontal MRI has the highest field strength MRI magnet in the world with a 400 mm bore and gradient strengths up to 1.5T/m; the 600 MHz 1.5-mm HTS cryoprobe

is the most mass-sensitive NMR probe in the world for  $^{13}\text{C}$  detection and is ideal for natural products research; the 5T DNP polarizer enables both fundamental studies of DNP mechanisms down to 1.2K as well as *in vivo* metabolism measurements when coupled to either the 4.7T or 11.1T systems. These systems support a broad range of science, including natural product identification, solid-state membrane protein structure determination, cardiac studies in animals and humans and correlation of neural structures with brain function and chemistry (Tab 2.b.1).

**Table 2.b.1: NMR & MRI Systems in the AMRIS Facility at UF in Gainesville**

$^1\text{H}$ Frequency	Field (T), Bore (mm)	Homogeneity	Measurements
800 MHz	18.8, 63	1 ppb	Solution/solid state NMR
750 MHz	17.6, 89	1 ppb	Solution/solid state NMR and MRI
600 MHz	14.1, 51	1 ppb	NMR and microimaging
600 MHz	14.1, 54	1 ppb	Solution NMR (CryoProbe)
600 MHz	14.1, 54	1 ppb	Solution NMR (HTS Cold Probe)
500 MHz	11.7, 54	1 ppb	Solution/solid state NMR
470 MHz	11.1, 400	0.1 ppm	DNP, MRI and NMR of animals
212 MHz	5.0, 89	1 ppm	DNP polarization
200 MHz	4.7, 330	0.1 ppm	DNP, MRI and NMR of animals
143 MHz	3.35, 52	1 ppm	DNP polarization
128 MHz	3.0, 900	0.1 ppm	MRI/S of humans, large animals
128 MHz	3.0, 900	0.1 ppm	MRI/S of humans

### Facility Developments and Enhancements

The installation of a  $^{13}\text{C}$ -optimized 10 mm cryoprobe at 600 MHz in combination with the Hypersense DNP polarizer previously installed now enables real-time metabolic measurements in functioning cardiac tissue. We are working directly with Bruker to test a new gradient setup on the 750 MHz system, which significantly increases SNR during imaging experiments. During 2018 our Bruker 600 MHz 5-mm CryoProbe system was upgraded with a new CryoPlatform and an Avance-Neo console. A 1.7-mm TCI CryoProbe is expected in 2019. We recently purchased and installed an 800 MHz 4 channel console and magnet ensuring that the high field NMR systems offer the latest in pulse sequence capabilities and multinuclear detection. User operation of the 800 MHz system is expected to begin in early 2019.

### Major Research Activities and Discoveries

This year we saw continued research growth in our major research focus areas. The first area was in fundamental DNP studies and their application to *in vivo* metabolic studies. A second area of growth was in supporting users pursuing quantitative studies for metabolomics and structural biology. A third area of growth was in the use of *in vivo* MRI and MRS to study structure/function/chemistry in rodent models up to 17.6T. Research in these areas led to and will leverage the enhancements described in section above. AMRIS facility users reported 61 peer-reviewed publications and five theses and dissertations for 2018.

### Facility Plans and Directions

In spite of the continued challenging budgetary climate, our users have consistently and successfully pursued federal funding to support their research programs in addition to assisting the AMRIS facility in writing proposals to upgrade instrumentation. The successful partnership of the NHMFL user program with individual investigator research grants also provides constant scientific motivation for our technology development. Last year we received an NIH P41 technology center grant. This five-year grant will fund the continued development of NMR probes with world-leading sensitivity for challenging biomolecular studies. We have also partnered with UCF to relocate 600 MHz and 800 MHz systems to AMRIS, enabling researchers to have improved access to high field spectrometers and expertise.

### Outreach to Generate New Proposals-Progress on STEM and Building User Community

In June of 2018, Kelly Deuerling replaced Elizabeth Webb as the NHMFL coordinator at the University of Florida. Deuerling and Webb, along with graduate students and postdoctoral fellows, visited 106 classrooms in 18 schools, reaching 2,100 students as part of the NHMFL classroom outreach program in



Gainesville. An additional 12 presentations reaching 20 students were made at Fort Clarke Middle School, the afterschool science program Webb initiated and Deuerling continued. Staff gave tours of the AMRIS facility to 11 groups reaching 210 individuals of diverse backgrounds.

This year, Webb volunteered at the Women in Science and Engineering (WiSE) Girls spring break camp with AMRIS engineer Malathy Elumalai. This weeklong camp brought middle school girls from Alachua County to the University of Florida to learn about a variety of different sciences. Webb and Elumalai lead one day of camp activities at the AMRIS facility, which included building electromagnets, running an NMR experiment and 3D printing.

In April, in association with Bruker, we hosted an MRI pulse programming course, which focused on development for the Paravision imaging software.

In May, we again held our very popular RF Coil building workshop in the AMRIS Facility. Five participants came for a week to learn the physics behind MRI, RF coil theory, and how to build RF coils. As part of the course, participants built a quadrature surface MRI coil to bring back to their home institutions.

Also in May, AMRIS faculty and staff led a NMR Metabolomics and <sup>13</sup>C Fluxomics Workshop. Eleven lecturers provided instruction about software, hardware and data handling in these areas of research. Participants acquired their own NMR spectra, and then subsequently analyzed those spectra with the assistance of expert instructors, both from AMRIS and from external collaborators.

Faculty associated with the AMRIS Facility mentored four NHMFL REU students over the summer and gave periodic tours of the AMRIS Facility. These faculty consistently have ~20 undergraduate and high school students working on projects at any given time.

### Facility Operations Schedule

The AMRIS facility operates year round, except during the last week of December when the University of Florida is shut down. Vertical instruments for ex vivo samples are scheduled 24/7, including holidays and weekends. Horizontals operate primarily 8 hrs/day, 5 days/week due to the difficulty in running animal or human studies overnight. The AMRIS facility operates as an auxiliary under federal cost accounting standards. Local and NHMFL-affiliated users pay for magnet time from federally funded projects (primarily individual investigator grants); the NHMFL funds magnet time for users from outside the UF system and development projects.

### DC FIELD FACILITY

*The DC Field Facility in Tallahassee serves a large and diverse user community by providing continuously variable magnetic fields in a range and quality unmatched anywhere in the world. The DC Field user community is made up of undergraduate students, graduate students, post docs and senior investigators from around the country and the world. State-of-the-art instrumentation is developed and coupled to these magnets through the efforts of our expert scientific and technical staff. The users of the DC Field Facility are supported throughout their visit by the scientific, technical and administrative staff to ensure that their visit is as productive as possible. The interaction between the NHMFL scientific and technical staff with the students, post docs and senior investigators who come to the DC Field Facility to perform their research results in a continuous mix of scientific ideas and advanced techniques that are passed both to and from users.*

### Unique Aspects of Instrumentation Capability

Table 2.b.2: DC Field Magnets

FLORIDA-BITTER and HYBRID MAGNETS		
Field, Bore, (Homogeneity)	Power (MW)	Supported Research
45T, 32 mm, (25 ppm/mm)	30.4	Magneto-optics – ultra-violet through far infrared; Magnetization; Specific heat; Transport – DC to microwaves; Magnetostriction; High Pressure; Temperatures from 30 mK to 1500K; Dependence of optical and transport properties on field, orientation, etc.; Materials processing; Wire, cable and coil testing. NMR, EMR and sub/millimeter wave spectroscopy.
41.5T, 32 mm, (25 ppm/mm)	32	
36T, 40 mm, (1 ppm/mm) <sup>2</sup>	14	
35T, 32 mm (x2)	19.2	
31T, 32 mm to 50 mm <sup>1</sup> (x2)	18.4	
25T, 32 mm bore (with optical access ports) <sup>3</sup>	27	

SUPERCONDUCTING MAGNETS		
Field, Bore	Sample Temperature	Supported Research
18/20T, 52 mm	20mK – 1K	Magneto-optics – ultra-violet through far infrared; Magnetization; Specific heat; Transport – DC to microwaves; Magnetostriction; High pressure; Temperatures from 20mK to 300K; Dependence of optical and transport properties on field, orientation, etc. Low to medium resolution NMR, EMR and sub/millimeter wave spectroscopy.
18/20T, 52 mm	0.3K – 300K	
17.5T, 47 mm	4K – 300K	
10T, 34 mm <sup>3</sup>	0.3K – 300K	

1. A coil for modulating the magnetic field and a coil for superimposing a gradient on the center portion of the main field are wound on 32 mm bore tubes.
2. Higher homogeneity magnet for magnetic resonance measurements.
3. Optical ports at field center with 4 ports each 11.4° vertical x 45° horizontal taken off of a 5mm sample space

**Table 2.b.2** lists the magnets in the DC Field Facility. The NHMFL leads the world in available continuous magnetic field strength, number of high field DC magnets available to users and accessibility for scientific research. The 45T hybrid magnet is the highest field DC magnet in the world, which is reflected in the number of proposals from PIs located overseas. The 41T resistive magnet is the highest field resistive magnet in the world. The 36T Series Connected hybrid magnet features two configurations: 40 mm bore with 1 ppm homogeneity for chem/bio NMR experiments and a 48 mm bore with 20 ppm homogeneity for condensed matter physics experiments in a top-loading cryogenic system. The 35T, 32 mm bore and 31T, 50 mm bore magnets are coupled to top loading cryogenic systems that have impressive performance, flexibility and ease of use. The 25T Split-Helix magnet is the highest field direct optical access / scattering magnet in the world. With four optical ports located at field center, each having a 11.4° vertical x 45° horizontal taken off of a 5mm opening, the ability to perform ultrafast, time resolved and x-ray scattering experiments are now a reality at high magnetic fields.

#### Facility Developments and Enhancements

**New 7 MW (2,000 ton) cooling power chillers installed in DC Field Facility Plant.** Beginning in early November 2018, work began on replacing the four 2,000-ton chillers (**Fig.2.b.1**), which were original to the construction of the DC Field Facility in 1992. These chillers were at the end of their service lives and utilized ozone-depleting R-22 (Freon) refrigerant that is due to be phased out completely in 2020. The new chillers use R-1233 refrigerant, which does not affect the ozone layer, operates at a lower pressure and features improved adaptability to the variable heat loads produced by the water-cooled magnets. The new chillers will also provide greatly improved reliability for operating the water-cooled magnets as well as being more energy efficient.

**High Voltage Disconnects for Power Supplies.** Four 12.5 kV disconnects were installed during the 2018 annual maintenance shutdown (**Fig.2.b.2**). These disconnects will



**Figure 2.b.1:** The first 7 MW (2,000 ton) chiller being installed.



**Figure 2.b.2:** 12.5 kV Power supply disconnect for power supply A and B.

become the energy isolation point for the

primary side of the power supply transformers—reducing wear and tear on the 12.5 kV, 1,500 A circuit breakers, which had been used as the energy isolation point when work needed to be done on the power supplies. The new disconnects eliminate the hazard of pulling the power supply breakers off of the high voltage bus (racking out), are much faster to operate, lock-out and provide a visual verification of open circuit condition.

### **Two New Magnets (SCM5 & SCM6) added to DC Field Facility User Program.**

Two new superconducting magnets were added to the DC Field Facility user program in 2018. A 9T Physical Property Measurement System (SCM6) and a 7T Magnetic Property Measurement System (SCM5) (Fig.2.b.3). These systems are part of our efforts to broaden participation in the user program and provide an important resource for users at colleges and universities with limited research capabilities as well as for users needing to perform initial low field measurements whose measurements don't require the higher fields of SCM1 and SCM2. SCM6 is able to accommodate AC and DC electrical transport, heat capacity, torque magnetometry and has a rotation stage with a temperature range from 1.9K – 400K. SCM5 is able to perform SQUID magnetometry and AC susceptibility with a temperature range of 1.9 – 400K.



Figure 2.b.3: SCM5 and SCM6

**Significant Improvement in FIR Measurement Capabilities** 2018 saw significant improvements in the FIR measurement capabilities of the DC Field Facility. Mike Ozerov made significant changes to key portions of the FIR instrumentation in cell 8 and SCM3 resulting in tremendous gains in the signal-to-noise ratios and a concomitant reduction in the amount of time needed to acquire spectra. An example is shown from a user experiment in SCM3 in Figure 2.b.4, demonstrating the dramatic improvement in the signal-to-noise ratio by greater than a factor of 20, coupled with a reduction in scan time from 20 minutes needed for the black trace to 1 minute needed for the red trace.

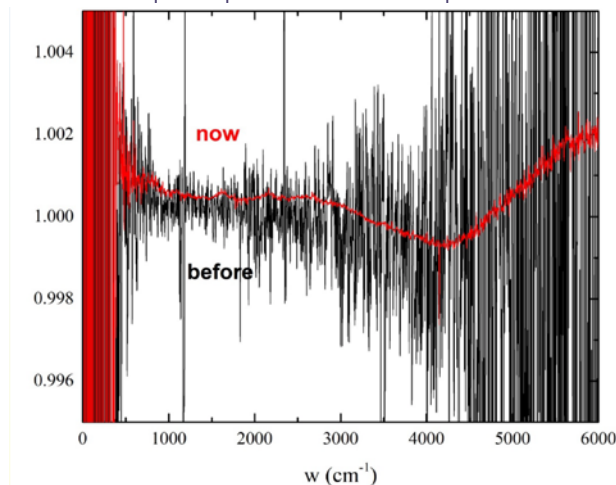


Figure 2.b.4: Demonstration of signal to noise improvement in SCM3 FIR measurement.

### **Major Research Activities and Discoveries**

Scientific exploration at the DC Field Facility encompassed a variety of topics in 2018, as shown in the annual research reports submitted by our users. A couple of notable examples are listed below.

**Research into the novel properties of graphene was carried out by a number of user groups**, including the group of Jun Zhu from Penn State University. Using SCM2, her group demonstrated switchable transmission of quantum Hall edge states in bilayer graphene using electrostatic gating. This is an important step in the development of an electron interferometer that can be used for the detection of non-Abelian collective electron excitations. These quasiparticle excitations are of interest as they are neither fermions nor bosons and therefore follow a different set of rules regarding their behavior.

**A topological excitonic insulator ground state** was observed in a mesoscopic InAs/GaSb double-gate, bilayer quantum well device. An excitonic insulator occurs when an electron-hole pair is created through weak correlations similar to how Cooper pairs are formed in BCS superconductors. This pairing opens a gap at the Fermi energy resulting in the dilute semimetal transforming into an insulator. Utilizing the portable dilution refrigerator coupled to the cell 8, 35 T magnet, a group from Rice University led by Rui Du measured the energy gap and observed edge states in the devices using non-local transport techniques.



**Bilayer graphene exhibits many fascinating fractional Quantum Hall States in strong magnetic fields (Fig. 2.b.5).**

The edge states carry important information about the low-energy, two-dimensional collective excitations in the bulk. Most notably, recently observed even-denominator fractional Quantum Hall States may be non-Abelian in nature, such that they could potentially be used to carry out topological quantum computations. The experimental detection of these collective excitations requires the construction of an electron interferometer, which is a daunting challenge in bilayer graphene due to the gapless nature of the electron bands. MagLab users have recently pioneered lithographic techniques to realize a bilayer graphene device in which electrons can tunnel between

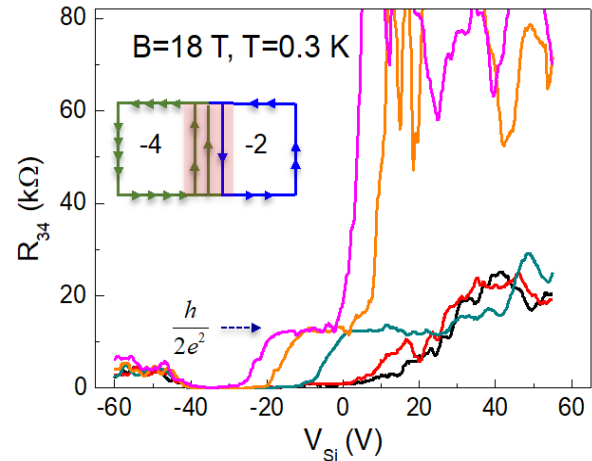
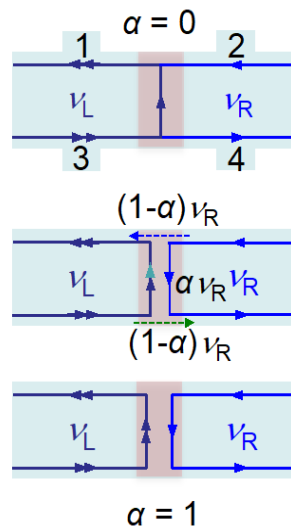


**Figure 2.b.5: Left:** The variable coupling of edge states between two lateral Quantum Hall States (blue regions). The backscattering rate  $a$  is controlled by the height of the tunneling barrier (gray region), which can be measured by longitudinal resistance across the barrier between contacts 3 and 4, denoted  $R_{34}$ . Three scenarios of  $a=0$ ,  $0 < a < 1$  and  $a=1$  are shown. **(At right)**  $R_{34}$  vs tunnel barrier gate voltage, which controls the barrier height. A vanishing  $R_{34}$  (as occurs around  $-35$  V) corresponds to perfect transmission of the edge states. A divergence (as occurs for pink and yellow traces for  $V > 10$  V) indicates no tunneling. A plateau at  $h/2e^2$ , as seen around  $-10$  V, indicates one of the two edge states on the right is completely reflected while the other transmits through, as illustrated by the inset.

two regions exhibiting Quantum Hall States (blue areas in the figure). This lateral quantum-Hall-to-quantum-Hall tunneling can be controlled electrically via a gate, where the height of the tunneling barrier is controlled by the gate voltage. By carrying out transport studies at the MagLab at fields up to 18 T at 0.3 K, MagLab users demonstrated gate-controlled transmission and pinch-off of quantum Hall edge states. This control mimics the action of a quantum point contact, which is a key milestone toward the

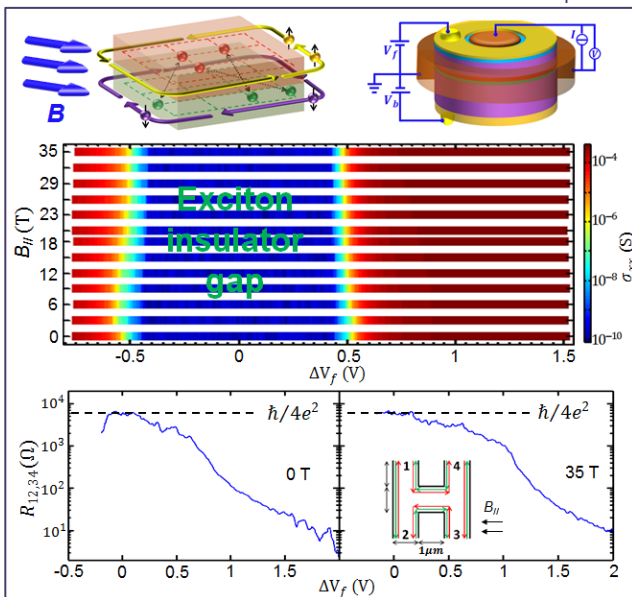


**Figure 2.b.6: Top:** Two depictions of the double quantum well device. **Middle:** Gate dependence of the conductance for a macroscopic Corbino device under inplane magnetic field from 0 T to 35 T. **Bottom:** Nonlocal transport measurement in meso-H bar under 0 T and 35 T.

future development of edge state interferometers. The success of this experiment enables the building of more complex interferometer devices using bilayer graphene to probe the unusual behaviors of collective excitations in the fractional quantum hall regime (J. Li, W. Hua, K. Watanabe, T. Taniguchi, and J. Zhu, *Gate-controlled Transmission of Quantum Hall Edge States in Bilayer Graphene*, Physical Review Letters 120, 057701 (2018).)

**In the 1960s, the exciton insulator (EI) was proposed to be an equilibrium ground state in which electrons and holes become paired through weak correlations, similar to Cooper pairs in a BCS superconductor (Fig 2.b.6).** This pairing opens a gap at the Fermi energy that transforms a dilute semimetal into an insulator. Recently the possibility of a topological EI has been proposed to explain the Quantum Spin Hall Effect, which features opposite propagation of edge states with reversed spins on the boundary of an EI. (See diagram at upper left) Thus far experimental evidence for the existence the EI state and counter-propagating edge states has remained elusive.

MagLab users fabricated macroscopic and mesoscopic double-gate devices in InAs/GaSb bilayer quantum wells, performing conductance measurements at temperatures down to 20mK and in magnetic fields up to 35T. Thermally activated conduction revealed the EI bulk energy gap, and non-local transport techniques revealed the edge states.

The data show that a topological Electronic Insulator state is indeed produced in these InAs/GaSb double quantum well devices. Realization of the nontrivial exciton state is a crucial step in exploring exotic phenomena of interacting topological insulators. Future work can be expected to access other correlated states, including bilayer superfluidity and Bose-Einstein condensation in this tunable system. (Evidence for a topological excitonic insulator in InAs/GaSb bilayers, L. Du, X. Li, W. Lou, G. Sullivan, K. Chang, J. Kono and R. R. Du, Nature Communications 8, 1971 (2017))

### Facility Plans and Directions

**The 41.5T resistive magnet will begin user operations in 2019.** The cryostat vibration isolation platform has been installed, tested and is ready to accept the cryostat. The start of user operations has been delayed due to the delivery date for the cryostat slipping by eight months from July 2018 to February 2019. The manufacturer experienced several setbacks and as a result the delivery was delayed.

**Replacement of the 12.5 kV – 480 V switchgear** used to supply electrical power to the DC Field Facility plant. Florida State University continues its longstanding support of the MagLab by funding the design, purchase and installation of the system of transformers, breakers, disconnects and buswork that is used to supply electrical power to the magnet cooling water pumps, helium liquefaction system, cooling towers and a host of other equipment necessary to operate magnets. The engineering work is underway now and replacement is anticipated to take place as part of the 2019 maintenance shutdown.

### Outreach to Generate New Proposals—Progress on STEM and Building User Community

The DC Field Facility continued to see heavy user demand in 2018, as shown by the usage tables in Appendix I. In spite of this oversubscription, however, the DC Field Facility has continued to make bringing new primary investigators (PIs) into the NHMFL a priority. We continue our efforts to reach out wherever possible



**Figure 2.b.7:** 2018 User Summer School participants.

in order to expand our user program and enable PIs from backgrounds underrepresented in the scientific community. In particular, the NHMFL sponsored a booth at the 2018 APS March Meeting in Los Angeles to advertise the capabilities and opportunities offered by the MagLab. The booth is staffed by NHMFL scientists and staff who explain the spectrum of research possibilities and user support available at the NHMFL. In addition, our DC Field Facility user support scientists regularly travel to conferences to present their results that showcase the capabilities of the laboratory and to recruit new users.

In 2018, the DC Field Facility continued to attract new researchers. Appendix A, DC Field Table 9, shows the DC Field Facility attracted 50 new PIs in 2018. This is in addition to the ten new PIs reported last year (2017) and 24 in 2016. Part of this large increase was due to the inaugural year of magnet operations with the Series Connected Hybrid that brought a number of new users into the DC Field Facility.

The DC Field Facility also hosted the **2018 NHMFL User Summer School**, which attracted 32 graduate students and post doc attendees (**Fig.2.b.7**). It is a five-day series of lectures and practical exercises in experimental condensed matter physics techniques developed and taught by members of the MagLab scientific staff as well as experts from scientific equipment companies. It has proven to be an excellent vehicle for communicating valuable experimental knowledge to the next generation of scientists from the enormous trove of experience encompassed by the MagLab scientific staff.

### Facility Operations Schedule

At the heart of the DC Field Facility are the four 14 MW, low noise, DC power supplies. Each 20 MW resistive magnet requires two power supplies to run the 45T hybrid magnet requires three power supplies and the 36T Series Connected Hybrid requires one power supply. Thus the DC Field Facility operates in



the following manner: in a given week there can be four resistive magnets and three superconducting magnets operating or the 45T hybrid, series connected hybrid, two resistive magnets and three superconducting magnets. The powered DC resistive and hybrid magnets operated for 45 weeks in 2018 with a six weeks shutdown for infrastructure maintenance from November 12 to December 23 and a one-week shutdown period for the university mandated holiday break from December 24, 2018, to January 2, 2019. The three superconducting magnets operated for 46 weeks out of the year with staggered maintenance periods as required. The hourly operation schedule for the resistive and hybrid magnets is as follows: 7 hours/day on Monday and 21 hours/day Tuesday–Friday. The superconducting magnets operate 24 hours/day, 7 days/week. The effects of Hurricane Michael in October resulted in a two-week shutdown of the DC Field Facility.

## EMR FACILITY

*Electron Magnetic Resonance (EMR) covers a variety of magnetic resonance techniques associated with the electron. The most widely employed is Electron Paramagnetic/Spin Resonance (EPR/ESR), which can be performed on anything that contains unpaired electron spins. EPR/ESR has thus proven to be an indispensable tool in a large range of applications in physics, materials science, chemistry and biology: including studies of impurity states; molecular clusters; molecular magnets; antiferromagnetic/ferromagnetic compounds in bulk, as well as thin films and nanoparticles; natural or induced radicals; optically excited paramagnetic states; electron spin-based quantum information devices; transition-metal based catalysts; and for structural and dynamical studies of metallo-proteins, spin-labeled proteins and other complex bio-molecules and their synthetic models.*

## Unique Aspects of Instrumentation Capability

The EMR facility at the NHMFL offers users several in-house developed, high-field and multi-high-frequency instruments covering the continuous frequency range from 9 GHz to ~1 THz, with additional frequencies up to 2.5 THz using a molecular gas laser. Several transmission probes are available for continuous-wave (CW) measurements, which are compatible with a range of magnets at the Lab, including the highest field 45T hybrid. Some of the probes can be configured with resonant cavities, providing enhanced sensitivity as well as options for in-situ rotation of single-crystal samples in the magnetic field and the simultaneous application of pressure (up to ~3 GPa). Quasi-optical (QO) reflection spectrometers are also available in combination with high-resolution 12T and 17T superconducting magnet systems; a simple QO spectrometer has also been developed for use in the resistive and hybrid magnets (up to 45T). EMR staff members can assist users in the DC field facility using broadband tunable homodyne and heterodyne spectrometers as well.

In addition to CW capabilities, the NHMFL EMR group boasts the highest frequency pulsed EPR spectrometer in the world, operating at 120, 240, 336 GHz, and now 395 GHz with <100 ns time resolution. A new quasi-optical 94 GHz spectrometer (HiPER) with 1 ns time resolution was recently upgraded for high power (1 kW) operation. A commercial Bruker Elexsys 680 operating at 9/94 GHz (X-/W-band) is also available upon request. This unique combination of CW and pulsed instruments may be used for a large range of applications in addition to EPR, including the study of optical conductivity, electron cyclotron resonance and Dynamic Nuclear Polarization.

## Facility Developments and Enhancements

The main area of development during 2018 centered around the use of field-modulated Fourier-transform infrared measurements, or Frequency-Domain Magnetic Resonance (FDMR). This work, which was carried out collaboratively with Mykhaylo Ozerov in the DC field facility, allows users to probe much higher frequency magnetic excitations associated with crystal field splittings and first-order spin orbit coupling. Many exciting new results were obtained with this capability, resulting in quite a few publications that are now appearing in print or are close to publication. The demand for this capability is high.

An important enhancement to the heterodyne pulsed EPR spectrometer was also implemented in 2018. New local oscillators were acquired, operating at 115 and 235 GHz (to complement the 120 and 240 GHz sources). These allow for the generation of a phase stable Intermediate Frequency (IF) from the multiplied frequency difference between the source and detector. This improved phase stability of the IF allows for experiments with increased repetition rates (> 200  $\mu$ s) and significantly enhances the sensitivity (>10 $\times$ ) of the spectrometer.

As noted in last year's report, a new narrow-band source operating at 395 GHz was acquired as part of the group's efforts to develop Dynamic Nuclear Polarization (DNP) enhanced NMR capabilities at 600 MHz. In addition to integrating this source into the DNP spectrometer, a separate layout was developed around the 15/17T magnet associated with the broadband homodyne spectrometer, where it can be used for pulsed EPR applications at 14.1T for  $g = 2$  spin species. Successful tests were performed last year, and this capability is now available to external users. Holders have also been manufactured for use in the 12.5T heterodyne spectrometer, where this capability can be used for species with  $g > 2.26$ .

In addition to the 395 GHz solid state source, the recently acquired 1 mW 950 GHz source and mixer-detector were successfully tested in the DC-field facility during 2018, as part of experiments with external user, Grace Morgan, from University College Dublin. This source was acquired for eventual use in the Series Connected Hybrid magnet. Work is ongoing to develop a dedicated dewar and probe for that magnet, which should be completed in the coming year (see below).

Last year we reported that our DNP efforts at 395 GHz have become part of a fully fledged solid-state MAS-DNP-enhanced NMR user program. During 2018, we supported our first user of the 395 GHz solution-state Overhauser DNP-enhanced NMR facility, Elzbieta Megiel, from the University of Warsaw. This project focused on the development of new organic radicals for solution-state DNP applications.

### Major Research Activities and Discoveries

A large number of research groups and projects were accommodated by the EMR program in 2018, resulting in the submission of 48 research reports (42 to EMR and six by EMR users submitted to the DC facility). In addition, 41 peer-reviewed journal articles were reported by our users (up from 37 the previous year), as well as numerous presentations at conferences. Many publications appeared in high-impact journals including: *Immunity* (1); *Nature Communications* (1); *J. Am. Chem. Soc.* (2); *Angew. Chem.* (1); *J. Phys. Chem. Lett.* (2); *Physical Review* (4); *Chem. Comm.* (3); *Inorganic Chemistry* (6); *Dalton Transactions* (4); and *Scientific Reports* (1). Projects in the facility spanned a range of disciplines, from applied materials research to studies of proteins; see also highlights below.

### Novel Metallofullerene Boosts Dynamic Nuclear Polarization

- Dynamic nuclear polarization (DNP) has gained tremendous popularity in recent years as an effective method to greatly boost the sensitivity of NMR and MRI. Upon application of a magnetic field, DNP is achieved by transferring the large electron spin polarization of a paramagnetic dopant to the NMR-active nuclei of interest. This polarization transfer is mediated by the saturation of electron spin resonance (ESR) transitions (e.g., in an organic radical mixed with the sample) via microwave irradiation of the sample. By combining DNP at low temperatures with rapid dissolution, researchers can achieve nuclear spin polarization enhancements that are as much as 10,000-fold over thermal equilibrium for solutions at room temperature. These DNP enhancements enable novel MRI applications, such as monitoring in vivo metabolism in real time (Fig. 2.b.8).

In this study, researchers added a low concentration of the endohedral metallofullerene (EMF)  $Gd_2@C_{79}N$  to DNP samples, finding that  $^1H$  and  $^{13}C$  enhancements increased by 40 percent and 50 percent, respectively, at 5T and 1.2K. Complementary multidimensional pulsed high-field ESR studies of the same sample provide important insights into the enhancement mechanism. While Gd reagents have previously been shown to enhance DNP at low fields, albeit at significantly higher Gd concentrations, this is the first time such increases have been observed at 5T. Importantly, the encapsulation of Gd in the EMF, along with the need for significantly lower concentrations, contribute to a significant reduction in toxicity of MRI for medical applications [X. Wang, J. E. McKay, B. Lama, J. van Tol, K. Kirkpatrick, Z. Gan, S. Hill, J. R. Long, H. C. Dorn, Gd based endohedral metallofullerene

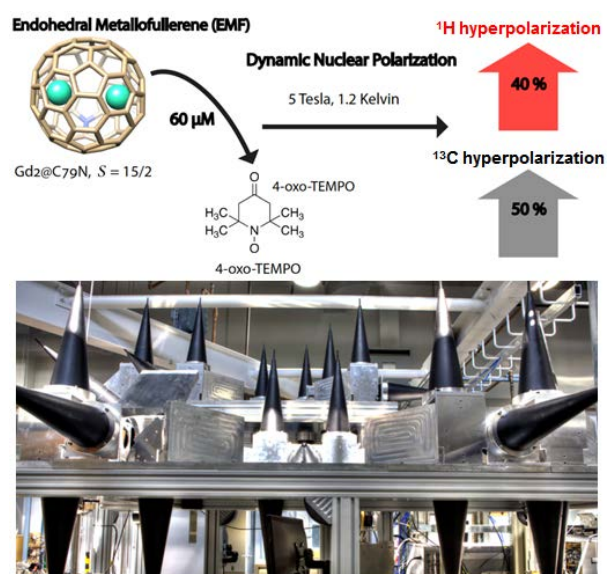


**Figure 2.b.8** (Top) A mixture of  $Gd_2@C_{79}N$  with the organic radical 4-oxo-TEMPO is shown to boost DNP efficiency, resulting in both  $^1H$  and  $^{13}C$  hyperpolarization. (Bottom) State-of-the-art spectrometer (HiPER) employed in this study, which combines expertise from the MagLab's EMR and NMR programs.

Gd<sub>2</sub>@C<sub>79</sub>N as a relaxation boosting agent for dissolution DNP at high fields, Chem. Comm. 54, 2425-2428 (2018)].

### Facility Plans and Directions

Over the past several years, a significant number of hardware acquisitions have resulted in remarkable enhancements to the instrumentation offered by the EMR program. Part of our longer-term plans involved the hiring of postdocs to support these instruments. During 2019, several new postdocs will join the group. In particular, Murari Soundararajan will join in February to boost the Overhauser DNP program; he will be supported by an NSF grant to Sungsool Wi (NMR facility) and EMR Director Steve Hill. In addition, Krishnendu Kundu will join the EMR program in early March to drive development of the HiPER spectrometer. Initial plans involve integration of the recently acquired Arbitrary Waveform Generator and development of an associated user software interface. He will also work on the development of a resonator for pulsed DNP applications at W-band. Two other postdocs are expected to join the EMR program during 2019, supported on external grants. Finally, we anticipate performing the first tests of the new 950 GHz source and mixer-detector in the Series Connected Hybrid Magnet (SCH) toward the end of the year.

### Outreach to Generate New Proposals—Progress on STEM and Building User Community

The total number of proposals that received magnet time during 2018 was 65, of which 20 were from first time users, meaning that 31 percent of our users were new to the program. Meanwhile, the EMR program assisted 160 individual researchers in 2018, of which over a quarter of those reporting were female (26 percent), and 9 percent minority. In an effort to attract new users, the EMR group continues to provide up to \$500 in financial support to first time visitors to the Lab (\$1,000 for overseas users). The EMR group also continues to maintain tremendous diversity among its own students and staff: 48 percent are female and 12 percent minority.

Members of the EMR group continue to make aggressive efforts to advertise the facility at regional, national and international workshops and conferences, as well as via seminars at universities around the globe (the EMR Director gave 18 such presentations in 2018). These efforts included attending and presenting at conferences outside of their own immediate research areas. In 2018, the EMR Director served as Program Chair for the American Physical Society's Topical Group on Magnetism and its Applications (GMAG) at the Annual March Meeting in Los Angeles. This involved placing ~1,000 abstracts, or 10 percent of the total March meeting program. The EMR group also organized or participated in Focused Sessions/Symposia at other major conferences, including the International Conference on Coordination Chemistry (ICCC) in Sendai, Japan (July 2018), where a two-day symposium entitled "Modern EPR: A Powerful Tool for Studies of Metal Complexes" featured many prominent NHMFL users. In addition, the EMR group provided financial support in the form of student travel grants for the two main EPR conferences in the U.S.—the Southeastern Magnetic Resonance Conference and the Rocky Mountain Conference on Magnetic Resonance—as well as the Gordon Research Conference on Conductivity and Magnetism in Molecular Materials. Finally, the EMR group has participated in several outreach activities, including the mentorship of undergraduate students and local high-school interns.

### Facility Operations Schedule

The most heavily used instrument in the program continues to be the 17T homodyne transmission spectrometer. This instrument has reached a point where it is significantly over-subscribed; it continues to be booked many months out, with users running seven days per week, 24 hours per day. The spectrometer was available for most of 2018; roughly five weeks of operations were lost due to the lab-wide shutdowns in October (Hurricane Michael) and December (Lab Maintenance). The usage (including tests/calibration) during 2018 was 255 days, implying that it was in use on every single weekday, as well as on ~25 weekend days and/or holidays. Of the 255 days of usage, only 41 days (16 percent) were allocated to NHMFL-affiliated and/or local users.

The 12T heterodyne/pulsed instrument had the same availability as the homodyne instrument, with time again lost during the lab shutdowns. This spectrometer is not straightforward to operate, requiring constant oversight by the EMR staff member (van Tol) responsible for the instrument. Consequently, users are not usually scheduled when this staff member is traveling. In 2018, 183 days of usage were reported constituting ~80 percent of the available working days (not including weekends and holidays). This usage is actually up from 2017, despite the disruptions due to the lab shutdowns. Of the 183 days of usage, 64 days (35 percent) were allocated to NHMFL-affiliated and/or local users.



The Bruker E680 spectrometer was also over-subscribed in 2018, with total usage of 288 days, which is exactly the same as in 2017 (in spite of the lab shutdowns). The instrument is shared between the FSU Biology Department and the EMR user program. Only 30 percent of the machine time was originally designated for the MagLab user program. In 2018, due to high demand from users, it was available to users 288 days, which constitutes 88 percent of the time (including holidays and weekends) that was not lost to the lab shutdowns. Of these 288 days, only 76 (26 percent) were allocated to NHMFL-affiliated users.

A total of 258 days were logged on the new high-power pulsed EPR spectrometer, HiPER, again representing an increase over its usage in 2017. It was thus operational essentially every single week day, as well as on ~28 weekend days and/or holidays. The number of days allocated to external users increased over the prior year (176 versus 150 in 2017). Of the 258 days of usage, 82 days (32 percent) were allocated to NHMFL-affiliated and/or local users.

The Mössbauer instrument was no longer available as a user facility during 2018, and we do not anticipate it being available to users in the foreseeable future. This is due to the departure of the EMR postdoc, Sebastian Stoian (now on the faculty at the University of Idaho), who single-handedly ran the facility for the past several years. It should be noted that this capability was originally funded via a UCGP and staffed by the Lab-funded Crow Postdoctoral Fellow. There are currently no plans to staff the facility going forward.

### HBT FACILITY

The High B/T facility provides users with access to unique combinations of high magnetic fields (up to 16T) and ultra-low temperatures down to 1mK for long durations (~weeks) using nuclear demagnetization refrigerators that have extended thermal links to the high magnetic field region. Studies at lower temperatures ~ 0.4mK for short times are possible, depending on the nature of the sample and proposed measurements. (Users should consult with staff on the best approaches to use.) Proposals for magnet time may be submitted at any time. A suite of specialized low temperature experimental cells is available for users for high sensitivity studies of magnetic or electric susceptibilities, nuclear magnetic resonance, transport, ultrasound and thermal properties of modern material. Each magnet station is located in an ultra-quiet environment designed for high-sensitivity studies.

Users work with NHMFL staff in selecting and designing the experimental cells and mounting the sample. Because the experiments can take a long time at ultra-low temperatures most users have the NHMFL staff record the measurements and direct changes in the field and temperatures from long distance.

### Unique Aspects of Instrumentation Capability *Multi-component demountable cells for magnetic and electric susceptibility measurements at ultra-low temperatures.*

A. Demountable and inter-changeable cells are available for measuring ac magnetic susceptibilities and dielectric constants down to sub-mK temperatures. The samples are immersed in liquid  $^3\text{He}$  to ensure thermal contact to a silver post that is an integral part of a nuclear refrigerator. Sintered silver heat exchangers (made from 50 $\mu\text{m}$  Ag powder) are also used to thermalize all electric leads entering and leaving the cells (**Fig.2.b.9.a, b**).

B. Experimental cells that allow tilting of the sample with respect to the applied magnetic field are available. This is accomplished (**Fig.2.b.10**) by using liquid  $^3\text{He}$  to pressurize a bellows that drives a

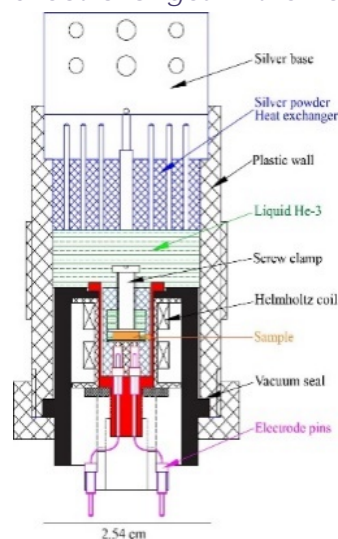


**Figure 2.b.9.a:** Dielectric susceptibility cell used for measuring the magneto-electric effects in a doped organic quantum magnet. [J. S. Xia et al., *J. Low Temp. Phys.* 187,627 (2017).]

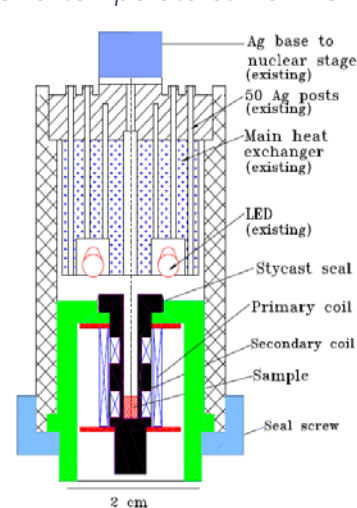


**Figure 2.b.9.b:** Magnetic susceptibility cell used for measuring phase changes to a Bose glass state at high magnetic fields and very low temperatures. [R. Yu et al., *Nature* 489, 379-384 (2012).]

platform mounted on jeweled bearings. Tilting angles of  $-10^{\circ}$  to  $90^{\circ}$  can be achieved. The device has been used to study exotic quantum Hall numbers in 2DES.

**High sensitivity NMR for studies at very low temperatures**—Two dedicated user-friendly spectrometers are available for low temperature NMR and NQR studies. They have been used for measurements of the nuclear spin relaxation dynamics of very dilute systems where the signal/noise is very low. Samples are placed in thermal contact with a silver post that is an integral part of a nuclear refrigerator and the NMR sample coil is matched in situ at low temperatures to a 50-ohm low-loss superconducting transmission line that feeds one arm of a wide-band hybrid tee at room temperature. In suitable cases, such as low-temperature bridge circuits, low-power RF amplifiers can be deployed at the sample site (using pHEMPT transistors) to create very low noise temperatures. The spectrometer is designed to reach 1,000 MHz (Fig. 2.b.11).

**Other specialized instrumentation**—A compact scalable user-friendly  $^3\text{He}$  purifier has been designed and assembled around a simple charcoal absorption column that is inserted in a regular liquid helium dewar

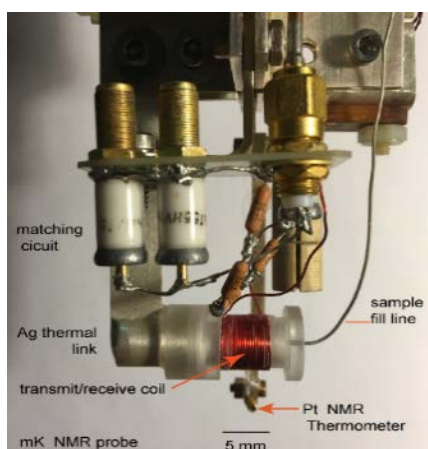


**Figure 2.b.11:** Single coil NMR probe mounted on silver post forms a nuclear demagnetization refrigerator. The capacitors are used to match the coil to transmission line that is connected to one arm of a broadband hybrid



**Figure 2.b.12:** New helium exhaust ducts installed above the three "bays" (magnet stations).

to adsorb the helium from an original contaminated sample. The temperature of the absorption column is controlled by the position in the dewar. By changing the temperature of desorption,  $^3\text{He}$  gas can be distilled preferentially leaving  $^4\text{He}$  or  $\text{H}_2$  gas impurities on the adsorber to be removed at a later stage. This separator is used to purify  $^3\text{He}$  to a few ppm which is needed with the wide use of liquid  $^3\text{He}$  as a thermalizing agent in ultra-low temperature systems and for large volume use in high circulation dilution refrigerators. The system was developed by undergraduate students supervised by Yoonseok Lee.

### Facility Developments and Enhancements

A new helium exhaust system (Fig. 2.b.12) has been installed above the magnet stations (Bays 1, 2 and 3) to automatically evacuate helium gas in event of a quench of one or more of the super-conducting magnets. The new exhaust system is normally shut off, and will start only upon detection of oxygen deficiency by sensors in each bay. After activation unconditioned makeup air is brought in through a new rooftop intake vent equipped with a normally closed gravity damper.

### Major Research Activities and Discoveries

**Pinning and melting of a quantum Wigner crystal**, T. Knighton, Z. Wu, J. Huang (Wayne State Univ.), K.W. Baldwin, K.W. West (Princeton Univ.), A. Serafin, J.-S. Xia (NHMFL High B/T)—Users performed measurements of a two-dimensional electron system in a perpendicular magnetic field at low temperatures. The sample was a low carrier density  $n = 4 \times 10^{-10} \text{ cm}^{-2}$  high mobility ( $3.0 \times 10^6 \text{ cm}^2/\text{Vs}$ ) s GaAs quantum well immersed in liquid  $^3\text{He}$ . A striking threshold behavior for the conductivity was observed for  $T \lesssim 35 \text{ mK}$ . The hole carriers are pinned within a narrow range of  $\pm 5 \text{ pA}$  (resistance  $> 1 \text{ G}\Omega$ ). The temperature dependence is non-activated and piecewise and interpreted as a two-stage first-order transition upon heating (Fig. 2.b.13).

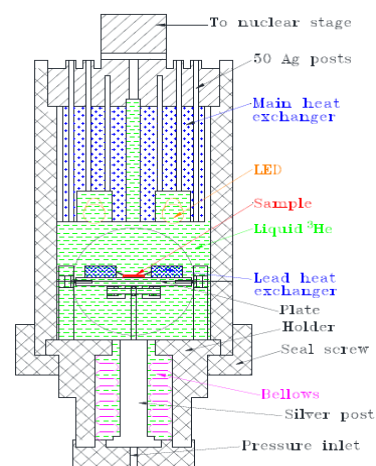


**Figure 2.b.10:** Ultra-low temperature tiltor using a bellows that to tilt a sample relative to an applied magnetic field. This cell has been used for transport studies of a GaAs-p quantum well. (Zhang et al., Phys. Rev. B85, 241302(2012).



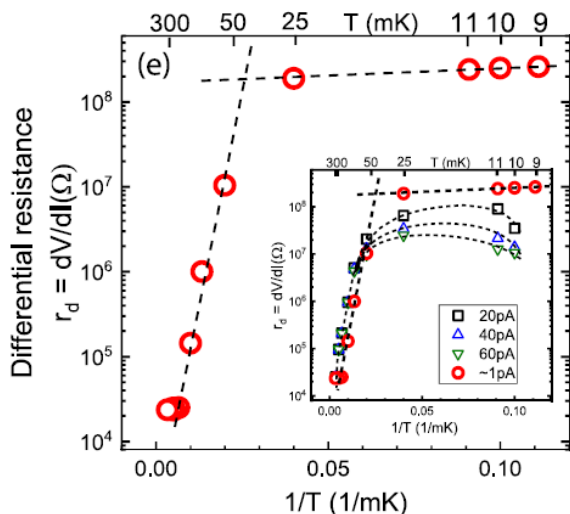


**Figure 2.b.13:** Temperature dependence of resistivity  $r_d(T) = dV/dI|_{V \rightarrow 0}$  for high mobility GaAs @DES. The inset: shows a comparison for higher current drives. T. Knighton et al., *Phys. Rev. B* 97, 085135 (2018).

temperature and pressure. The design will be based on the successful 32T magnet in the NHMFL DC facility. This new facility would use the UF Physics High bay space that could accommodate up to three HTS magnet systems that would also include a magnet dedicated to AMRIS.

#### High B/T Outreach. Progress on STEM and Building User Community

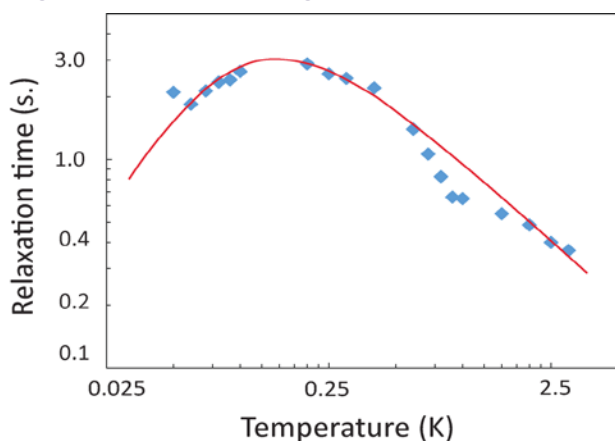


**Figure 2.b.14:** Temperature dependence of the nuclear spin-lattice relaxation time  $T_1$ , of  $^3\text{He}$  in MCM-41, showing the expected peak at  $T=2T_F$ . The red line is the predicted temperature dependence for a Fermi temperature of 95 mK. J. Adams et al., *J. Low Temp. Phys.* (in press).

college high school students and teachers; participated in four Family Science Nights at local middle and elementary schools, reaching approximately 1,300 students; presented at three career fairs, reaching 475 middle and high school students; judged posters at the Florida Regional Junior Science, Engineering, and Humanities Symposium; and judged middle school science fairs as well as the Alachua County Science Fair.

**Quantum fluids in one dimension: Luttinger liquid behavior  $^3\text{He}$  in MCM-41**, D. Candela (Univ. Massachusetts), J. Adams, M. Lewkowicz, C. Huan, N. Masuhara (NHMFL High B/T)—High sensitivity NMR studies were used to probe the dynamics of  $^3\text{He}$  constrained to move in the 1D hexagonal channels of tinc of MCM-41. The walls of the MCM-41 were plated with  $^4\text{He}$  atoms to reduce the wall interactions and to reduce the diameter of the channels to better approach 1D conditions. The volume of  $^3\text{He}$  added was chosen to result in a line density appropriate for  $T_F$  in the 100–200 mK range. The temperature dependence follows the theoretical predictions with  $T_1 \propto T$  at low temperatures and  $T_1 \propto T^{-1/2}$  at high temperatures (Fig. 2.b.14).

#### Facility Plans and Directions

We have proposed to the NHMFL Management and to the University of Florida the development of a special High Temperature Superconducting (HTS) magnet facility that will include a 32T HTS magnet and a refrigeration system for advanced high sensitivity studies of quantum matter at the extremes of field,

In June of 2018, Kelly Deuerling replaced Elizabeth Webb as the NHMFL coordinator at the University of Florida. Deuerling and Webb, along with graduate students and postdoctoral fellows, visited 106 classrooms in 18 schools, reaching 2,100 students as part of the NHMFL classroom outreach program in Gainesville. An additional 12 presentations reaching 20 students were made at Fort Clarke Middle School in the afterschool science program initiated by Webb and continued by Deuerling.

This year, Webb co-organized the Women in Science and Engineering (WiSE) Girls spring break camp with AMRIS employee Malathy Elumalai. This weeklong camp brought middle school girls from Alachua County to the University of Florida to learn about a variety of different sciences and included a tour of and magnet demonstration at the High B/T Facility (Fig.2.b.15).

Engaging with teachers and school groups is an annual practice at High B/T, and this year, facility leadership and staff lead three tours, reaching 40

### Facility Operations Schedule

The majority of the experiments conducted at the High B/T Facility need a dedicated study of the experimental cell in order to be certain that the sample can reach ultra-low temperatures in the course of the measurements being proposed by users. This study is necessary because of the high Kapitza thermal resistance at ultra-low temperatures. Users work closely with High B/T staff in the design, construction and testing of the cells. The experiments can take one to nine months to complete and for this reason the facility operated 24/7 for 290 days in 2018. Normal shutdowns are planned to occur whenever possible at the same time as major scientific meetings in the fields, notably for the March APS meetings and the International Low Temperature Physics Conferences.

### Performance Goals—Present and Future

The current waiting time for users who have approved proposals for magnet time is about nine months. This could be reduced by opening another nuclear demagnetization refrigerator (0.1mK, 8T) for user operations. The timing for this improvement is dependent on available funding as it requires obtaining additional staff and new equipment funding.

### ICR FACILITY

During 2018, the Fourier Transform Ion Cyclotron Resonance (ICR) Mass Spectrometry program continued instrument and technique development as well as pursuing novel applications of FT-ICR mass spectrometry. These methods are made available to external users through the NSF National High-Field FT-ICR Mass Spectrometry Facility. The facility features seven staff scientists who support instrumentation, software, biological, petrochemical and environmental applications, as well as a machinist, technician and several rotating postdocs who are available to collaborate and/or assist with projects.

### Unique Aspects of Instrumentation Capability

The Ion Cyclotron Resonance facility provides operations for sample analysis that requires the ultrahigh resolution ( $m/\Delta m_{50\%} > 1,000,000$  at  $m/z$  500, where  $\Delta m_{50\%}$  is the full mass spectral peak width at half-maximum peak height) and sub-ppm mass accuracy only achievable by FT-ICR MS coupled to high magnetic fields. The facility's four FT-ICR mass spectrometers feature high magnetic fields < 21 tesla and are compatible with multiple ionization and fragmentation techniques (Tab.2.b.3).

**Table 2.b.3:** ICR Systems at the Magnet Lab in Tallahassee

Field (T), Bore (mm)	Homogeneity	Ionization Techniques
21, 123	< 1ppm	ESI, AP/LIAD-CI, APCI, DART, MALDI
14.5, 104	1 ppm	ESI, AP/LIAD-CI, APCI, DART
9.4, 220	1 ppm	ESI, AP/LIAD-CI, APCI, APPI FT-ICR, DART, DAPPI
9.4, 155	1 ppm	FD, LD FT-ICR

### Facility Developments and Enhancements

In 2015, the ICR facility revealed the design and initial performance of the **first actively shielded 21 tesla Fourier transform ion cyclotron resonance mass spectrometer**. The 21 tesla magnet is the highest field superconducting magnet ever used for FT-ICR and features high spatial homogeneity, high temporal stability and negligible liquid helium consumption (J. Am. Soc. Mass Spectrom., 26, 1626-1632 (2015)).

Mass resolving power of 150,000 ( $m/\Delta m_{50\%}$ ) is achieved for bovine serum albumin (66 kDa) for a 0.38 second detection period (see Fig.2.b.16), and greater than 2,000,000 resolving power is achieved for a 12-second detection period.

Externally calibrated broadband mass measurement accuracy is typically less than 150 ppb rms, with resolving power greater than 300,000 at  $m/z$  400 for a 0.76 second detection period. Combined analysis of electron transfer and collisional dissociation spectra results in 68 percent sequence coverage for carbonic anhydrase. The instrument is part of the NSF High-Field FT-ICR User Facility and is available free of charge to qualified users (Fig.2.b.17).



**Figure 2.b.15:** Dr. Huan and Dr. Sullivan give a tour of the UF NHMFL High B/T Facility to students from the Student Science Training Program.

The instrument includes a commercial dual linear quadrupole trap front end that features high sensitivity, precise control of trapped ion number and collisional and electron transfer dissociation. A third linear quadrupole trap offers high ion capacity and ejection efficiency, and rf quadrupole ion injection optics deliver ions to a novel dynamically harmonized ICR cell.

FT-ICR mass spectrometry has become the method of choice for detailed chemical characterization of natural complex mixtures. The high mass-resolving power, mass accuracy and dynamic range of FT-ICR enable resolution and confident elemental formula assignment for tens of thousands of unique components in complex organic mixtures. Here, we present complex mixture characterization on the newly developed NHMFL 21T FT-ICR mass spectrometer.

An **actively shielded 14.5T**, 104 mm bore system offers the highest mass measurement accuracy (<300 parts-per-billion rms error) and highest combination of scan rate and mass resolving power available in the world. The spectrometer features electrospray; atmospheric pressure photoionization (APPI); atmospheric pressure chemical ionization sources (APCI); linear quadrupole trap for external ion storage, mass selection and collisional dissociation (CAD); and automatic gain control (AGC) for accurate and precise control of charge delivered to the ICR cell. The combination of AGC and high magnetic field make sub-ppm mass accuracy routine without the need for an internal calibrant. Mass resolving power > 200,000 at  $m/z$  400 is achieved at one scan per second, which is ideal for de novo sequencing (Int. J. Mass Spectrom., 427, 107-113 (2018)) and facilitates automated data reduction for H/D exchange experiments (Biochemistry, 57, 5672-5682 (2018)). Robotic sample handling allows unattended or remote operation. An additional pumping stage has been added to improve resolution of small molecules.

The **9.4T, passively shielded**, 220 mm bore system offers a unique combination of mass resolving power ( $m/\Delta m = 8,000,000$  at mass 9,000 Da) and dynamic range (>10,000:1), as well as high mass range, mass accuracy, dual-electrospray source for accurate internal mass calibration, efficient tandem mass

spectrometry (as high as  $MS^8$ ) and long ion storage period (J. Am. Soc. Mass Spectrom., 25, 943-949 (2014)). A redesign to the custom-built mass spectrometer coupled to the 9.4T, 200 mm bore superconducting magnet designed around custom vacuum chambers has improved ion optical alignment, minimized distance from the external ion trap to magnetic field center and facilitates high conductance for effective differential pumping. (J. Am. Soc. Mass Spectrom. 22, 1343-1351, (2011)). The length of the transfer optics is 30 percent shorter than the prior system, for reduced time-of-flight mass discrimination and increased ion transmission and trapping efficiency at the ICR cell. The ICR cell, electrical vacuum feed through and cabling have been improved to reduce the detection circuit capacitance (and improve detection sensitivity) 2-fold (Rev. Sci. Instrum., 85, 066107 (2014)). When applied to compositionally complex organic mixtures such as dissolved organic matter (Proc. Natl. Acad. Sci. USA, 115, 549-554 (2018); Water Research, 131, 52-1 (2019); Env. Sci. Technol., 50, 3391-3398 (2016); J. Geophys. Res. Biogeosci., 123, 2998-3015 (2018), biofuels (Fuel, 216, 341-348 (2018)

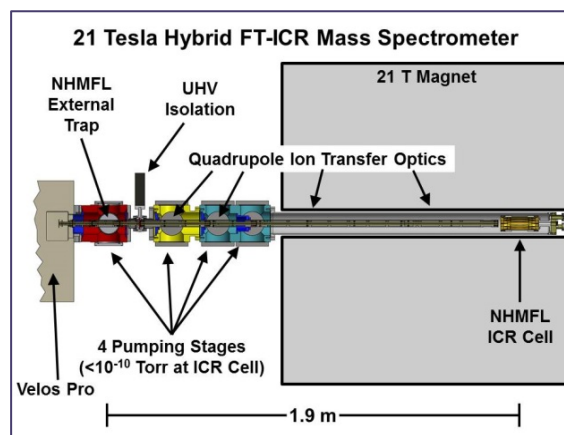


**Figure 2.b.16:** Schematic of the 21 tesla FT-ICR mass spectrometer. Approximately half of the magnet cross-section is shown. Differentially pumped vacuum chambers are shown in red, yellow and blue (the blue chamber contains two differentially pumped regions, the second of which includes the ICR cell). The scale at the bottom shows the approximate distance from the external quadrupole trap to the ICR cell.

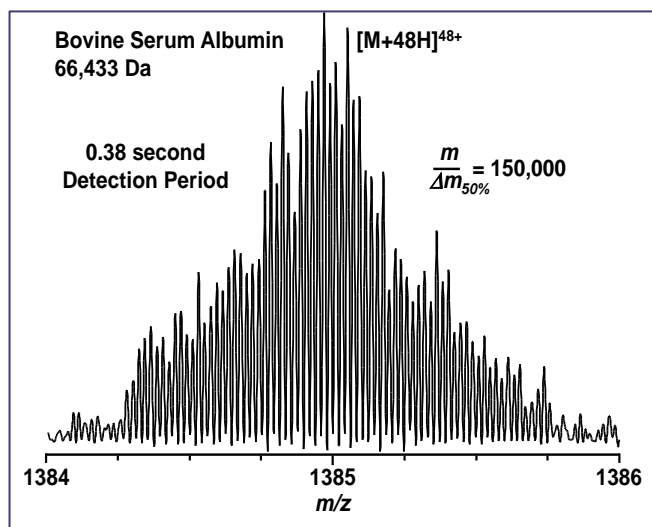


**Figure 2.b.17:** Single-scan electrospray FT-ICR mass spectrum of the isolated 48+ charge state of bovine serum albumin following a 12 s detection period. Mass resolving power is approximately 2,000,000, and the signal-to-noise ratio of the most abundant peak is greater than 500:1. The ion accumulation period was 250 ms and the ion target was 5,000,000.



and petroleum fractions (Energy Fuels, 32, 12198–12204 (2018), mass spectrometer performance improves significantly, because those mixtures are replete with mass “splits” that are readily separated and identified by FT-ICR MS (Energy Fuels, 30, 3962–3966 (2016)). The magnet is passively shielded to allow proper function of all external mass selection prior to ion injection for further increase in dynamic range and rapid (~100 ms time scale) MS/MS (Anal. Chem., 75, 3256–3262 (2003)). Available dissociation techniques include collision-induced (CID), infrared multiphoton-induced (IRMPD) (J. Am. Soc. Mass Spectrom., 23, 644–654 (2012)) and electron capture-induced (ECD) (J. Phys. Chem. A., 117, 1189–1196 (2013)).

The **9.4T actively shielded** FT-ICR instrument is available for analysis of complex nonpolar mixtures and instrumentation development. The 9.4T magnet is currently used for elemental cluster analysis and reported the formation of the smallest fullerene by stabilization through cage encapsulation of a metal by use of a pulsed laser vaporization cluster source (Molecular Physics, 113, 15–16 (2015)). The functionalization of endohedral metallofullerenes by halogenation has not been previously reported and remains a challenging endeavor in carbon nanoscience. In this work, we show that halogenation of endohedral metallofullerenes is predicted to be feasible based on thermodynamic grounds by means of DFT computations, combined within in situ experimental investigations. (Carbon., 129, 750–757 (2018)).

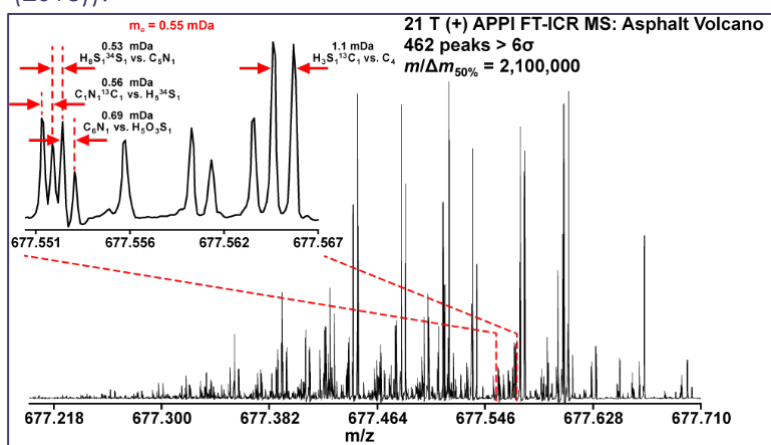


**Figure 2.b.18:** Mass scale expanded segment of 21T (+) APPI FT-ICR mass spectrum of an asphalt volcano sample after ion trap isolation. Inset illustrates the need for ultrahigh mass-resolving power to resolve ions with a mass difference on the order of the mass of an electron ( $m_e = 0.55$  mDa).

and identified in a single spectrum of any kind and represents the highest broadband resolving power for any petroleum mass spectrum and emphasizes the need for ultrahigh resolving power achievable only by 21T FT-ICR MS sufficient to separate isobaric overlaps prevalent in complex seep samples (Fig.2.b.18, Anal. Chem., 90, 2041–2047 (2018)).

The detailed characterization of large protein assemblies in solution remains challenging to impossible. Nonetheless, these large complexes are common and often of exceptional importance. **Hydrogen/Deuterium exchange (HDX)** experiments reveal changes in deuteration over time to examine protein-protein contacts. Proteins are diluted into a  $D_2O$  solution to induce the exchange of hydrogen atoms with deuterium. The degree of protection from deuterium exchange is indicative of local structure as well as dynamics. (Fig.2.b.19).

Human glucokinase (GCK) acts as the body’s primary glucose sensor and plays a critical role in glucose homeostatic maintenance. We report the results of comparative hydrogen–deuterium exchange mass spectrometry (HDX-MS) of wild-type GCK and representative activated variants. HDX-MS was conducted on the 21T FT-ICR MS (Biochemistry, 57, 1632–1639, (2018)).

The, 9.4T and 14.5T instruments are primed for immediate impact in **environmental and petrochemical analysis**, where previously intractably complex mixtures are common. The field of “petroleomics” has been developed largely due to the unique ability of high-field FT-ICR mass spectrometry to resolve and identify all of the components in petroleum samples.

**Major Research Activities and Discoveries**  
**Complex mixture analysis** by FT-ICR MS at 21T can The high mass-resolving power, mass accuracy and dynamic range of FT-ICR enable resolution and confident elemental formula assignment for tens of thousands of unique components in complex organic mixtures. Here, we present complex mixture characterization on the newly developed NHMFL 21T FT-ICR mass spectrometer. Combined with absorption-mode data processing, mass resolving power increases as much as a factor of two higher than conventional magnitude-mode display, an improvement otherwise requiring a more expensive increase in magnetic field strength. To the best of our knowledge, this mass spectrum represents the most peaks resolved and

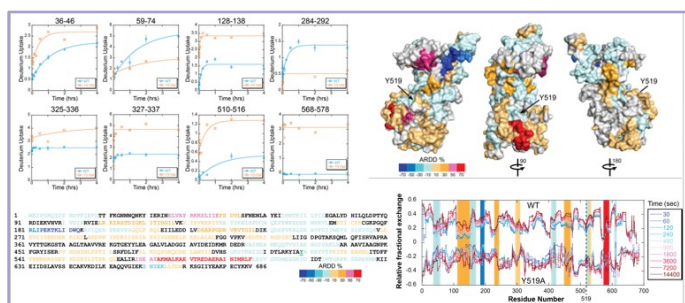


**Figure 2.b.19:** HDX uptake profiles for WT SsoMCM and Y519A. (A) Deuterium incorporation during the H/D exchange period for representative peptides, showing differences between the two conditions. Average relative deuterium uptake difference (ARDD) percent difference color coding for (B) the primary sequence of SsoMCM (Y519 is underlined and colored green) and (C) peptide regions with significant ARDD percent differences (Y519A minus WT) color-mapped onto the surface of the SsoMCM monomer. (D) HDX butterfly plots for WT SsoMCM (positive values) vs Y519A (negative values) showing relative fractional exchange as a function of amino acid residue number. Lines are color-coded from shades of blue to red from the 30 to 14,400 s deuterium exchange period. Y519A is indicated by a dashed line. Shaded regions correspond to significant changes in relative fractional change kinetics correlated with ARDD colors.

comprised of primarily  $N_xO_y$  species. After hydrotreatment, FT-ICR mass spectra of all three biocrudes revealed a significant reduction in mass spectral complexity (observed as the loss of Ox, Nx and  $N_xO_y$  species) and the formation of hydrocarbon compounds, as expected (Energy Fuels, 32, 8483–8493 (2018)).

**Dissolved Organic Matter (DOM)** consists of soluble organic materials derived from the partial decomposition of organic materials (Env. Sci. Technol., 52, 5, 2538–2548 (2018); Env. Sci. Technol., 52, 16, 9380–9390 (2018); J. Geophys. Res. Biogeosci., 123, 5, 1475–1485 (2018); Biogeosciences, 15, 6637–6648 (2018)). Marine dissolved organic matter (DOM) contains one of the largest active organic carbon pools

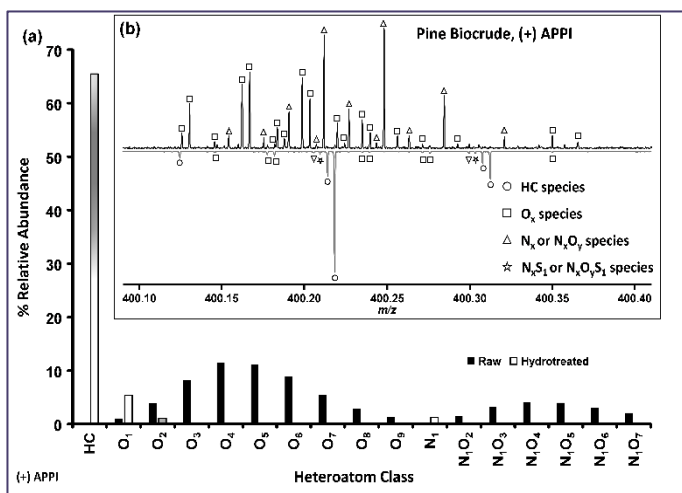


**Figure 2.b.20:** a) Heteroatom class distributions derived from the (+) APPI mass spectra of the raw (gray) and hydrotreated (blue) biocrude from pine feedstock. b) Zoom inset at  $m/z$  400 within the raw (gray, top) and hydrotreated (blue, bottom) pine biocrude mass spectra.

on Earth. A key step in the marine carbon cycle occurs when bacteria transport carbon from the oceanic pool and transform it chemically. This is a challenging link to understand, however, because of the thousands of compounds that make up the DOM pool, each with different biological turnover rates. **Figure 2.b.21** Elemental composition of compounds in the initial DOM (T0) and those changed in relative abundance (depleted or enriched) after a 24 h incubation experiments. Values shown are the fraction of the molecular formulae in each category (T0, enriched or depleted) that contained only CHO, CHON, CHOS or CHONS. The sum of each category equals 100 percent.  $n = 3$  (Env. Microbiol., 20, 3012–3030 (2018)).

Fourier transform ion cyclotron resonance mass spectrometry (FT-ICR MS) is utilized for direct comparison of the chemical composition of **hydrothermal liquefaction biocrudes** from of 100 percent pine, 100 percent algae, 75 : 25 pine:algae, and 50 : 50 pine:algae feedstocks. (Fuel, 216, 341–348 (2018)). **Figure 2.b.20** shows FT-ICR MS analysis of the raw biocrudes showed predominantly Ox species whereas raw microalgae and sewage sludge biocrudes are

comprised of primarily  $N_xO_y$  species. After hydrotreatment, FT-ICR mass spectra of all three biocrudes revealed a significant reduction in mass spectral complexity (observed as the loss of Ox, Nx and  $N_xO_y$  species) and the formation of hydrocarbon compounds, as expected (Energy Fuels, 32, 8483–8493 (2018)).

Of the estimated 5 million barrels of crude oil released into the Gulf of Mexico from the Deepwater Horizon oil spill, a fraction washed ashore onto sandy beaches from Louisiana to the Florida



panhandle. Targeted petroleomics characterized petrogenic material isolated from the Pensacola Beach sand displays greater than two-fold higher molecular complexity than the MWO constituents, most notably in oxygenated species absent in the parent crude oil. Surprisingly, the diverse oxygenated hydrocarbons in the Pensacola Beach sediment extracts were dominant in all ionization modes investigated, ( $\pm$ ) ESI. Thus, the molecular-level information highlighted oxygenated species for subsequent “targeted” analyses (Energy Fuels, 32, 2901–2907 (2018)).

**Geochemistry.** Porphyrins are the molecular fossils of chlorophylls. Our recent discovery of porphyrins from 1.1 billion-year-old marine black shales of the Taoudeni Basin in Mauritania pushes back the geological record for photosynthesis by 600 million years (Proc. Natl. Acad. Sci. USA, 115, 1–9, (2018)). These porphyrins are nitrogen-containing molecules preserved from bacteriochlorophylls and quantitation of their nitrogen isotopic composition provides quantitative information about the type of organisms in past ecosystems that utilized sunlight energy to synthesize organic compounds for nutrition. Fourier Transform Ion Cyclotron Resonance (FT-ICR) mass spectrometry resolved and identified porphyrins from the tens of thousands of other organic compounds in each shale. Indeed, FT-ICR MS was able to identify the elemental composition and structure for nickel and vanadyl porphyrins in this highly preserved shale.

**Endohedral metallofullerenes**, which are metal-encapsulated nanoscale carbon cages, are of particular interest because of their unique properties that offer promise in biomedicine and photovoltaics. An understanding of chemical formation mechanisms is essential to achieve effective yields and targeted products. One of the most challenging endeavors is synthesis of molecular nanocarbon. Nevertheless, the mechanism of formation from metal-doped graphite has largely eluded experimental study, because harsh synthetic methods are required to obtain them (Nat. Commun. 5:5844, 1–8 (2014)). **Figure 2.b.22** (right) shows molecular cage behavior and reactivity of PR@C<sub>82</sub> (I) under synthetic conditions that generate EMFs, namely at high temperature, in the presence of carbon evaporated from graphite and at a low-pressure of He (Carbon, 129, 750–757 (2018)).

### Facility Plans and Directions

The ICR facility will continue to expand its user facility to include user access to the world's first 21 tesla FT-ICR mass spectrometer.

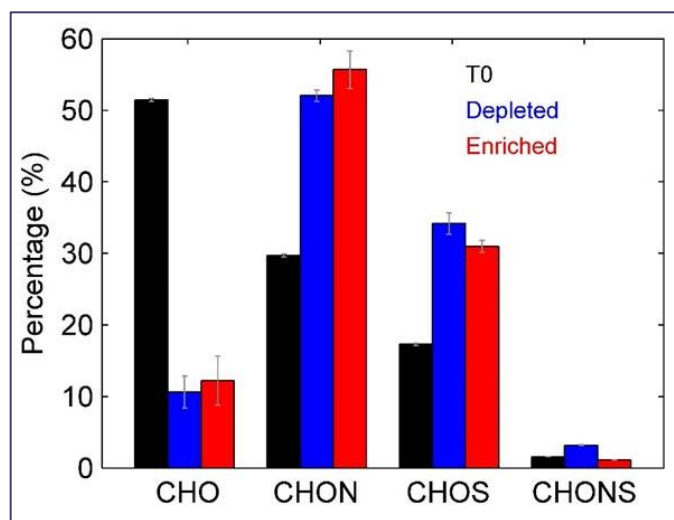


**Figure 2.b.21:** Percentage of assigned molecular formulae determined by FT-ICR MS analysis for the different organic soil horizons before and after incubation.

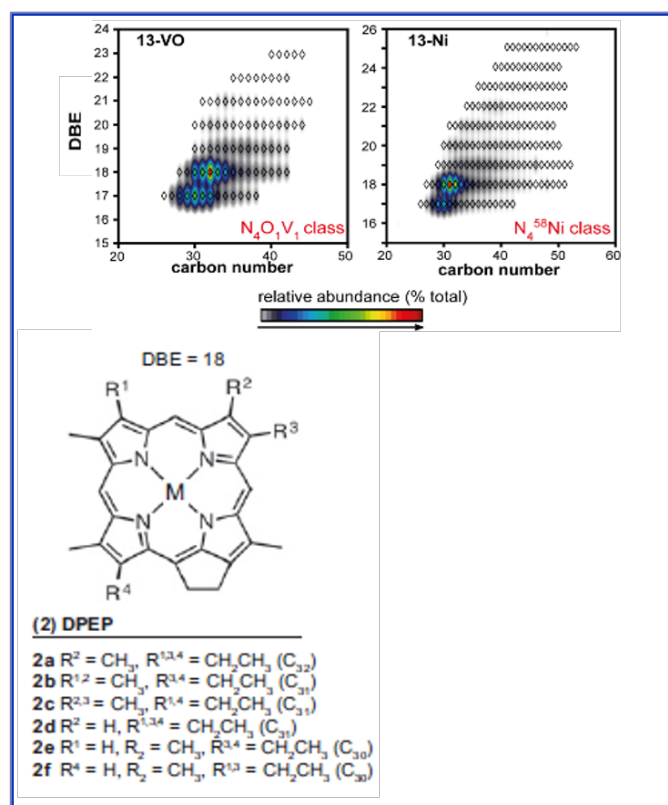


**Figure 2.b.22: Top:** Identification of two classes of Ni- and VO-porphyrins by FT-ICR MS, plotting relative abundance versus double-bond equivalents (DBEs) and carbon number. **Left:** The structure of C<sub>30</sub> to C<sub>32</sub> DPEP, one of the many porphyrin structures identified supports phototrophs as dominant photosynthesizing organisms on Earth 1.1 billion years ago. Identified porphyrins likely derived from oxygenic phototrophs and anoxygenic phototrophic bacteria.

### **Outreach to Generate New Proposals—Progress on STEM and Building User Community**

The ICR program had 28 new principal investigators in 2018. The ICR program also enhanced its undergraduate research and outreach program for six undergraduate scientists. The ICR program in 2018 supported the attendance of research faculty; postdoctoral associates; and graduate, undergraduate and high school students at numerous national conferences to present current results.

### **Facility Operations Schedule**

The ICR facility operates year-round, with weekend instrument scheduled. Two shifts (eight hours each) are scheduled for each instrument year-round, including holiday shut-downs, which are utilized for routine instrument maintenance.

### **The Future Fuel Institute**

The Future Fuels Institute completed its sixth full year in 2018, with two full share members (\$250K each/year for four years) to support research to address challenges associated with petroleum production, processing and upgrading. The Future Fuels Institute currently supports one fulltime technician and 2.5 fulltime research faculty to pursue analytical method development. For 2015/2016 the corporate members were: Reliance and Total. Additionally, the FFI partners with two instrument manufacturers (Leco Instruments, Waters Instrument Company) for state-of-the-art instrumentation prior to commercial release.

### **NMR FACILITY**

*The NMR and MRI User Program in Tallahassee is a partner with the AMRIS facility of the NHMFL at the Univ. of Florida Gainesville. The Tallahassee facility offers scientists access to high magnetic fields with the world's highest sensitivity NMR and MRI probe technology. Our flagship 900 MHz ultra-wide bore spectrometer is the world's highest field instrument for in vivo imaging and spectroscopy and also offers leading capabilities in materials and biological solid state NMR. Lower field instruments offer users additional unique capabilities in solution, solid state NMR and imaging. In the past year our 600 MHz DNP instrument has become fully operational for bio-solids research and for materials research. Coupled with this solids instrument is our Overhauser solution DNP, which generated our first successful solution spectra this past year. Much of our technology efforts continue to be focused on the development of innovative probes for triple resonance solid state spectroscopy, high field in vivo imaging and spectroscopy, as well as very high mass sensitivity solution NMR probes. This past year was the first year of successful Series Connected Hybrid user operations at 35.2T for both bio and materials solid state NMR spectroscopy. The transition from superconducting NMR spectroscopy to NMR on a power magnet has been very challenging, but the spectra of quadrupolar nuclei for both of these scientific arenas have been spectacular at a field strength that is and continues to be 50 percent higher than any commercial instruments. Maybe the most surprising results have come from  $^{17}\text{O}$  spectroscopy of the interactions between water and a transmembrane peptide channel. The interactions are characterized and found to be orders of magnitude longer lasting than previously thought.*

### **Unique Aspects of Instrumentation Capability**

Last year we reported on the first year of SCH operations (2017), a commissioning year, in which the first probes were tested, field stability and homogeneity were optimized and initial science demonstrated. This past year (2018) was the first year of SCH User operations. This was not without challenges. All of our users are accustomed to operating perfectly stable magnets, which can be run for a week or even several weeks of time (24 hours a day, seven days a week) to obtain a single multidimensional data set on a single sample. Here, we are restricted to an eight hour shift, although spectra from day to day can be summed, but it has been rare that a factor of two improvement in signal-to-noise ratio merits so the time and expense associated with a week of SCH operations, but this does not mean that we will not do this on occasion, when we believe the science merits the instrument time. While a supercon NMR instrument with power back up rarely fails more than once over the course of a year, the SCH can trip from field multiple times during the 30 hours of operation in a given week. Consequently, experiments that require more than an hour of data collection are saved every 20 minutes. The overall result has generated some very exciting data and numerous success stories from the 20 different research groups that participated in the SCH user program this past year. Indeed, where spectral resolution was enhanced dramatically major steps forward in science were made.

### Facility Developments and Enhancements

The 600 MHz solid state DNP system has been assembled around a new wide bore field swept 600 MHz magnet, a demo gyrotron and spectrometer from Bruker, and a quasi-optic table is now the DNP instrument in the country with the highest operational up-time thanks to superb scientific and engineering staff. Numerous publications are being generated from this instrument as well as a very strong user program.

Major technology enhancements were achieved late in the 2018 SCH year of operation, demonstrating significant enhancement in magnet stability. This represented the many years of effort by Prof. Jeff Schiano at Penn State working with Bill Brey and colleagues for the development of the Cascade Field Regulation (CFR) system replacing the Bruker Lock system, which itself had outperformed our resolution expectations. Now the CFR results in a further reduction of resonance linewidths by a factor of two, largely due to the field stabilization in the frequency range of 1-60 Hz where it is difficult for the Bruker lock system to be effective. The CFR represents a decade-long effort that dates back to initial experiments with the Keck magnet, long before the SCH was assembled.

The facility is looking forward to a greatly enhanced 900 MHz MRI and MRS console and gradient set that will be the first major upgrade to this system in nearly a decade. The uniqueness of the ultra-wide-bore 900 magnet makes the commercial/MagLab partnership very challenging to accomplish and yet there is a strong will on both sides due to the uniqueness of the MagLab instrumentation to make this happen. We anticipate that the instrument specifications will be agreed upon before the middle of 2019 and that the instrument will then soon be delivered.

### Major Research Activities and Discoveries

A partnership between Florida State University, University of Illinois at Chicago, Wayne State University, Pukyong National University, and the MagLab obtained  $^{17}\text{O}$  spectroscopy at 35.2T SCH illustrating unique long-lived water-protein interactions in the monovalent cation channel, gramicidin A. The ultra-high sensitivity and spectral resolution for  $^{17}\text{O}$  at this field strength made these characterizations possible.

A team of researchers from the Max Delbrück Center and the MagLab were using a cryogenic quadrature probe for  $^{19}\text{F}$  MRI illustrated dramatic  $B_0^2$  sensitivity gains. In mice the increase in sensitivity permitted the detection of inflamed regions of the brain at 21.1T (the MagLab's UWB 900) that were undetectable at 9.4T. Researchers from Washington University in St. Louis and the MagLab teamed up to study materials for  $\text{CO}_2$  capture from high concentration sources such as flue gasses with solid amine sorbents. Experiments at low temperature (100 K) were performed to uniquely demonstrate two magnetically inequivalent environments that were baseline resolved compared to room temperature where only a motionally averaged signal was observed. Penn State University researchers are working with a MagLab scientist to characterize a structure for the Nitrogen Regulator protein (NR11) in native *E. coli* membranes. This is an exciting step forward in studying membrane proteins in their native environment. To do this they labeled all amino acids except Proline and Phenylalanine with  $^{15}\text{N}$  and  $^{13}\text{C}$  and then selected for the rare  $^{15}\text{N}$ - $^{12}\text{C}$  pairs in the protein backbone—resolving single sites in native *E. coli* membranes.

A research partnership from UC Davis, Corning Inc. and the MagLab has worked on chalcogen glasses of S and Se that have important glass properties for photonics, non-volatile memories and remote sensing. The  $^{77}\text{Se}$  spectroscopy shows that the glasses consist of two topological elements: polymeric  $[\text{Se}_y\text{S}]_n$  chains and eight-membered  $\text{Se}_y\text{S}_{8-y}$  rings. The specificity of these elements prevents a random or homogeneous mixing between the elements.

Life-threatening fungal infections affect more than 2 million people worldwide but effective antifungal medications are very limited, thus resulting in high mortality (**Fig. 2.b.23**). The fungal cell wall is a promising target for future antifungal drugs as it contains polysaccharides that are absent in humans. However, our knowledge of the fungal cell wall architecture remains ambiguous due to technical constraints of traditional experimental techniques. Experiments on the high-field magnets at the MagLab provide unprecedented NMR resolution from a variety of polysaccharides and proteins (**Figs. 2.b.23.a, b**). Magic Angle Spinning (MAS) Dynamic Nuclear Polarization (DNP) provides a 30-fold sensitivity

enhancement (Fig. 2.b.23.c), which enabled this collaboration to determine the spatial proximities between different biomacromolecules (Fig. 2.b.23.d). This information on intermolecular packing, together with site-specific information on molecular hydration and dynamics, led to a new structural model of the fungal cell wall that substantially differs from any preceding impressions of the structure of fungal cell walls.

The revised model will serve as the structural basis for designing better antifungal drugs that inhibit a broader spectrum of infectious fungi. The methods highlighted in this experiment can be widely applied to a variety of carbohydrate-rich biomaterials, such as the cell walls in plants, bacteria and algae. (X.Kang, A.Jirui, A.Muszyński, M.C.D. Widanage, A.Chen, P.Azadi, P. Wang, F. Mentink-Vigier, T. Wang, "Molecular architecture of fungal cell walls revealed by solid-state NMR", *Nature Comm* 9 (1), 2747 (2018) DOI: 10.1038/s41467-018-05199-0.)

Oxygen is one of the most important elements in chemistry, biology and material sciences due to its active role in reactions (Fig.2.b.24). The potential of  $^{17}\text{O}$  NMR for obtaining detailed structural, dynamic and functional information has yet to be fully realized, primarily due to  $^{17}\text{O}$  having a low gyromagnetic ratio ( $\gamma = -5.774 \text{ MHz T}^{-1}$ ), low natural isotopic abundance (0.037 percent) and an  $I = 5/2$  spin, which produces complex quadrupolar NMR spectra. High magnetic fields are critical to fully enable  $^{17}\text{O}$  NMR because they dramatically enhance spectral resolution and sensitivity, particularly when coupled with a reduction of the residual second-order quadrupolar broadening under magic-angle spinning (MAS).

The MagLab has recently commissioned a 36T Series-Connected-Hybrid (SCH) magnet that offers 50 percent higher magnetic fields than the highest superconducting NMR magnet available today. The magnetic field is homogeneous and stable to better than one ppm over one  $\text{cm}^3$  DSV. This field quality enables high-resolution multidimensional NMR experiments for  $^{17}\text{O}$  and, in future experiments, for other quadrupolar nuclei throughout the periodic table.

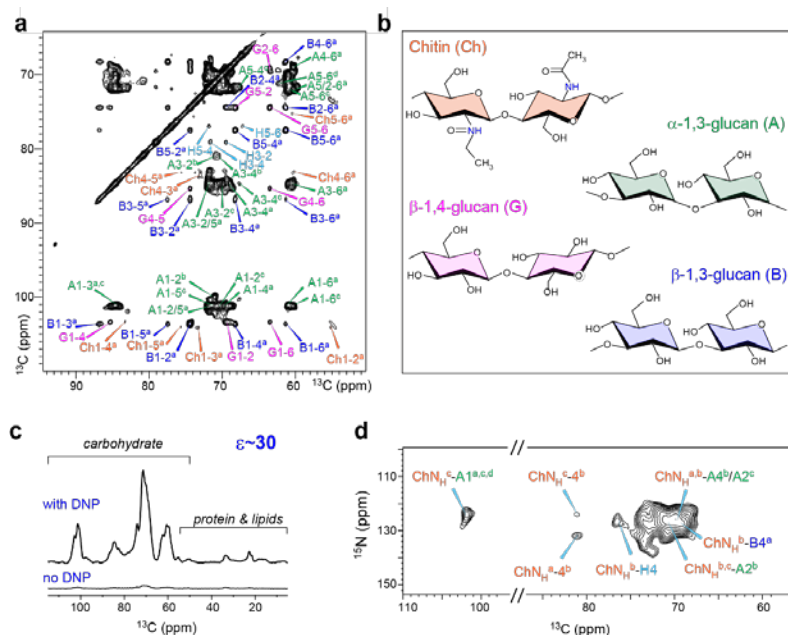


**Figure 2.b.23:** The structural determination of intact fungal cell walls. **a**, Two-dimensional  $^{13}\text{C}$ - $^{13}\text{C}$  spectra. **b**, Representative structure of glycans. **c**, Thirty-fold sensitivity enhancement by MAS-DNP. **d**, Intermolecular-only  $^{15}\text{N}$ - $^{13}\text{C}$  correlation spectrum reports many sub-nanometer contacts under the sensitivity enhancement provided by the MagLab's MAS-DNP.

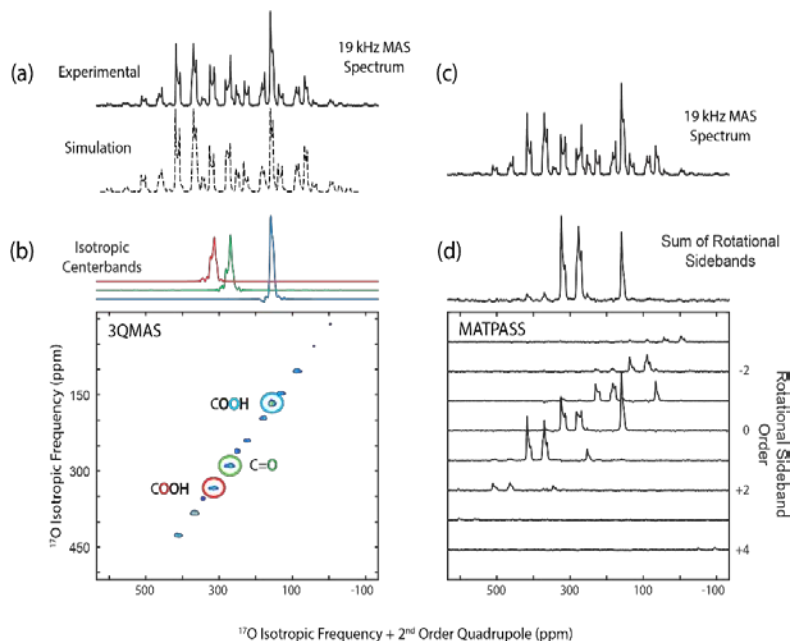


**Figure 2.b.24:** NMR from the SCH magnet: **a**) 1D  $^{17}\text{O}$  magic-angle spinning, **b**) two-dimensional 3-quantum magic-angle spinning, **c**) and **d**) magic-angle turning phase-adjusted separated sideband spectra of *N*-acetyl-L-valyl-L-leucine



Researchers from MIT partnered with MagLab scientists to record the first  $^{17}\text{O}$  NMR spectra of biological samples taken in a 35.2T magnetic field (corresponding to a 1.5GHz resonance frequency for  $^1\text{H}$ ). The results demonstrate the field qualities of the SCH magnet and advantages of the 35.2T field for  $^{17}\text{O}$  NMR. The SCH magnet is now open to researchers from around the world. (Keeler, E.G.; Michaelis, V.K.; Colvin, M.T.; Hung, I.; Gor'kov, P.L.; Cross, T.A.; Gan, Z. and Griffin, R.G.,  $^{17}\text{O}$  MAS NMR Correlation Spectroscopy at High Magnetic Fields. *J. Am. Chem. Soc.* (2017), 139, 17953–17963. ; Gan, Z.; Hung, I.; Wang, X.; Paulino, J.; Wu, G.; Litvak, I.M.; Gor'kov, P.L.; Brey, W.W.; Lendi, P.; Schiano, J.L.; Bird, M.D.; Dixon, I.R.; Toth, J.; Boebinger, G.S. and Cross, T.A., NMR spectroscopy up to 35.2 T using a series-connected hybrid magnet, *Journal of Magnetic Resonance* 284 (2017) 125–136.)

### Facility Plans and Directions

During the past four years the NMR facility in Tallahassee has received two 800 MHz mid-bore magnets from other institutions essentially for the price of de-energizing the magnets, shipping the magnets and re-energizing them. Our partner AMRIS facility has recently received three such magnets. Not only is this a great cost savings for the MagLab, but it is recognition by the community that such magnets that are no longer being supported by industry can be supported at the MagLab for the community at large. The concept of repurposing such magnets for which up-to-date commercial probes are not available has proven to be very successful.

For the past few years we have had at 500 MHz, and more recently at 800 MHz, 1.3 mm Fast Magic Angle Spinning (Fast MAS) probes that can achieve, depending on the samples, between 50 and 60 kHz revolution rates. These probes have been built at the MagLab using Bruker MAS stators. Now, JEOL has a 0.9 mm rotor and stator that can spin up to 110 kHz. The MagLab has two of these stators. The first is to be integrated into one of our 800 MHz systems, and a 1.3 mm probe will be built for the SCH. This capability is revolutionary as the spinning serves to decouple the protons in the spectral sample without having to apply high power proton decoupling. Furthermore, this means that for solid state NMR spectroscopy, which can uniquely characterize membrane proteins in a native like lipid bilayer environment,  $^1\text{H}$  detection can be used.  $^1\text{H}$  detection is vastly more sensitive than  $^{13}\text{C}$  detection and in the 1980s for solution NMR this development made the characterization of protein structures in aqueous solution – today solution NMR accounts for 20 percent of protein structures in Protein Data Bank. It is possible that a similar scientific result will occur for Fast MAS solid state NMR.

### Outreach to Generate New Proposals—Progress on STEM and Building User Community

Our primary mechanism for recruiting new users involves one-on-one contact with potential users at national and international meetings with follow up to bring those users here. All of our staff scientists go to important national and international meetings annually, and one of their tasks at these meetings is to identify new users and to follow up with them when they return to the MagLab. A greater challenge that we are beginning to work on is to recruit users who are not NMR spectroscopists, but scientists that could use NMR data for the science they do. This opens the MagLab facility to a much broader and more diverse community of biological and chemical scientists.

### Facility Operations Schedule

The NMR and MRI facility of the NHMFL is open 24/7 52 weeks of the year. The SCH is operational for NMR spectroscopy for ~25 hours/week and for ~30 weeks or a total of 750 hours – i.e., equivalent to approximately one month of continuous operation per year. The 800 MHz 63 #2 magnet did not start operation until September 3, 2018.

### PULSED FIELD FACILITY

*The National High Magnetic Field Laboratory—Pulsed Field Facility (NHMFL-PFF) is located in Los Alamos, New Mexico, at the Los Alamos National Laboratory (LANL). The NHMFL-PFF utilizes LANL and U.S. Department of Energy (DOE)-owned equipment and resources to provide world record pulsed magnetic fields to users from the scientific and engineering community worldwide. The pulsed field user program provides researchers with both the highest research magnetic fields available at the Mag Lab and a suite of robust scientific diagnostics specifically designed to operate in transient field environments. The connection with the DC Field Facility is strong and complementary in expertise, with both facilities often contributing to a given user's research. Users are encouraged to take full advantage of this through a common application process, under which experiments can be requested at both facilities under a single overarching scientific proposal. Although achieving the highest research magnetic fields possible is a fundamental competency at the NHMFL-PFF, we also pride ourselves upon*



maintaining the very best high-field research environment by providing users with support from the world's leading experts in pulsed magnet science. All of the user support scientists are active researchers and collaborate with multiple users per year. A fully multiplexed (8-output) computer controlled, 4.0 mega-Joule (32 mF @ 16 kV) capacitor bank system is at the heart of the short pulse magnet activities. Many thousands of 20-millisecond-long high magnetic field pulses up to 65 tesla are fired for the user program, which accommodates approximately 150 different users each year. Beyond the workhorse short pulse magnets, we provide users with access to the highest non-destructive magnetic fields worldwide. The hundreds of mega-Joules necessary are provided by a 1.4 GW AC generator, a truly unique pulsed power supply. The AC rectification enables control of pulsed power waveform so as to optimize performance of the associated magnet system (enabling technology for both the 100T multishot and 60T controlled waveform magnets) and sample diagnostics. Pulsed field users have access to magnetic fields exceeding 100 tesla using the semi-destructive Single Turn magnet system, which produces 6 microsecond duration magnetic field pulses to 300 tesla.

### Unique Aspects of Instrumentation Capability

Table 2.b.4 lists the pulsed magnets available to users of the NHMFL-PFF. The short pulse magnets serve the majority of users with maximum fields currently in the 65 tesla range. The 100T multi-shot magnet is the first and only magnet in the world to successfully perform a magnetic field pulse to 100 tesla in a non-destructive manner. The expertise in pulsed power engineering and access to world-class materials scientists at both LANL and FSU focus attention on development and characterization of the best materials for magnets. The PFF at LANL is also home to the 60 T Controlled Waveform (aka "Long Pulse") magnet, which has the ability to customize pulse waveforms for optimal user research. The 300 tesla single turn magnet at the PFF (development and installation was funded by LANL) provides users with access fields in excess of 100T – routine pulses are to 170 tesla with a pulse duration of 6 microseconds. In addition to optical studies, including FBG dilatometry, the platform has recently been updated with an inductive contactless method enabling thin (~micron thickness conductors) to be studied at extremes of high magnetic fields.

**Table 2.b.4:** Pulsed magnets available to users of the NHMFL-PFF

Capacitor Driven Pulsed Magnets		
Magnet, Field, Bore	Duration FWHM (ms)	Supported Research
Cell 1, 65T, 15.5 mm	20	Magneto-optics (IR through UV), magnetization (susceptibility, extraction, and torque), magneto-transport, (DC- MHz & GHz conductivity), Pulse Echo Ultrasound spectroscopy, Fiber Bragg grating dilatometry. Sample environments from 350mK to 300K, pressures up to 170 GPa, and in-situ sample rotation and are available for compatible techniques.
Cell 2, 65T, 15.5 mm	20	
Cell 3, 65T, 15.5 mm	20	
Cell 4, 65T, 15.5 mm	20	
Duplex & 100T Insert Test Cell	15	
Optics Cell, 30T, 15 mm	1	
Single Turn, 300T, 10mm	0.003	
Generator Driven Magnets		
Magnet, Field, Bore	Duration FWHM (ms)	Supported Research
100T Multi-Shot, 101T, 10 mm	15	All techniques listed above including magnetothermal studies (heat capacity and magnetocaloric measurements) FIR and THz optics and larger sample volumes in the long pulse magnets.
60T Controlled Waveform, 60T, 32 mm	100 (plateau)	

### Facility Developments and Enhancements

In 2018 the most significant facility developments have been part of a series of multiyear enhancements to the 1.4 GW motor-generator and pulsed power infrastructure. These include the following institutional investments from LANL: \$1.445million for a new drive and exciter systems to be installed in the fall of 2019, \$186 thousand to resurface the sliprings and upgrade the brushes, \$291 thousand to replace the oil check valve, \$221 thousand in engineering support and \$114 thousand in general facility upgrades. Similar scale investments are planned for 2019 and beyond. The new drive and exciter systems are being

manufactured by ABB in Switzerland, so to date this work has not interrupted the generator run cycle. However, the slipring and brush upgrade were precipitated by damage caused by the carbon brushes reaching “end-of-life” during the regular operation of 100T magnet for user in March 2018 as seen in

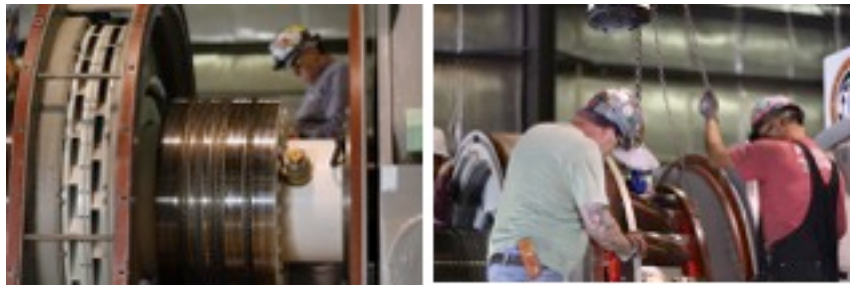


**Figure 2.b.25:** Work to resurface the generator sliprings and upgrade the carbon brush configuration to enable high current operation in the future.

**Figure 2.b.25:** The shut down for slipring maintenance was combined with an overhaul of the generator main lubrication system. This was triggered by the need to service the auxiliary oil pump and replace the associated check valve, the operation of which had become intermittent, necessitating the use of the emergency oil pump to provide the necessary lubrication to bring the generator to rest. The completion of both of these decadal overhauls by General Electric will, in part, ensure the reliability of the unique pulsed power infrastructure for the next generation of high field magnets. In December 2018, 100T operations resumed.

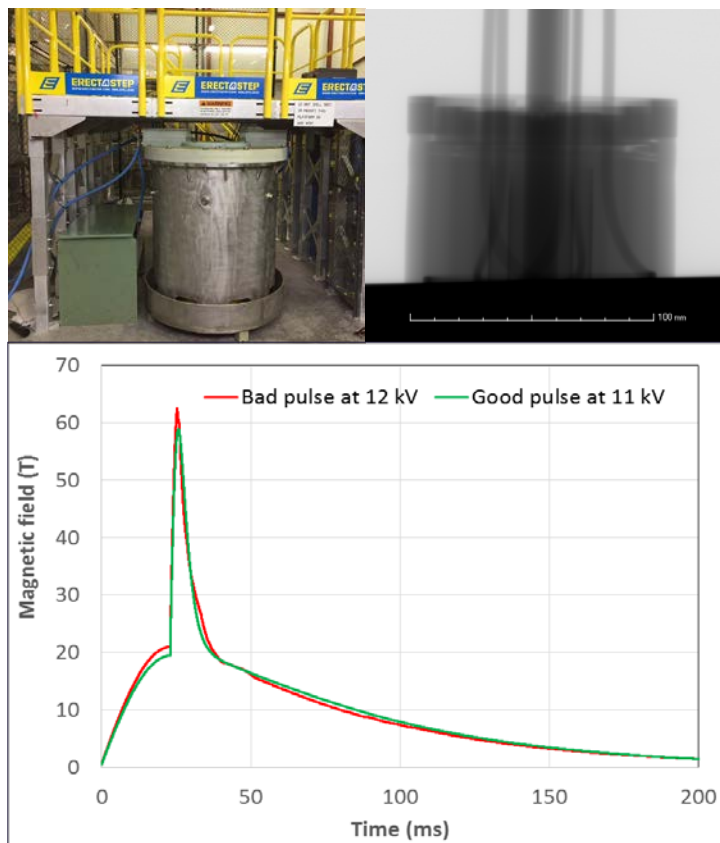


**Figure 2.b.26:** The duplex cell, Xray image indicates the delamination of the end-spool of layer 5 of the inner coil, caused by the large axial push-out force during the winding of pre-tension Zylon fiber, the measured waveform of magnetic field generated by duplex magnet for two pulses. Despite the end spool issue identified during winding, the magnet was tested to failure at 12 kV.

powers our four 65T magnet cells was upgraded in 2018 to enable duplex magnet operation. The addition of new selector switches, combined with a trigger and control system upgrade, enables one-quarter to three-quarters split of the delivered energy. Specifically, independent control of the charge and timing of each sub module allows separate powering of (nested) coils to both reduce the driving voltages and increase control over the pulse duration to maximize field intensity. Design and construction of a prototype duplex magnet with two separately powered nested coils was completed in 2017. Ultimately such a duplex magnet is designed to 80T with sufficient engineering margin to provide

2018 has also seen progress in upgrading the outsert coils of the 100T system: The inner most coils (coils 1 and 2) of the 100T outsert experience the highest stress during operation. The magnet teams at LANL and FSU have collaborated to build upgraded version of those coils with the stronger Cu-Nb conductor (~ 50 percent stronger than the glid-cop AL60 wires used in the present coils). This project has been underway since March 2018 and is expected to be completed and installed in the third quarter of 2019. The successful fabrication of these coils will allow the 100T outsert magnet to operate at a considerably more conservative margin and is part of the pulsed field facilities long-term goal to increase the peak magnetic field routinely available to users. Progress on the rebuild of coils 3, 4 and 7 of the 60T controlled waveform magnet was delayed significantly in 2018 because the quality of conductors did not meet the requirements. To mitigate these issues in 2019, we are pursuing multiple routes to accelerate the production of the conductor for these coils (see the Material Section for details). The metal reinforcing shells and other materials for electrical insulation have been in-stock, ready to start to fabricate these coils as soon as good conductors are obtained.

**Test cell and short pulse bank upgrades:** The pulsed field facility 4 MJ capacitor bank that

75T for routine user operations. The prototype duplex magnet was successfully tested to destruction demonstrating the ability of such a design to exhibit a “soft failure” in excess of 2MJ.

Lessons learned from winding this prototype will inform future design: The duplex magnet relies heavily on Zylon fiber for high hoop stress at 80 Tesla. Zylon fibers are overwrapped outside conductor windings as reinforcement with pre-tension to compensate for their negative thermal expansion when cooled down to 77K. Applying a considerable amount of Zylon fiber with 20-pound pre-tension causes a significant “push-out” axial force on the G-10 end-spools, which contains the Zylon fibers. For the prototype, these forces caused delamination on the end-spools, resulting in voids between the end-spool and the conductor winding. This was detected during winding and imaged via x-ray radiography (Fig.2.b.26). Consequently, the magnet failed quite prematurely at 64T due to the loose conductor winding and Zylon fiber reinforcement. Figure 2.b.26 is the waveform of the 64T pulse of our duplex magnet. Based on the lessons learned from the autopsy of the failed magnet, tooling and fabrication processes are being modified to prevent delamination due to the large push-out force during future fabrication. The next generation of duplex magnet is expected to be tested in quarter three of 2019.

### Major Research Activities and Discoveries

The PFF continues to develop world-class experimental capabilities at the milli- to micro-second time scale as necessary in pulsed magnet fields. In 2018 pulsed field research played an important role in understanding new classes of quantum materials. The monolayer transition-metal dichalcogenides such as WSe<sub>2</sub> or MoS<sub>2</sub> are members of a new class of atomically-thin direct-gap semiconductors exhibiting very strong light-matter coupling, making them interesting for future ultrathin and efficient optoelectronics. However, in order to rationally design such devices, fundamental material properties such as the mass of electrons, holes and excitons, their size and dimensionality must be determined. Historically, such fundamental properties of traditional semiconductors have been revealed via

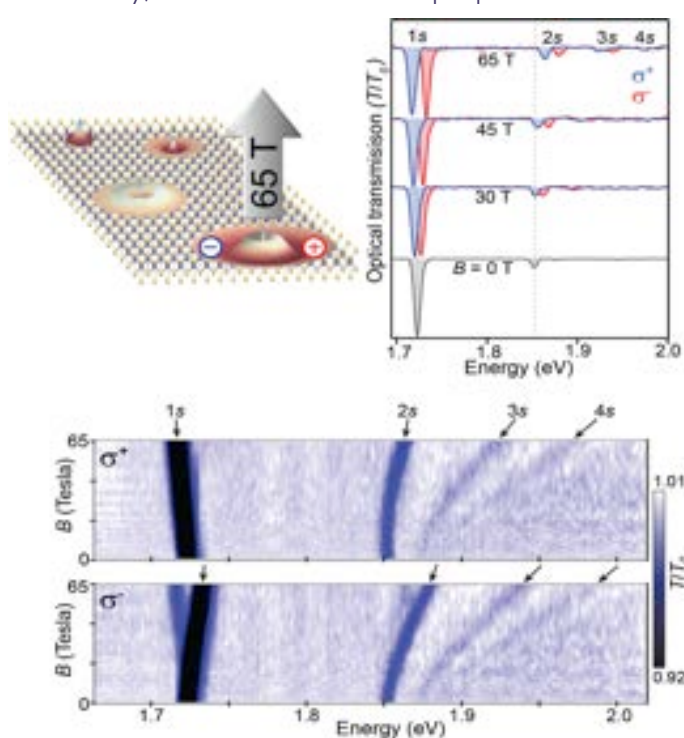


**Figure 2.b.27:** Using hBN-encapsulated WSe<sub>2</sub> monolayers placed over the core of single-mode fibers, we measure circularly polarized optical spectra from 0-65T. 1s, 2s, 3s, and 4s Rydberg states of the neutral exciton are revealed.

magneto-optical spectroscopy in moderately strong magnetic fields <10T. In the new monolayer semiconductors, extremely high fields (>50T) are needed to compete with the very large Coulomb interactions. By positioning very clean monolayers of encapsulated WSe<sub>2</sub> over the core of single-mode optical fibers, we measured the polarized transmission spectra in pulsed fields to 65T, revealing for the first time the size and binding energy of the first four Rydberg states of the neutral exciton (1s, 2s, 3s, 4s). Crucially, the nearly linear shift of the 3s and 4s Rydberg states at high field directly reveals the exciton’s reduced mass ( $m_r=0.20m_e$ ), a fundamental material parameter that to date was inferred from theory alone. This information will help to guide not only theoretical models but also the rational design and engineering of future optoelectronic devices based on this new class of 2D semiconductors—see A.V. Stier, N.P. Wilson, K.A. Velizhanin, J. Kono, X. Xu, S.A. Crooker, “Magneto-Optics of Exciton Rydberg States in a Monolayer Semiconductor”, Physical Review Letters 120, 057405 (2018)[Fig.2.b.27].

Pulsed fields also enabled the exploration of topologically non-trivial states of matter such as the Weyl semi-metals. The spin up and spin down electrons in Dirac materials, such as

graphene, share a Dirac-cone in momentum space. Weyl semimetals split this degeneracy into two Weyl-nodes with opposite handedness of spin-chirality; this provides the possibility of observing new phenomena. Weyl electrons, for example, are predicted to give rise to a chiral anomaly, whereby parallel electric and magnetic fields can pump an imbalance between the Weyl nodes leading to a topologically protected current. To date all Weyl metals not only possess Weyl electrons but also trivial electrons, complicating the search for the associated phenomena. The use of extreme magnetic fields



(95 tesla) to drive the Weyl metal TaAs deep into its quantum limit where only the purely chiral zeroth Landau levels are populated, enables the transport signature of the chiral anomaly to be observed. This illustrates an important future role of high magnetic fields—to overcome material constraints and access a state composed purely of Weyl fermions—and points the way to inducing new correlated states of matter composed of these exotic quasiparticles—see B.J. Ramshaw, K.A. Modic, A. Shekhter, Y. Zhang, E.-A. Kim, P.J.W. Moll, M. Bachmann, M.K. Chan, J.B. Betts, F. Balakirev, A. Migliori, N.J. Ghimire, E.D. Bauer, F. Ronning, and R.D. McDonald, Quantum limit transport and destruction of the Weyl nodes in TaAs, Nature Communications 9: 2217 (2018) [Fig.2.b.28].

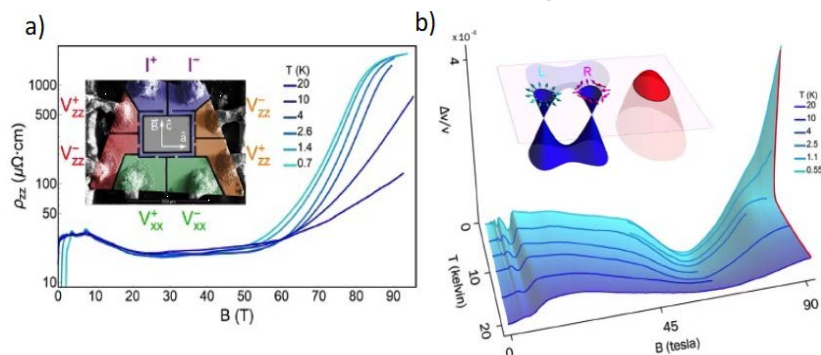


**Figure 2.b.28:** a) Resistivity of the Weyl semimetal, TaAs, for both current and magnetic field along the c-axis from  $T=20\text{K}$  to  $0.7\text{K}$ . Quantum oscillations from the Weyl pockets are visible up to  $7.5\text{T}$ , followed by a decrease and then saturation of the resistivity in temperature and field up to  $50\text{T}$ . Above  $50\text{T}$ , there is a two-order-of-magnitude increase resistivity at low temperature, signifying the opening of an energy gap. The inset shows single-crystal TaAs microstructured using focused-ion-beam (FIB) lithography for both  $r_{zz}$  and  $r_{xx}$  measurements. b) Change of the longitudinal sound speed measured at  $315\text{ MHz}$  for both the sound propagation and magnetic field along the c-axis. Above  $2.5\text{K}$ , the sound velocity flattens out above  $80\text{T}$  and the attenuation is only weakly field dependent. Below  $2.5\text{K}$ , however, both the sound velocity and the ultrasonic attenuation increase rapidly with field. The red line at  $90\text{T}$  highlights the abruptness of the high-field transition as a function of temperature. The inset illustrates the hole dispersion (red), and electron-like Weyl fermions (blue), separated into distinct right and left-handed chiralities.

pulsed field facility plans to continue the multiyear development of a horizontal-bore  $65\text{T}$  short pulse magnet with optical access.

### Facility Plans and Directions

The Pulsed Field Facility is planning a series of upgrades to the pulsed power capabilities. Beyond the current contract with ABB to complete the upgrades to the generator drive and exciter in 2019, we are planning for future upgrades of the PSRs that control the rectification delivering the bespoke current waveforms that power the  $100\text{T}$  outsert and  $60\text{T}$  long-pulse magnet—a multi-million-dollar contract with ABB. Further overhaul of the  $4\text{ MJ}$  short pulse capacitor bank to replace and upgrade the 10-year-old cell-selector switches and reversing switches is planned for 2019 to ensure long term reliability of the short-pulse user facilities. During 2018, the pulsed field facility has developed a far infrared spectroscopy capability centered around time-domain THz spectroscopy and a  $30\text{T}$  sub-millisecond rise time mini-magnet. This enables a complete  $200\text{ GHz}-2\text{ THz}$  spectrum to be recorded every  $625\text{ }\mu\text{s}$ . During 2019, the

### Outreach to Generate New Proposals—Progress on STEM and Building User Community

During 2018, the PFF hosted and participated in numerous outreach events, including the Expanding Your Horizons conference in Santa Fe, a STEM program to foster middle-school girl's interest in science in northern New Mexico, of which the MagLab is the leading sponsor. PFF scientists also visited local elementary and middle schools where they gave presentations on the physics of magnetism and electricity (Fig.2.b.29). PFF scientist Scott Crooker also gave electricity and magnetism demonstrations at the local

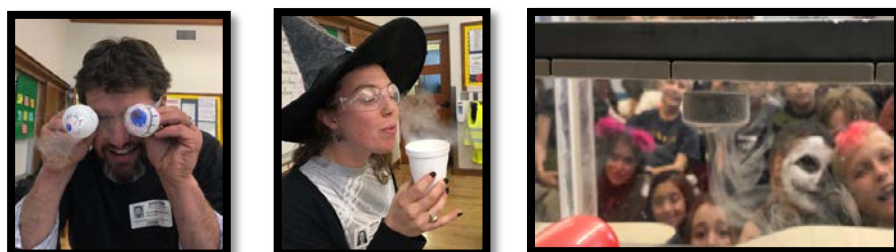


**Figure 2.b.29:** NHMFL-PFF scientists Ross McDonald and Laurel Winter perform Halloween-themed outreach at Carlos Gilbert Elementary School, including spooky levitating superconductors.

Bradbury Science Museum as part of the Scientist Ambassador program. A diverse number of tours were also given of the facility including groups of local high school students, undergraduates from the University of New Mexico, Arizona State University and the McDermott Scholars group from UT Dallas.

### Facility Operations Schedule

The Pulsed- and DC-Field Facilities solicit proposals through a common call tri-annually to streamline the application process and encourage cross-facility collaboration. Such scheduling enables users to coordinate access to high field resources and ensures the availability of support scientists. Hours of operation for large magnets energized by the 1.43 MW motor generator are from 8:00 a.m. to 5:00 p.m. Monday through Friday. The 16 kV, four MJ capacitor bank driven, 65T short pulse magnets in the four cells are in use Monday through Friday 8:00 a.m. to 6:00 p.m. on regular schedule, 6:00 p.m. to 11:00 p.m. on extended after-hours schedule. Maintenance is scheduled each Monday 8:00 a.m. to 10:00 a.m., or performed on an as needed basis. Typically, no more than three out of four of the short pulse cells are scheduled for user experiments on any given week to enable rapid turnaround and continuation of an experiment following a magnet failure.



### 3. EDUCATION AND OUTREACH

In 2018, the education and outreach efforts of the MagLab continued to reach thousands of students and members of the general public at all three sites and across the nation through outreach demonstrations, including the USA Science & Engineering Festival in Washington D.C. and our website. The Center for Integrating Research and Learning (CIRL) conducts the K–16 educational activities for the MagLab as well as facilitates mentoring and professional development for undergraduates, graduate students and postdocs. Public Affairs focuses on community outreach and helping scientists communicate their research.

#### Diversity and Inclusion in Education and Outreach

Diversity and inclusion is a large part of all of the MagLab's educational and outreach activities. The **table 3.1** highlights the demographics for our long-term programs (e.g., one week or longer).

**Table 3.1: Diversity of Education Programs**

2018	Total	% Women	% African American	% Hispanic	% American Indian/ Native American
Research Experiences for Undergraduates (REU) summer	18 undergraduates	67%	22%	17%	0%
Research Experiences for Teachers (RET) summer	10 K–12 teachers	30%	20%	10%	0%
Middle School Mentorship (Fall)	21 middle school students	43%	29%	5%	5%
Internship	26 (high school and college students)	69%	15%	15%	0%
Camp TESLA (Two weeklong camps)	48 (middle school students)	46%	31%	8%	2%
SciGirls Summer camp (Two two-week camps)	40 (middle school students)	100%	30%	10%	7.5%
SciGirls Coding Camp (One weeklong camp)	14 (middle school students)	100%	36%	0%	0%

#### K–12 STUDENTS

##### On-Site and Classroom Outreach Conducted through CIRL

CIRL staff and MagLab scientists conduct outreach in local K–12 schools each year. The outreach is recorded according to the school year as opposed to the calendar year. During the 2017–2018 school year, CIRL's Director of K–12 Programs, Carlos Villa, and CIRL Educational Intern Enri Henry, provided outreach to over 5,000 students from school districts in North Florida, South Florida and Southwest Georgia. Title I schools made up the bulk of these visits, accounting for 41 of the 59 school visits (72 percent). CIRL continued to offer 12 types of outreach activities. The most popular activities were based on the science at the MagLab: Build an Electromagnet, Magnet Exploration and the Static & Current Electricity activities. (For more information on the activities listed and all of CIRL's outreach activities, please visit the [outreach website](#)). Elementary school students represented 43 percent of the visits, followed by middle school students (22 percent) and high school students (10 percent) (The remaining 25 percent were mixed grade groups). The evaluation surveys are given to the classroom teachers who receive the program. All responding educators indicated on their survey that they learned instructional strategies for teaching science based on the presentation. They also indicated that they believed the structure of the outreach made the content more understandable to their students.

At the MagLab's UF facility, Elizabeth Webb conducted outreach efforts during the school year. Webb and fellow UF personnel reached 2,071 students through classroom outreach—75 percent of these were Title I schools. Villa trained and reviewed the use of the outreach materials with UF personnel, leaving six outreach activities and materials in Gainesville. In 2018, the Magnet Explorations lesson was the most frequently requested lesson. The "Build an Electromagnet" lesson and the "What Is Science" lessons were tied for the next most popular. Approximately 88 percent of these outreach lessons were presented to elementary students, with the remaining 12 percent of the presentations being to middle school students. Additionally, Webb coordinated activities to afterschool science programs and school-

wide science nights, reaching an additional 1,160 elementary and middle school students through those efforts.

The staff at LANL also conducted outreach in local schools. Dr. Laurel Winter Stritzinger has developed an outreach lesson using what was offered at the MagLab in Tallahassee and adapting it to the unique science at LANL. The LANL staff has reached nearly 400 students, almost all of them elementary students. They also participated in several programs aimed at increasing girls' interest in STEM careers, working with older middle school girls in Santa Fe. The LANL group also gave a series of presentation on STEM careers at the NHMFL and LANL throughout the year. These presentations were aimed at underrepresented minorities, mostly Hispanic youth. These talks reached over 100 participants.

### Middle School Mentorship

The MagLab Middle School Mentorship Program hosted its largest group for the fourth consecutive year. In 2018, the program included 21 students from middle schools in Leon County. These students worked with 13 MagLab scientist mentors: Dr. Ryan Baumbach, Dr. Ernesto Bosque, Dr. Lloyd Engel, Alyssa Henderson, Dr. Amy McKenna, Lucas Nelson, Dr. Rongmei Niu, Dr. Dmitry Smirnov, Vince Toplosky, Dr. Hans VanTol, Bob Walsh and Gary White. The students meet their mentors every Friday morning in lieu of school, and do so for the entire fall semester. The program culminates in a poster presentation session attended by their family, teachers, principals and mentors. A full list of the 2018 participants and their projects can be found at our [Middle School Mentorship website](#).



*Figure 3.1: Two Middle School Mentorship students show off the piezoelectric crystal they grew.*

### Summer Programs

In 2018, CIRL housed five middle school summer camps (Camp TESLA 1 and 2, SciGirls 1 and 2 and SciGirls Coding Camp) reaching over 100 students. Villa oversees all of the summer camps and supervises the camp teachers.

#### Camp Tesla

Summer Camp TESLA (Technology, Engineering, & Science in a Laboratory Atmosphere) is a one-week coed summer camp held every June for boys and girls interested in science. The camp activities are planned by camp teachers and highlight MagLab science and engineering research and/or disciplines. There are two identical sessions offered in back-to-back weeks. In 2018, 48 students participated in one of the two one-week sessions. 46 percent of the campers were female, 31 percent of the campers were African American, 8 percent were Hispanic, and 2 percent were Native American. Post camp evaluation surveys indicated that participants cited the following activities as positively changing their views of science and engineering: building speakers from household materials, the design and construction of chaos towers and the construction of an electric motor.

#### SciGirls Summer Camp

In 2018, SciGirls Summer camp completed its 13<sup>th</sup> year. This program is based on a partnership between the MagLab and our local public television station, WFSU. The program is closely associated with the SciGirls Connect program, an NSF-funded national SciGirls Program associated with Twin Cities Public Television. The camp includes two two-week camps for middle school girls. Based on post survey responses, the girls cited the following as the activities that positively influenced their views of STEM: creating a hologram projection with a MagLab REU student, a chemistry activity with MagLab scientist McKenna, a geological dig at a local rock quarry, 3D design and printing at FSU's Innovation Hub, along with meeting women scientists throughout the camp who served as role models including many from the MagLab

#### SciGirls Coding Camp

In 2018, we continued our SciGirls Coding Camp which introduces middle school girls to coding and computer science – fields with a low representation of women. The 2018 class of Coding Camp Students included fourteen middle school girls who participated in the one-week program where they learned

the basics of computer programming. The group consisted of 29 percent African American students. They developed projects such as coding with Spheros and a robotics coding field trip to FSU's Innovation Hub and to Diverse Computing Inc. with guest speaker Desiree Fraser. Post camp survey responses indicated that all of the participants mentioned how the camp helped them to realize their talents and connect those to computer programming.

## **K-12 TEACHERS**

### **Los Alamos and Santa Fe, NM, Teacher Workshop**

In 2018, CIRL expanded their teacher workshops to include the Los Alamos and Santa Fe area. Villa and Jose Sanchez created MagLab Pulsed Field specific teacher workshop and outreach kit at Los Alamos National Lab (LANL). The curriculum focused on the pulse magnet science and NMR research technique, translating these topics into an elementary school level activity. Over two days, 20 Santa Fe and Los Alamos area teachers received information on research techniques used at LANL and training on how to implement lessons related to these techniques. The topics covered in the workshop included: Electricity, Circuits, Pulse Magnets, Spectrums and NMR. The kit is available to teachers in the Los Alamos and Santa Fe area and LANL staff.

### **Leon County Schools Workshop**

The Leon County Schools district continued their STEAM Bowl Challenge with teams participating from all of the districts' elementary schools. CIRL staff members, Sanchez and Villa, worked closely with the county school board and implemented a training for the elementary teachers as well as classroom support throughout the semester. The 2018 program began with a January workshop that helped teachers understand how to incorporate engineering and art concepts and problem-solving activities in their classrooms and clubs. Additionally, throughout the spring semester, Villa and Sanchez were available to answer questions as each elementary school club prepared for the culminating event—the STEAM Bowl Challenge. In May, the final STEAM Bowl was held. All twenty-four public elementary schools participated in the Challenge, which included 120 students and over 30 teachers and administrators. The teachers credited the success of the STEAM challenge to CIRL's dedication to the project. This partnership is further evidence of CIRL and the MagLab's commitment to education in Leon County.

### **Research Experiences for Teachers (RET)**

The 2018, RET program hosted 10 teachers (two elementary school and eight secondary school) from seven different counties in Florida. This program is run by Director of RET, REU and Internships, Sanchez. A large part of the success of this year's program is due to the MagLab scientists who mentor and work closely with the teachers over the six weeks. In 2018, 80 percent of the teachers came from Title I schools. A list of the participants and their projects can be found at our [RET website](#).

### **MagLab Educators Club**

The MagLab Educators Club is an email list that CIRL utilizes to send information about MagLab community events, outreach, programs and other exciting opportunities at the lab. We have nearly 600 members, providing further evidence of the interest of educators in MagLab programs.

### **Magnet Academy—For Teachers**

The [Magnet Academy](#) is the outreach portion of the MagLab's website. This site has a page that focuses on teachers. This page provides lesson plans, science demonstrations and interactive activities for teachers of students of all ages. Page views to the MagLab's education page makes up 47 percent of all traffic to the MagLab website. Of these visits, 90 percent went to MagLab Academy.

## **PUBLIC OUTREACH**

Public Outreach is spearheaded by the Public Affairs team. In 2018, this team used large-scale events and a wide variety of communications tools to share high magnetic field research and trends with the MagLab's diverse audiences, including 19 news releases, the website, videos, events and fields magazine.

## Website & Social Media

In 2018, the website continued to grow with more than 1.3 million pageviews, an increase of 13 percent over 2017.

Sections of the site, by percentage of all pageviews, January to December 2018:

Education:	48%
Homepage:	10%
User Facilities:	10%
Personnel & Publication Databases:	4%
News/Events:	5%
Research:	4%
Staff:	4%
About:	5%
Magnet Development:	4%
User Resources:	2%

In addition, the website saw growth in sessions, users and traffic:

- Number of sessions up 20%
- Number of users up 23%
- Percentage of new users up 24%
- Percentage of users on a tablet up 23% and mobile up 25%
- Organic search traffic is up 24%, indicating better performance of site content in search engines.
- Traffic from Social up 15%
- Number of pageviews to Magnet Academy up 30%

In addition, all of the MagLab's social media accounts grew in 2018 (Fig. 3.2; Tab.3.2.):



Figure 3.2: 2018 Social Media Trend

Table 3.2: 2018 YouTube Analytics

	2017	2018	Increase (%)
Views	1,074,506	2,949,452	174%
Watchtime	2,260,455	6,143,910	172%
NEW Subscribers	23,075	45,629	98%
Likes	10,647	29,803	357%
Shares	6,892	21,678	318%

Events:

### Open House

More than 8,200 visitors came to see how science and sports team up at the National MagLab's open house on February 24, 2018. Nearly 100 hands-on science demonstrations were set up, including a number of special sports-themed activities like radar running, MRI of common sports injuries, magnetic mini golf, science of speed skating, air pressure in footballs and superconducting race cars. A unique partnership with Florida State's Institute of Science and Sports Medicine (ISSM) helped explore the science that goes into sports.

Survey data shows (Tab.3.3) -

- 39.5% of survey attendees visited the lab for the first time this open house, and this was the first open house attendance for 45.9% of survey respondents.
- 15.3% of survey respondents had not heard of the MagLab prior to attending their first Open House.
- Before open house, respondents rated the lab at an average score of 8.49 for a net promoter score of 40.6. After open house, respondents rated the lab at 9.49 for a net promoter score of 88.9.

Table 3.3: Open House Survey Statistics

Attendee Income	Percent
Less than \$30,000	12.1%
\$30,000 to \$49,999	13.4%
\$50,000 to \$69,999	16.6%
\$70,000 to \$99,999	12.7%
\$100,000 +	26.1%
Prefer not to Respond	14.0%



The MagLab also helped present the Tallahassee Science Festival on November 3, 2018, at Kleman Plaza in partnership with Tallahassee Community College. More than 3,500 people came to experience the festival.

### See-Thru Science Video Series

This collection of animated videos show viewers what electricity and magnetism might look like if they weren't invisible. Collectively, these videos received about 3.5 million total views in 2018.

- How Capacitors Work
- How Electromotive Forces Work
- How Ignition Coils Work
- How Microwaves Work
- What Oersted Discovered with his Compass
- The Lorenz Force
- How Van de Graaff Generators Work
- How DC Motors Work
- How MRI Machines Work
- Right & Left Hand Rules

### Fields Magazine

This magazine continued to tell stories of high magnetic field research from around the world in 2018. More than 7,000 print magazines are distributed each issue and the online magazine has more than 12,000 page views.

The Subatomic Smackdown (**Fig. 3.3**) began as print articles for fields and symmetry magazines and reached about 20,000 people in that form. But millions of people were ready to rumble as four worthy particles took to the ring in one of the greatest science showdowns of all time.

The Smackdown was then staged as a performance at our sports-themed 2018 open house event and 2018 APS March Meeting.

Finally, the Smackdown culminated in a very successful, weeklong audience engagement on social media:

- 9.3 million+ impressions
- ~530 people voted in poll to select the winner
- Worldwide engagement
- Participants ranged from scientists to teachers to science fans and institutions like DOE, NSF, CERN, ORNL, Brookhaven National Lab, APS, Science Friday, SLAC and Fermilab.
- An equal number of women and men participated in the Smackdown.

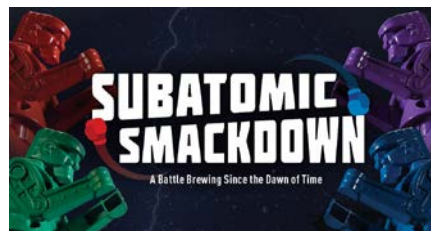


Figure 3.3: Smackdown graphics

### UNDERGRADUATE, GRADUATE AND POSTDOCS

#### Magnet Lab Internship Program (For students 17 years or older)

Over the last six years the MagLab's internship program has grown in recognition among local students from Florida State University, Tallahassee Community College and our local high schools. Jose Sanchez directs this program and facilitates MagLab scientists' selection of student interns each semester. In 2018, the students worked as volunteers in an unpaid position throughout the academic year. Mentors often offer some of these successful students paid positions over the summer. Based on the post program survey recommendations, Jose plans to have summer interns present posters on their research and to have scientists create a job description to match interns in a more effective way.

#### Undergraduate – Research Experiences for Undergraduates (REU)

The 2018, REU cohort hosted 18 undergraduates (**Fig.3.4**). All of 2018 participants and their projects can be found at that [REU website](#). Based on the post program survey, Jose plans to make the following changes in 2018:



Figure 3.4: 2018 REU Participants

- Mentors will create job descriptions for students to apply to specific positions. Also mentors will create a list of preparatory work that students use to prepare to enter their respective labs.

### Graduate Students and Postdocs

Kari Roberts is the MagLab's Postdoc Liaison. She serves as a resource for graduate students and postdocs to connect them to relevant resources at FSU, UF, LANL and via the web. Postdocs and graduate students can visit her at any time to seek support and connections to outside resources. The most common requests she received in 2018 were for assistance securing travel funding, connections to the FSU career center and information related to onboarding tasks.

In 2018, we utilized a different model for our professional development sessions. High-demand organizations came to the lab at regular intervals to host "office hours" where anyone at the lab could come to meet with representatives from FSU resources one-on-one to receive tailored support. In 2018, three offices at FSU participated in office hours.

- Dirac Science Libraries came to the MagLab twice a month to assist MagLab staff and students with literature searching, citation management, data management plans, research metrics, accessing and uploading to data repositories and new tools for project management.
- The Office of Proposal Development came to the MagLab once a month during the spring semester to help MagLab staff and students with the proposal submission process, from finding funding sources all the way up to submitting final drafts to funding agencies.
- The FSU Career Center came to the College of Engineering (walking distance from the lab) once per month in the fall semester to provide staff and students with support on any topic related to career development, including searching for job postings, resume and CV review and preparing for interviews.

In addition to these office hours, FSU career center came to the lab to host a professional development session on creating and updating CVs. The session was attended by eight people: two staff members, three graduate students and three postdocs.

We also offer a postdoc seminar for any postdoc who wishes to give a practice talk. These have been used to prepare for upcoming conference presentations and practice job talks.

### Professional Development Resources at FSU, UF, and LANL

In addition to MagLab-specific resources, postdocs and graduate students have access to professional development resources at their affiliate campuses. FSU, UF and LANL all offer additional resources to graduate students and postdocs that connect these early career scientists to their larger campuses and to resources beyond the scope of what the MagLab can currently provide. Examples of resources provided at each of the three campuses can be found in **table 3.4**:

**Table 3.4:** Resources provided at FSU, UF and LANL

FSU	UF	LANL
<ul style="list-style-type: none"> <li>• An official Office of Postdoctoral Affairs</li> <li>• Twice yearly postdoc workshops including outside speakers and a poster session.</li> <li>• Career Center</li> <li>• Regular professional development sessions</li> <li>• Travel Funding</li> <li>• Postdoc-level Preparing Future Faculty and Preparing Future Professionals programs</li> <li>• Free membership to the National Postdoc Association</li> </ul>	<ul style="list-style-type: none"> <li>• An official Office of Postdoctoral Affairs</li> <li>• Annual Postdoc Research Symposium</li> <li>• Career Center</li> <li>• Regular professional development sessions</li> <li>• Travel Funding</li> <li>• Free membership to the National Postdoc Association</li> </ul>	<ul style="list-style-type: none"> <li>• Regular online and in-person professional development opportunities</li> <li>• A matched mentorship program</li> <li>• Awards and recognition opportunities specifically for postdocs</li> <li>• Paid maternity leave</li> </ul>

### Mentoring for MagLab Postdocs

Postdocs are an important piece of the overall mentoring landscape at the MagLab, as indicated by our [Postdoc Mentoring Plan](#). While at the lab, they have the opportunity to be a mentor to younger students and be mentored by our faculty. Postdocs often serve as important mentors to graduate

students and undergraduate students in the lab setting. For the last two years, students have mentioned the value of the mentoring they receive from postdocs on the annual Climate Survey. Postdocs are also eligible to participate as mentors in CIRL's long-term outreach programs. Kari Roberts serves as a support for both postdocs and supervisors during the annual evaluation process.

### Annual Survey to Postdocs

The annual survey to postdocs is included each year as a section of the lab's annual Climate Survey. The survey helps gauge the quality of the mentoring and supervision that postdocs receive at the lab. This year, 100 percent of postdocs who responded to the survey said they were satisfied with their overall experience at the lab. When asked to rate their interactions with their supervisor and mentors, 100 percent of postdocs indicated they had regular meetings with their supervisor, and 92 percent of postdocs were satisfied with the frequency of these meetings. Postdocs rated their supervisors at 4.5 out of 5 for treating them with respect and being accessible. 83 percent of postdocs indicated that they were satisfied with the mentoring they have received at the lab.

The demographics for our postdocs are in **tables 3.5, 3.6, and 3.7**. These numbers are taken directly from the internal MagLab personnel system on January 10, 2019.

**Table 3.5: Race and Ethnicity — Excluding Affiliates**

Race/Ethnicity	Number	Percentage (N= 29)
Hispanic or Latino/a	3	10.3%
Asian	18	62.1%
Black/African American	0	0%
American Indian or Alaska Native	0	0%
Native Hawaiian or Pacific Islander	0	0%
White/Caucasian	10	34.5%
Prefer not to disclose	1	3.4%

**Table 3.6: Gender- Excluding Affiliates**

Male	Female
18 (62.1%)	11 (37.9%)

**Table 3.7: Citizenship Status — Excluding Affiliates**

US Citizen or Permanent Resident	Visa Holder
7 (24.1%)	22 (75.9%)

## NHMFL SCIENTISTS' AND STAFFS' COMMITMENT TO OUTREACH

### NHMFL Personnel Outreach

In 2018, 95 scientists and staff reported conducting outreach to communicate information about the MagLab to the community. Together, these scientists reached 9,739 people. The large majority (75 percent) of this audience were K–12 students. Of the 95 scientists who conducted outreach in 2018, 52 conducted long-term outreach working with K–12 students, K–12 teachers, or undergraduate students. These scientists mentored a total of 105 individuals this year. Of these individuals, 76 (72 percent) were matched with their mentor through a CIRL program. A summary of the types of short-term outreach conducted and outreach audience for each department is presented in **tables 3.8 and 3.9**.

**Table 3.8: Short-Term Outreach**

Department	Tour of MagLab Facility		Presentation		Visit K–12 classroom		Judged a Science Fair	
	# of Scientists	# of people reached	# of Scientists	# of people reached	# of Scientists	# of people reached	# of Scientists	# of people reached
ICR	3	111	5	1060	1	160	3	90
CMS	1	65	1	450			1	12
ASC					1	200		
EMR	1	1	2	70	1	200		
NMR	4	44	2	160	1	20	2	119
UF	15	420	3	3231	3	311	3	80
LANL	2	25	3	335	2	170		
MS&T	1	10	2	160				
DC	1	38	1	912	1	30		
Geochem			1	280	2	680		
Directors Office			1	290				

**Table 3.9: Outreach Audience: Short- and Long-Term Outreach**

Department	# of Scientists	Number of People Reached				
		Elementary Students	Middle/High Students	Undergraduate and Graduate Students	General Public	K-12 Teachers
ASC	3	200	2			1
NMR	10	141	20	53	54	
EMR	3		17	37		
ICR	13	245	198	132	754	
CMS	14	401	165	9	23	6
UF	19	1350	1877	67	350	204
DC	3		38	2	942	
Geochem	8	400	143	8		
MS&T	11	100	6	15	60	2
Director's Office*	3			92	201	
LANL	7	150	271	43	75	

\*Includes Public Affairs, Safety, CIRL and WAG

## RESEARCH AND EVALUATION

### Evaluation

Evaluation for all education programs at the MagLab is conducted by Kari Roberts. She stays up to date on the best practices in evaluation as outlined by experts in evaluation and the social sciences and the National Science Foundation. The evaluations conducted for each education program at the lab allow for data-driven decision making when it comes to designing and modifying education programs at the lab. Evaluation methodology for each program is described in **table 3.10**.

**Table 3.10: Evaluation methodology for each program**

Outreach	Form of Evaluation
<i>Classroom outreach</i>	Post-survey to teachers after outreach conducted (formative assessment), post-survey to students who come to the lab for outreach
<i>RET/REU/Internship</i>	Pre-/post-survey measuring attitudes toward STEM careers, perceptions of STEM careers and self-efficacy in STEM (for teachers in teaching STEM) Regular tracking of past participants to determine persistence over time
<i>Summer Camps/Middle School Mentorship</i>	Pre-/Post-survey measuring STEM Identity, STEM Self-Efficacy, perceptions of scientists and science careers. Regular tracking of past participants to determine how their interest in STEM evolves over time.
<i>Graduate Student/ Postdoc Professional Development</i>	Annual survey to current postdocs to determine professional development needs and assess mentoring and annual tracking of graduate students and postdocs to determine career trajectories.
<i>MagLab Users Summer School</i>	Pre-/Post-survey assessing perceived value of program on their career trajectories.
<i>Winter Theory School</i>	Post-survey assessing participants perceived value of the Winter Theory School and how they will apply what they learned in the program
<i>Open House</i>	Post-experience surveys and brief interviews given to attendees of the annual open house to assess perceived benefits of the annual open house and provide feedback for future years.

### Research

In 2018, Hughes led the research team for the SciGirls CONNECT2 NSF grant, which included staff member Kari Roberts and FSU graduate student Jennifer Schellinger. The team completed an article focused on the coding identity work of middle school girls during the SciGirls Coding Camp. The article has been resubmitted as a revise and resubmit. Two other articles are under review. Roberts, K. & Hughes, R. (Submitted). The Role of STEM Self-Efficacy on STEM Identity for Middle School Girls After Participation in a Single-Sex Informal STEM Education Program, *Research in Science Education*.

- Hughes, R. & Roberts, K. (Submitted). STEM Identity Growth in Co-Educational and Single-Sex STEM Summer Camps, *International Journal of Gender, Science, and Technology*.



- Hughes, R. & Roberts, K. (Under review). STEM Identity Growth in Co-Educational and Single-Sex STEM Summer Camps, *International Journal of Gender, Science, and Technology*.
- Hughes, R., Schellinger, J., & Roberts, K. (Revise and Resubmit). The Role of Recognition in Coding Identity for Girls. *Journal of Women and Minorities in Science and Engineering*.
- Roberts, K. & Hughes, R. (Under review). The Role of STEM Self-Efficacy on STEM Identity for Middle School Girls After Participation in a Single-Sex Informal STEM Education Program, *Journal of STEM Outreach*.

In 2018, Hughes and another FSU graduate student, Shannon Davidson, published an article based on research conducted with the MagLab RET program.

### BROADENING OUTREACH

In addition to the *Diversity and Education* sections, which speak to the MagLab's work in broadening outreach through education and underrepresented groups, the Lab's staff are regularly presenting new research and sharing information about our user program at national and international conferences, workshops and seminars. Each presentation, poster or abstract opportunity offers the chance for scientists around the world to learn more about the Lab's research capabilities and broaden our user program to appeal to new scientists from varying levels – from graduate students and postdocs to seasoned scientists.

In 2018, MagLab staff gave 294 lectures, talks and presentations across 19 countries and nearly 30 states (**Fig.3.5., 3.6**), including American Physical Society March Meeting, American Chemical Society, ASMS Conference on Mass Spectrometry and Allied Topics, International Bologna Conference on Magnetic Resonance in Porous Media (MRPM14), Experimental Nuclear Magnetic Resonance Conference, Applied Superconductivity Conference, International Conference on Materials and Mechanisms of Superconductivity and High Temperature Superconductors (M2S), International Cryogenic Engineering Conference (ICEC), Rocky Mountain Conference on Magnetic Resonance Solid - state NMR Symposium and International Battery Seminar.

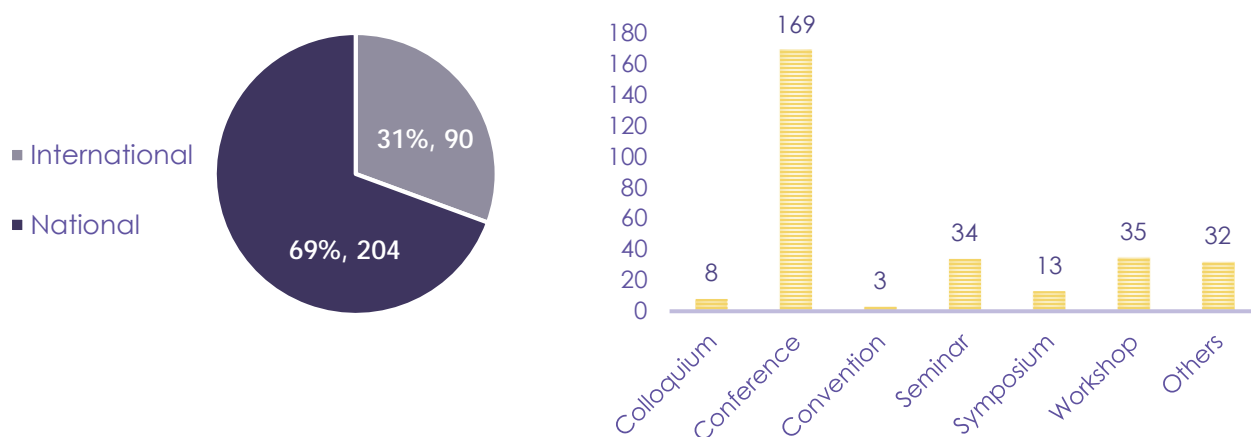


**Figure 3.5:** Geographic Distribution of Presentations    **Figure 3.6:** 2018 Presentation Types

Throughout the year, the MagLab hosts or sponsors a variety of workshops and conferences related to our science.

**Table 3.11:** List of 2018 sponsored workshops and conferences

Date	Name	Location	About
Jan 8–12	Theory Winter School	Tallahassee, FL	This year, lectures introduced and explained concepts explored in quantum information theory, such as entanglement, and answered outstanding questions in many-body physics.
Jan 13	Frontiers in Many-Body Physics	Tallahassee, FL	A one-day memorial symposium to honor the memory of Lev P. Gor'kov focusing on recent developments in many-body physics.

Date	Name	Location	About
Feb 18–22	The 14th International Bologna Conference on Magnetic Resonance in Porous Media (MRPM14)	Gainesville, FL	The MRPM conference series addresses questions concerning the structure, interactions and dynamics in natural and synthetic porous materials as well as the development and application of magnetic resonance techniques to these systems.
May 7–11	NMR Metabolomics and <sup>13</sup> C Fluxomics Workshop	Gainesville, FL	The workshop will focus on technical details of sample preparation, data acquisition, data processing and statistical analysis. Significant time will be spent in lab preparing samples and acquiring both <sup>1</sup> H and <sup>13</sup> C data.
May 14–18	User Summer School	Tallahassee, FL	The weeklong summer school features tutorials on measurement techniques, practical exercises and plenary talks from experts in the field of condensed matter physics.
May 17–19	BigMAG	UC Santa Barbara	A workshop to identify transformational science that would be enabled by coupling a ~30 T magnet to UCSB's Terahertz Free-Electron Lasers.
June 24–28	The 12th International Conference on Research in High Magnetic Fields (RHMF 2018)	Santa Fe, NM	The 12th International Conference on Research in High Magnetic Fields (RHMF 2018) is devoted to all aspects of research in high magnetic fields and covers areas such as magnetism, semiconductor physics, superconductivity, studies of strongly correlated electron systems, low-dimensional and nano-scale materials, spin liquids, topological materials, molecular systems, high magnetic field technology and new high-field experimental techniques. The conference is hosted by the National High Magnetic Field Laboratory-Pulsed Field Facility at the Los Alamos National Laboratory.
July 21–25	60th Annual Rocky Mountain Conference on Magnetic Resonance	Denver, Colorado	Electron Paramagnetic Resonance (EPR) Solid-State Nuclear Magnetic Resonance (SSNMR) (biennial; the next year to be held is 2020)
Aug 6–17	Advanced School and Workshop on Correlations in Electron Systems – from Quantum Criticality to Topology	Trieste (Italy)	<ul style="list-style-type: none"> <li>• Novel theories of quantum criticality in metals and Mott insulators</li> <li>• Superconductivity and competing orders</li> <li>• Novel approaches to spin liquids</li> <li>• Correlated systems with strong spin-orbit coupling</li> <li>• Coulomb interaction in topological systems</li> <li>• Topological superconductors</li> </ul>
Oct 13	Fall 2018 STEM Santa Fe Expanding Your Horizons Conference	Santa Fe, NM	A conference for girls in 5th–8th grade. This day-long event will include hands-on workshops in science, technology, engineering and math (STEM) led by women professionals. This year's event was attended by 165 5th through eighth grade girls. This conference featured 16 workshops, a STEM and college careers fair and a keynote address by Jessica Perea Houston, Associate Professor in the Chemical and Materials Engineering department at New Mexico State University.

## 4. IN-HOUSE RESEARCH

### a. Geochemistry

*The facility primarily investigates natural processes, both recent and ancient, through the analysis of trace element contents and isotopic compositions.*

#### Introduction

The Geochemistry Program main funding is through grants from the Geoscience directorate at NSF, NASA and the USGS. On average the program has about 15 active grants with average budget per grant of \$150,000/year. All tenure-track faculty have their appointments in FSU's College of Arts and Sciences. Honors: This year Geochemistry Program member Robert Spencer was awarded the Yentsch Schindler Award Prize by the Association for the Science of Limnology and Oceanography for his research into the carbon cycle in the Amazon and Congo Watershed; Salters was elected fellow of the American Geophysical Union for: "Fundamental contributions to mantle evolution and dynamics through hafnium isotopes and trace element geochemistry."

The facility has seven mass spectrometers, which are available to outside users. Three instruments are single collector inductively coupled plasma mass spectrometers for elemental analysis. One is dedicated to in-situ trace element analyses on solid materials using laser ablation. The other two are dedicated to elemental analyses of solutions. The facility has four mass spectrometers dedicated to determination of isotopic compositions. One is a multi-collector inductively coupled plasma mass spectrometer (NEPTUNE) used for determination of isotopic abundances of metals. A second is a thermal ionization multi-collector mass spectrometer, which is mainly used for Sr-isotopic compositions. The third mass spectrometer is designed for the measurement of the light stable isotope compositions (C, N O). A fourth mass spectrometer dedicated to sulfur isotope analyses.

#### Publications and Outreach

The program members have published 30 peer-reviewed publications and a similar number of presentations at meetings and invited presentations at other institutions. The program involves a large number of undergraduate students in their research.

#### Science Highlights

The extinction of the dinosaurs at the end of the Cretaceous 65 million years ago caused by a meteorite impact has been a fascinating story. How quickly life recovered from the impact was addressed obtaining the sedimentary record, through drilling, of the impact site. Owens and colleagues determined the geochemistry of this record to investigate whether there were high concentrations of metal just after the impact as evidence for metal poisoning. In addition, they measured elemental ratios that are sensitive to redox state. Their results together with detailed stratigraphy and paleontological studies were published in the journal Nature. The conclusion of these combined studies shows that life reappears years after the impact and that high productivity was reestablished within 30,000 years.

Atmospheric nitrogen (N) deposition is an important determinant of N availability for natural ecosystems worldwide. A study by Spencer and his students presented the first field data from tropical Africa and showed high nitrogen deposition in the region. Utilizing the facilities at the NHMFL, they elucidated the deposited nitrogen is predominantly derived from intensive seasonal burning of biomass on the African continent. This high N deposition has important implications for the ecology of the Congo Basin and for global biogeochemical cycles more broadly. This work was published in the Proceedings of the National Academy of Sciences

A third highlight is a study on the Lanzo peridotite in collaboration with colleagues at University of Pavia, Italy. Evidence has been mounting recently that the Earth's mantle is more heterogeneous than previously assumed and especially that a larger proportion is ultra depleted material. The presence of this ultra depleted component affects the amount of melt the mantle can produce and the depth of melting at, for example, mid-ocean ridges. In Lanzo we found isotopic evidence of the presence of melts with an ultra depleted signature. This work is published in Earth and Planetary Science Letters

#### Progress on Stem and Building the User Community

The facility is open to users of all disciplines, and we have a long-time collaboration with the USGS and the South Florida Water Management District. During the summer we hosted one undergraduate student from the REU program; eighteen undergraduate students are involved in research throughout

the year. In the last year, 69 users, of which 52 percent were female, used our analytical facilities. Graduate student users were 65 percent female. Within the area of Geosciences, the faculty has collaborations with researchers throughout the US, Europe as well as Asia. The disciplines for which we do service analyses at a more local level range from magnet science to pharmacy.

### b. Cryogenics

The Cryogenics Laboratory located at the National High Magnetic Field Laboratory is a fully developed facility for conducting low temperature experimental research and development. A number of specialized experimental equipment are available in the lab, which include the Cryogenic Helium Experimental Facility (CHEF) for horizontal single and two-phase heat transfer and flow research; the Liquid Helium Flow Visualization Facility (LHFVF) for high Reynolds number superfluid helium (He II) flow visualization research; the Laser Induced Fluorescence Imaging Facility (LIFIF) for high precision molecular tagging velocimetry measurement in both gaseous and liquid helium; and the Cryogenic Magnetic Levitation Facility (CMLF) for studying cryogenic fluid hydrodynamics in micro-gravity. The laboratory supports in-house development projects as well as contracted scientific work directed by Prof. Guo of the Mechanical Engineering department at Florida State University. The major research focus of the cryogenics lab currently includes: 1) fundamental turbulence and heat transfer research in cryogenic helium; 2) quantized vortex-line imaging in levitated helium drops; 3) catastrophic loss of vacuum in liquid helium cooled pipes. These research activities are supported by external funding agencies including the National Science Foundation, the Department of Energy, the Army Research Office and our industrial partners.

#### Turbulence Research with He II

Many flows in nature have extremely high Reynolds ( $Re$ ) or Rayleigh ( $Ra$ ) numbers, such as those generated by flying aircraft and atmospheric convection. Better understanding of these flows can have

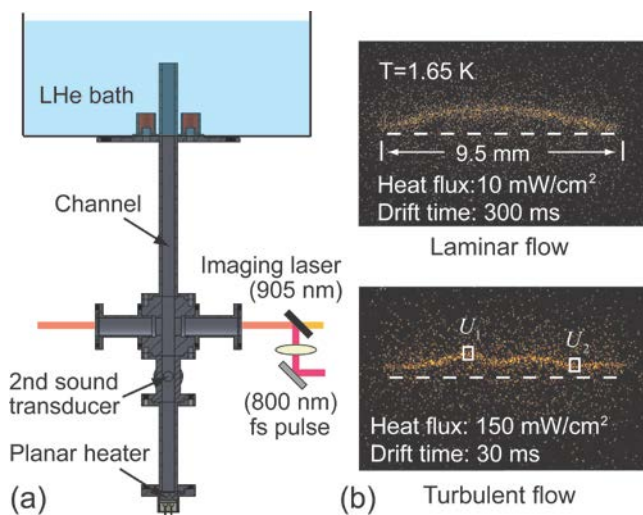


**Figure 4.b.1:** (a) Schematic diagram of the experimental setup for flow visualization using He<sub>2</sub> molecules. A high intensity femto-second laser (red beam) through the windows ionizes helium atoms and creates a tracer line of He<sub>2</sub> excimer molecules. Then the imaging laser at 905 nm (yellow beam) drives the tracers to produce fluorescent light (640 nm) for the imaging. (b) Typical images of the tracer line in thermal counterflow generated by an applied heat flux in He II. The deformation of the tracer lines provides quantitative information about the velocity field in He II.

profound positive impacts on everyday life, such as improving the design in energy efficient applications and our understanding of climate change. To achieve large  $Re$  values in laboratory, a common route is to increase the characteristic length of the flow, which normally requires the construction of expensive and energy-consuming large-scale flow facilities and wind tunnels. An alternative method is to use a fluid material with very small kinematic viscosity. At the cryogenics lab, we adopt helium-4 as the working fluid.

Helium-4 has extremely small kinematic viscosity (three orders of magnitudes smaller than that for air), which enables the generation of highly turbulent flows in compact table-top equipment. Furthermore, when helium-4 is cooled below about 2.17K, it undergoes a phase transition into a superfluid phase (He II), which consists of two miscible fluid components: a viscous normal component and an inviscid superfluid fluid component. Turbulence in He II is a cutting-edge research area that is important both in fundamental science and in practical applications of He II as a coolant. In order to make quantitative flow field measurements, we have developed two powerful flow visualization techniques. One is the so-called molecular-line tagging velocimetry technique which is developed based on tracking thin lines of He<sub>2</sub> excimer tracers

created via femtosecond-laser field ionization of helium atoms (see Fig.4.b.1). Besides this technique, a particle tracking velocimetry method in He II using seeded micron-sized frozen hydrogen particles has also been developed and implemented. The application of these techniques to the study of heat induced flows in He II has revealed a novel form of turbulence (counterflow turbulence). A systematic



characterization of this turbulence will be indispensable for developing a theoretical understanding that will potentially benefit the design of He II based cooling systems. This year, we have also designed and fabricated a new towed-grid system for studying turbulence in He II generated via mechanical forcing. This system will allow us to conduct interesting high Re flow research utilizing the unique properties of helium.

### Vortex Imaging in Levitated Helium Drops

The motion of quantized vortex lines is responsible for a wide range of phenomena, such as the decay of quantum turbulence and the initiation of dissipation in type-II superconductors, and it is also implicated in the appearance of glitches in neutron star rotation and the formation of cosmic strings in the early universe. A systematic study of vortex-line dynamics promises broad significance spanning multiple physical science disciplines. In He II, vortex lines can be directly visualized by imaging tracer particles trapped on the lines. However, producing tracers in helium at low temperatures and imaging the trapped tracers remains challenging, and the container walls can often affect the vortex-line motion. In the cryogenics lab, a special cryostat with a superconducting magnet in it has been restored and tested recently. The magnet, when it is charged, can levitate a large drop of liquid helium. We plan to create quantized vortices in the drop via fast evaporative cooling of the drop and controlled drop rotation (see Fig.4.b.2). These vortices will be decorated with He<sub>2</sub> excimer tracers or fluorescence nano-particles which can be imaged via laser-driven fluorescence. This process can enable unprecedented insight into the behavior of a rotating superfluid drop and will untangle some key issues in quantum turbulence research.

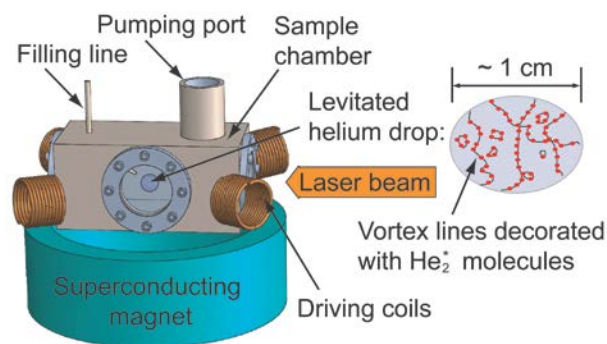


**Figure 4.b.2:** Schematic of the experimental apparatus inside the optical cryostat for visualizing quantized vortex lines in a magnetically levitated helium drop.

### Loss-of-Vacuum Heat and Mass Transfer

High performance superconducting magnets and superconducting radio frequency (SRF) cavities are essential components of almost all future high energy particle accelerators. These magnets and SRF cavities are normally cooled by liquid helium. The study of the heat and mass transfer processes that can occur during a sudden catastrophic loss of vacuum (SCLV) incident in a liquid-helium cooled system is therefore of great importance to the design and safe operation of the superconducting magnets and SRF cavities. A project has been launched in the cryogenics lab to study how a gas such as atmospheric air/nitrogen will condense inside a liquid-helium cooled vacuum tube while the gas simultaneously propagates down the vacuum tube. In the past year, we have implemented a new experimental rig that incorporates a vacuum tube of helical geometry designed for He II immersion experiments (see Fig.4.b.3). Systematic study on the propagation of condensable gas (air or nitrogen) in this tube cooled by liquid helium at 4.2K has been conducted. The variations of the temperatures at different locations along the tube following the vacuum break were measured at controlled inlet gas pressure. We have observed exponential deceleration of the gas front velocity as the gas propagates along the vacuum tube. More recently, a theoretical model has been developed which explains the deceleration as a consequence of the gas condensation on the inner wall of the tube. Preliminary numerical simulation based on this model can indeed reproduce the observed slowing down of gas front velocity along the tube. A more systematic comparison of the experimental data and the simulation in the future will allow us to extract valuable information such as the sticking coefficient of the gas molecules on the cold wall.

On the education side, our research projects have allowed us to support both undergraduate and graduate students. We have also been able to engage postdoctoral researchers, interns, visiting students and scholars. These students have obtained training and experiences in fluid dynamics, cryogenics, advanced laser technologies, electronics and data analysis techniques. These skills are applicable to nearly all STEM related fields, giving these students the technical dexterity necessary to excel in today's science-and-technology-dominated market. Our cryogenics lab is also involved in various outreach activities, such as presenting science demonstrations for the annual open house event at the NHMFL.

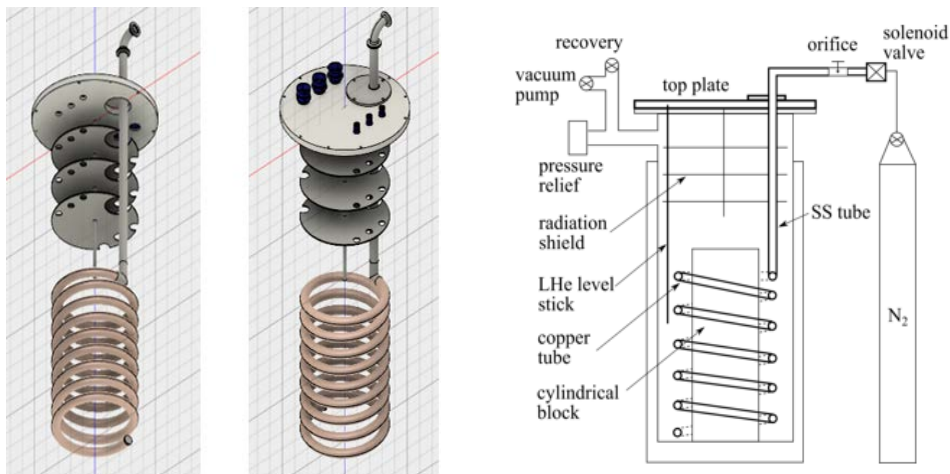


**Figure 4.b.3:** (a) Schematic of the helix tube and the top flange of the cryostat. (b) Schematic diagram of the vacuum break experiment in He II.

## Funding

In 2018, we received about \$740,000 from six different awarded external grants.

**Table 4.b.1:** Awards received that provided 2018 funding for the cryogenics in-house research.

PI and co-PI(s) – indicate if you are the PI or a co-PI	Agency	Title	Time period	Total award	Annualized 2018 award. Amount to you if you are the sole PI or your share if there are multiple PIs.
W. Guo	NSF	Flow Visualization Study of Quantum Hydrodynamics in Superfluid Helium-4	8/1/2018 to 7/31/2021	\$335,023	about \$108K
W. Guo (PI) and L. Cattafesta (co-PI)	NSF	High Reynolds Number Turbulence Research in Cryogenic Helium	6/1/2018 to 5/31/2021	\$375,003	about \$120K
W. Guo (PI) and L. Cattafesta (co-PI)	Army Research Office	Advanced Molecular Tagging Velocimetry In Cryogenic Helium	12/21/2018 to 12/20/2019	\$216,893	about \$180K
W. Guo (PI) and Van Sciver (co-PI)	DOE	Liquid Helium Fluid Dynamics Studies	4/01/2016 to 3/31/2019	\$765,000	about \$255K
W. Guo	NSF	Visualization Study of Vortex-Line Dynamics in a Magnetically Levitated Helium-4 Superfluid Drop	05/01/2015 to 05/01/2018	\$302,362	about \$50K
W. Guo	Oak Ridge National Lab	High Resolution Validation of Next Generation Turbulent Flow Models	10/1/2017 to 9/30/2018	\$34,780	about \$25K

### c. CMS/UF Physics/ UF Chemistry

Here we have taken a few exciting research discoveries from our both Teaching and Research MagLab faculty that are not driven by our users, but by our faculty themselves. We present this because, although the MagLab is primarily a user facility, our faculty are internationally known for their front-line science. This provides a world-class scientific environment for our in-house science and drives innovation for our user program. The international acclaim brings new users and stresses the eminence of our MagLab. There are many more examples of exciting in-house research than shown here – these were chosen for impact as decided by our chief scientist.

We start with 2D materials – as the MagLab has always led worldwide research in this area – from the Quantum Hall and Fractional Quantum Hall effect to the non-time-reversal breaking phenomena of topologically protected states and graphene. Then we show some ground-breaking work on the high-

temperatures superconducting cuprates, extremely high-field pulsed work on the quantum critical material CeRhIn5. Then we coming back to some brand new work on flux quantization but in asymmetric superconducting rings. The last two findings have to do with spin textures in frustrated magnets and some computations on a near-ideal Heisenberg antiferromagnet.

### Fermi Surfaces for Dirac Type II Semimetal Candidates and High-Energy Physics

Recently, condensed matter is borrowing a number of concepts inherent to high energy physics, such as Dirac, Weyl or Majorana fermions. These particles were predicted to exist in the free vacuum, however only in solid state systems we found Landau quasiparticles behaving as Weyl or Majorana fermions. More

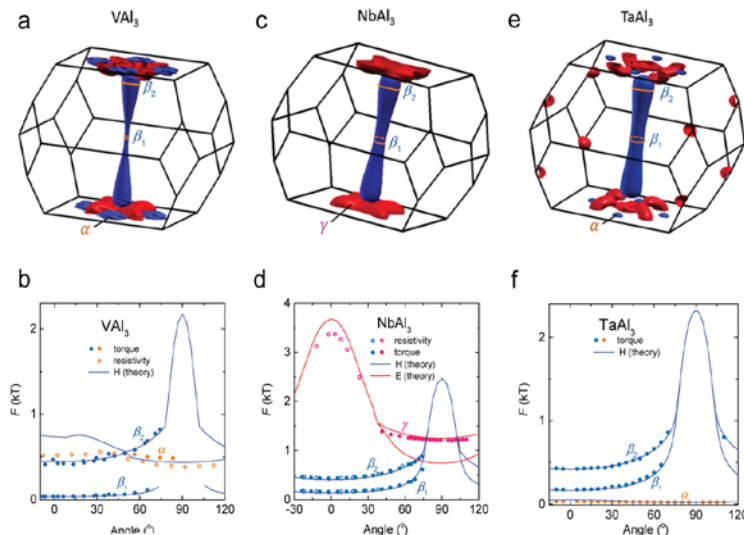


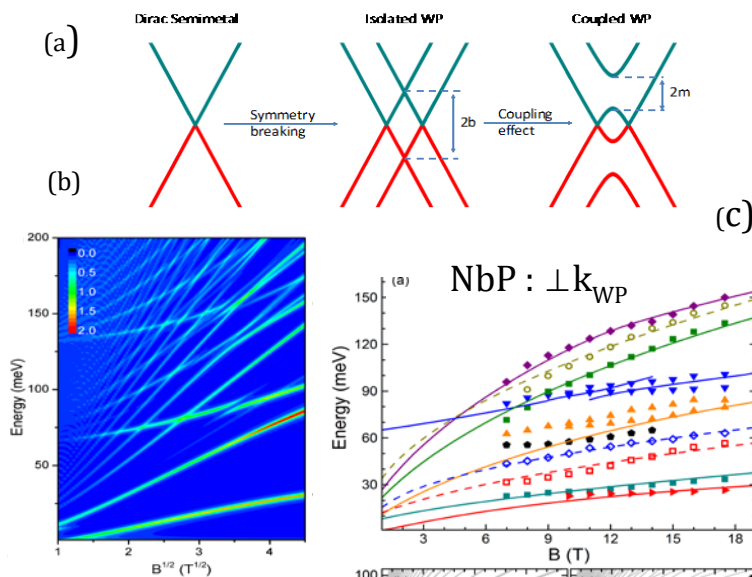
**Figure 4.c.1:** Fermi surfaces for the Dirac type-II semimetal candidates a) VAAl<sub>3</sub> (c) NbAl<sub>3</sub> (e) TaAl<sub>3</sub> respectively. Hole- and electron-like pockets are depicted in blue and in red, respectively.  $\beta_1$  and  $\beta_2$  orbits match the frequencies calculated for the “neck” and the “belly” cross sectional areas of the dumbbell like pockets; a orbit can be associated to a hole-like ellipsoid of topologically trivial character.  $\gamma$  orbit can be associated with the large “helix” like electron pocket. (b), (d), (f) Cyclotron frequencies  $F$  as functions of the angle  $\theta$  relative to crystallographic  $c$ -axis. Solid lines depict the angular dependence of the FS extremal cross-sectional areas predicted theoretically. K.-W. Chen, X. Lian, Y. Lai, N. Aryal, Y.-C. Chiu, W. Lan, D. Graf, E. Manousakis, R. E. Baumbach, and L. Balicas Phys. Rev. Lett. 120, 206401 (2018).

recently, other systems like Weyl type II and Dirac type-II that do not have analogs in high energy physics, were predicted to exist in certain compounds. The standard particle model of high energy physics assumes Lorentz invariance, or that the laws of physics are independent of the position or the direction of movement. However, Dirac type II systems are characterized by tilted Dirac cones, meaning that there is no simple and isotropic relation between energy and momentum; for a given energy the momentum is direction dependent.

We found excellent agreement between calculations and experiments for the topography of the Fermi surface of the MAI<sub>3</sub> compounds (where M= V, Nb, and Ta). This implies that these calculations are correct or that these compounds indeed display tilted Dirac nodes in its dispersion being good candidates for displaying Dirac type-II quasiparticles (Fig.4.c.1).

**Landau Quantization in Coupled Weyl Points (CSP): Semimetal NbP** Weyl semimetal (WSM) is a newly discovered quantum phase of matter that exhibits topologically protected states characterized by two separated Weyl points (WPs) with linear dispersion in all directions. In the vicinity of the WPs, the band structure is very similar to that of Dirac semimetal.

**Figure 4.c.2:** a) Band structure evolution of Dirac and Weyl semimetals under the action of symmetry breaking and band hybridization. b) Calculated optical conductivity featuring a complex pattern of Landau Levels crossings/anticrossings originating from WP's coupling. Only a single pair of WPs is considered for simplicity. c) Magnetic field dependence of the major inter-LL spectra (symbols). The dash and solid lines are best fits calculated within the model with two types of coupled WPs in NbP Y. Jiang Z.L. Dun, S. Moon, H.D. Zhou, M. Koshino, D. Smirnov, Z. Jiang Nano Lett. 18, 7726–7731 (2018).





However, the band hybridization can significantly modify the electronic structure of a WSM and provide a new twist to the protected states. We have demonstrated both theoretically and experimentally the essential role of the coupling effect between WPs in an established WSM, NbP. The band structure analysis predicts several unique spectroscopic features originated from the WPs that were largely confirmed in magneto-spectroscopy experiments. These results emphasize the importance of coupling between WPs both for fundamental understanding of Weyl fermions in realistic condensed matter systems and for future device applications (Fig. 4.c.2).

### Wigner Solid of an Interlayer-Correlated Bilayer State

In wide quantum wells (WQWs), 2D electron systems (2DESs) can change from a single-layer to a bilayer [1] by increasing the 2DES density or by applying inplane field. Just at the transition to bilayer the integer quantum Hall state (IQHS) at Landau filling  $\nu=1$  is interlayer-correlated, and is understood as the famous Halperin Y111 state. Near integer  $\nu$ , quasiparticles or -holes of IQHSs form Wigner solids (WSs). The signature of a WS is a pinning mode, in which the carriers oscillate within the residual disorder potential (Fig. 4.c.3).

### Electron Correlations in Twisted Bilayer Graphene near the Magic Angle

Recent remarkable experiments on twisted bilayer graphene (tBLG) discovered correlated insulator phases—and the neighboring superconductivity—at simple integer commensurate charge concentrations, apparently corresponding to partial filling of the four nearly flat electron bands near the charge neutrality point. This discovery quickly stimulated a flurry of activity among experimentalists and theorists alike, with the goal of characterizing the nature and the mechanism of the insulating and superconducting phases. To understand the electron correlation effects, Jian Kang and Oskar Vafek (NHMFL) used the microscopic model of the tBLG electrons to construct Wannier states (WSs) for the active four narrow bands. Such WSs serve as the localized basis spanning the same subspace as the well-known delocalized Bloch waves. As a byproduct, they also constructed the corresponding low energy tight binding model and showed that it reproduces the results from the microscopic model. Although the tBLG moire superstructure forms a triangular superlattice, the symmetry arguments force the WSs to be centered on the dual honeycomb lattice. Each WS has three peaks at its neighboring triangular moire lattice sites (Fig. 4.c.4).

### Charge Dynamics in Cuprates with Stripes

The dynamics of charge-ordered states observed in all underdoped cuprate high- $T_c$  superconductors, and the search for fluctuations of the incipient charge order ("fluctuating order", or "dynamic stripes"), have been the subject of intensive research with the goal to clarify their relationship to high- $T_c$  superconductivity. However, only static short-range charge-order (CO) domains have been detected in almost all cuprates. A group led by NHMFL scientist Dragana Popović has reported a novel

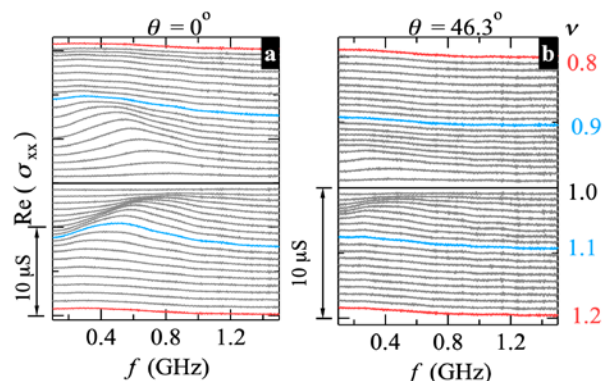


**Figure 4.c.3:** By studying a 2DES in a WQW as density and in-plane field are increased at  $\nu=1$ , Engel's group [2], in collaboration with M. Shayegan, has used pinning modes to locate the transition to Y111 from the single-layer  $\nu=1$ . The modes of the Y111 state (Fig. 1b) are shifted to lower frequency relative to those in the single-layer state. The pinning mode shift is the first observed signature of a new state of matter: a WS of excitations of the Y111 state. 1. H. C. Manoharan, Y. W. Suen, M. B. Santos, and M. Shayegan *Phys. Rev. Lett.* 77, 1813 (1996). 2. A. T. Hatke, Yang Liu, L. W. Engel, L. N. Pfeiffer, K. W. West, K. W. Baldwin, and M. Shayegan, *Phys. Rev. B* 98, 195309 (2018).

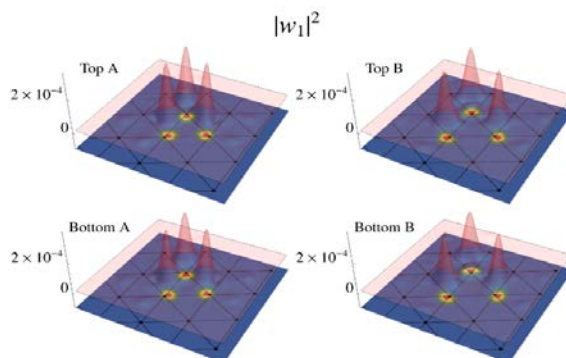


**Figure 4.c.4:** Based on the obtained WSs, Kang and Vafek then identified the favored ground states at simple integer commensurate charge concentrations in the strong coupling limit. They found that the projected (gate-screened) Coulomb interactions contain the terms beyond the cluster Hubbard model and favor the  $SU(4)$  ferromagnetic insulator at one quarter (or three quarters) filling of the four narrow bands. The kinetic terms, treated as the perturbation, break the  $SU(4)$  symmetry and favor the state in which two valleys with opposite spins are equally mixed. Furthermore, the stripe ferromagnetic insulator is proposed as the ground state at  $1/8$  filling.



study of domain dynamics in cuprates, based on time-dependent, nonequilibrium charge transport: They track the resistance of the system as it responds to a change in temperature and to an applied magnetic field. In  $\text{La}_{1.48}\text{Nd}_{0.4}\text{Sr}_{0.12}\text{CuO}_4$ , which has “striped” charge and spin orders, they find evidence for metastable states, collective behavior, such as avalanches in the resistance (Fig. 4.c.5) and criticality. Magnetoresistance (MR) measurements on another striped cuprate,  $\text{La}_{1.7}\text{Eu}_{0.2}\text{Sr}_{0.1}\text{CuO}_4$ , in which the structural and CO transitions are well separated in temperature, support the conclusion that the nonequilibrium dynamics obtained from the negative MR in  $\text{La}_{1.48}\text{Nd}_{0.4}\text{Sr}_{0.12}\text{CuO}_4$  (Fig. 4.c.5) is related to the CO and not to the structural transition. These findings provide the long-sought evidence for the fluctuating order across the CO transition and also set important constraints on theories of dynamic stripes [Baity, P. G.; Sasagawa, T. and Popović, D., Phys. Rev. Lett. 120, 156602 (2018)]. A related study [Stanley, L. J. *et al.*] led by D. Popović using the same technique has already revealed similar evidence of dynamic behavior on a stripe-ordered  $\text{La}_{1.875}\text{Ba}_{0.125}\text{CuO}_4$  in response to a temperature change. These experiments demonstrate that nonequilibrium protocols in charge transport can be a powerful tool to probe charge domain dynamics in correlated-electron systems.

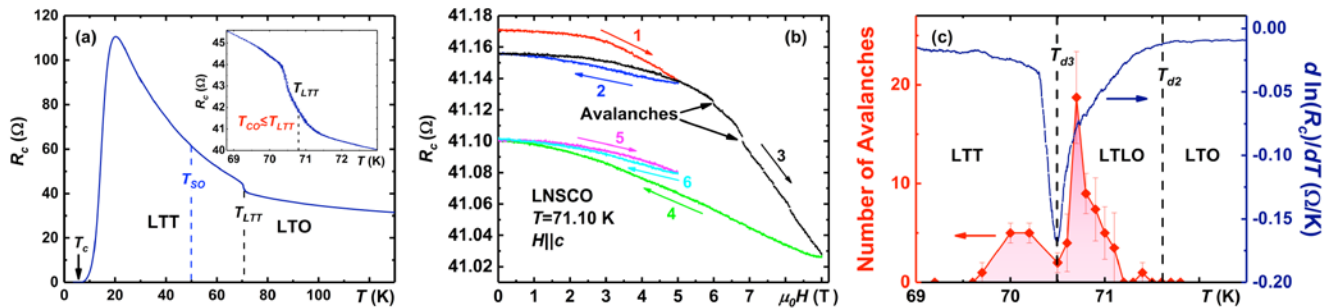


**Figure 4.c.5:** a) Out-of-plane resistance ( $R_c$ ) vs temperature ( $T$ ) in  $\text{La}_{1.48}\text{Nd}_{0.4}\text{Sr}_{0.12}\text{CuO}_4$ . Inset: Jump in  $R_c(T)$  is observed in the region of the transition from a low-temperature tetragonal (LTT) to low-temperature orthorhombic (LTO) phase at  $T = T_{LTT}$ ; TSO and TCO TLTT are the onset of static spin and charge stripe orders, respectively. b)  $R_c$  vs magnetic field ( $H$ ) after warming to  $T = 71.10$  K. The arrows and numbers show the direction and the order of field sweeps. MR exhibits a hysteresis with avalanches. Avalanches are observed only with sweeps to  $H$  higher than those applied previously, and only upon warming, as opposed to cooling, to the measurement temperature, i.e. as the system evolves from the CO/LTT phase. c) The average number of avalanches per MR measurement (red diamonds), after warming, vs  $T$ . In general, fluctuations are expected to peak at the phase transition, so the presence of two peaks is tentatively attributed to the onset of CO and precursor nematic order in the LTT and LTLO regions, respectively.

### Optical Conductivity of Overdoped Cuprate Superconductors: Application to LSCO

Recent measurements on both the superfluid density  $\rho_s$  and the optical conductivity  $\sigma_1$  of high quality LSCO films [1,2] showed properties apparently inconsistent with BCS theory, particularly a proportionality of  $\rho_s$  and  $T_c$  and a lack of any gap feature in  $\sigma_1(\omega)$ . Recently NHMFL theorist Peter Hirschfeld showed that these effects can be understood almost entirely within the theory of disordered BCS d-wave superconductors [3, 4]. The large scattering rates deduced from experiments were shown to arise predominantly from weak scatterers, probably the Sr dopants out of the  $\text{CuO}_2$  plane, and correspond to significant suppression of  $T_c$  relative to a pure reference state with the same doping. Recently, Hirschfeld and collaborators compared the results of dirty d-wave theory for LSCO and TI-2201 against experimental data. TI-2201 is found to be a factor of three cleaner, explaining the existence of quantum oscillations observed in this system, but still follows dirty d-wave predictions in the weak scattering limit. These results suggest that the

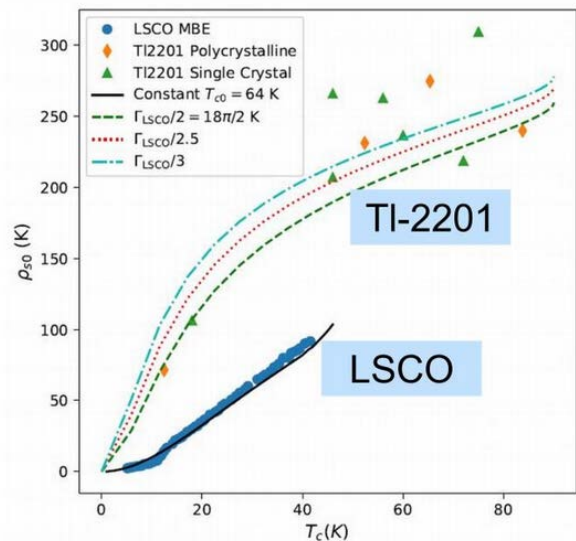


**Figure 4.c.6:** Superfluid density vs.  $T_c$  (left) and Sommerfeld coefficient vs. doping (right) for LSCO and TI-2201. Symbols experimental data and solid lines represent ranges of theoretical scattering rates compatible with data (same for left and right panels). N. R. Lee-Hone, V. Mishra, D. M. Broun, P. J. Hirschfeld, Phys. Rev. B 98, 054506 (2018).

overdoped cuprates can be understood within a theoretical framework based on the Landau-BCS paradigm (Fig.4.c.6).

### High-field Magnetostriction of Strongly Correlated CeRhIn<sub>5</sub>

Understanding, predicting and ultimately manipulating quantum ground states stemming from strong electron-electron interactions remains one of the central questions in physics, and CeRhIn<sub>5</sub> is a prototypical material to address this question.

Here, we use *state-of-the-art* optical dilatometry to probe the lattice response of CeRhIn<sub>5</sub> in high magnetic fields. We observe an expansion of the crystal lattice at  $B^* \sim 30$ T that is consistent with a change of the quantum mechanical ground state of this material (Fig. 4.c.7).

Understanding quantum materials not only advances our fundamental knowledge, but also enables their use in future technologies. This work particularly sheds light on the ground state of CeRhIn<sub>5</sub>, which is believed to share the same pairing mechanism found in high-temperature superconductors.

The new state of matter discovered in CeRhIn<sub>5</sub> only occurs above  $B^* \sim 30$ T, making NHMFL the only suitable facility in the US for this investigation.

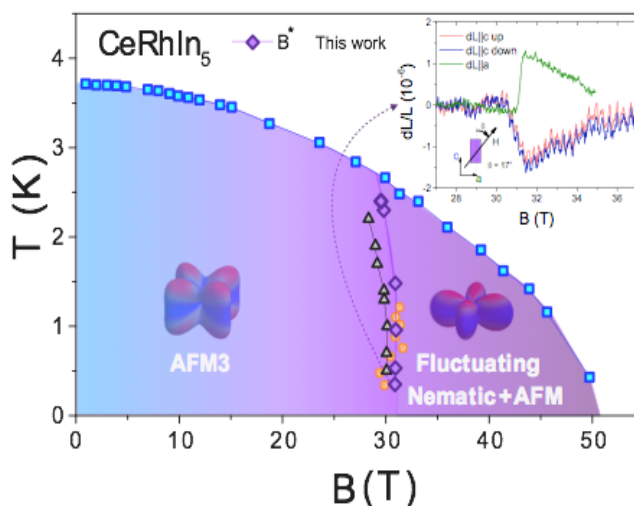


**Figure 4.c.7:** Magnetic field-temperature phase diagram of CeRhIn<sub>5</sub>. A field-induced change of the Ce *f*-electron ground state gives rise to enhanced hybridization that in turn promotes electronic nematicity. P. F. S Rosa, S. M. Thomas, F. F. Balakirev, E. D. Bauer, R. M. Fernandes, J. D. Thompson, F. Ronning, M. Jaime. *Physical Review Letters* 122, 016402 (2019).

### Flux Quantization in Asymmetric Superconducting Rings

A fundamental concept in superconducting loops is the well-known flux quantization condition. This law enforces a relationship between an electric current biased through the two branches of a loop and a persistent current, self-generated by the loop, such that the total flux is an integer multiple of flux quanta  $\Phi_0$ . A collaborative effort between the groups of Dr. P. Xiong and Dr. I. Chiorescu aims to get insight on

the details on this relationship in the case of asymmetric rings, for which either the cross-section or the length (or both) of each branch are tunable variables. At half-integer flux quanta (see Fig.4.c.8) a discontinuous behavior is expected, although it has yet to be observed experimentally. The study can have significant impact in the way classical or quantum superconducting electronics can be used and designed.

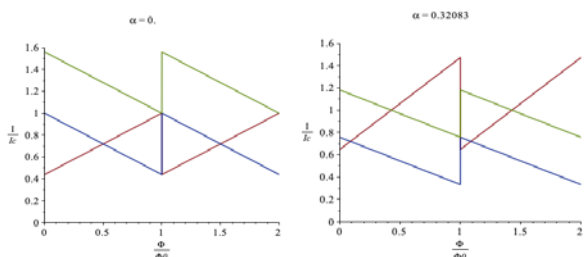


**Figure 4.c.8:** Switch at  $\Phi_0/2$  for the  $I_{sw}$  vs external flux  $F$ : With no asymmetry (left), the sequence is blue-red while for large length asymmetry (right), a jump blue-green is expected at  $\Phi_0/2$ . The length asymmetry parameter ' $\alpha$ ' is the ratio of branches length difference and the total perimeter.

of CoV<sub>2</sub>O<sub>4</sub> display an orbital glass transition associated with a small first order structural transition and a small amount of spin canting on the V-site at 90 K. The group of Prof. Christianne Beekman has been the first to grow a series of CoV<sub>2</sub>O<sub>4</sub> thin films onto SrTiO<sub>3</sub> substrates. In contrast to the weak effects seen in bulk samples, magnetization and neutron experiments on her films demonstrate distinct and unmistakable signatures of spin canting, and structural effects, which can be associated with longranged orbital order below 90 K. This implies that she has driven the system deeper into the insulating state. This work clearly shows that structural tuning associated with thin film growth is a viable knob to tune spin and orbital states, frustration, and itinerancy in spinel vanadate thin films. [Thompson C.J. et al ...: C. Beekman *Phys. Rev. Mat.* 2, 104411 (2018)]. (Fig. 4.c.9)

### Novel Noncollinear Spin Textures in Thin Films of Frustrated Magnets

Near-itinerant spinel vanadates, poster materials for orbital physics in frustrated antiferromagnets, provide an ideal test system to gain a better understanding on how orbital order can help relieve spin degeneracy. Ferrimagnetic below 150 K, bulk powders and single crystals

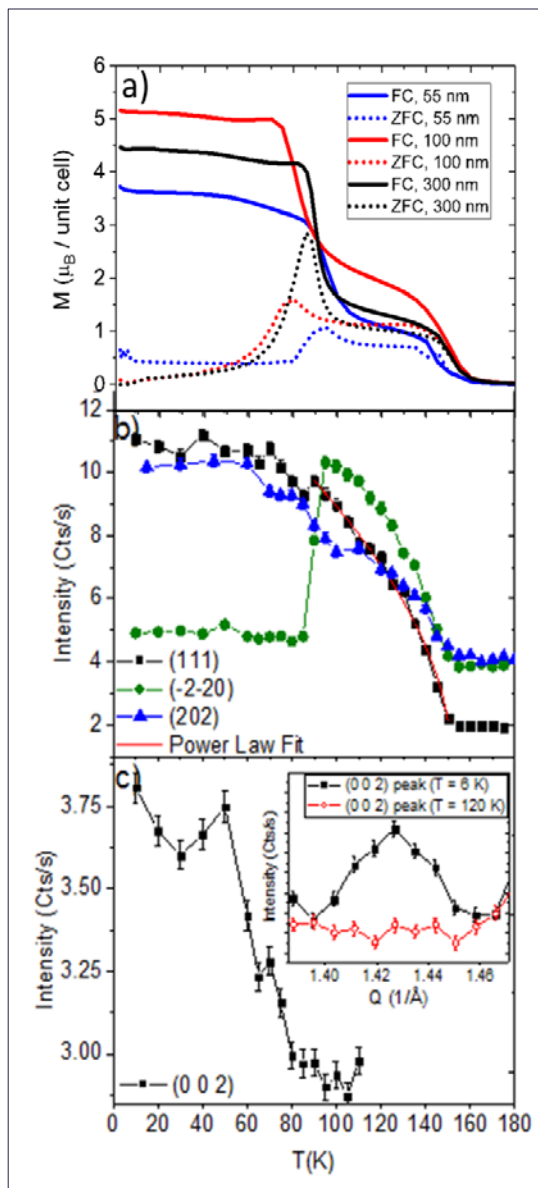
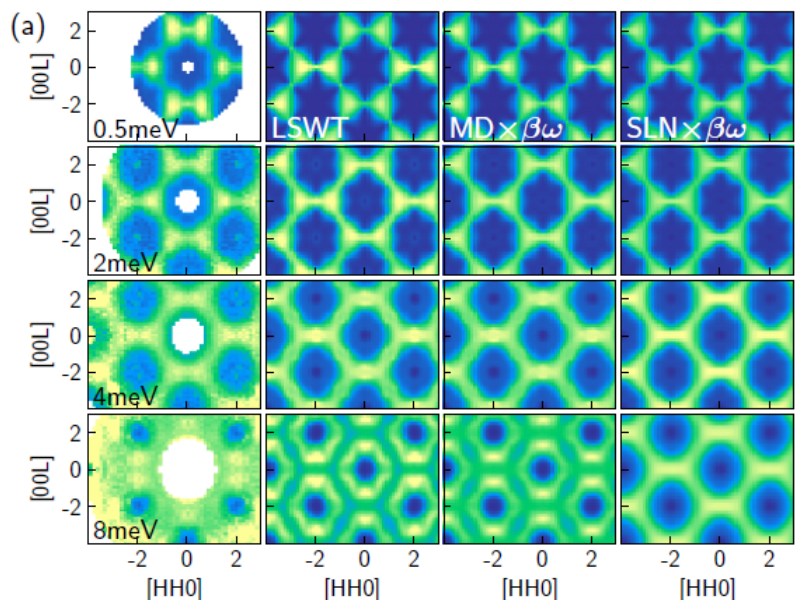


**Figure 4.c.9 left:**  $M$  vs  $T$  for a 55 (blue line), 100 (red line) and 300 nm (black line) film measured while warming in  $H = 1000$  Oe after cooling the sample in zero field (ZFC, dotted line), and after cooling the sample in the measurement field (FC, solid line). The field is applied in the  $ab$  plane. **b)** Neutron scattering measurements on a 300 nm thin film: (111) (black squares), (-2-20) (green circles), and (202) (blue triangles) Bragg peak intensities as a function of temperature. The red line is a power law fit. **c)** (002) Bragg peak intensity as a function of temperature. Inset: radial scan of the (002) Bragg peak at 6K (black squares) and at 120 K (red circles).

### Continuum of Excitations in a Near-Ideal $S=1$ Heisenberg Antiferromagnet on the Pyrochlore Lattice

Conventional crystalline magnets are characterized by symmetry breaking and normal modes of excitation called magnons with quantized angular momentum  $\hbar$ . Prominent exceptions are so called “quantum spin liquids” (QSL) – a prime example of a QSL being the one-dimensional spin-1/2 chain which has no magnetic order and where magnons accordingly fractionalize into spinons with angular momentum  $\hbar/2$ . This is spectacularly revealed by a continuum of inelastic neutron scattering associated with two-spinon processes and the absence of magnetic Bragg diffraction. We report evidence for these same key features of a QSL in the three-dimensional Heisenberg antiferromagnet  $\text{NaCaNi}_2\text{F}_7$ . Through specific heat and neutron scattering measurements, Monte Carlo simulations and a study of spin-dynamics, we have shown that  $\text{NaCaNi}_2\text{F}_7$  is an almost ideal realization of the spin-1 antiferromagnetic Heisenberg model on a pyrochlore lattice. Magnetic Bragg diffraction is absent and 90 percent of the spectral weight forms a continuum of magnetic scattering not dissimilar to that of the spin-1/2 chain but with low energy pinch points indicating  $\text{NaCaNi}_2\text{F}_7$  is in a Coulomb phase. The residual entropy and diffuse elastic scattering points to an exotic state of matter driven by frustration, quantum fluctuations and weak exchange disorder (Fig. 4.c.10).

**Figure 4.c.10 (right):** Comparison between inelastic neutron scattering data for the dynamical structure factor in the  $[HHL]$  plane compared to our theoretical modelling of it. The colors are indicative of the intensity – yellow is more intensity, blue is less intensity. Three theoretical methods were investigated: LSWT (linear spin wave theory in real space applied to inhomogeneous ground states), MD (molecular dynamics) and SLN (stochastic large- $N$  approach). The clear observation of “pinch points” at low energy is the hallmark of a Coulombic spin liquid. K.W. Plumb, H. J. Changlani, et al., *Nature Physics*, 15, 54-59 (2019); S. Zhang, H.J. Changlani et al., under review in *Phys. Rev. Lett.* (2019).





#### d. Magnets and Magnet Materials

*A central feature of the MagLab's mission is the provision of unique, high-performance magnet systems that exploit the latest materials and magnet design developments for our users. As we move forward, maintaining a balance of development of new magnet systems with new technology is of critical importance to keep us at the forefront. Collaborations with other leading industrial, academic and government groups that develop these new magnet technologies is built into many of these thrusts.*

#### Executive Summary

At the end of 2017 the MagLab announced completing the construction of the world's first 32T all-superconducting magnet. This constituted an 8T step beyond the previous record of 24T set earlier the same year by the High Field Laboratory for Superconducting Materials in Tohoku, Japan.

This year we are pleased to announce the start of the next major new magnet project: a 40T all-superconducting magnet funding for the first year of this project was received from NSF in the fourth quarter of 2018. The project is initially considering four different magnet technologies that might be appropriate for such a system: insulated Rare Earth Barium Copper Oxide (REBCO), no-insulation (NI-)REBCO, Bi-2212 and Bi-2223. Advantages and disadvantages of these four technologies are being considered, design calculations are being performed and test coils are being made. As data from the tests is analyzed and models updated, we intend to soon start down-selecting toward the technology that will be used for the final user system.

Of these three conductors, REBCO became available first in a high-strength form in 2007 and was chosen, with insulation, for the 32T magnet. Extending this technology to 40 seems feasible, but is not trivial. The tape being produced today has higher performance than what was available a few years ago. Consequently a 40T magnet will need to be designed for higher current than the 32T, which means more steel reinforcement and copper stabilizer are required. Higher field also means protecting a larger magnet from a larger amount of stored energy, which requires upgrading from a battery-base system to a capacitor based one. Finally, it requires confidence in the uniformity of tape that is provided, which is still a concern at this point.

Using REBCO without insulation results in much less copper stabilizer being required in each electrical turn of conductor. This makes a smaller magnet, which results in lower stress. Hence less steel reinforcement is required and the magnet gets smaller still. This approach resulted in a test coil that produced 14T in a 31T background field (45T total) in 2017, but there is not yet a clear plan of how to protect such magnets when they quench.

In addition, the MagLab has been working with the High energy Physics (HEP) community for several years and has produced dramatically improved Bi-2212 wire by improving the quality of Ag powder used in fabrication. In addition, over-pressure heat treatment has resulted in higher current densities within the wire. Recent test coils with internal reinforcement have demonstrated that highly stressed coil should be possible, however, there is still a lot of work required to scale this technology to the 40 T level.

In the pulsed magnet arena, the first duplex magnet was tested in 2018 and construction of the large pulsed coils has been moved from the commercial sector to the FSU-branch of the MagLab. This has resulted in better quality control being implemented in the conductor-inspection process and the coil-winding processes. This shows good promise for higher quality coils in the Pulsed Field Facility in coming years.

#### HTS Magnets and Materials

##### **32T Magnet Project**

As reported last year, the 32T superconducting magnet reached its design magnetic field in December 2017 and passed all the planned tests during its first test in liquid helium. To date that still represents the highest field reached with a superconducting user magnet. For comparison, the highest field superconducting user magnet in routine service is the 24 tesla magnet at Tokoku University, Sendai, Japan.

As planned, the 32T magnet was warmed up after the first test for inspection. While the magnet generally looked pristine, some deformation was observed at two of the HTS terminals that suggested a further investigation was warranted. After partial disassembly and a detailed analysis of the available test data, it was determined that the root cause of the problem is in the mechanical structure of the supports for the coil flanges. When the magnet is energized, Lorentz forces compress the coil axially. While the magnet was designed to accommodate this motion, and the prototype coils did accommodate this motion properly, the strain relief system was not working properly in the full-scale



coils. While the magnet can be operated as intended, leaving this unaddressed would likely result in a short lifetime for the magnet. Proposed minimally invasive solutions were first tested stand-alone, before selecting and implementing changes to the flange support structure and modifying the terminals. Additional instrumentation will monitor relative movements of various magnet components in the future to help verify the modifications are working as intended.

Currently the 32T magnet system has been fully reassembled. Both of the REBCO coils have had modifications and both are now reassembled. The two REBCO coils have nested within each other and have been installed in the LTS coils, which were then installed in the cryostat in February 2019. The cryostat is in its permanent location in the new Millikelvin building extension and the Variable Temperature Insert had previously been verified to fit the magnet. Tasks remaining are mainly completion of various aspects of the control, protection and user-interface hardware and software.

#### **40T Magnet Development**

The MagLab has initiated the world's first project to construct a superconducting (SC) magnet to routinely serve condensed matter physics (CMP) users at 40T. Funding for the first year of the project was awarded by NSF in September 2018. The 40T superconducting magnet is expected to establish another new international standard for Ultra-High Field (UHF) operations, joining the MagLab's other unique facilities such as the 100T pulsed magnet, 45T hybrid, 41.5T resistive magnet, 32T SC magnet and 21.1T MRI and ICR magnets. It will also serve to develop technology that may enable the construction of CMP magnets beyond 40T as well as help enable other types of SC magnets for NMR, x-ray and neutron scattering, etc. As the technology matures, the targets will be reviewed and updated. As a fully superconducting magnet, the system confers intrinsically lower noise for experimentalists than resistive magnets, as well as opportunity to dwell at high fields for extended periods of time. These capabilities would enable a 40T SC magnet to support higher-sensitivity measurements than possible in present-day resistive and hybrid magnets—high-magnetic-field measurements that will be uniquely capable of addressing physics questions from previously inaccessible perspectives on a number of expanding frontiers in condensed matter physics.

Realization of a 40T SC magnet requires technology that is beyond the present state-of-the-art. Quench and stress management present the most challenging risks, which are presently without mitigation strategies for either a single or a combination of HTS material approaches. Three presently viable insulated HTS conductors (REBCO, Bi-2212, Bi-2223), as well as a fourth no-insulation REBCO alternative (NI-REBCO) provide complementary and somewhat independent lines to attack the significant technical challenges. Insulated REBCO (I-REBCO) formed the basis for the MagLab 32T superconducting magnet, and further development of quench management could allow a conceptual design to draw heavily from this success. No-Insulation REBCO (NI-REBCO) was used in a MagLab test coil that reached 14T in a 31T resistive magnet, for total of 45T, in 2017, and this approach offers the opportunity to make UHF coils very compact and possibly much cheaper than other approaches. Bi-2212 coils take advantage of huge improvements in wire performance, achieved by MagLab in partnership with Department of Energy programs and other advances in coil technology over recent years that now make this component worth consideration. Bi-2223 has been demonstrated in several coils in Japan and elsewhere, which has attractive features due to improvements in reinforcement technology.

While no basis exists at present for a conceptual 40T SC magnet design, maturity of the options above should retire some risks by late 2019, and even more by 2020, to allow design of a viable base concept with alternatives. This is a prerequisite to begin a more formal construction project with appropriate baseline and governance. The maturation of technology follows the inner turns of a spiral as shown in **Figure 4.d.1**. The whole spiral traces a risk-retirement approach, originally introduced in the software-development industry. The spiral process is iterative: The start of the process (point 1) considers the available concepts and their known unknowns, and then performs risk analysis to help determine what technology gaps need be closed to advance key technology components. Focused tasks, analysis and prototyping (in the 40T SC case test coils) generate data regarding the risks as well as revealing other uncertainties (unknown unknowns) of the technology. The spiral completes at a critical decision stage where the increased technology maturity is applied to improvement and advancement of concepts, which could result in retirement of some approaches. The next spiral starts with a more detailed design and alternatives and applies new risk analysis. The process repeats with each successive spiral reducing risk further until a final design with a well-supported baseline, cost controls, key performance parameters and other project requirements can be created and defended, at which

point a construction project for the final magnet can start. Only one spiral is planned at a time and each spiral ends with the planning of the next spiral or completion of the user magnet. The scope is managed by continuous delivery of increments based on technical milestones.

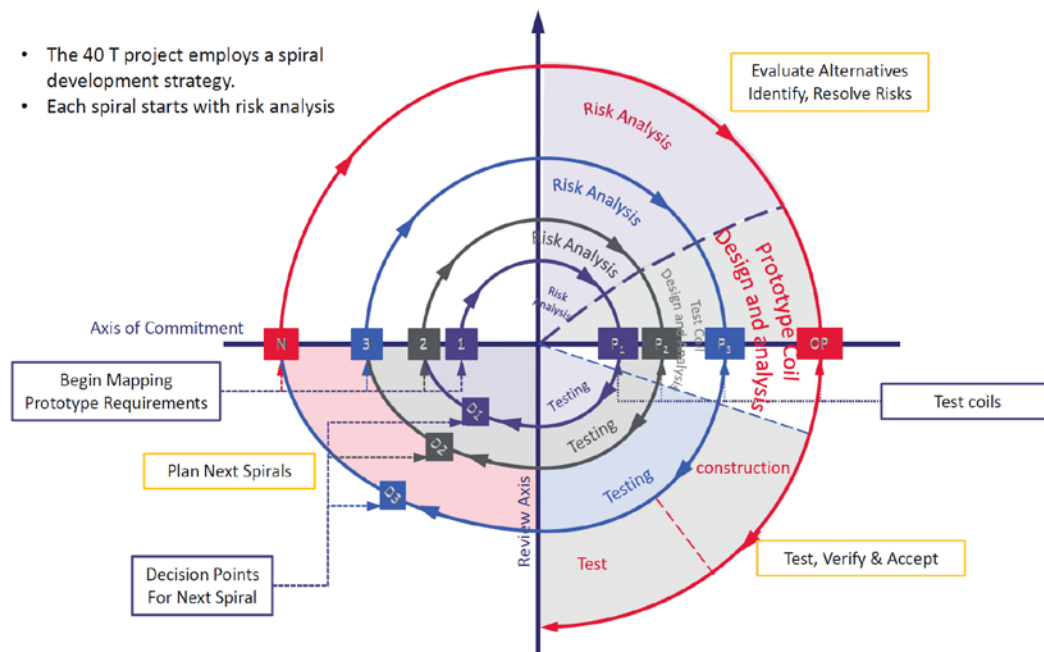


Figure 4.d.1: Spiral management plan for the 40T superconducting magnet project.

In Spiral One we are consolidating and validating technology through analysis and small coils testing. Each test provides critical knowledge and demonstration of increased technology maturity toward conceptual designs of the 40T superconducting magnet. Spiral one will advance each technology path, target and remove risks and facilitate down-selection decisions as soon as possible. In late 2018, Spiral One of the 40T project was planned and each technology has started to implement the plan. The driving questions and risks of each technology were analyzed, the scope of spiral one was defined, the work breakdown structure (WBS) was created and the tasks are scheduled and resources have been assigned. Microsoft Project is used for the scheduling and resources assignment. Spiral one was baselined and it will last one and a half years.

#### **No-insulation REBCO (NI-REBCO) Coil-Development**

The objective of the research performed this year on No-Insulation Coil Technology with REBCO coated conductors was to develop technology suitable for UHF CMP magnets. Some of the work was a continuation of quench analysis work that had started years earlier while part was analysis of screening currents undertaken as part of the 40T effort and to enable a large-bore NI-REBCO magnet that was proposed to be built. Much additional work was inspired by the “Little Big Coil” (LBC) tests.

The LBCs were a series of NI-REBCO test coils that were made to fit within a 31T resistive magnet for the purpose of pushing the envelope of high field magnet technology. In fact, a record field strength of 45.5T was generated with the third LBC (LBC-III) in 2017 [1]. In examinations of the HTS tape from this test coil, it was observed that plastic deformation of the high strength Hastelloy substrate and fracture and delamination of the copper plating and REBCO layer occurred in many of the coil pancakes resulting from a high-field quench. We have identified that screening current, induced even in a normal charging operation as well as upon a quench, plays an important role in the stress state of the conductor. While the transport current flows along the length of the conductor (theta-direction in the coil) the screening currents are positive and negative currents on the edges of the tape, one in the same direction as the transport current, the other in the opposite direction. While the transport current interacts with the axial component of field to give a Lorentz force that is radially outward, the screening current typically generates radially inward force on the tape edge closest to the mid-plane of the coil and outward force on the edge further from the mid-plane. This effectively adds a “diamagnetic torque” to the tape which will result in stresses higher than what would occur if there were no screening current. This can result in plastic deformation of the tape and cracking of the REBCO layer. Also, when a quench occurs in an NI-REBOC coil, it induces extra current in neighboring turns. The manufacturing process of slitting HTS tape

to the desired width exacerbates the problem by creating cracks, which can be fracture initiation sites. Orienting cracks away from the tape edge being placed in tension has shown that this failure mode can be mitigated [2], which we discuss further below. Therefore, a key aspect of NI magnet technology is a proper orientation of the not-slit edge to mitigate the damage to the superconducting REBCO layer during plastic deformation of the composite tapes in an ultra-high field magnet [1].

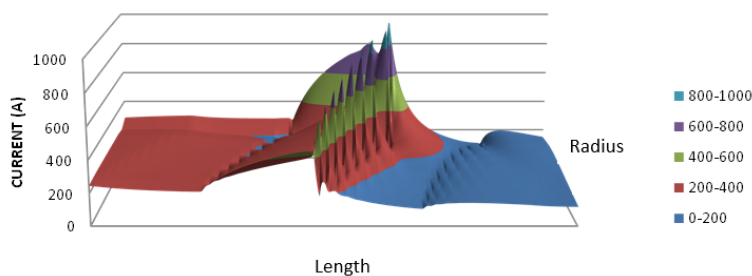


**Figure 4.d.2:** Results of LBC quench analysis showing propagation of induced currents starting from the right side of the graph and sweeping down the coil.

Quench analyses of LBC-III were performed which simulate the behavior of the induced currents. A snapshot of the computed current distribution in the coil is shown in **Figure 4.d.2**. The coil was initially at 250 A. A quench was initiated on the right side of the plot (end pancake) and the wave of induced currents flows through the windings. We see that peak currents may be >800 amps. Given that this coil is operating inside the magnetic field of the resistive magnet which is still energized, the stresses due to these current spikes might cause damage.

A systematic study was performed with short versions of the LBC solenoids tested in the 31T, 50 mm bore resistive magnet. Three coils were tested, all of the same dimensions but with variations on the orientation of the conductor's slit edge and of the applied radial field (altering the induced screening currents). It was demonstrated that if the slit edge of the conductor was oriented outward from the coil's mid-plane and placed in a region of high radial field, then yielding and fracturing was more likely to occur. Tensile stress at the tape edge drives cracks across the width. **Figure 4.d.3** shows typical images of conductor examined after testing. In contrast, when the slit edge was oriented inward toward the coil's mid-plane, yielding and fracture did not occur. Compressive stress at the edge was created for this orientation, which did not drive cracks across the tape.

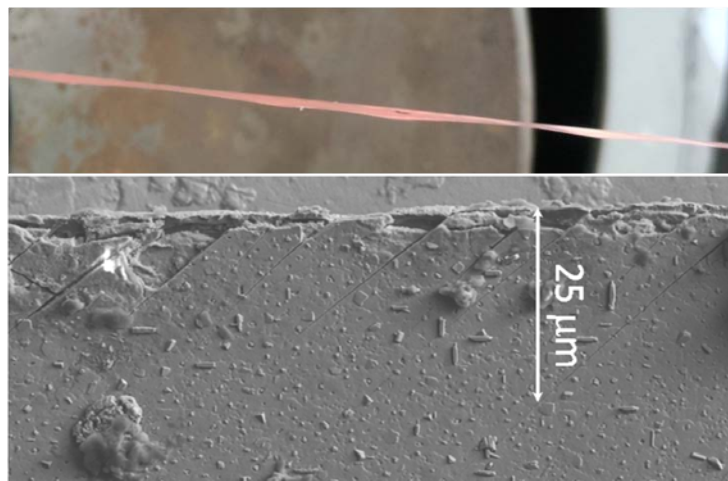


**Figure 4.d.3:** Images from examination of REBCO tape after operation in UHF test coil. Macroscopic plastically deformation is seen in composite tape (above) as well as micro-cracks within the REBCO layer (below).

This was performed again in a 15T background field on small coils that were wound with a conductor that does not have a mechanically slit edge. The results are similar where plasticity occurred in the coil placed in relatively high radial field yet the REBCO layer did not fracture. The conductor did not show any permanent degradation after reaching field, which indicated that, although the stress level was high enough to yield the substrate, it was not high enough to delaminate the REBCO layer.

Commercial REBCO composite tape consists of a high-strength substrate with buffer layers, a thin film (~1 micron) of REBCO, Ag and Cu. Some suppliers use stainless steel 310 for the substrate while others use Hastelloy. The yield strengths of the two materials can be similar. However,

formation of the REBCO superconducting film requires deposition at a temperature in the 750-800 °C range. Test performed at the MagLab [3] indicate that this high-temperature deposition can anneal the SS310 sufficiently to reduce its yield strength, while the nickel-based Hastelloy actually experiences an increase in strength due to age-hardening. These data are shown in **Figure 4.d.4** [3].

Additionally, studies on the ability to prescribe the contact resistance between turns of conductor have been carried out. During charging of no-insulation coils, the charging current initially flows radially through the coil through a resistive path and moves into the superconducting spiral path at a rate given by the inductance and resistance of the coil. Consequently, the field generated is not proportional to

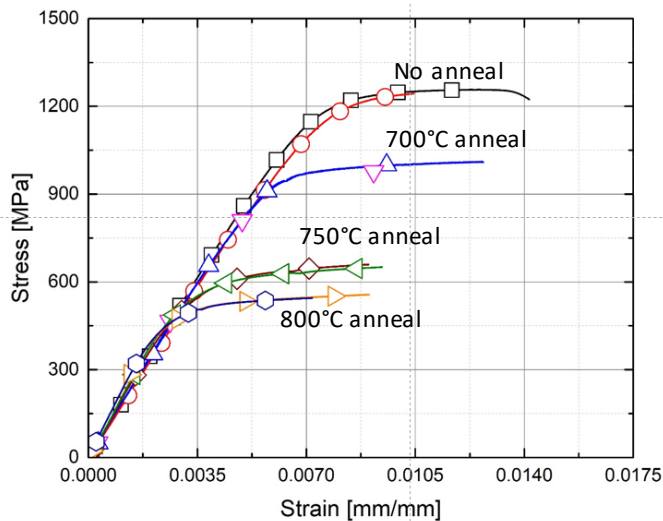


**Figure 4.d.4:** Stress-strain of substrate material stainless steel 310 subjected to elevated temperatures.

temperature and fatigue have begun for evaluating various conductors. A processing line to modify the surface conditions of REBCO and reinforcing co-wind tapes is being fabricated in order to prescribe the contact resistance over long lengths of material. A series of small test coils are in design with the objectives to study fatigue, screening currents and quench propagation. A typical coil configuration is shown in Figure 4.d.5

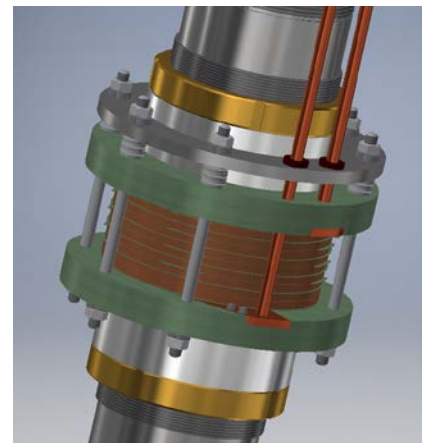
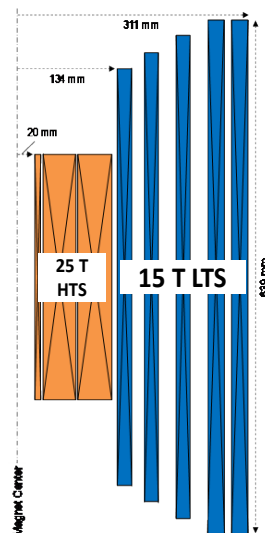
#### References

- [1] Seungyong Hahn, Kwanglok Kim, Kwangmin Kim, Xinbo Hu, Thomas Painter, Iain Dixon, Seokho Kim, Kabindra Bhattarai, So Noguchi, Jan Jaroszynski, and David Larbalestier, "World Record DC Magnetic Field using an REBa<sub>2</sub>Cu<sub>3</sub>O<sub>x</sub> (RE = Y,Gd) Superconducting Magnet" *Nature*, to appear.
- [2] Xinbo Hu, "Studies on the origins and nature of critical current variations in rare earth barium copper oxide coated conductors", dissertation for PhD in materials science and engineering, Florida State University, 2017.
- [3] Kyle Radcliff, "Mechanical properties of superpower and Sunam REBCO coated conductors", master's thesis for mechanical engineering at Florida State University, 2018.
- [4] Lu, J.; Levitan, J.; McRae, D.; Walsh, R., "Contact resistance between two REBCO tapes: the effects of cyclic loading and surface coating", *Superconductor Science and Technology*, 31, 085006 (2018).

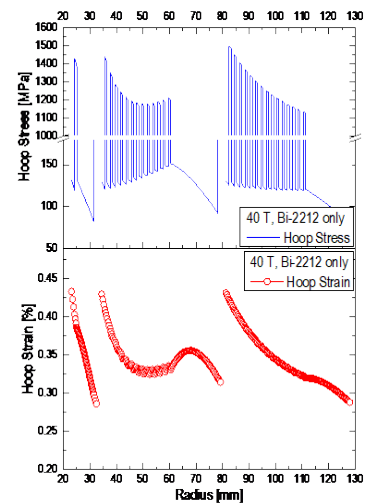
#### Bi-2212 Coil Technology

Efforts on the application of Bi-2212 round wire for high field nested solenoids and accelerator magnets for the HEP community are further

**Figure 4.d.6:** Left: Hypothetical 40T magnet design using a 25 T Bi-2212 insert. The stresses on the coil reinforcement are exceptionally high. Right: Performance of LBNL made and NHMFL OPHT<sup>ed</sup> race-track coils over the past years. OPHT and new Bi-2212 powders dramatically boosted their transport properties.



**Figure 4.d.5:** Mechanical model of a six double pancake test coil for fatigue studies.





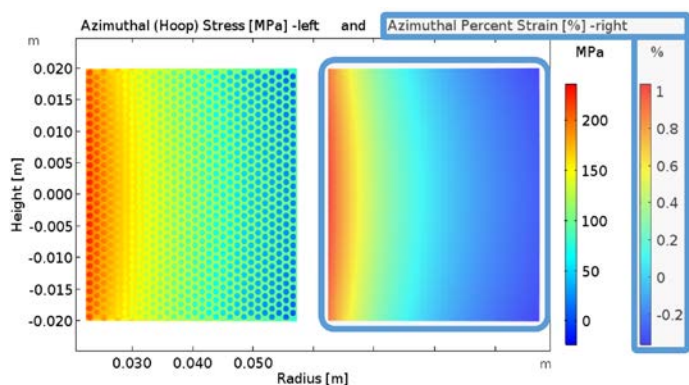


**Figure 4.d.7:** Stress test coil to operate in 14T background. The coil specifications are: 44.5 mm ID, 116.5 mm OD, 30 layers, 30 turns, 40.5 mm tall. It will use 228 m of 1.0 mm dia. wire. Unmitigated strain will be on the order of ~1percent, which makes it a good candidate to evaluate the efficiency of coil reinforcement schemes.

in high background fields of up to 14T. The designs are based on FEA models that are laid out to mitigate stresses so that peak strains of less than 0.4 percent can be achieved anywhere in the coil. An FEA model of non-reinforced test coil in a 14T background field is shown in **Figure 4.d.7**. It can clearly be seen that under unmitigated conditions, peak strains raise beyond 1 percent, which would destroy the coil immediately. These conditions make this coil a good candidate to explore various reinforcement schemes. A superconducting magnet made by Cryogenic LLC has recently been installed and put into commission at the ASC (**Fig. 4.d.8**). It will be used as a high field test bed for these coils. With background fields of up to 14T and a large cold-bore of 161 mm it will allow for coil mechanics tests that were not possible to accomplish in our existing 8 T magnet system. To evaluate the mechanical properties of coils reinforced with high strength alloy tape, two coils have been made and tested using aspected conductor with a high strength alloy tape bonded to it and aspected conductor with high strengths alloy tape added as a co-wind, respectively. The bonded conductor was provided by Solid Materials Solutions (SMS) Inc. These coils were tested in our 8T cryo-cooled magnet, **Fig. 4.d.9.a, b**. Two more race-track coils made with Bi-2212 17-strand Rutherford cable were made by LBNL. One coil, RC-6, was over pressure heat treated (OPHT) and tested while the other coil, RC-7, will be OPHT'ed and tested soon.



**Figure 4.d.8:** The 14T LTS background magnet made by Cryogenic LLC.

Both coils wound with aspected conductor performed well during the tests. The coil made with SMS wire mitigated a maximum stress of ~300 MPa before degradation while the co-wound coil could not be degraded in the 8T background and may be tested again in the now available 14T cryogenic magnet. In tests at LBNL RC-6 achieved a critical current of ~8600 A, which is the highest performance among all Bi-2212 race-track coils made at LBNL so far. The desire of heat treating larger race-track coils as well as solenoids has generated funding through DOE and NSF for a project

gaining momentum. For high field solenoids, Bi-2212 is currently being explored as a part of the NHMFL's ongoing 40T project. Operating conditions at 40T are extremely demanding on the coil mechanics and have yet to be explored in HTS coils in general. A series of test coils will be built and tested in the coming year to evaluate various coil reinforcement schemes, **Figure 4.d.6 left**. For HEP several more race-track coils have been made at LBNL and over pressure heat treated in our high pressure furnace. Performance test that were successfully carried out at LBNL showed very high transport properties and also that an upper critical current limit has yet to be reached, **Figure 4.d.6 right**.

Bi-2212 round wire wound solenoids carrying various amounts of reinforcement are currently being designed, which will be tested



**Figure 4.d.9.a, b:** Two test coils made with a) aspected conductor made by SMS and b) aspected conductor co-wound with high strengths alloy tape. The high stresses caused the winding pack of coil a) to completely snap at one location.

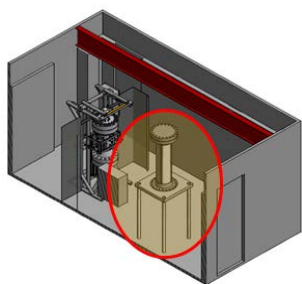


**Figure 4.d.10:** New over-pressure furnace sitting next to its current counterpart in our furnace room. It will be about 81" tall with a furnace tube diameter of 18". First heat is expected during the first half of 2020.

to build a larger over pressure furnace to accommodate these needs. All of our over pressure heat treatments so far were carried out at a pressure of 50 bar. Though some additional conductor densification can be achieved applying 100 bar of pressure (the original design of our current over pressure furnace), there is only small further gain in transport properties. Hence the new furnace has been designed to operate at a maximum pressure of 50 bar. Particularly to accommodate larger racetrack coils, the furnace will have a homogeneous working hot zone of 1 m and a working diameter of 305 mm. This project has just started and the new furnace is expected to be completed within a time frame of two years, **Fig. 4.d.10**.

This work is supported by the National Science Foundation under DMR-1157490 and the State of Florida. A portion of this work was also supported by a grant from the National Institute of Health under 1 R21 GM111302-01 amplified the U.S. Magnet Development Program (MDP) funded by the US Department of Energy.

#### Bi2223 Coil Development

Fabrication and testing of layer-wound coils made with Sumitomo Bi-2223 Type HT-NX conductor is ongoing. A test coil, named 'Tall-Thin' (**Fig. 4.d.11**), was made and operated at 1.3T in a 10.4 Tesla background to perform an NMR measurement at 500 MHz. An NMR map of the field was performed, which confirmed expectations for field magnitude and homogeneity (**Fig. 4.d.12**).



**Figure 4.d.11:** Bi-2223 test coil 'Tall-Thin' 1- The measured field homogeneity of the 'Tall-Thin' coil in the IMPDAHMA background magnet at 500 MHz was 116 ppm, which was in substantial agreement with the calculated homogeneity of 128 ppm.

During the test of the 'Tall-Thin' coil, the commercial outer coils suffered a quench during the ramp to a 600 MHz field. A subsequent test of the commercial coil set was performed with extra voltage taps to identify the location of the failed section. Findings

from the test indicated that the failure was on one of the inner Nb<sub>3</sub>Sn coils.

The test also indicated that the remaining coils are healthy. A design study was performed and we are considering replacing some of the coils from the LTS coil set to upgrade this important test facility.

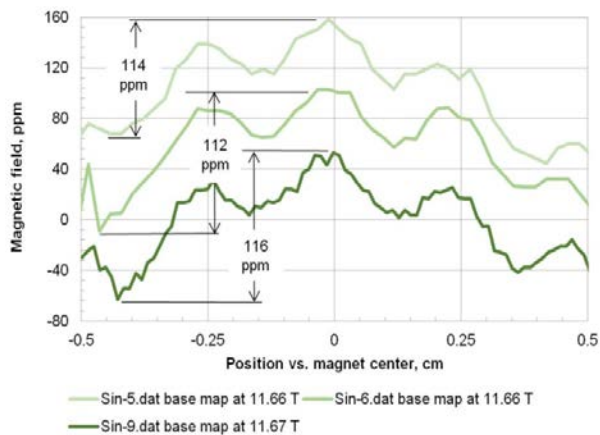


**Figure 4.d.12:** NMR field maps of Tall-Thin and IMPDAHMA at 500 MHz.[1]

whom have been supported under DOE-HEP SBIR awards since 2014. As we know, no magnet is ever better than its conductor and no Bi-2212 conductor will be better than its powder. The powder quality depends on its composition, phase assemblage, particle size distribution, tap density and content of carbon, hydrogen and impurity elements. Most of our effort on Bi-2212 powder since 2016 has been focused on characterizing Bi-2212 powders produced by nGimat and MetaMateria. Our main tasks include identifying the amount of hard particles, impurity phases and any contamination picked up during production. In 2018 we did overpressure heat treatment (OPHT) for all the DOE-HEP SBIR supported powder producers and their Bruker-OST manufactured wires so as to evaluate the outcome in a consistent way and to provide feedback to the powder manufacturers for further improvement in their

#### Bi-2212 Conductor Development

An essential component of Bi-2212 wire is the precursor powder because it affects the wire performance significantly. Nexans in Germany was the only supplier of Bi-2212 powder for the past decade but they stopped Bi-2212 powder production when they moved their operation from Cologne to Hannover in early 2015. To replace Nexans powder, we have been working closely with nGimat and MetaMateria, both of

product. Critical currents of fully processed Bi-2212 wires were measured in a 31.2T resistive magnet at the NHMFL.

Figure 4.d.13 shows engineering critical current density  $J_E(B)$  and critical current density  $J_C(B)$  for wires pmm170123 (55x18, 0.8 mm dia.) made from nGimat powder LXB-52 and pmm171024 (55x18, 0.8 mm) made from MetaMateria powder MM318. For comparison  $J_E$  and  $J_C$  data are shown for wire pmm151103 (121x18, 1.0 mm) made with Nexans lot 87, which was the best Nexans powder lot. Record  $J_C(4.2K, 15T)$  of 6860 A/mm<sup>2</sup> and  $J_E(4.2K, 15T)$  of 1365 A/mm<sup>2</sup> were achieved for wire pmm170123.  $J_C(4.2K, 15T)$  was increased by over 60 percent over the previous record  $J_C$  of 4200 A/mm<sup>2</sup> for wire pmm151103 (Nexans

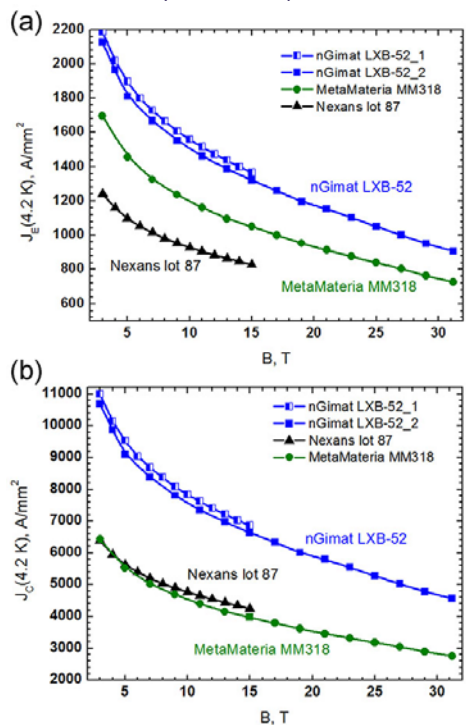


Figure 4.d.13: Comparison of wires pmm170123 (nGimat LXB-52), pmm171024 (MetaMateria MM318) and pmm151103 (Nexans lot 87). (a)  $J_E(4.2K)$  and (b)  $J_C(4.2K)$  as a function of applied field.

lot 87). The  $n$  values for pmm170123 are about 30, which is higher than the range of 15 to 20 of previous 0.8 mm wires, which we believe indicates that the filaments are more longitudinally uniform. Based on our OPHT evaluation, nGimat later donated their SBIR wire pmm170123 to LBNL for racetrack coil testing and wire pmm170725 to LBNL for CCT coil testing. LBNL achieved new record critical currents for the racetrack coil made from pmm170123. nGimat wire pmm170823 was used for Bruker-OST twisting test, and we did OPHT for this twisted wire.

Both nGimat and MetaMateria have made significant progress in manufacturing Bi-2212 powder in the past three years. Our contribution to the powder development has resulted in the establishment of LXB-52 as nGimat's standard composition for current commercial powder production. In 2017 and 2018, Bruker-OST produced nine 2 kg billets and eight 10 kg billets using the powders made by nGimat and four billets of 2 kg from MetaMateria powders. A most recent 10 kg wire (pmm180928) with a diameter of 1.0 mm made with nGimat powder was delivered to FSU in a single piece of 1355 m. This is by far longer than tapes of REBCO and Bi-2223, at least in the strengthened Bi-2223-NX needed for magnet use.

#### References

[1] Jiang, J.; Bradford, G.; Hossain, S. I.; Brown, M. D.; Cooper, J.; Miller, E.; Huang, Y.; Miao, H.; Parrell, J. A.; White, M.; Hunt, A.; Sengupta, S.; Revur, R.; Shen, T.; Kametani, F.; Trociewitz, U. P.; Hellstrom, E. E.; Larbalestier, D. C. "High-Performance Bi-2212 Round Wires Made With Recent Powders", *IEEE Trans. Appl. Supercond.*, 29 (5), 6400405 (2019).

## Resistive Magnets and Materials

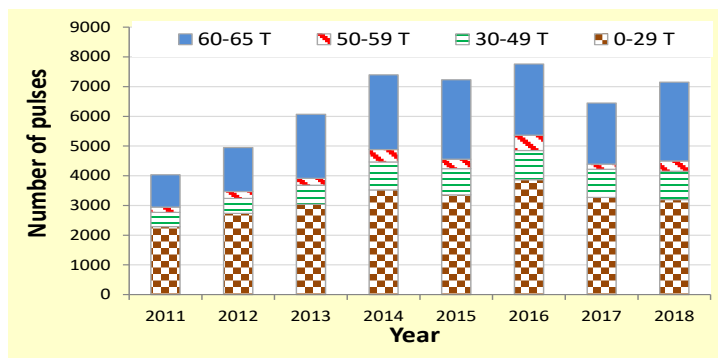
### DC Magnets

In 2018, the resistive magnet team witnessed the first full year of operations of the 36T series-connected hybrid magnet, which provided a record amount of magnet time without maintenance (1,770 hours). In addition, the new 41T magnet was modified and tested to 41.6T, presently the highest field worldwide for resistive magnets. Fifteen coils were built for use at the MagLab and a spare coil was delivered to the Helmholtz Zentrum Berlin.

### Pulsed Magnets

**Short-pulsed magnets developed at LANL:** As seen in Figure 4.d.14, the four user cells of 65T workhorse magnets delivered a total of ~7,100 shots in 2018, of which ~2,700 shots are 60T and above. These numbers are comparable with those of recent years,

Figure 4.d.14: Number of pulses and their peak magnetic field distribution delivered by 65T magnets in period 2011–2018.





although the 4 MJ capacitor bank (cap-bank), which is used to power the 65T magnets, were shut down three weeks in June 2018 for maintenance and adding new switches for the new duplex magnet cell. We have successfully maintained the magnets available in all four cells at all time during the year for users and always have a few spare magnets on the shelf. In 2018, seven new magnets have been built and six magnets were retired after their service in the user program.

To date, the capacitor-driven magnets have consisted of a single circuit. All coils electrically in series driven by a single capacitor bank. Separately powering (nested) coils allows us to both reduce the driving voltages and have a further degree of control over the pulse duration and/or current density in the various section of a magnet to maximize field. Design and construction of a duplex magnet with two nested coils powered separately by two capacitors was completed in 2017. In 2018, the PFF-NHMFL focused on modifying the hardware and control software of 4 MJ capacitor bank to enable the safe testing of the first duplex magnet. A new power transmission line with associated safety switches was installed to safely deliver the energy from the 4 MJ capacitor bank to the new duplex magnet cells. The switching system and the control of the 4 MJ capacitor bank were reconfigured so that the operation the new duplex magnet does not impact the performance of 65T workhorse magnets. The duplex magnet was designed to test to 80T and should provide 75T to users during regular operations. The design of the duplex magnet relies heavily on Zylon fiber to bear for high hoop load at 80 Tesla. Zylon fibers are wound with pre-tension at the outer diameter of the coil. It can thus provide mechanical support despite its slight thermal expansion during cool-down to 77K. However, it is also known that winding Zylon fiber under tension produces significant axial pressure at the ends of the winding pocket (poisson ratio). Unfortunately in this first 80T coil

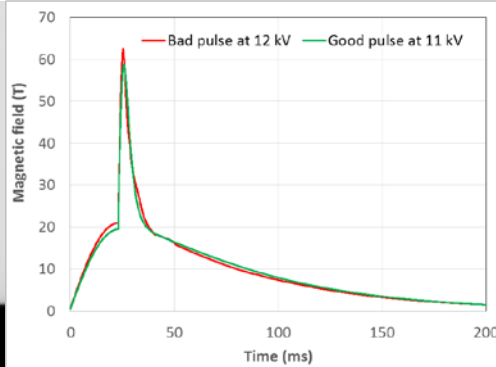
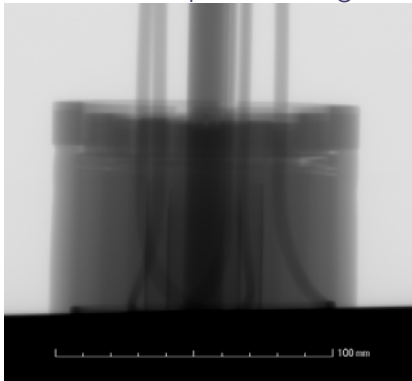


**Figure 4.d.15:** (Left) Xray image indicates the delamination of the end-spool of layer five of the inner coil, caused by insufficient winding pocket strength. (Right) The measured waveform of the magnetic field generated by the duplex magnet for two pulses. The magnet failed at 12 kV during the training process.

the winding pocket was not sufficiently strong and these forces causes the delamination on the end-spools (Fig.4.d.15: left) and voids between the end-spool and the conductor winding. Consequently, the magnet failed quite prematurely at 64T during training. **Figure 4.d.15 right** is the waveform of the 64T pulse of our duplex magnet. Based on the lessons learned from the autopsy of the failed magnet, tooling and fabrication

processes are being modified to contain the Zylon. The second duplex magnet is expected to be tested in the third quarter of 2019.

**100T magnet system activities at LANL:** The collector rings of the 1.4 GW generator were damaged when the carbon brushes reached end-of-life during the regular operation of the 100T magnet for a user in March 2018. Consequently, 100T operations were temporarily shut down for nearly the rest of the year for repairing and refurbishing the collector rings and jacking oil system. With the institutional investment from Los Alamos National Laboratory, the Pulsed Field Facility contracted with General Electric to successfully repair those components and the generator was re-operated to full power by December of 2018. Because of the generator maintenance, the 100T system delivered only 60 shots in 2018, of which 15 shots are in the range of 90T and above.

The innermost coils (coils 1 and 2) of the 100T outsert experience the highest stress during pulses reaching 100T, posing some risk for the magnet to deliver that field strength. The magnet teams at LANL and FSU have collaborated to build upgraded versions of those coils with the stronger Cu-Nb conductor (~ 50 percent stronger than the glid-cop AL60 wires used in the present coils). The successful fabrication of these coils will allow the 100T outsert magnet to operate at considerably more conservative margin or possibly increase the peak magnetic field slightly.

**60T controlled waveform (CW) magnet: Activities on 60T LP and 100T magnet at FSU:** Recently a new initiative commenced to fabricate large pulsed coils at the MagLab in Tallahassee. This allows the quality controls and fabrication procedures developed for large superconducting coils to be applied to pulsed





**Figure 4.d.16:** Winding of Coil #3 of the 100T Outsert.

coils and provides better communications between magnet designers and production engineers. Construction of the smaller, short-pulse magnets and insert coils remains in Los Alamos. Two projects are underway, the rebuild of coils 3, 4 and 7 for the 60T long pulse magnet and replacement of the coils 1 and 2 of the 100T outsert. The biggest change in the procedure has been better quality assurance of wire prior to winding. In particular, all wire is now subjected to visual and eddy-current examination.

Coil number 3 of the 100T outsert has been wound using a high-strength composite of Cu-Nb (**Fig. 4.d.16**). Its Nitronic 60 reinforcing shell has been fabricated and installed. The coil has been impregnated with epoxy and should be ready for shipment to LANL in March 2019 where over-banding will take place. However, the rebuild of coil

2 is presently on hold because internal flaws were found in the CuNb wire.

The rebuild of coils 3, 4 and 7 of the 60T long pulse magnet has been delayed significantly because of poor quality commercially produced GlidCop (Cu + Al<sub>2</sub>O<sub>3</sub>) conductors. Surface inclusions were found visually, which had to be ground out while internal chevron cracks were found via eddy-current testing. We are simultaneously pursuing several routes to accelerate the production of satisfactory conductors for these coils (see the Material Section for details). The metal reinforcing shells and other materials for electrical insulation have been in-stock, ready to start to fabricate these coils as soon as good conductors are obtained.

### **High-Strength Materials for Resistive Magnets**

Resistive magnets need both conductive and structural materials. The MagLab has conducted intensive research on both. Most of the high strength conductors used in our resistive magnets are manufactured from Cu matrix composites. One of the most important composites is reinforced with alumina particles (GlidCop, 0.15-0.6 wt%). The fabrication of this conductor requires high deformation strain, which creates high densities of dislocations and reduced particle spacing. Both mechanical strength and electrical conductivity can be predicted from particle spacing and dislocation density. At relatively low levels of deformation strain, mechanical strength increase depends mainly on dislocation density increase, but once dislocation density reaches a certain value, mechanical properties depend mainly on the size, the shape and the distribution of the particles themselves. In 2018, we focused our research on two of the most important factors related to the above parameters 1) dislocations near the interface between particle and matrix and 2) stress concentration near the particles. By engineering these variations, we devised ways to optimize the properties of Cu-alumina composite conductors for use in high field pulsed magnets. Large stress and dislocation concentrations near the large particles may result in premature failure of the composite. We studied the impact of die parameters, lubricants and drawing speed on both the stress-concentration and the quality of Cu-alumina wires. We also established parameters for using the Eddy current method to test the integrity of these wires and detect the presence of metallic inclusions and voids[1]. In collaboration with our commercial partners Sam Dong and North American Höganäs, we are now applying what we have learned to fabricating wires for our short-pulsed magnets and our 60T long-pulsed magnet.

Another important composite is Cu matrix reinforced with niobium. Wires formed from this conductor material must be bent to small diameters (~9 mm) to form pulsed magnets. Heat treatment is usually applied during wire fabrication in order to reduce the residual stress arising from cold work so that greater deformation is possible. We have studied the effect of annealing on the microstructure of Cu-Nb microcomposite wires. The microstructure of these wires is very stable below 500 °C due to the dragging effect of the triple points formed at intersections between Cu and Nb grains. Most triple points are composed of low-angle grain boundaries in Nb ribbons and Cu-Nb interfaces of (111)Cu//(011)Nb. At 500 °C or above, the elastic energy induced by stress at triple joints is the principal cause for the primary morphology changes we observed in Nb ribbons [2]. Based on our current understanding of the effect of heat treatment on deformed wires, we and our collaborators at Nanoelectro have begun developing Cu-Nb wires for 100+T magnets.

Poly-p-phenylene-benzobisoxazole (PBO, or Zylon) has been used as reinforcement material for pulsed magnets. Because PBO has both high strength (5.8 GPa) and high modulus (180 ~ 280 GPa), it

shows promise for use in superconducting as well as pulsed high-field magnets. Zylon fibers, however, exhibit an unusual sensitivity to light. By comparing samples kept in a dark bag to those exposed to laboratory lighting, we investigated the degradation of the mechanical strength of both single and strand Zylon fiber over time. Samples remained stable and strong after aging without exposure to light for eight years. Mechanical testing data indicated that subsequent prolonged exposure to laboratory lighting resulted in gradual strength degradation. Light-aging induced a transition from well-oriented crystallinity to amorphous structure, producing surface defects and debris and consequently leading to a decrease in mechanical strength. Our results indicate that it is necessary to protect Zylon from long-term light exposure during storing, manufacturing and operation of magnets [3].

Austenitic stainless steels are good reinforcement materials and have long been used successfully for high field magnets. The stable face-centered cubic structure of austenitic stainless steels also indicates that they are tough even at cryogenic temperatures [4,5]. The materials, however, may become brittle at cryogenic temperatures if their manufacture is undertaken improperly or quality control is incomplete [6]. We have tightened quality control in the manufacturing of austenitic stainless steel shells for the large pulsed coils. The materials produced so far under our new quality control protocol have consistently met the requirements for three of the four shells required in our proposed 100 +T pulsed magnet.

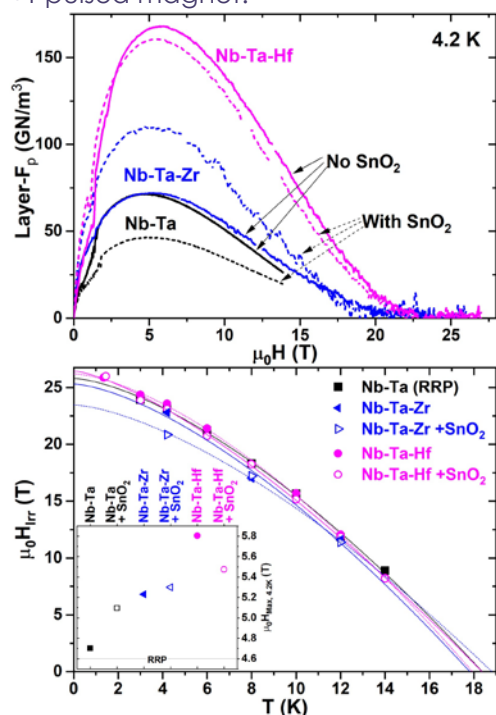


**Figure 4.d.17:** (Top) Layer  $F_p$  curves for in-house quaternary  $Nb_3Sn$  wires showing a significant  $F_p$  enhancement for wires made with Nb-Ta-Zr and Nb-Ta-Hf alloys instead of the standard Nb-Ta. (Bottom) Temperature dependence of  $H_{irr}$  of the wires prepared with new alloys compared to a commercial state-of-the-art RRP wire. In the inset the position of the  $F_p$  maximum for all home-made wires.

$Nb_4Ta_1Hf$ , and compare them to the commercially used  $Nb_4Ta$  (typical  $\mu_0 H_{irr}=23.2T$  with  $F_p$  maximum at  $\mu_0 H_{Max}=4.7T$ ). Ta-doping was introduced to increase  $H_{irr}$  whereas Zr or Hf are intended to enhance pinning force density  $F_p$ . The conductors were fabricated both with and without  $SnO_2$ , and the A15 reaction was performed at 670 °C for 100h. The samples were measured by VSM in the DC facility at NHMFL in the 35T magnet in the temperature range between 14 and 1.3K. From the hysteresis loops, we obtained the layer  $J_c$  and the pinning force density,  $F_p$ .

**Figure 4.d.17** reports the layer  $F_p$  curves obtained at 4.2K (with the position of the peak summarized in the inset) and the temperature dependence of  $H_{irr}$ . We observed that adding  $SnO_2$  is detrimental to

## References

- [1] K. Han, R.E. Goddard, V.J. Toplosky, R. Niu, J. Lu, R. Walsh, IEEE Transactions on Applied Superconductivity (2018).
- [2] L. Deng, B. Wang, K. Han, R. Niu, H. Xiang, K.T. Hartwig, X. Yang, Journal of Materials Science 54 (2019) 840-850.
- [3] R. Niu, K. Han, R.P. Walsh, K. Buchholz, R.E. Goddard, T. Besara, T.M. Siegrist, IEEE Transactions on Applied Superconductivity 28 (2018) 1-4.
- [4] K. Han, V. Toplosky, N. Min, J. Lu, Y. Xin, R. Walsh, IEEE Transactions on Applied Superconductivity 28 (2018) 1-5.
- [5] K. Han, Y. Xin, R. Walsh, S. Downey, P.N. Kalu, Materials Science and Engineering a-Structural Materials Properties Microstructure and Processing 516 (2009) 169-179.
- [6] J.R. Sims, J.B. Schillig, G.S. Boebinger, H. Coe, A.W. Paris, M.J. Gordon, M.D. Pacheco, T.G. Abeln, R.G. Hoagland, M.C. Mataya, K. Han, A. Ishmaku, IEEE Transactions on Applied Superconductivity 12 (2002) 480-483.

## LTS Conductor Advances

High R&D superconducting  $Nb_3Sn$  wires were fabricated at the Applied Superconductivity Center employing new in-house fabricated alloys, in order to investigate the feasibility of wires with enhanced high field properties for future accelerator magnets for the proposed Future Circular Collider (FCC), as well as U.S.-Magnet Development Program (MDP) projects. The target non-Cu critical current density,  $J_c$ , at 4.2K, 16T for FCC is 1,500 A/mm<sup>2</sup>, value far out of sight of any prior  $Nb_3Sn$  conductor. Previous experiments used Nb-Zr precursor rods surrounded by  $SnO_2$ , which generates  $ZrO_2$  precipitates in the reacted  $Nb_3Sn$  acting as pinning centers [1]. However, the use of Zr leads to a suppression of the irreversibility field  $H_{irr}$ . Here we show results obtained with two new ternary alloys,  $Nb_4Ta_1Zr$  and

the (standard) Nb<sub>4</sub>Ta sample, whereas it clearly increases the  $F_p$  maximum, shifting the  $F_p$  peak to 5.3T for the Nb<sub>4</sub>Ta1Zr alloy. However, the Nb<sub>4</sub>Ta1Zr+SnO<sub>2</sub> sample has a reduced  $H_{irr}$  (20.9T at 4.2K) that limits the  $J_c$  improvement at 16T. To our surprise, the most striking results were obtained with Nb<sub>4</sub>Ta1Hf; with or without SnO<sub>2</sub> the  $F_p$  maximum is more than twice that obtained with the Nb<sub>4</sub>Ta alloy, reaching more than 150 GN/m<sup>3</sup>. Because for Hf additions  $H_{irr}$ (4.2 K) is 23.1-23.6T, the  $J_c$ (16T) values are not suppressed with respect to commercial wires and  $H_{irr}$  is actually enhanced when SnO<sub>2</sub> is not used. The net result is that  $J_c$ (16T) more than doubles, achieving the hitherto thought impossible FCC target [2].

These findings for the Nb-Ta-Hf alloyed Nb<sub>3</sub>Sn wires demonstrate that Nb<sub>3</sub>Sn conductor performance can be greatly improved. We believe that this new alloy can easily be implemented into commercial wires without the difficulty of incorporating SnO<sub>2</sub>. We estimate that a conventional (RRP®) wire using Nb-Ta-Hf alloy could attain a non-Cu  $J_c$ (16T, 4.2K) of over 2200 A/mm<sup>2</sup>, well above FCC specification.

## References

- [1] Xu X, Sumption M, Peng X and Collings E W 2014 Refinement of Nb<sub>3</sub>Sn grain size by the generation of ZrO<sub>2</sub> precipitates in Nb<sub>3</sub>Sn wires. *Appl. Phys. Lett.* **104** 082602.  
 [2] Balachandran S, Tarantini C, Lee P J, Kametani F, Su Y F, Walker B, Starch W L, and Larbalestier D C 2019 Beneficial influence of Hf and Zr additions to Nb<sub>4</sub>at.%Ta on the vortex pinning of Nb<sub>3</sub>Sn with and without an O source. *Supercond. Sci. Technol.* in press <https://doi.org/10.1088/1361-6668/aaff02>

## Structural Materials for LTS Magnets

High-strength structural materials are required for both conductor reinforcement and coil support in high field magnets. Austenitic stainless steel is one of the most important high-strength materials used for these purposes. The ITER central solenoid is a highly stressed superconducting magnet that utilizes a Cable-in-Conduit-Conductor (CICC) technology. In collaboration with the US-ITER organization (funded by US-DOE) we studied the fatigue life of the conduit made from the austenitic steel JK2LB. US-ITER sought to collaborate with MagLab's MS&T division because of our expertise in CICC materials and low-temperature testing capabilities. Tests of full-scale conduit specimens that incorporate geometric stress concentrations present in the design required our 500kN cryogenic/mechanical materials test system. The results from eight samples confirmed the average fatigue life of the components meets the system requirements (> 540,000 cycles). Additionally, localized strain data from strain gage rosettes used on two of the tests were used to confirm FEA predicted stress models generated at Oak Ridge National Lab.

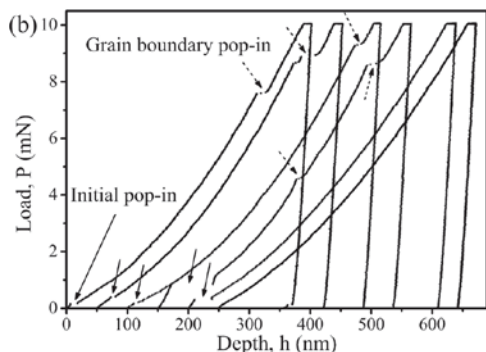


**Figure 4.d.18:** Representative load-depth curves event in aged steels showing both initial pop-in and grain boundary pop-in.

In steel fatigue, plastic deformation usually appears once materials begin to yield. Reinforcement materials can be used either after aging or as-received. We used tensile tests, nanoindentation measurements and carbon concentration analyses to test these two conditions [1]. In the aged samples, tensile tests showed the presence of yield-point phenomenon, a yielding feature that reflects a drop in stress where a rise would normally be observed. Nano-indentation measurements revealed sudden increases in displacement, known as 'pop-ins,' that occur during the mechanical contact of the indenter. Both an initial pop-in and multiple grain boundary pop-ins were in evidence (Fig. 4.d.18). Carbon concentration analysis showed that carbon content decreased significantly in the matrix in these samples. In the as-received samples, tensile tests showed no yield point phenomenon. Nano-indentation showed only an initial pop-in but no grain boundary pop-ins. Carbon concentration analysis showed that carbon content in the matrix was significantly greater than in the aged samples. We concluded that the presence of both yield point phenomena and grain boundary pop-ins in the aged samples was attributable to lower carbon content in the matrix.

Because nickel has a higher Young's modulus than iron, nickel-based alloys have the potential to produce higher modulus and higher mechanical strength materials than iron-based alloys (steels) for use in high field magnets, so we also studied several nickel-based alloys in hopes of developing a material superior to steel for use in high field magnets[2]. Nickel-based alloys have the added advantage of high resistance to fracture propagation, and their stable fcc structure also makes them tougher even at cryogenic temperatures. We studied mainly the modulus of nickel-based alloys in 2018. Nickel-chromium-based alloys (i.e., Haynes alloys), with their higher modulus, can replace stainless steels in

order to reach higher magnetic fields than ever before. In most cases, the addition of alloying elements further enhances mechanical properties, but contrary to expectations, the addition of certain high modulus elements such as molybdenum and tungsten does not further significantly increase the modulus of nickel-chromium-based alloys. Even so, alloys designed around nickel and molybdenum have higher modulus than other alloys that may be candidates for cryogenic magnet applications. Nickel-cobalt-molybdenum alloy (i.e. MP35N) has both high modulus and very high mechanical strength. Deformation and aging further enhance Young's modulus in this alloy. Because of their modulus, strength and cryogenic fracture toughness, all fcc-matrix Ni-based alloys are highly recommended for either reinforcement components in magnets or as reinforced substrates for superconductors.

#### References

- [1] Z.Y. Shen, B.L. Wang, G.F. Liang, Y.H. Zhang, K. Han, C.J. Song, ISIJ INTERNATIONAL 58 (2018) 373-375.
- [2] K. Han, V. Toplosky, N. Min, J. Lu, Y. Xin, R. Walsh, IEEE Transactions on Applied Superconductivity 28 (2018) 1-5.



## 5. PUBLICATIONS

The Laboratory continued its strong record of publishing, with **380** articles appearing in peer-reviewed scientific and engineering journals in 2018. Among these, 291 acknowledge NSF support for the operation of the NHMFL and 167 (44 percent) appeared in significant journals.

**Table 5.1.** provides an overview about NSF-acknowledged peer-reviewed and significant peer reviewed publications by user facility, followed by Applied Superconductivity Center, Magnet Science & Technology, Center for Integrating Research & Learning at FSU, the Condensed Matter Theory/Experiment group, Geochemistry, MBI and Physics at UF.

**Table 5.1:** Submitted peer-reviewed publications from OPMS live database. The point-in-time snapshot was on February 7, 2019. A total number of publications per year should NOT be drawn from this report because a submitter may, as appropriate, link a publication to two or more facilities. We note that the State of Florida contributes significantly to NHMFL and hired faculty at UF and FSU to enhance NHMFL programs. Publications from these professors are included as they significantly enhance the NHMFL research effort and are listed here in the UF physics and CMT/E categories.

Facility	2018 Peer Reviewed	Acknowledges Core Grant	2018 Significant Peer Reviewed	Acknowledges Core Grant
AMRIS at UF	30	16	8	3
DC Field at FSU	80	74	55	52
EMR at FSU	41	40	15	15
High B/T at UF	6	6	3	3
ICR at FSU	42	40	18	17
NMR at FSU	45	39	20	18
PF at LANL	37	32	18	15
ASC	19	16	15	12
MS&T	26	22	14	12
Education at FSU	1	1	0	0
CMT/E	53	41	29	25
Geochemistry	20	6	1	0
MBI at UF	31	4	3	0
UF Physics	7	7	4	4

291 of the 380 publications acknowledge NSF support for the operation of the MagLab. **Table 5.2** summarizes the publications generated by external users and in-house research activities. A detailed lists of these publications can be found below table 5.2.

**Table 5.2:** Overview of publications generated by external users and in-house research activities.

Facility	All Internal Authors		Internal Corresponding Author(s) with External Co-Authors		External Corresponding Author(s) with Internal Co-Authors		All External Authors		Totals		Total Pubs for 2018
	NSF Core Grant Cited	NSF Core Grant Not Cited	NSF Core Grant Cited	NSF Core Grant Not Cited	NSF Core Grant Cited	NSF Core Grant Not Cited	NSF Core Grant Cited	NSF Core Grant Not Cited	NSF Core Grant Cited	NSF Core Grant Not Cited	
AMRIS at UF	-	-	8	4	8	9	-	1	16	14	30
DC Field at FSU	3	-	5	2	56	4	10	-	74	6	80
EMR at FSU	-	-	8	-	27	-	5	1	40	1	41
High B/T at UF	-	-	4	-	2	-	-	-	6	-	6
ICR at FSU	6	-	8	-	16	2	10	-	40	2	42
NMR at FSU	2	-	12	2	24	2	1	2	39	6	45
PF at LANL	1	-	8	2	23	3	-	-	32	5	37

Facility	All Internal Authors		Internal Corresponding Author(s) with External Co-Authors		External Corresponding Author(s) with Internal Co-Authors		All External Authors		Totals		Total
	NSF Core Grant Cited	NSF Core Grant Not Cited	NSF Core Grant Cited	NSF Core Grant Not Cited	NSF Core Grant Cited	NSF Core Grant Not Cited	NSF Core Grant Cited	NSF Core Grant Not Cited	NSF Core Grant Cited	NSF Core Grant Not Cited	Pubs for 2018
ASC	1	-	3	-	12	3	-	-	16	3	19
MS&T	9	-	5	2	8	2	-	-	22	4	26
Education at FSU	-	-	1	-	-	-	-	-	1	-	1
CMT/E	5	1	12	4	24	6	-	1	41	12	53
Geochemistry	2	-	2	1	2	13	-	-	6	14	20
MBI at UF	-	-	2	3	-	11	2	13	4	27	31
UF Physics	-	-	4	-	3	-	-	-	7	-	7
<b>Total of Publications</b>	<b>23</b>	<b>1</b>	<b>69</b>	<b>18</b>	<b>171</b>	<b>52</b>	<b>28</b>	<b>18</b>	<b>291</b>	<b>89</b>	<b>380</b>
<b>% of Publications</b>	<b>6%</b>	<b>0%</b>	<b>18%</b>	<b>5%</b>	<b>45%</b>	<b>14%</b>	<b>7%</b>	<b>5%</b>	<b>77%</b>	<b>23%</b>	<b>100%</b>

Besides 380 peer reviewed publications, the following other products have also been published at the MagLab in 2018:

- Books: 2
- Patents: 3
- Disseminations: 7
- Awards: 7
- Grants: 15
- M.S. Theses: 3
- Ph.D. Theses: 26

The full listing of these products is available on the [MagLab's website](#).

#### Publications acknowledging NSF core grant generated by:

##### 1) All Internal Authors (23)

Bird, M.D.; Brey, W.W.; Cross, T.A.; Dixon, I.R.; Griffin, A.; Hannahs, S.T.; Kynoch, J.; Litvak, I.M.; Schiano, J.L.; Toth, J., Commissioning of the 36 T Series-Connected Hybrid Magnet at the NHMFL, IEEE Trans. Appl. Supercond., 28 (3), 4300706 (2018)
Chacon Patino, M.L.; Rowland, S.M.; Rodgers, R.P., Advances in Asphaltene Petroleomics. Part 2: A Selective Separation Method that Reveals Fractions Enriched in Island and Archipelago Structural Motifs by Mass Spectrometry, Energy Fuels, 32 (1), 314-328 (2018)
Chacon Patino, M.L.; Rowland, S.M.; Rodgers, R.P., Advances in Asphaltene Petroleomics. Part 3. Dominance of Island or Archipelago Structural Motif Is Sample Dependent, Energy Fuels, 32 (9), 9106-9120 (2018)
Chen, K.-W.; Lian, X.; Lai, Y.; Aryal, N.; Chiu, Y.-C.; Lan, W.; Graf, D.; Manousakis, E.; Baumbach, R. E. and Balicas, L., Bulk Fermi Surfaces of the Dirac Type-II Semimetallic Candidates MAI <sub>3</sub> (Where M=V, Nb, and Ta), Phys. Rev. Lett., 120, 206401 (2018)
Han, K.; Goddard, R.E.; Toplosky, V.J.; Niu, R.; Lu, J.; Walsh, R.P., Alumina Particle Reinforced Cu Matrix Conductors, IEEE Trans. Appl. Supercond., 28 (3), 7000305 (2018)
Han, K.; Toplosky, V.J.; Min, N.A.; Lu, J.; Xin, Y.; Walsh, R.P., High Modulus Reinforcement Alloys, IEEE Trans. Appl. Supercond., 28 (3), 1-5 (2018)

He, L.; Weisbrod, C.R.; Marshall, A.G., Protein de novo Sequencing by Top-down and Middle-down MS/MS: Limitations Imposed by Mass Measurement Accuracy and Gaps in Sequence Coverage, <i>Int. J. Mass Spectrom.</i> , 427, 107-113 (2018)
Kang, J.; Vafeek, O., Symmetry, Maximally Localized Wannier States, and a Low-Energy Model for Twisted Bilayer Graphene Narrow Bands, <i>Phys. Rev. X</i> , 8 (3), 031088 (2018)
liou, S.; Yang, K., Quench dynamics across topological quantum phase transitions, <i>Phys. Rev. B</i> , 97, 235144 (2018)
Lu, J.; Levitan, J.; McRae, D.; Walsh, R., Contact resistance between two REBCO tapes: the effects of cyclic loading and surface coating, <i>Superconductor Science and Technology</i> , 31, 085006 (2018)
Marshall, W.S.; Bird, M.D.; Larbalestier, D.C.; McRae, D.M.; Noyes, P.D.; Voran, A.J.; Walsh, R.P., Fabrication and Testing of a Bi-2223 Test Coil for High Field NMR Magnets, <i>IEEE Trans. Appl. Supercond.</i> , 28 (3), 1-4 (2018)
Mastracci, B.; Guo, W., An apparatus for generation and quantitative measurement of homogeneous isotropic turbulence in He II, <i>Rev. Sci. Instrum.</i> , 89, 015107 (2018)
Mastracci, B.; Guo, W., An exploration of thermal counterflow in He II using particle tracking velocimetry, <i>Phys. Rev. Fluids</i> , 3, 063304 (2018)
Nguyen, Q.V.M.; Torres, L.; Nguyen, D.N., Electromagnetic Interaction Between the Component Coils of Multiplex Magnets, <i>IEEE Trans. Appl. Supercond.</i> , 28 (3), 4300804 (2018)
Niu, R.; Han, K.; Walsh, R.P.; Buchholz, K.; Goddard, R.E.; Besara, T.; Siegrist, T.M., Aging effect of Zylon, <i>IEEE Trans. Appl. Supercond.</i> , 28 (3), 4 (2018)
Ruddy, B.M.; Hendrickson, C.L.; Rodgers, R.P.; Marshall, A.G., Positive Ion Electrospray Ionization Suppression in Petroleum and Complex Mixtures, <i>Energy &amp; Fuels</i> , 32 (3), 2901-2907 (2018)
Smith, D.; Podgorski, D.C.; Rodgers, R.P.; Blakney, G.T.; Hendrickson, C.L., 21 Tesla FT-ICR Mass Spectrometer for Ultrahigh-Resolution Analysis of Complex Organic Mixtures, <i>Anal. Chem.</i> , 90 (3), 2041-2047 (2018)
Sur, S.; Gong, S.S.; Yang, K.; Vafeek, O., Quantum anomalous Hall insulator stabilized by competing interactions, <i>Phys. Rev. B</i> , 98, 125144 (2018)
Toth, J.; Bole, S.T., Design, Construction and First Testing of a 41.5 T All-Resistive Magnet at the NHMFL in Tallahassee, <i>IEEE Trans. Appl. Supercond.</i> , 28 (3), 1051-8223 (2018)
Ware, R.L.; Rowland, S.M.; Lu, J.; Rodgers, R.P.; Marshall, A.G., Compositional and Structural Analysis of Silica Gel Fractions from Municipal Waste Pyrolysis Oils, <i>Energy &amp; Fuels</i> , 32 (7), 7752-7761 (2018)
Yang, S.; Humayun, M.; Salters, V. J. M., Elemental Systematics in MORB Glasses from the Mid-Atlantic Ridge, <i>Geochem. Geophys. Geosyst.</i> , 19, 4236 (2018)
Yang, S.; Humayun, M.; Salters, V.J.M., Elemental Systematics in MORB Glasses From the Mid-Atlantic Ridge, <i>Geochem. Geophys. Geosyst.</i> , 19 (11), 4236-4259 (2018)
Zheng, J.; Hu, Y.Y., New Insights into the Compositional Dependence of Li-Ion Transport in Polymer-Ceramic Composite Electrolytes, <i>ACS Applied Materials Interfaces</i> , 10 (A), 4113-4120 (2018)

## 2) Internal Corresponding Author(s) with External Co-Authors (69)

Abad, N.; Rosenberg, J.T.; Hike, D.C.; Harrington, M.G.; Grant, S.C., Dynamic Sodium Imaging at Ultra-High Field Reveals Progression in a Preclinical Migraine Model, <i>Pain</i> , 159 (10), 2058-2065 (2018)
Archer, D.B.; Coombes, S.A.; Chu, W.T.; Chung, J.W.; Burciu, R.G.; Okun, M.S.; Shukla, A.W.; Vaillancourt, D.E., A widespread visually-sensitive functional network relates to symptoms in essential tremor, <i>Brain</i> , 141, 472-485 (2018)
Badisa, R.B.; Wi, S.; Jones, Z.; Mazziro, E.; Zhou, Y.; Rosenberg, J.T.; Latinwo, L.M.; Grant, S.C.; Goodman, C.B., Cellular and molecular responses to acute cocaine treatment in neuronal-like N2a cells: potential mechanism for its resistance in cell death, <i>Cell Death Discovery</i> , 5, 13 (2018)
Baity, P.G.; Sasagawa, T.; Popovic, D., Collective dynamics and strong pinning near the onset of charge order in La <sub>1.48</sub> Nd <sub>0.48</sub> Sr <sub>0.12</sub> CuO <sub>4</sub> , <i>Phys. Rev. Lett.</i> , 120, 156602 (2018)
Balk, A.L.; Li, F.; Gilbert, I.; Unguris, J.; Sinitsyn, N.A.; Crooker, S.A., Broadband Spectroscopy of Thermodynamic Magnetization Fluctuation through a Ferromagnetic Spin-Reorientation Transition, <i>Phys. Rev. X</i> , 8, 031078 (2018)
Bao, S.; Guo, W.; L'vov, V.S.; Pomyalov, A., Statistics of turbulence and intermittency enhancement in superfluid 4He counterflow, <i>Phys. Rev. B</i> , 98, 174509 (2018)
Berens, S.; Chmelik, C.; Hillman, F.; Karger, J.; Jeong, H.K.; Vasenkov, S., Ethane diffusion in mixed linker zeolitic imidazolate framework-7-8 by pulsed field gradient NMR in combination with single crystal IR microscopy, <i>Phys. Chem. Chem. Phys.</i> , 20 (37), 23967-23975 (2018)
Besara, T.; Ramirez, D.; Sun, J.; Falb, N.; Lan, W.; Neu, J.; Whalen, J.; Singh, D.; Siegrist, T., Synthesis and Crystal Structure of the Layered Lanthanide Oxychlorides Ba(3)Ln(2)O(5)Cl(2), <i>Inorg. Chem.</i> , 57 (4), 1727-1734 (2018)
Cheggour, N.; Stauffer, T.C.; Starch, W.L.; Lee, P.J.; Splett, J.D.; Goodrich, L.F.; Ghosh, A.K., Precipitous change of the irreversible strain limit with heat-treatment temperature in Nb <sub>3</sub> Sn wires made by the restacked-rod process, <i>Nature Scientific Reports</i> , 8, 13048 (2018)

Chen, H.; Nelson, R.K.; Swarthout, R.F.; Shigenaka, G.; H.B. de Oliveira, A.; Reddy, C.M.; McKenna, A.M., Detailed Compositional Characterization of the 2014 Bangladesh Furnace Oil Released into the World's Largest Mangrove Forest, <i>Energy Fuels</i> , 32 (3), 3232-3242 (2018)
Chen, K.W.; Aryal, N.; Dai, J.; Graf, D.; Zhang, S.; Das, S.; Le Fèvre, P.; Bertran, F.; Yukawa, R.; Horiba, K.; Kumigashira, H.; Frantzeskakis, E.; Fortuna, F.; Balicas, L.; Santander-Syro, A.F.; Manousakis, E.; Baumbach, R.E., Converting topological insulators into topological metals within the tetradymite family, <i>Phys. Rev. B</i> , 97, 165112 (2018)
Chien, P.H.; Feng, X.; Tang, M.; Rosenberg, J.T.; O'Neill, S.; Zheng, J.; Grant, S.C.; Hu, Y.Y., Li Distribution Heterogeneity in Solid Electrolyte Li <sub>10</sub> GeP <sub>2</sub> S <sub>12</sub> upon Electrochemical Cycling Probed by <sup>7</sup> Li MRI, <i>J. Physical Chemistry Letters</i> , 9 (8), 1990-1998 (2018)
Colon-Perez, L.M.; Pino, J.A.; Saha, K.; Pompilus, M.; Kaplitz, S.; Choudhury, N.; Jagarine, D.A.; Geste, J.R.; Levin, B.A.; Wilks, I.; Setlow, B.; Bruijnzeel, A.W.; Khoshbouei, H.; Torres, G.E.; Febo, M., Functional connectivity, behavioral and dopaminergic alterations 24 hours following acute exposure to synthetic bath salt drug methylenedioxypyrovalerone, <i>Neuropharmacology</i> , 137, 178-193 (2018)
Davidson, S.G.; Hughes, R., Communities of Practice as a Framework to Explain Teachers' Experiences within the Community of Science, <i>Journal of Research on Science Teaching</i> , 55 (9), 1287-1312 (2018)
Drake, T.W.; Guillemette, F.; Hemingway, J.D.; Chanton, J.P.; Podgorski, D.C.; Zimov, N.S.; Spencer, R.G.M., The Ephemeral Signature of Permafrost Carbon in an Arctic Fluvial Network, <i>J. Geophys. Res. Biogeosci.</i> , 123 (5), 1475-1485 (2018)
Dubroca, T.; Smith, A.N.; Pike, K.J.; Froud, S.; Wylde, R.; Trociewitz, B.; McKay, J.; Mentink-Vigier, F.; van Tol, J.; Wi, S.; Brey, W.; Long, J.R.; Frydman, L.; Hill, S., A quasi-optical and corrugated waveguide microwave transmission system for simultaneous dynamic nuclear polarization NMR on two separate 14.1 T spectrometers, <i>J. Magn. Reson.</i> , 289, 35-44 (2018)
Dutta, A.R.; Sekar, P.; Dvoyashkin, M.; Bowers, C.; Ziegler, K.J.; Vasenkov, S., Possible role of molecular clustering in single-file diffusion of mixed and pure gases in dipeptide nanochannels, <i>Microporous and Mesoporous Materials</i> , 269, 83-87 (2018)
Feng, X.; Tang, M.; O'Neill, S.; Hu, Y., In Situ Synthesis and In Operando NMR Studies of High-Performance Ni <sub>5</sub> P <sub>4</sub> -Nanosheet Anode, <i>J. Materials Chemistry A</i> , 6 (44), 22240-22247 (2018)
Fu, R.; Hernández-Maldonado, A.J., Boosting sensitivity and suppressing artifacts via multi-acquisition in direct polarization NMR experiments with small flip-angle pulses, <i>J. Magn. Reson.</i> , 293, 34-40 (2018)
Gan, Z.; Hung, I.; Nishiyama, Y.; Amoureux, J.P.; Lafon, O.; Nagashima, H.; Trebosc, J.; Hu, B.W., N-14 overtone nuclear magnetic resonance of rotating solids, <i>J. Chem. Phys.</i> , 149 (6), 064201 (2018)
Gao, J.; Guo, W.; Yui, S.; Tsubota, M.; Vinen, W.F., Dissipation in quantum turbulence in superfluid <sup>4</sup> He above 1K, <i>Phys. Rev. B</i> , 97, 184518 (2018)
Giraldo Gallo, P.; Galvis, J.; Stegen, Z.; Modic, K.; Balakirev, F.; Betts, J.; Lian, X.; Moir, C.; Riggs, S.; Wu, J.; Bolliger, A.; He, X.; Bozovic, I.; Ramshaw, B.; McDonald, R.; Boebinger, G.; Shehter, A., Scale-invariant magnetoresistance in a cuprate superconductor, <i>Science</i> , 361, 479 (2018)
Gor'kov, L.P.; Kresin, V.Z., Colloquium: High pressure and road to room temperature superconductivity, <i>Review of Modern Physics</i> , 90 (1), 011001 (2018)
Greer, S.M.; Oakley, R.T.; van Tol, J.; Shatruk, M.; Hill, S., Investigating the thermally- and light-induced interconversion of bisdithiazolyl radicals and dimers with high-field EPR, <i>Polyhedron</i> , 153, 99-103 (2018)
Heald, S.M.; Tarantini, C.; Lee, P.J.; Brown, M.D.; Sung, Z.H.; Ghosh, A.K.; Larbalestier, D.C., Evidence from EXAFS for Different Ta/Ti Site Occupancy in High Critical Current Density Nb <sub>3</sub> Sn Superconductor Wires, <i>Nature Scientific Reports</i> , 8 (1), 4798 (2018)
Huan, C.; Masuhara, N.; Adams, J.; Lewkowicz, M.; Sullivan, N.S., Probing the dynamics of <sup>3</sup> He atoms adsorbed on MCM-41 with pulsed NMR, <i>Journal of Physics, Conf. Series</i> , 969 (1), 012001 (2018)
Hur, M.; Ware, R.L.; Park, J.; McKenna, A.M.; Rodgers, R.P.; Nikolau, B.J.; Wurtele, E.S.; Marshall, A.G., Statistically Significant Differences in Composition of Petroleum Crude Oils Revealed by Volcano Plots Generated from Ultrahigh Resolution Fourier Transform Ion Cyclotron Resonance Mass Spectra, <i>Energy &amp; Fuels</i> , 32 (2), 1206-1212 (2018)
Jackson, D.E.; VanGennep, D.; Bi, W.L.; Zhang, D.Z.; Materne, P.; Liu, Y.; Cao, G.H.; Weir, S.T.; Vohra, Y.K.; Hamlin, J.J., Superconducting and magnetic phase diagram of RbEuFe <sub>4</sub> As <sub>4</sub> and CsEuFe <sub>4</sub> As <sub>4</sub> at high pressure, <i>Phys. Rev. B</i> , 98 (1), 014518 (2018)
Jarvis, J.M.; Billing, J.M.; Corilo, Y.; Schmidt, A.J.; Hallen, R.T.; Schaub, T.M., FT-ICR MS Analysis of Blended Pine-microalgae Feedstock HTL Biocrudes, <i>Fuel</i> , 216, 341-348 (2018)
Johnston, S.E.; Shorina, N.; Bulygina, E.; Vorobjeva, T.; Chupakova, A.; Kilmov, S.I.; Kellerman, A.M.; Guillemette, F.; Shiklomanov, A.; Podgorski, D.C.; Spencer, R.G.M., Flux and Seasonality of Dissolved Organic Matter From the Northern Dvina (Severnaya Dvina) River, Russia, <i>J. Geophys. Res. Biogeosci.</i> , 123 (3), 1041-1056 (2018)
Kang, J.; Chubukov, A.V.; Fernandes, R.M., Time-reversal symmetry-breaking nematic superconductivity in FeSe, <i>Phys. Rev. B</i> , 98 (6), 064508 (2018)



Kang, J.; Fernandes, R.M.; Abrahams, E.; Wolfle, P., Superconductivity at an antiferromagnetic quantum critical point: Role of energy fluctuations, <i>Phys. Rev. B</i> , <b>98</b> , 214515 (2018)
Kang, J.; Fernandes, R.M.; Chubukov, A., Superconductivity in FeSe: The Role of Nematic Order, <i>Phys. Rev. Lett.</i> , <b>120</b> , 267001 (2018)
Kellerman, A.M.; Guillemette, F.; Podgorski, D.C.; Aiken, G.R.; Butler, K.D.; Spencer, R.G.M., Unifying Concepts Linking Dissolved Organic Matter Composition to Persistence in Aquatic Ecosystems, <i>Environ. Sci. Technol.</i> , <b>52</b> (5), 2538-2548 (2018)
Kim, J.S.; VanGennep, D.; Hamlin, J.J.; Wang, X.; Sefat, A.S.; Stewart, G.R., Unusual effects of be doping in the iron-based superconductor FeSe, <i>J. Phys.-Condens. Mat.</i> , <b>30</b> , 445701 (2018)
Kim, J.W.; Mun, E.D.; Ding, X.; Hansen, A.; Jaime, M.; Harrison, N.; Yi, H.T.; Chai, Y.S.; Sun, Y.; Cheong, S.W.; Zapf, V.S., Metastable states in the frustrated triangular compounds $\text{Ca}_3\text{Co}_2\text{-xMn}_x\text{O}_6$ and $\text{Ca}_3\text{Co}_2\text{O}_6$ , <i>Phys. Rev. B</i> , <b>98</b> , 024407 (2018)
Krajewski, L.C.; Lobodin, V.V.; Johansen, C.; Bartges, T.E.; Maksimova, E.V.; MacDonald, I.R.; Marshall, A.G., Linking Natural Oil Seeps from the Gulf of Mexico to Their Origin by Use of Fourier Transform Ion Cyclotron Resonance Mass Spectrometry, <i>Environ. Sci. Technol.</i> , <b>52</b> (3), 1365-1374 (2018)
Lai, Y.; Bone, S.E.; Minasian, S.; Ferrier, M.G.; Lezama-Pacheco, J.; Mocko, V.; Ditter, A.S.; Kozimor, S.A.; Seidler, G.T.; Nelson, W.L.; Chiu, Y.C.; Huang, K.; Potter, W.; Graf, D.; Albrecht-Schmitt, T.E.; Baumbach, R.E., Ferromagnetic quantum critical point in $\text{CePd}_2\text{P}_2$ with Pd $\rightarrow$ Ni substitution, <i>Phys. Rev. B</i> , <b>97</b> (22), 224406 (2018)
liou, S.; Hu, Z.; Yang, K., Topological phase transition in a two-species fermion system: Effects of a rotating trap potential or a synthetic gauge field, <i>Phys. Rev. B</i> , <b>97</b> , 245140 (2018)
Liu, J.; Wang, Y.; Wang, Y.; Guan, Y.; Dong, J.; Li, T., A multi-proxy record of environmental changes during the Holocene from the Haolaihu Paleolake sediments, Inner Mongolia., <i>Quaternary International</i> , <b>479</b> , 148-159 (2018)
Manson, J.L.; Brambleby, J.; Goddard, P.A.; Spurgeon, P.M.; Villa, J.A.; Liu, J.; Ghannadzadeh, S.; Foronda, F.; Singleton, J.; Lancaster, T.; Clarke, S.J.; Thomas, I.O.; Xiao, F.; Willaims, R.C.; Pratt, F.L.; Blundell, S.J.; Topping, C.V.; Baines, C.; Campana, C.; Noll, B., Implications of bond disorder in a $S=1$ kagome lattice, <i>Scientific Report</i> , <b>8</b> , 4745 (2018)
Marbey, J.; Gan, P.R.; Yang, E.C.; Hill, S., Magic-angle effects in a trigonal $\text{MnIII}_3$ cluster: Deconstruction of a single-molecule magnet, <i>Phys. Rev. B</i> , <b>98</b> , 144433 (2018)
Mihalik, M.; Mihalik, M.A.; Zentkova, M.; Uhlírova, K.; Kratochvílová, M.; Fitta, M.; Quintero, P.A.; Meisel, M.W., Tuning of magnetism in $\text{DyMn}(1-x)\text{Fe}_x\text{O}(3)$ ( $x < 0.1$ ) system by iron substitution, <i>Physica B</i> , <b>536</b> , 102-106 (2018)
Orsini, C.A.; Colon-Perez, L.; Heshmati, S.C.; Setlow, B.; Febo, M., Functional Connectivity of Chronic Cocaine Use Reveals Progressive Neuroadaptations in Neocortical, Striatal, and Limbic Networks, <i>eNeuro</i> , <b>5</b> (4), 1 (2018)
Pan, J.; Dalzini, A.; Khadka, N.K.; Aryal, C.M.; Song, L., Lipid Extraction by a Synuclein Generates Semi-Transmembrane Defects and Lipoprotein Nanoparticles, <i>ACS Omega</i> , <b>3</b> (8), 9586-9597 (2018)
Patrick, C.E.; Kumar, S.; Gotze, K.; Pearce, M.J.; Singleton, J.; Rowlands, G.; Balakrishnan, G.; Lees, M.R.; Goddard, P.A.; Staunton, J.B., Field-induced canting of magnetic moments in $\text{GdCo}_5$ at finite temperature: first-principles calculations and high-field measurements, <i>J. Phys.-Condens. Mat.</i> , <b>30</b> , 32LT01 (2018)
Perez, P.D.; Hall, G.; Zubcevic, J.; Febo, M., Cocaine differentially affects synaptic activity in memory and midbrain areas of female and male rats: an in vivo MEMRI study, <i>Brain Imaging and Behavior</i> , <b>1</b> (1), 1-16 (2018)
Podgorski, D.C.; Zito, P.; McGuire, J.T.; Martinovic-Weigelt, D.; Cozzarelli, I.M.; Bekins, B.; Spencer, R.G.M., Examining Natural Attenuation and Acute Toxicity of Petroleum-Derived Dissolved Organic Matter (DOMHC) with Optical Spectroscopy, <i>Environ. Sci. Technol.</i> , <b>52</b> (11), 6157-6166 (2018)
Pradhan, N.R.; Garcia, C.; Isenberg, B.; Rhodes, D.; Feng, S.; Memaran, S.; Xin, Y.; McCreary, A.; Hight Walker, A.R.; Raelarijaona, A.; Terrones, M.; McGill, S.; Balicas, L., Phase Modulators Based on High Mobility Ambipolar $\text{ReSe}_2$ Field Effect Transistors, <i>Nature Scientific Reports</i> , <b>8</b> , 12745 (2018)
Ran, Y.; Fanucci, G.E., Characterization of the Lipid Binding Pocket in GM2AP and SapB with EPR Spectroscopy, <i>Appl. Magn. Reson.</i> , <b>49</b> (11), 1181-1199 (2018)
Roussel, T.; Rosenberg, J.T.; Grant, S.C.; Frydman, L., Brain investigations of rodent disease models by chemical exchange saturation transfer at 21.1 T, NMR in Biomedicine, <b>31</b> (11), e3995 (2018)
Sertphon, D.; Harding, P.; Murray, K.S.; Moubaraki, B.; Chilton, N.F.; Marbey, J.; Hill, S.; Adams, H.; Davis, C.G.; Jameson, G.N.L.; Harding, D.J., Self-assembly of a mixed-valence $\text{Fe}^{\text{II}}\text{-Fe}^{\text{III}}$ tetranuclear star, <i>Dalton Trans. Chem.</i> , <b>47</b> , 7118-7122 (2018)
Shafieizadeh, Z.; Xin, Y.; Koochpayeh, S.M.; Huang, Q.; Zhou, H.D., Superdislocations and point defects in pyrochlore $\text{Yb}_2\text{Ti}_2\text{O}_7$ single crystals and implication on magnetic ground states, <i>Nature Scientific Reports</i> , <b>8</b> , 17202 (2018)
Sirusi, A.; Suh, E.H.; Kovacs, Z.; Merritt, M., The effect of $\text{Ho}^{3+}$ doping on $^{13}\text{C}$ dynamic nuclear polarization at 5 T, <i>Phys. Chem. Chem. Phys.</i> , <b>20</b> (2), 728-731 (2018)
Stier, A.V.; Wilson, N.P.; Velizhanin, K.A.; Kono, J.; Xu, X.; Crooker, S.A., Magneto-optics of Exciton Rydberg States in a Monolayer Semiconductor, <i>Phys. Rev. Lett.</i> , <b>120</b> (5), 057405 (2018)

Tarantini, C.; Iida, K.; Sumiya, N.; Chihara, M.; Hatano, T.; Ikuta, H.; Singh, R.K.; Newman, N.; Larbalestier, D.C., Effect of a-particle irradiation on a NdFeAs(O,F) thin film, <i>Superconductor Science and Technology</i> , 31, 034002 (2018)
Them, T.R.; Gill, B.C.; Caruthers, A.H.; Gerhardt, A.M.; Gröcke, D.R.; Marroqin, S.M.; Lyons, T.W.; Nielsen, S.G.; Trabucho-Alexandre, J.P.; Owens, J.D., Thallium isotopes reveal protracted anoxia during the Toarcian (Early Jurassic) associated with volcanism, carbon burial, and mass extinction, <i>Proceeding of the National Academy of Sciences</i> , 115 (26), 6596-6601 (2018)
Thompson, C.J.; Reig-i-Plessis, D.; Kish, L.; Aczel, A.A.; Zhang, B.; Karapetrova, E.; MacDougall, G.J.; Beekman, C., Spin canting and orbital order in spinel vanadate thin films, <i>Phys. Rev. Materials</i> , 2, 104411 (2018)
Tian, C.; Yang, K.; Fang, P.; Zhou, X.; Wang, J., Hidden thermal structure in Fock space, <i>Phys. Rev. E Rapid Commun.</i> , 98, 060103 (2018)
Varga, E.; Gao, J.; Guo, W.; Skrbek, L., Intermittency enhancement in quantum turbulence in superfluid 4He, <i>Phys. Rev. Fluids</i> , 3, 094601 (2018)
Wang, K.; Zhang, Z.; Ding, X.; Tian, F.; Huang, Y.; Chen, Z.; Fu, R., Spin-echo based diagonal peak suppression in solid-state MAS NMR homonuclear chemical shift spectra, <i>J. Magn. Reson.</i> , 287, 91 (2018)
Wang, K.; Zhang, Z.Y.; Ding, X.Y.; Tian, F.; Huang, Y.Q.; Chen, Z.; Fu, R., Spin-echo based diagonal peak suppression in solid-state MAS NMR homonuclear chemical shift correlation spectra, <i>J. Magn. Reson.</i> , 287, 91-98 (2018)
Wang, X.; McKay, J.E.; Lama, B.; van Tol, J.; Kirkpatrick, K.; Gan, Z.; Hill, S.; Long, J.R.; Dorn, H.C., Gadolinium based endohedral metallofullerene Gd <sub>2</sub> @C <sub>79</sub> N as a relaxation boosting agent for dissolution DNP at high fields, <i>Chem. Commun.</i> , 54, 2425 (2018)
Weickert, D.F.; Civale, L.; Maiorov, B.; Jaime, M.; Salamon, M.B.; Carleschi, E.; Strydom, A. M.; Fittipaldi, R.; Granata, V.; Vecchione, A., In-depth study of the H-T phase diagram of Sr <sub>3</sub> Ru <sub>4</sub> O <sub>10</sub> by magnetization experiments, <i>Physica B</i> , 536, 634 (2018)
Weickert, D.F.; Gegenwart, P.; Geibel, C.; Steglich, F., Observation of two critical points linked to the high-field phase B in CeCu <sub>2</sub> Si <sub>2</sub> , <i>Phys. Rev. B</i> , 98, 085115 (2018)
Wi, S.; Schurko, W.R.; Frydman, L., Broadband adiabatic inversion cross-polarization phenomena in the NMR of rotating solids, <i>Solid State Nucl. Mag. Reson.</i> , 94, 31-53 (2018)
Xia, J.S.; Ozarowski, A.; Spurgeon, P.M.; Graham, A.G.; Manson, J.L.; Meisel, M.W., Unusual Magnetic Response of an S = 1 Antiferromagnetic Linear-Chain Material, <i>J. Phys.: Conf. Series</i> , 969 (012121), 1-6 (2018)
Xin, Y.; Huang, Q.; Shafieizadeh, Z.; Zhou, H.D., B-site cation order/disorder and their valence states in Ba <sub>3</sub> MnNb <sub>2</sub> O <sub>9</sub> perovskite oxide, <i>J. Solid State Chem.</i> , 262, 8-15 (2018)
Zheng, W.; Schoenemann, R.; Aryal, N.; Zhou, Q.; Rhodes, D.; Chiu, Y. C.; Chen, K.W.; Kampert, E.; Forster, T.; Martin, T.J.; McCandless, G.T.; Chan, J.Y.; Manousakis, E.; Balicas, L., Detailed Study of the Fermi Surfaces of XTe <sub>2</sub> (where X= Pd, Pt), <i>Phys. Rev. B</i> , 97, 235154 (2018)

### c) External Corresponding Author(s) with Internal Co-Authors (171)

Abad, N.; Rosenberg, J.T.; Roussel, T.; Grice, D.C.; Harrington, M.G.; Grant, S.C., Metabolic Assessment of a Migraine Model Using Relaxation-Enhanced 1H Spectroscopy at Ultrahigh Field, <i>Magnet. Reson. Med.</i> , 79 (3), 1266-1275 (2018)
Afaneh, T.; Sahoo, P.K.; Nobrega, I.A.P.; Xin, Y.; Gutiérrez, H.R., Laser-Assisted Chemical Modification of Monolayer Transition Metal Dichalcogenides, <i>Adv. Funct. Mater.</i> , 28, 1802949(1-7) (2018)
Ahlschwede, K.M.; Curran, G.L.; Rosenberg, J.T.; Grant, S.C.; Sarkar, G.; Jenkins, R.B.; Ramakrishnan, S.; Poduslo, J.F.; Kandimalla, K.K., Cationic carrier peptide enhances cerebrovascular targeting of nanoparticles in Alzheimer's disease brain, <i>Nanomedicine</i> , 1876, 1-38 (2018)
Alberi, K.; Fluegel, B.; Beaton, D.A.; Steger, M.; Crooker, S.A.; Mascarenhas, A., Origin of deep localization in GaAs <sub>1-x</sub> Bix and its consequences for alloy properties, <i>Phys. Rev. Materials</i> , 2, 114603 (2018)
Anders, M.A.; Lenahan, P.M.; Cochrane, C.J.; van Tol, J., Physical nature of electrically detected magnetic resonance through spin dependent trap assisted tunneling in insulators, <i>J. Appl. Phys.</i> , 124 (21), 215105 (2018)
Bastiaansen, J.A.M.; Yoshihara, H.A.I.; Capozzi, A.; Schwitter, J.; Gruetter, R.; Merritt, M.E.; Comment, A., Probing cardiac metabolism by hyperpolarized 13C MR using an exclusively endogenous substrate mixture and photo-induced nonpersistent radicals, <i>Magnet. Reson. Med.</i> , 79 (5), 2451-2459 (2018)
Battesti, R.; Budker, D.; Crooker, S.A.; Beard, J.; Boser, S.; Bruyant, N.; Daw, E.; Flambaum, V.; Inada, T.; Irastorza, I.; Karbstein, F.; Kim, D.; Kozlov, M.; Melhem, Z.; Phipps, A.; Pugnati, P.; Rikken, G.; Rizzo, C.; Schott, M.; Semertzidis, Y.; ten Cate, H.; Zavattini, G., High magnetic fields for fundamental physics, <i>Physics Reports</i> , 765-766, 1-39 (2018)
Baumbach, R.; Balicas, L.; McCandless, G.T.; Sotelo, P.; Zhang, Q.R.; Evans, J.; Camdzic, D.; Martin, T.J.; Chan, J.Y.; Macaluso, R.T., One-dimensional tellurium chains: Crystal structure and thermodynamic properties of PrCu <sub>x</sub> Te <sub>2</sub> (x ~ 0.45), <i>J. Solid State Chem.</i> , 269, 553 (2018)

Bauters, M.; Drake, T.W.; Verbeeck, H.; Bode, S.; Herve-Fernandez, P.; Zito, P.; Podgorski, D.C.; Boyemba, F.; Makelele, I.; Ntaboba, L.C.; Spencer, R.G.M.; Boeckx, P., High Fire-derived Nitrogen Deposition on Central African Forests, <i>P. Natl. Acad. Sci. U.S.A.</i> , 115 (3), 549-554 (2018)
Bindra, J.K.; Gutsev, L.G.; van Tol, J.; Singh, K.; Dalal, N.S.; Strouse, G.F., Experimental Validation of Ferromagnetic–Antiferromagnetic Competition in FexZn1–xSe Quantum Dots by Computational Modeling, <i>Chem. Mater.</i> , 30 (6), 2093-2101 (2018)
Bindra, J.K.; Kurian, G.; Christaian, J.H.; van Tol, J.; Singh, K.; Dalal, N.S.; Mochena, M.; Stoian, S.A.; Strouse, G.F., Evidence of Ferrimagnetism in Fe-Doped CdSe Quantum Dots, <i>Chem. Mater.</i> , 30 (23), 8446–8456 (2018)
Blancon, J.C.; Stier, A.V.; Tsai, H.; Nie, W.; Noe, T.; Kono, J.; Crooker, S.A.; Kanatzidis, M.G.; Even, J.; Mohite, A.D., Scaling law for excitons in 2D perovskite quantum wells, <i>Nature Comm.</i> , 9, 2254 (2018)
Bonhomme, C.; Wang, X.L.; Hung, I.; Gan, Z.; Gervais, C.; Sassoie, C.; Rimsza, J.; Du, J.C.; Smith, M.E.; Hanna, J.V.; Sarda, S.; Gras, P.; Combes, C.; Laurencin, D., Pushing the limits of sensitivity and resolution for natural abundance Ca-43 NMR using ultra-high magnetic field (35.2 T), <i>Chemical Communications</i> , 54 (69), 9591-9594 (2018)
Bonura, M.; Avitabile, F.; Barth, C.; Jiang, J.; Larbalestier, D.; Fête, A.; Leo, A.; Bottura, L.; Senatore, C., Very-high thermal and electrical conductivity in overpressure-processed Bi2Sr2CaCu2O8+x wires, <i>Materials Research Express</i> , 5 (5), 056001 (2018)
Brazin, K.N.; Mallis, R.J.; Boeszoermyeni, A.; Feng, Y.; Yoshizawa, A.; Rech, P.A.; Kaur, P.; Bi, K.; Hussey, R.E.; Duke-Cohan, J.S.; Song, L.; Wagner, G.; Arthanari, H.; Lang, M.J.; Reinherz, E.L., The T-cell Antigen Receptor a Transmembrane Domain Coordinates Triggering through Regulation of Bilayer Immersion and CD3 Subunit Associations, <i>Immunity</i> , 49, 1-13 (2018)
Brinzari, T.V.; Rajan, D.; Ferreira, C.F.; Stoian, S.A.; Quintero, P.A.; Meisel, M.W.; Talham, D.R., Light-induced magnetization changes in aggregated and isolated cobalt ferrite nanoparticles, <i>J. Appl. Phys.</i> , 124 (10), 103904 (2018)
Campbell, D.J.; Wang, L.M.; Eckberg, C.; Graf, D.; Hodovanets, H.; Paglione, J., CoAs: The line of 3d demarcation, <i>Phys. Rev. B</i> , 97 (17), 174410 (2018)
Can, T.V.; McKay, J.E.; Weber, R.T.; Yang, C.; Dubroca, T.; van Tol, J.; Hill, S.; Griffin, R.G., Frequency-Swept Integrated and Stretched Solid Effect Dynamic Nuclear Polarization, <i>J. Physical Chemistry Letters</i> , 9, 3187-3192 (2018)
Cao, W.; Wang, W.D.; Xu, H.S.; Sergeyev, I.V.; Struppe, J.; Wang, X.; Mentink-Vigier, F.; Gan, Z.; Xiao, M.X.; Wang, L.Y.; Chen, G.P.; Ding, S.Y.; Bai, S.; Wang, W., Exploring Applications of Covalent Organic Frameworks: Homogeneous Reticulation of Radicals for Dynamic Nuclear Polarization, <i>J. Am. Chem. Soc.</i> , 141, 6969–6977 (2018)
Cepeda, M.R.; McGarry, L.; Pennington, J.M.; Krzystek, J.; Stroupe, M.E., The role of extended Fe4S4 cluster ligands in mediating sulfite reductase hemoprotein activity, <i>Biochim. Biophys. Acta - Proteins and Proteomics</i> , 1866, 933-940 (2018)
Chang, N.B.; Wen, D.; McKenna, A.M.; Wanielista, M.P., The Impact of Carbon Source as Electron Donor on Composition and Concentration of Dissolved Organic Nitrogen in Biosorption-Activated Media for Stormwater and Groundwater Co-Treatment, <i>Environ. Sci. Technol.</i> , 52 (16), 9380-9390 (2018)
Chen, C.H.; Shimon, D.; Lee, J.J.; Mentink-Vigier, F.; Hung, I.; Siever, C.W.; Jones, C.; Hayes, S.E., The "Missing" Bicarbonate in CO2 Chemisorption Reactions on Solid Amine Sorbents, <i>J. Am. Chem. Soc.</i> , 140 (28), 8648-8651 (2018)
Chen, H.; Laws, E.A.; Martin, J.L.; Berhane, T.K.; Gulig, P.A.; Williams, H.N., Relative Contributions of Halobacteriovorax and Bacteriophage to Bacterial Cell Death under Various Environmental Conditions, <i>mBio</i> , 9 (4), 1-13 (2018)
Chen, P.; Holinsworth, B.; O'Neal, K.; Luo, X.; Topping, C.; Cheong, S.; Singleton, J.; Choi, E.; Musfeldt, J., Frustration and glass-like character in RIn1-xMnxInO3, <i>Inorg. Chem.</i> , 57, 12501 (2018)
Ciuchi, S.; DiSante, D.; Dobrosavljevic, V.; Fratini, S., The origin of Mooij correlations in disordered metals, <i>npj Quantum Materials (Nature)</i> , 3, 44 (2018)
Collet, A.; Craig, G.A.; Heras Ojea, M.; Wilson, C.; Bhaskaran, L.; Hill, S.; Murrie, M., Slow magnetic relaxation in a {CollCollII2} complex containing a high magnetic anisotropy trigonal bipyramidal Coll, <i>Dalton Trans. Chem.</i> , 47, 9237-9240 (2018)
Cui, J.Y.; Li, J.; Liu, X.; Peng, X.H.; Fu, R., Engineering spin Hamiltonians using multiple pulse sequences in solid state NMR spectroscopy, <i>J. Magn. Reson.</i> , 294, 83-92 (2018)
Curtis, J.A.; Burch, A.D.; Barman, B.; Linn, A.G.; McClintock, L.M.; O'Berine, A.L.; Stiles, M.J.; Reno, J.L.; McGill, S.A.; Karaskaj, D.; Hilton, D.J., Broadband ultrafast terahertz spectroscopy in the 25 T Split Florida-Helix, <i>Rev. Sci. Instrum.</i> , 89, 073901 (2018)
Cyr-Choinière, O.; LeBoeuf, D.; Badoux, S.; Dufour-Beauséjour, S.; Bonn, D.A.; Hardy, W.N.; Liang, R.; Graf, D.; Doiron-Leyraud, N.; Taillefer, L., Sensitivity of Tc to pressure and magnetic field in the cuprate superconductor YBa2Cu3Oy: Evidence of charge-order suppression by pressure, <i>Phys. Rev. B</i> , 98, 064513 (2018)

Dai, Y.T.; Xu, Z.S.; Luo, Z.P.; Han, K.; Zhai, Q.J.; Zheng, H.X., Phase formation kinetics, hardness and magnetocaloric effect of sub-rapidly solidified LaFe <sub>1.6</sub> Si <sub>1.4</sub> plates during isothermal annealing, <i>J. Magn. Magn. Mater.</i> , 454, 356-361 (2018)
Davila, S.; Liu, P.; Smith, A.; Marshall, A.G.; Pedigo, S., Spontaneous Calcium-Independent Dimerization of the Isolated First Domain of Neural Cadherin, <i>Biochemistry</i> , 57 (45), 6404-6415 (2018)
Davis, I.; Koto, T.; Terrell, J.R.; Kozhanov, A.; Krzystek, J.; Liu, A., High-Frequency/High-Field Electron Paramagnetic Resonance and Theoretical Studies of Tryptophan-Based Radicals, <i>J. Phys. Chem. A</i> , 122 (12), 3170-3176 (2018)
Dhakal, P.; Chetri, S.; Balachandran, S.; Lee, P.J.; Ciovati, G., Effect of low temperature baking in nitrogen on the performance of a niobium superconducting radio frequency cavity, <i>Physical Review Accelerators and Beams</i> , 21 (3), 032001 (2018)
Ding, X.; Chai, Y.S.; Balakirev, F.; Jaime, M.; Yi, H.T.; Cheong, S.W.; Sun, Y.; Zapf, V.S., Measurement of the angle dependence of magnetostriction in pulsed magnetic fields using a magnetoelectric voltage sensor, <i>Rev. Sci. Instrum.</i> , 89, 085109 (2018)
Diroll, B.; Cho, W.; Coropceanu, I.; Harvey, S.M.; Brumberg, A.; Holtgrewe, N.; Crooker, S.A.; Wasielewski, M.R.; Prakapenka, V.B.; Talapin, D.V.; Schaller, R.D., Semiconductor Nanoplatelet Excimers, <i>Nano Letters</i> , 18, 6948 (2018)
Dordevic, S.V.; Lei, H.; Petrovic, S.; Ludwig, J.; Li, Z.; Smirnov, D., Observation of cyclotron antiresonance in the topological insulator Bi <sub>2</sub> Te <sub>3</sub> , <i>Phys. Rev. B</i> , 98, 115138 (2018)
Drichko, I.L.; Smirnov, I.YU.; Nestoklon, M.O.; Suslov, A.V.; Kamburov, D.; Baldwin, K.W.; Pfeiffer, L.N.; West, K.W.; Golub, L.E., Intersubband scattering in n-GaAs/AlGaAs wide quantum wells, <i>Phys. Rev. B</i> , 97, 075427 (2018)
Dubraja, L.A.; Juric, M.; Lafargue-Dit-Hauret, W.; Pajic, D.; Zorko, A.; Ozarowski, A.; Rocquefelte, X., First crystal structures of oxo-bridged [CrIII TaV] dinuclear complexes: spectroscopic, magnetic and theoretical investigations of the Cr–O–Ta core, <i>New J. Chemistry</i> , 42, 10912-10921 (2018)
Dudukovic, N.A.; Hudson, B.C.; Paravastu, A.K.; Zukoskid, C.F., Self-assembly pathways and polymorphism in peptide-based nanostructures, <i>Nanoscale</i> , 10 (3), 1508-1516 (2018)
Dutoit, C.E.; Stepanov, A.; van Tol, J.; Orio, M.; Bertaina, S., Superlattice Induced by Charge Order in the Organic Spin Chain (TMTTF) <sub>2</sub> X (X=SbF <sub>6</sub> , AsF <sub>6</sub> , and PF <sub>6</sub> ) Revealed by High-Field Electron Paramagnetic Resonance, <i>J. Physical Chemistry Letters</i> , 9 (18), 5598-5603 (2018)
Dutta, A.; Tyminska, N.; Zhu, G.; Collins, J.; Lively, R.P.; Schmidt, J.R.; Vasenkov, S., Influence of Hydrogen Sulfide Exposure on the Transport and Structural Properties of the Metal-Organic Framework ZIF-8, <i>J. Physical Chemistry C</i> , 122 (13), 7278-7287 (2018)
Ermolaev, M.; Suchalkin, S.; Belenky, G.; Kipshidze, G.; Laikhtman, B.; Moon, S.; Ozerov, M.; Smirnov, D.; Svensson, S.P.; Sarney, W.L., Metamorphic narrow-gap InSb/InAsSb superlattices with ultra-thin layers, <i>Appl. Phys. Lett.</i> , 113, 213104 (2018)
Escobar, L.B.L.; Guedes, G.P.; Soriano, S.; Cassaro, R.A.A.; Marbey, J.; Hill, S.; Novak, M.A.; Andruh, M.; Vaz, M.G.F., Synthesis, Crystal Structures, and EPR Studies of First MnIII LnIII Hetero-binuclear Complexes, <i>Inorg. Chem.</i> , 57, 326-334 (2018)
Felts, A.C.; Slimani, A.; Cain, J.M.; Andrus, M.J.; Ahir, A.; Abboud, K.A.; Meisel, M.W.; Boukheddaden, K.; Talham, D.R., Control of the Speed of a Light-Induced Spin Transition through Mesoscale Core-Shell Architecture, <i>J. Am. Chem. Soc.</i> , 140 (17), 5814-5824 (2018)
Ferentinos, E.; Raptopoulou, C.P.; Psycharis, V.; Terzis, A.; Krzystek, J.; Kyritsis, P., Magnetostructural correlations in S = 1 trans-[Ni{(OPPh <sub>2</sub> )(EPh <sub>2</sub> N) <sub>2</sub> (dmsO) <sub>2</sub> }] <sub>2</sub> , E = S, Se, and related complexes, <i>Polyhedron</i> , 151, 177-184 (2018)
Fortune, N.; Agosta, C.; Hannahs, S.; Schleuter, J., Magnetic-field-induced 1st order transition to FFLO state at paramagnetic limit in 2D superconductors, <i>J. Phys.: Conf. Series</i> , 996, 012072 (2018)
Garcia, C.; Pradhan, N.R.; Rhodes, D.; Balicas, L.; McGill, S.A., Photogating and high gain in ReS <sub>2</sub> field-effect transistors, <i>J. Appl. Phys.</i> , 124, 204306 (2018)
Garg, P.; Balachandran, S.; Adlakha, I.; Lee, P.J.; Bieler, T.R.; Solanki, K.N., Revealing the role of nitrogen on hydride nucleation and stability in pure niobium using first-principles calculations, <i>Superconductor Science and Technology</i> , 31 (11), 115007 (2018)
Gatto, R.G.; Mustafi, S.M.; Amin, M.Y.; Mareci, T.H.; Wu, Y.C.; Magin, R.L., Neurite orientation dispersion and density imaging can detect presymptomatic axonal degeneration in the spinal cord of ALS mice, <i>Functional Neurology</i> , 33 (3), 155-163 (2018)
Giraldo-Dávila, D.; Chacon Patino, M.; McKenna, A.M.; Blanco-Tirado, C.; Combariza, M.Y., Correlations Between Molecular Composition and the Adsorption, Aggregation and Emulsifying Behavior of Petrophase 2017 Asphaltene and their TLC Fractions, <i>Energy Fuels</i> , 32 (3), 2769-2780 (2018)
Gosh, S.; Wasala, M.; Pradhan, N.R.; Rhodes, D.; Patil, P.D.; Fralalde, M.; Xin, Y.; McGill, S.A.; Balicas, L.; Talapatra, S., Low temperature photoconductivity of few layer p-type tungsten diselenide (WSe <sub>2</sub> ) field-effect transistors (FETs), <i>Nanotechnology</i> , 29, 484002 (2018)
Graham, B.W.; Bougoulas, M.E.; Dodge, K.L.; Thaxton, C.T.; Olasso, D.; Tao, Y.; Young, N.L.; Marshall, A.G.; Trakselis, M.A., Control of Hexamerization, Assembly, and Excluded Strand Specificity for the <i>Sulfolobus solfataricus</i> MCM Helicase, <i>Biochemistry</i> , 57 (39), 5672-5682 (2018)



Greer, S.M.; McKay, J.; Gramigna, K.M.; Thomas, C.M.; Stoian, S.A.; Hill, S., Probing Fe-V Bonding in a C3-Symmetric Heterobimetallic Complex, <i>Inorg. Chem.</i> , <b>57</b> , 5870-5878 (2018)
Gu, G.C.; Zhao, Z.Y.; Chen, X.L.; Lee, M.; Choi, E.S.; Ling, L.S.; Zhang, Y.H.; Yang, Z.R.; Zhou, H.D.; Sun, X.F., Field-Driven Quantum Criticality in the Spinel Magnet ZnCr <sub>2</sub> Se <sub>4</sub> , <i>Phys. Rev. Lett.</i> , <b>120</b> , 147204 (2018)
Gubkin, A.F.; Wu, L.S.; Nikitin, S.E.; Suslov, A.V.; Podlesnyak, A.; Prokhnenko, O.; Prokeš, K.; Yokaichiya, F.; Keller, L.; Baranov, N.V., Field-induced magnetic phase transitions and metastable states in Tb <sub>3</sub> Ni, <i>Phys. Rev. B</i> , <b>97</b> , 134425 (2018)
Gueneli, N.; McKenna, A.M.; Ohkouchi, N.; Boreham, C.J.; Beghin, J.; Javaux, E.J.; Brocks, J.J., 1.1 Billion Years Old Porphyrins Establish a Marine Ecosystem Dominated by Bacterial Primary Producers, <i>P. Natl. Acad. Sci. U.S.A.</i> , <b>115</b> , 1-9 (2018)
Harstein, M.; Toews, W.H.; Hsu, Y.H.; Zeng, B.; Chen, X.; Hatnean, M.; Ciomaga, M.; Zhang, Q.R.; Nakamura, S.; Rodway-Gant, G.; Berk, J.; Kingston, M.K.; Zhang, G.H.; Chan, M.K.; Yamashita, S.; Sakakibara, T.; Takano, Y.; Park, J.H.; Balicas, L.; Harrison, N.; Shitsevalova, N.; Balakrishnan, G.; Lonzarich, G.G.; Hill, R.W.; Sutherland, M.; Sebastian, S.E., Fermi surface in the absence of a Fermi liquid in the Kondo insulator SmB <sub>6</sub> , <i>Nature Physics</i> , <b>14</b> , 166 (2018)
Hayes, I.M.; Hao, Z.; Maksimovic, N.; Lewin, S.K.; Chan, M.K.; McDonald, R.D.; Ramshaw, B.J.; Moore, J.E.; Analytis, J.G., Magnetoresistance Scaling Reveals Symmetries of the Strongly Correlated Dynamics in BaFe <sub>2</sub> (As <sub>1-x</sub> Px) <sub>2</sub> , <i>Phys. Rev. Lett.</i> , <b>121</b> , 197002 (2018)
Hediger, S.; Lee, D.; Mentink-Vigier, F.; De Paepe, G., MAS-DNP Enhancements: Hyperpolarization, Depolarization, and Absolute Sensitivity, <i>eMagRes</i> , <b>7</b> , 105-116 (2018)
Higgins, J.S.; Chan, M.K.; Sarkar, T.; McDonald, R.D.; Greene, R.L.; Butch, N.P., Quantum oscillations from the reconstructed Fermi surface in electron-doped cuprate superconductors, <i>New J. Phys.</i> , <b>20</b> , 043008 (2018)
Holinsworth, B.; Harms, N.; Fan, S.; Mazumdar, D.; Gupta, A.; McGill, S.; Musfeldt, J., Magnetic field control of charge excitations in CoFe <sub>2</sub> O <sub>4</sub> , <i>APL Mater.</i> , <b>6</b> , 066110 (2018)
Hu, J.; Zhu, Y.; Gui, X.; Graf, D.; Tang, Z.; Xie, W.; Mao, Z., Quantum oscillation evidence of a topological semimetal phase in ZrSnTe, <i>Phys. Rev. B</i> , <b>97</b> , 155101 (2018)
Hughey, K.; Clune, A.; Yokosuk, M.; Li, J.; Abyankar, N.; Ding, X.; Dalal, N.; Xiang, H.; Smirnov, D.; Singleton, J.; Musfeldt, J., Structure-property relations in multiferroic [(CH <sub>3</sub> ) <sub>2</sub> NH <sub>2</sub> ]M(HCOO) <sub>3</sub> (M=Mn, Co, Ni), <i>Inorg. Chem.</i> , <b>57</b> , 11569 (2018)
Iida, K.; Haenisch, J.; Tarantini, C., Fe-based superconducting thin films on metallic substrates: growth, characteristics and relevant properties, <i>Applied Physics Reviews</i> , <b>5</b> , 031304 (2018)
Ji, H.; Dhomkar, S.; Wu, R.; Ludwig, J.; Lu, Z.; Smirnov, D.; Tamargo, M.C.; Bryant, G.W.; Kuskovsky, I.L., Long spin-flip time and large Zeeman splitting of holes in type-II ZnTe/ZnSe submonolayer quantum dots, <i>J. Appl. Phys.</i> , <b>124</b> , 144306 (2018)
Jiang, T.; Hoover, M.E.; Holt, M.V.; Freitas, M.A.; Marshall, A.G.; Young, N.L., Middle-Down Characterization of the Cell Cycle Dependence of Histone H4 Posttranslational Modifications and Proteoforms, <i>Proteomics</i> , <b>18</b> , 1700442 (2018)
Jiang, Y.; Dun, Z. L.; Monn, S.; Zhou, H.D.; Koshino, M.; Smirnov, D.; Jiang, Z., Landau Quantization in Coupled Weyl Points: A Case Study of Semimetal NbP, <i>Nano Letters</i> , <b>18</b> (12), 7726 (2018)
Jin, W.; Schiros, T.; Lin, Y.; Ma, J.; Lou, R.; Dai, Z.; Yu, J.X.; Rhodes, D.; Sadowski, J.T.; Tong, X.; Qian, T.; Hashimoto, M.; Lu, D.; Dadap, J.I.; Wang, S.; Santos, E.J.G.; Zang, J.; Pohl, K.; Ding, H.; Hone, J.; Balicas, L.; Pasupathy, A.N.; Osgood, Jr., R.M., Phase transition and electronic structure evolution of MoTe <sub>2</sub> induced by W substitution, <i>Phys. Rev. B</i> , <b>98</b> , 144114 (2018)
Joshi, G.; Teferi, M.Y.; Miller, R.; Jamali, S.; Baird, D.; van Tol, J.; Malissa, H.; Lupton, J.; Boehme, C., Isotropic Effective Spin-Orbit Coupling in a Conjugated Polymer, <i>J. Am. Chem. Soc.</i> , <b>140</b> (22), 6758-6762 (2018)
Joshi, G.; Teferi, M.Y.; Miller, R.; Jamali, S.; Groesbeck, M.; van Tol, J.; McLaughlin, R.; Vardeny, Z.V.; Lupton, J.M.; Malissa, H.; Boehme, C., High-Field Magnetoresistance of Organic Semiconductors, <i>Physical Review Applied</i> , <b>10</b> (2), 024008 (2018)
Kamiya, Y.; Ge, L.; Hong, T.; Qiu, Y.; Quintero-Castro, D.L.; Lu, Z.; Cao, H.B.; Matsuda, M.; Choi, E.S.; Batista, C.D.; Mourigal, M.; Zhou, H.D.; Ma, J., The nature of spin excitations in the one-third magnetization plateau phase of Ba <sub>3</sub> CoSb <sub>2</sub> O <sub>9</sub> , <i>Nature Comm.</i> , <b>9</b> , 2666 (2018)
Kang, J.; Xie, L.; Wang, Y.; Lee, H.; Campbell, N.; Jiang, J.; Ryan, P.J.; Keavney, D.J.; Lee, J.; Kim, T.H.; Pan, X.; Chen, L.; Hellstrom, E.E.; Rzechowski, M.S.; Liu, Z.; Eom, C.B., Control of Epitaxial BaFe <sub>2</sub> As <sub>2</sub> Atomic Configurations with SubstrateSurface Terminations, <i>Nano Letters</i> , <b>18</b> (10), 6347-6352 (2018)
Kang, X.; Kirui, A.; Muszyński, A.; Widanage, M.C.D.; Chen, A.; Azadi, P.; Wang, P.; Mentink-Vigier, F.; Wang, T., Molecular architecture of fungal cell walls revealed by solid-state NMR, <i>Nature Comm.</i> , <b>9</b> (1), 2747 (2018)
Kim, J.C.; Kim, J.; Xin, Y.; Lee, J.H.; Kim, Y.G.; Subhash, G.; Singh, R.K.; Arjunan, A.C.; Lee, H.G., Micro-architecture embedding ultra-thin interlayer to bond diamond and silicon via direct fusion, <i>Appl. Phys. Lett.</i> , <b>112</b> (21), 211601-4 (2018)
Kirui, A.; Ling, X.K.; Dickwella Widanage, M.C.; Mentink-Vigier, F.; French, A.D.; Wang, T., Atomic resolution of cotton cellulose structure enabled by dynamic nuclear polarization solid-state NMR, <i>Cellulose</i> , <b>6</b> , 1-11 (2018)

Klotz, J.; Goetze, K.; Sheikin, I.; Foerster, T.; Graf, D.; Park, J.H.; Choi, E.S.; Hu, R.; Petrovic, C.; Wosnitza, J.; Green, E.L., Fermi surface reconstruction and dimensional topology change in Nd-doped CeCoIn <sub>5</sub> , <i>Phys. Rev. B Rapid Commun.</i> , <b>98</b> , 081105 (2018)
Knighnton, T.; Wu, Z.; Huang, J.; Serafin, A.; Xia, J.S.; Pfeifer, L.N.; West, K.W., Evidence of two-stage melting of Wigner solids, <i>Phys. Rev. B</i> , <b>97</b> , 085135 (2018)
Komijani, D.; Ghirri, A.; Bonizzoni, C.; Klyatskaya, S.; Moreno-Pineda, E.; Ruben, M.; Soncini, A.; Affronte, A.; Hill, S., Radical-Lanthanide Ferromagnetic Interaction in a TbIII Bis-Phthalocyaninato Complex, <i>Phys. Rev. Materials</i> , <b>2</b> , 024405 (2018)
Lengyel, J.; Stoian, S.A.; Dalal, N.; Shatruck, M., Directed Synthesis and Magnetic Properties of a Hexanuclear Ferric Cluster, <i>Polyhedron</i> , <b>151</b> (1), 446-451 (2018)
Li, H.; Shan, X.; Neu, J.; Geske, T.; Davis, M.; Mao, P.; Xiao, K.; Siegrist, T.; Yu, Z., Lead-free halide double perovskite-polymer composites for flexible X-ray imaging, <i>J. Materials Chemistry C</i> , <b>6</b> , 11961-11967 (2018)
Li, H.; Wang, L.; Xiao, H.; Xu, J.; Zheng, S.; Zhai, Q. J.; Han, K., Hardening Low-Carbon Steels by Engineering the Size and Distribution of Inclusions, <i>Metall. Mater. Trans. A</i> , <b>11</b> , 1-12 (2018)
Li, M.; Wang, Y.; Chen, A.P.; Naidu, A.; Napier, B.S.; Li, W.Y.; Rodriguez, C.L.; Crooker, S.A.; Omenetto, F.G., Flexible magnetic composites for light-controlled actuation and interfaces, <i>P. Natl. Acad. Sci. U.S.A.</i> , <b>115</b> , 8119 (2018)
Li, Q.; Liu, Z.G.; Zheng, F.; Liu, R.; Lee, J.; Xu, G.L.; Zhong, G.; Hou, X.; Fu, R.; Chen, Z.H.; Amine, K.; Mi, J.X.; Wu, S.Q.; Grey, C.P.; Yong, Y., Identifying the Structural Evolution of the Sodium Ion Battery Na <sub>2</sub> FePO <sub>4</sub> F Cathode, <i>Angew. Chem. Int. Ed.</i> , <b>57</b> , 11918-11923 (2018)
Li, W.; Han, K.; Niu, R.; Liang, T.; Lai, C.; Zhang, X.H., Effect of Si and Y <sub>2</sub> O <sub>3</sub> Additions on the Oxidation Behavior of Ni-xAl (x = 5 or 10 wt%) Alloys at 1150 °C, <i>Oxid Met.</i> , <b>89</b> (5-6), 731-753 (2018)
Li, Z.; Wang, T.; Lu, Z.; Jin, C.; Chen, Y.; Meng, Y.; Taniguchi, T.; Watanabe, K.; Zhang, S.; Smirnov, D.; Shi, S., Revealing the biexciton and trion-exciton complexes in BN encapsulated WSe <sub>2</sub> , <i>Nature Comm.</i> , <b>9</b> , 3719 (2018)
Luo, W.; Kar, S.; Li, X.F.; Galstyan, E.; Kochat, M.; Sandra, J.; Jaroszynski, J.; Abraimov, D.; Selvamanickam, V., Superior critical current of Symmetric Tape Round (STAR) REBCO wires in ultra-high background fields up to 31.2 T, <i>Superconductor Science and Technology</i> , <b>31</b> , 12LT01 (2018)
Ma, J.Z.; He, J.B.; Xu, Y.F.; Chen, D.; Zhu, W.L.; Zhang, S.; Kong, L.Y.; Gao, X.; Rong, L.Y.; Huang, Y.B.; Richard, P.; Xi, C.Y.; Choi, E.S.; Shao, Y.; Wang, Y.L.; Gao, H.J.; Dai, X.; Fang, C.; Weng, H.M.; Chen, G.F.; Qian, T.; Ding, H., Three-component fermions with surface Fermi arcs in tungsten carbide, <i>Nature Physics</i> , <b>14</b> , 349 (2018)
Majkic, G.; Pratap, R.; Xu, A.; Galstyan, E.; Higley, H.C.; Prestemon, P.; Wang, X.; Abraimov, A.; Jaroszynski, J.; Selvamanickam, V., Engineering Current Density over 5 kA/mm <sup>2</sup> at 4.2 K, 14 T in Thick Film REBCO Tapes, <i>Superconductor Science and Technology</i> , <b>31</b> , 10LT01 (2018)
Majkic, G.; Pratap, R.; Xu, A.; Galstyan, E.; Higley, H.C.; Prestemon, S.O.; Wang, X.; Abraimov, D.; Jaroszynski, J.; Selvamanickam, V., Engineering current density over 5 kA mm <sup>-2</sup> at 4.2 K, 14 T in thick film REBCO tapes, <i>Superconductor Science and Technology</i> , <b>31</b> (10), 10LT01 (2018)
Malissa, H.; Miller, R.; Baird, D.L.; Jamali, S.; Joshi, G.; Bursch, M.; Grimme, S.; van Tol, J.; Lupton, J.M.; Boehme, C., Revealing weak spin-orbit coupling effects on charge carriers in a $\Pi$ -conjugated polymer, <i>Phys. Rev. B Rapid Commun.</i> , <b>97</b> , 161201 (2018)
Marsay, C.; Aguilar-Islas, A.; Fitzsimmons, J.; Hatta, M.; Jenson, L.; John, S.; Kadko, D.; Landing, W.; Lanning, N.; Morton, P.L.; Pasqualini, A.; Rauschenberg, S.; Sherrell, R.; Shiller, A.; Twining, B.; Whitmore, L.; Zhang, R.; Buck, C.S., Dissolved and particulate trace elements in late summer Arctic melt ponds, <i>Mar. Chem.</i> , <b>204</b> , 70-85 (2018)
Marsay, C.M.; Kadko, D.; Landing, W.M.; Morton, P.L.; Summers, B.A.; Buck, C.S., Concentrations, provenance and flux of aerosol trace elements during US GEOTRACES Western Arctic cruise GN01, <i>Chemical Geology</i> , <b>502</b> , 1-14 (2018)
Mentink-Vigier, F.; Marin-Montesinos, I.; Jagtap, A.P.; Halbritter, T.; van Tol, J.; Hediger, S.; Lee, D.; Sigurdsson, S.T.H.; De Paepe, G., Computationally Assisted Design of Polarizing Agents for Dynamic Nuclear Polarization Enhanced NMR: The AsymPol Family, <i>J. Am. Chem. Soc.</i> , <b>140</b> (35), 11013-11019 (2018)
Modic, K.; Bachman, M.; Ramshaw, B.; Arnold, F.; Shirer, K.; Estry, A.; Betts, J.; Ghimire, J.; Bauer, E.; Schmidt, M.; Baenitz, M.; Svaizde, M.; McDonald, R.; Shekter, A.; Moll, P., Resonant torsion magnetometry in anisotropic quantum materials. , <i>Nature Comm.</i> , <b>9</b> , 3975 (2018)
Modic, K.A.; Bachmann, M.D.; Ramshaw, B.J.; Arnold, F.; Shirer, K.R.; Estry, A.; Betts, J.; Ghimire, G.J.; Bauer, E.D.; Schmidt, M.; Svanidze, E.; McDonald, R.D.; Shekter, A.; Moll, P.J.W., Resonant torsion magnetometry in anisotropic quantum materials, <i>Nature Comm.</i> , <b>9</b> , 3975 (2018)
Moreno-Vicente, A.; Mulet-Gas, M.; Dunk, P.W.; Poblet, J.M.; Rodriguez-Forte, A., Probing the Formation of Halogenated Endohedral Metallofullerenes: Predictions Confirmed by Experiments, <i>Carbon</i> , <b>129</b> , 750-757 (2018)
Moseley, D.H.; Stavretis, S.E.; Thirunavukkuarasu, K.; Ozerov, M.; Cheng, Y.; Daemen, L.; Ludwig, J.; Lu, Z.; Smirnov, D.; Brown, C.M.; Pandey, A.; Ramirez-Cuesta, A.J.; Lamb, A.C.; Atanasov, M.; Bill, E.; Neese, F.; Xue, Z., Spin-phonon couplings in transition metal complexes with slow magnetic relaxation, <i>Nature Comm.</i> , <b>9</b> , 2572 (2018)

Nesterova, O.V.; Nesterov, D.S.; Jezierska, J.; Pombeiro, A.J.L.; Ozarowski, A., Copper(II) Complexes with Bulky N-Substituted Diethanolamines: High-Field Electron Paramagnetic Resonance, Magnetic, and Catalytic Studies in Oxidative Cyclohexane Amidation, <i>Inorg. Chem.</i> , 57 (19), 12384-12397 (2018)
Nikolo, M.; Singleton, J.; Solenov, D.; Jiang, J.; Weiss, J.; Hellstrom, E.E., Upper critical and irreversibility fields in Ni- and Co-doped pnictide bulk superconductors, <i>Physica B</i> , 536, 833-838 (2018)
Nikolo, M.; Weiss, J.D.; Singleton, J.; Jiang, J.; Hellstrom, E.H., Critical Properties of Bulk-Doped BaFe <sub>2</sub> As <sub>2</sub> Pnictides for Magnet Design, <i>IEEE Trans. Appl. Supercond.</i> , 28 (3), 7300104 (2018)
Nolan, M.M.; Touchton, A.J.; Richey, N.E.; Ghiviriga, I.; Rocca, J.R.; Abboud, K.A.; McElwee-White, L., Synthesis and Characterization of Tungsten Nitrido Amido Guanidinato Complexes as Precursors for Chemical Vapor Deposition of WN <sub>x</sub> Cy Thin Films, <i>Eur. J. Inorg. Chem.</i> , 1, 46-53 (2018)
Nowak, J.A.; Shrestha, P.M.; Weber, R.J.; McKenna, A.M.; Chen, H.; Coates, J.D.; Goldstein, A.H., Comprehensive Analysis of Changes in Crude Oil Chemical Composition during Biosouring and Treatments, <i>Environ. Sci. Technol.</i> , 52 (3), 1290-1300 (2018)
Oyler, B.L.; Khan, M.M.; Smith, D.F.; Harberts, E.M.; Kilgour, D.P.A.; Ernst, R.K.; Cross, A.S.; Goodlett, D.R., Top Down Tandem Mass Spectrometric Analysis of a Chemically Modified Rough-Type Lipopolysaccharide Vaccine Candidate, <i>J. Am. Soc. Mass Spectr.</i> , 29 (6), 1221-1229 (2018)
Pan, W.; Lu, P.; Ihlefeld, J.F.; Lee, S.R.; Choi, E.S.; Jiang, Y.; Jia, Q.X., Electrical-current-induced magnetic hysteresis in self-assembled vertically aligned La <sub>2</sub> /3S <sub>1</sub> /3MnO <sub>3</sub> :ZnO nanopillar composites, <i>Phys. Rev. Materials</i> , 2 (2), 021401(R) (2018)
Park, E.; Lee, S.; Ronning, F.; Thompson, J.; Zhang, Q.; Balicas, L.; Lu, X.; Park, T., Spectroscopic evidence for two-gap superconductivity in the quasi-one dimensional chalcogenide Nb <sub>2</sub> Pd <sub>0.81</sub> S <sub>5</sub> , <i>J. Phys.-Condens. Mat.</i> , 30, 165401 (2018)
Patel, A.; Baskys, A.; Mitchell-Williams, T.; McCaul, A.; Coniglio, W.; Hänisch, J.; Lao, M.; Glowacki, B.A., A trapped field of 17.7 T in a stack of high temperature superconducting tape, <i>Superconductor Science and Technology</i> , 31 (9), 09LT01 (2018)
Paukovich, N.; Xue, M.; Elder, J.R.; Redzic, J.S.; Blue, A.; Pike, H.; Miller, B.G.; Pitts, T.M.; Pollock, D.D.; Hansen, K.; D'Alessandro, A.; Eisenmesser, E.Z., Biliverdin Reductase B Dynamics Are Coupled to Coenzyme Binding, <i>J. Mol. Biol.</i> , 430 (18), 3234-3250 (2018)
Pinchetti, V.; Di, Q.M.; Lorenzon, M.; Camellini, A.; Fasoli, M.; Zavelani-Rossi, M.; Meinardi, F.; Zhang, J.T.; Crooker, S.A.; Brovelli, S., Excitonic pathway to photoinduced magnetism in colloidal nanocrystals with nonmagnetic dopants, <i>Nature Nanotechnology</i> , 13, 145 (2018)
Pope, G.M.; Hung, I.; Gan, Z.; Mobarak, H.; Widmalm, G.; Harper, J.K., Exploiting C-13/N-14 solid-state NMR distance measurements to assign dihedral angles and locate neighboring molecules, <i>Chemical Communications</i> , 54 (49), 6376-6379 (2018)
Potter, W.M.; Lai, Y.; Cao, H.; Baumbach, R.E.; Lattner, S., U <sub>8</sub> Al <sub>19</sub> Si <sub>6</sub> , A Uranium Aluminide Silicide with a Stuffed Supercell Grown from Aluminum Flux, <i>Chem. Mater.</i> , 30, 3806 (2018)
Pustogow, A.; Borjes, M.; Lohle, A.; Rosshuber, R.; Zhukova, E.; Gorshunov, B.; Tomic, S.; Schluter, J.A.; Hubner, R.; Hirimitsu, T.; Yoshida, Y.; Saito, G.; Kato, R.; Lee, T.H.; Dobrosavljevic, V.; Fratini, S.; Dressel, M., Quantum spin liquids unveil the genuine Mott state, <i>Nature Mater.</i> , 17, 773-777 (2018)
Pustogow, A.; Saito, Y.; Zhukova, E.; Gorshunov, B.; Kato, R.; Lee, T.H.; Fratini, S.; Dobrosavljevic, V.; Dressel, M., Low-Energy Excitations in Quantum Spin Liquids Identified by Optical Spectroscopy, <i>Phys. Rev. Lett.</i> , 121, 056402 (2018)
Putman, J.C.; Gutiérrez Sama, S.; Barrère-Mangote, C.; Rodgers, R.P.; Lobinski, R.; Marshall, A.G.; Bouyssière, B.; Giusti, P., Analysis of Petroleum Products by Gel Permeation Chromatography Coupled Online with Inductively Coupled Plasma Mass Spectrometry and Offline with Fourier Transform Ion Cyclotron Resonance Mass Spectrometry, <i>Energy Fuels</i> , 32 (12), 12198-12204 (2018)
Rai, B.K.; Chikara, S.; Ding, X.; Oswald, I.W.H.; Schoenemann, R.; Loganathan, V.; Hallas, A.M.; Cao, H.B.; Stavinoha, M.; Chen, T.; Man, H.; Carr, S.; Singleton, J.; Zapf, V.; Benavides, K.A.; Chan, J.Y.; Zhang, Q.R.; Rhodes, D.; Chiu, Y.C.; Balicas, L.; Aczel, A.A.; Huang, Q.; Lynn, J.W.; Gaudet, J.; Sokolov, D.A.; Walker, H.C.; Adroja, D.T.; Dai, P.; Nevidomskyy, A.H.; Huang, C.L.; Morosan, E., Anomalous Metamagnetism in the Low Carrier Density Kondo Lattice YbRh <sub>3</sub> Si <sub>7</sub> , <i>Phys. Rev. X</i> , 8, 041047 (2018)
Ramshaw, B.J.; Modic, K.A.; Shehter, A.; Zhang, Y.; Kim, E.A.; Moll, P.J.W.; Bachman, M.; Chan, M.K.; Betts, J.; Balakirev, F.; Migliori, A.; Ghimire, N.J.; Bauer, E.D.; Ronning, F.; McDonald, R.D., Quantum limit transport and destruction of the Weyl nodes in TaAs, <i>Nature Comm.</i> , 9, 2217 (2018)
Rasheed, W.; Draksharapu, A.; Banerjee, S.; Young, V.G.; Fan, R.; Guo, Y.; Ozerov, M.; Nehrkorn, J.; Krzystek, J.; Telsler, J.; Que Jr., L., Crystallographic evidence for a sterically induced ferryl tilt in a non-heme oxoiron(IV) complex that makes it a better oxidant, <i>Angew. Chem. Int. Ed.</i> , 57, 9387-9391 (2018)
Ren, W.; Wang, A.; Graf, D.; Liu, Y.; Zhang, Z.; Yin, W.G.; Petrovic, C., Absence of Dirac states in BaZnBi <sub>2</sub> induced by spin-orbit coupling, <i>Phys. Rev. B</i> , 97, 035147 (2018)
Rosenberg, J.T.; Xuegang, Y.; Helsper, S.; Bagdasarian, F.A.; Ma, T.; Grant, S.C., Effects of labeling human mesenchymal stem cells with superparamagnetic iron oxides on cellular functions and magnetic resonance contrast in hypoxic environments and long-term monitoring, <i>Brain Circulation</i> , 4 (3), 133-138 (2018)

Roy, B.; Kennett, M. P.; Yang, K.; Juricic, J., From Birefringent Electrons to a Marginal or Non-Fermi Liquid of Relativistic Spin-1/2 Fermions: An Emergent Superuniversality, <i>Phys. Rev. Lett.</i> , 121 (15), 157602 (2018)
Sahoo, P.K.; Memaran, S.; Xin, Y.; Balicas, L.; Gutiérrez, H.R., One-pot growth of two-dimensional lateral heterostructures via sequential edge-epitaxy, <i>Nature</i> , 553, 63-67 (2018)
Sakhratov, Y.A.; Kweon, J.J.; Choi, E.S.; Zhou, H.D.; Svistov, L.E.; Reyes, A.P., Search for a nematic phase in the quasi-two-dimensional antiferromagnet CuCrO <sub>2</sub> by NMR in an electric field, <i>Phys. Rev. B</i> , 97, 094409 (2018)
Sanabria, C.; Field, M.; Lee, P.J.; Miao, H.; Parrell, J.; Larbalestier, D.C., Controlling Cu-Sn Mixing so as to Enable Higher Critical Current Densities in RRP@ Nb <sub>3</sub> Sn Wires, <i>Superconductor Science and Technology</i> , 31 (6), 064001 (2018)
Sellappan, P.; Cote, J.; Kreth, P.A.; Schepkin, V.D.; Darkazalli, A.; Morris, D.R.; Alvi, F.S.; Levenson, C.W., Variability and uncertainty in the rodent controlled cortical impact model of traumatic brain injury, <i>J. Neurosci. Methods</i> , 312, 37-42 (2018)
Shen, J.; Terskikh, V.; Wang, X.L.; Hung, I.; Gan, Z.; Wu, G., A Quadrupole-Central-Transition O-17 NMR Study of Nicotinamide: Experimental Evidence of Cross-Correlation between Second-Order Quadrupolar Interaction and Magnetic Shielding Anisotropy, <i>J. Phys. Chem. B</i> , 122 (18), 4813-4820 (2018)
Shen, Z.Y.; Wang, B.L.; Liang, G.F.; Zhang, Y.H.; Han, K.; Song, C.J., Grain Boundary Pop-in, Yield Point Phenomenon and Carbon Segregation in Aged Low Carbon Steel, <i>ISIJ International</i> , 58 (2), 373-375 (2018)
Sohn, E.; Xi, X.; He, W.Y.; Jiang, S.; Wang, Z.; Kang, K.; Park, J.H.; Berger, H.; Forro, L.; Law, K.T.; Shan, J.; Mak, K.F., An unusual continuous paramagnetic-limited superconducting phase transition in 2D NbSe <sub>2</sub> , <i>Nat. Mat.</i> , 17, 504-508 (2018)
Steele, J.L.; Tahsini, L.; Sun, C.; Elinburg, J.K.; Kotyk, C.M.; McNeely, J.; Stoian, S.A.; Dragulescu-Andrasi, A.; Ozarowski, A.; Ozerov, M.; Krzystek, J.; Telsler, J.; Bacon, J.W.; Golen, J.A.; Rheingold, A.L.; Doerrer, L.H., Square-planar Co(III) in {O <sub>4</sub> } coordination: Large ZFS and reactivity with ROS, <i>Chem. Commun.</i> , 54, 12045-12048 (2018)
Stepanov, P.; Che, S.; Shcherbakov, D.; Yang, J.; Chen, R.; Thilagar, K.; Voigt, G.; Bockrath, M.W.; Smirnov, D.; Watanabe, K.; Taniguchi, T.; Lake, R.K.; Barlas, Y.; MacDonald, A.H.; Lau, C.N., Long-distance spin transport through a graphene quantum Hall antiferromagnet, <i>Nature Physics</i> , 14, 907 (2018)
Sternisha, S.M.; Liu, P.; Marshall, A.G.; Miller, B.G., Mechanistic Origins of Enzyme Activation in Human Glucokinase Variants Associated with Congenital Hyperinsulinism, <i>Biochemistry</i> , 57 (10), 1632-1639 (2018)
Stevens, C.E.; Paul, J.; Cox, T.; Sahoo, P.K.; Gutiérrez, H.R.; Turkowski, V.; Semenov, D.; McGill, S.A.; Kapetanakis, M.D.; Perakis, I.E.; Hilton, D.J.; Karaiskaj, D., Biexcitons in monolayer transition metal dichalcogenides tuned by magnetic fields, <i>Nature Comm.</i> , 9, 3720 (2018)
Stevens, C.E.; Stroucken, T.; Stier, A.V.; Paul, J.; Zhang, H.; Dey, P.; Crooker, S.A.; Koch, S.W.; Karaiskaj, D., Superradiant coupling effects in transition-meta dichalcogenides, <i>Optica</i> , 5, 749 (2018)
Suarez, D.; Steven, E.; Laukhina, E.; Gomez, A.; Crespi, A.; Mestres, N.; Rovira, C.; Choi, E. S.; Veciana, J., 2D organic molecular metallic soft material derived from BEDO-TTF with electrochromic and rectifying properties., <i>Nature Flex Electron</i> , 2 (1), 29 (2018)
Suchalkin, S.; Belenky, G.; Ermolaev, M.; Moon, S.; Jiang, Y.; Graf, D.; Smirnov, D.; Laikhtman, B.; Shtrengas, L.; Kipshidze, G.; Svensson, S.P.; Sarney, W.L., Engineering Dirac Materials: Metamorphic InAs 1-xSb x/InAs 1-ySb y Superlattices with Ultralow Bandgap, <i>Nano Letters</i> , 18, 412 (2018)
Switlicka, A.; Machura, B.; Penkala, M.; Bienko, A.; Bienko, D.C.; Tifis, J.; Rajnak, C.; Boca, R.; Ozarowski, A.; Ozerov, M., Slow Magnetic Relaxation in Cobalt(II) Field-Induced Single-Ion Magnets with Positive Large Anisotropy, <i>Inorg. Chem.</i> , 57, 12740-12755 (2018)
Tabatabai, B.; Chen, H.; Lu, J.; Giwa-Otusajo, J.; McKenna, A.M.; Shrivastava, A.K.; Sittler, V., Fremyella Diplosiphon as a Biodiesel Agent: Identification of Fatty Acid Methyl Esters via Microwave-Assisted Direct In Situ Transesterification, <i>BioEnergy Research</i> , 11 (3), 528-537 (2018)
Tala, S.R.; Singh, A.; Lensing, C.J.; Schnell, S.M.; Freeman, K.T.; Rocca, J.R.; Haskell-Luevano, C., 1,2,3-Triazole Rings as a Disulfide Bond Mimetic in Chimeric AGRP-Melanocortin Peptides: Design, Synthesis, and Functional Characterization, <i>ACS Chemical Neurosci.</i> , 9 (5), 1001-1013 (2018)
Tennakoon, S.; Peng, Y.; Mookherjee, M.; Speziale, S.; Manthilake, G.; Besara, T.; Andreu, L.; Rivera, F., Single crystal elasticity of natural topaz at high-temperatures, <i>Scientific Report</i> , 8, 1372 (2018)
Terashima, T.; Hirose, H.T.; Graf, D.; Ma, Y.; Mu, G.; Hu, T.; Suzuki, K.; Uji, S.; Ikeda, H., Fermi Surface with Dirac Fermions in CaFeAsF Determined via Quantum Oscillation Measurements, <i>Phys. Rev. X</i> , 8, 011014 (2018)
Tian, W.; Cao, H.; Clune, A.; Hughey, K.; Hong, T.; Yam, J.; Argawal, H.; Singleton, J.; Sales, B.; Fishman, R.; Musfeldt, J.; Fernandez-Baca, J., Electronic phase separation and magnetic-field-induced phenomena in molecular multiferroic (ND <sub>4</sub> ) <sub>2</sub> FeCl <sub>5</sub> D <sub>2</sub> O, <i>Phys. Rev. B</i> , 98, 054407 (2018)
Uji, S.; Iida, Y.; Sugiura, S.; Isono, T.; Sugii, K.; Kikugawa, N.; Terashima, T.; Yasuzuka, S.; Akutsu, H.; Nakazawa, Y.; Graf, D.; Day, P., Fulde-Ferrell-Larkin-Ovchinnikov superconductivity in the layered organic superconductor beta''-(BEDT-TTF)(4)[(H <sub>3</sub> O)Ga(C <sub>2</sub> O <sub>4</sub> )(3)]C <sub>6</sub> H <sub>5</sub> NO <sub>2</sub> , <i>Phys. Rev. B</i> , 97 (14), 144505 (2018)
Vieru, V.; Iwahara, N.; Lan, Y.; Komijani, D.; Hill, S.; Wernsdorfer, W.; Chibotaru, L., Towards a Microscopic Understanding of the Magnetization Behavior of Multimolecular Single Crystal of Radical-Bridged [DyIII <sub>4</sub> ] Cubane Units: A Joint Ab Initio, Micro-SQUID and EPR Study, <i>J. Physical Chemistry C</i> , 122, 11128-11135 (2018)



Von Morze, C.; Reed, G.D.; Larson, P.E.; Mammoli, D.; Chen, A.P.; Tropp, J.; Van Criekeing, M.; Ohliger, M.A.; Kurhanewicz, J.; Vigneron, D.B.; Merritt, M.E., In vivo hyperpolarization transfer in a clinical MRI scanner, <i>Magnet. Reson. Med.</i> , 80 (2), 480-487 (2018)
Waiczies, S.; Rosenberg, J.T.; Kuehne, A.; Starke, L.; Delgado, P.R.; Millward, J.M.; Prinz, C.; Periquito, J.S.; Pohlmann, A.; Waiczies, H.; Niendorf, T., Fluorine-19 MRI at 21.1 T: enhanced spin-lattice relaxation of perfluoro-15-crown-5-ether and sensitivity as demonstrated in ex vivo murine neuroinflammation, <i>Magma</i> , 31 (5), 13 (2018)
Wang, L.; Yin, M.; Khan, A.; Muhtadi, S.; Asif, F.; Choi, E.S.; Datta, T., Scatterings and Quantum Effects in (Al,InN)/GaN Heterostructures for High-Power and High-Frequency Electronics, <i>Physical Review Applied</i> , 9 (2), 024006 (2018)
Wang, Y.; Xu, Y.; Spencer, R.G.M.; Zito, P.; Kellerman, A.; Podgorski, D.; Xiao, W.; Wei, D.; Rashid, H.; Yang, Y., Selective Leaching of Dissolved Organic Matter From Alpine Permafrost Soils on the Qinghai-Tibetan Plateau, <i>J. Geophys. Res. Biogeosci.</i> , 123 (3), 1005-1016 (2018)
Wehinger, B.; Fiolka, C.; Lanza, A.; Scatena, R.; Kubus, M.; Grokowiak, A.; Coniglio, W.A.; Graf, D.; Skoulatos, M.; Chen, J.H.; Gukelberger, J.; Casati, N.; Zaharko, O.; Macchi, P.; Krämer, K.W.; Tozer, S.; Mudry, C.; Normand, B.; Rüttig, CH., Giant Pressure Dependence and Dimensionality Switching in a Metal-Organic Quantum Antiferromagnet, <i>Phys. Rev. Lett.</i> , 121, 117201 (2018)
Whittles, Z.; Marple, M.; Hung, I.; Gan, Z.; Sen, S., Structure of BaO-TeO <sub>2</sub> glasses: A two-dimensional Te-125 NMR spectroscopic study, <i>J. Non-Crystalline Solids</i> , 481, 282-288 (2018)
Wilfong, B.; Zhou, X.; Vivanco, H.; Campbell, D.J.; Wang, K.; Graf, D.; Paglione, J.; Rodriguez, E., Frustrated magnetism in the tetragonal CoSe analog of superconducting FeSe, <i>Phys. Rev. B</i> , 97 (10), 104408 (2018)
Williams, C.M.; Rocca, J.R.; Edison, A.S.; Allison, D.B.; Morgan, T.J.; Hahn, D.A., Cold adaptation does not alter ATP homeostasis during cold exposure in <i>Drosophila melanogaster</i> , <i>Integrative Zoology</i> , 13 (4), 471-481 (2018)
Willmering, M.M.; Sesti, E.L.; Hayes, S.E.; Wood, R.M.; Bowers, C.R.; Thapa, S.K.; Stanton, C.J.; Reyes, A.P.; Kuhns, P.; McGill, S., Probing the magnetic field dependence of the light hole transition in GaAs/AlGaAs quantum wells using optically pumped NMR, <i>Phys. Rev. B</i> , 97, 075303 (2018)
Wu, C.Y.; Satapati, S.; Gui, W.; Wynn, R.M.; Sharma, G.; Lou, M.; Qi, X.; Burgess, S.C.; Malloy, C.R.; Khemtong, C.; Sherry, A.D.; Chuang, D.T.; Merritt, M.E., A novel inhibitor of pyruvate dehydrogenase kinase stimulates myocardial carbohydrate oxidation in diet-induced obesity, <i>J. Biol. Chem.</i> , 293 (25), 9604-9613 (2018)
Xia, Y.Q.; Marple, M.A.T.; Hung, I.; Gan, Z.; Sen, S., Network Structure and Connectivity in SnO-P <sub>2</sub> O <sub>5</sub> Glasses: Results from 2D P-31 and Sn-119 NMR Spectroscopy, <i>J. Phys. Chem. B</i> , 122 (29), 7416-7425 (2018)
Xiang, Z.; Kasahara, Y.; Asaba, T.; Lawson, B.; Tinsman, C.; Chen, L.; Sugimoto, K.; Kawaguchi, S.; Sato, Y.; Li, G.; Yao, S.; Chen, Y.L.; Iga, F.; Singleton, J.; Matsuda, Y.; Li, L., Quantum oscillations of electrical resistivity in an insulator, <i>Science</i> , 362, 65 (2018)
Yang, H.; Schmidt, M.; Suess, V.; Chan, M.K.; Balakirev, F.; McDonald, R.D.; Parkin, S.; Felser, C.; Yan, B.; Moll, P.J.W., Quantum oscillations in the type-II Dirac semi-metal candidate PtSe <sub>2</sub> , <i>New J. Phys.</i> , 20, 043008 (2018)
Yang, H.Y.; Gaudet, J.; Aczel, A.A.; Graf, D.E.; Blaha, P.; Gaulin, B.D.; Taffi, F., Interplay of magnetism and transport in HoBi, <i>Phys. Rev. B</i> , 98 (4), 045136 (2018)
Yang, J.; Tran, S.; Wu, J.; Che, S.; Stepanov, P.; Taniguchi, T.; Watanabe, K.; Baek, H.; Smirnov, D.; Chen, R.; Lau, C.N., Integer and Fractional Quantum Hall effect in Ultrahigh Quality Few-layer Black Phosphorus Transistors, <i>Nano Letters</i> , 18, 229 (2018)
Yang, L.; Li, X.; Ma, X.; Shan, X.; Liu, P.; Tang, Y.; Cheng, S.; Hu, Y.; Liu, M.; Chen, H., Design of high-performance cathode materials with single-phase pathway for sodium ion batteries: A study on P <sub>2</sub> -Nax(LiyMn1-y)O <sub>2</sub> compounds, <i>J. Power Sources</i> , 381, 171-180 (2018)
Yankowitz, M.; Jung, J.; Laksono, E.; Leconte, N.; Chittari, B.L.; Watanabe, K.; Taniguchi, T.; Adam, S.; Graf, D.; Dean, C.R., Dynamic band-structure tuning of graphene moiré superlattices with pressure, <i>Nature</i> , 557, 404-408 (2018)
Ye, Z.; Waldecker, L.; Ma, E.Y.; Rhodes, D.; Antony, A.; Kim, B.; Zhang, X.X.; Deng, M.; Jiang, Y.; Lu, Z.; Smirnov, D.; Watanabe, K.; Taniguchi, T.; Hone, J.; Heinz, T., Efficient generation of neutral and charged biexcitons in encapsulated WSe <sub>2</sub> monolayers, <i>Nature Comm.</i> , 9, 3718 (2018)
Yoo, K.; Koteswara, B.; Kang, J.; Nam, W.; Balakirev, F.; Zapf, V.S.; Harrison, N.; Guda, A.; Ter-Oganessian, N.; Kim, K.H., Magnetic field induced ferroelectricity in a S=1/2 kagome staircase compound PbCu <sub>3</sub> TeO <sub>7</sub> , <i>Nature Quantum Materials</i> , 3, 45 (2018)
Young, R.B.; Avneri-Katz, S.; McKenna, A.M.; Chen, H.; Bahureksa, W.; Polubesova, T.; Chefetz, B.; Borch, T., Composition-Dependent Sorptive Fractionation of Anthropogenic Dissolved Organic Matter by Fe(III)-Montmorillonite, <i>Soil Systems</i> , 2 (1), 14 (2018)
Yousif, M.; Wannipurage, D.; Huizenga, C.D.; Washnock-Schmid, E.; Peraino, N.J.; Ozarowski, A.; Stoian, S.A.; Lord, R.L.; Groysman, S., Catalytic Nitrene Homocoupling by an Iron(II) Bis(alkoxide) Complex: Bulking Up the Alkoxide Enables a Wider Range of Substrates and Provides Insight into the Reaction Mechanism, <i>Inorg. Chem.</i> , 57 (15), 9425-9438 (2018)
Yuan, B.; Zhu, W.; Hung, I.; Gan, Z.; Aitken, B.; Sen, S., Structure and Chemical Order in S-Se Binary Glasses, <i>J. Phys. Chem. B</i> , 122 (50), 12219-12226 (2018)

Yuan, X.; Yan, Z.; Song, C.; Zhang, M.; Li, Z.; Zhang, C.; Liu, Y.; Wang, W.; Zhao, M.; Lin, Z.; Xie, T.; Ludwig, J.; Jiang, Y.; Zhang, X.; Shang, C.; Ye, Z.; Wang, J.; Chen, F.; Xia, Z.; Smirnov, D.; Chen, Z.; Wang, Z.; Yan, H.; Xiu, F., Chiral Landau levels in Weyl semimetal NbAs with multiple topological carriers, <i>Nature Comm.</i> , 9, 1854 (2018)
Zhang, K.; Higley, H.; Ye, L.; Gourlay, S.; Prestemon, S.; Shen, T.; Bosque, E.; English, C.; Jiang, J.; Kim, Y.; Lu, J.; Trociewitz, U.; Hellstrom, E.; Larbalestier, D., Tripled critical current in racetrack coils made of Bi-2212 Rutherford cables with overpressure processing and leakage control, <i>Superconductor Science and Technology</i> , 31 (10), 105009 (2018)
Zhang, Z.; Jiang, J.; Wang, Q.; Larbalestier, D.C.; Hellstrom, E.E., Optimization of a Novel Melt-Growth Heat Treatment of YbBa <sub>2</sub> Cu <sub>3</sub> O <sub>7-δ</sub> /Ag Tapes, <i>IEEE Trans. Appl. Supercond.</i> , 28 (4), 6900204 (2018)
Zhao, J.; Yu, J.H.; Han, K.; Zhong, H.G.; Li, R.X.; Zhai, Q.J., Improving the Solidified Structure by Optimization of Coil Configuration in Pulsed Magneto-Oscillation, <i>Acta Metallurgica Sinica (English Letters)</i> , 31 (12), 1334-1344 (2018)
Zhao, Y.; Xie, H.; Wang, L.; Shen, Y.; Chen, W.; Song, B. E.; Zhang, Z.; Zheng, A.; Lin, Q.; Fu, R.; Wang, J.; Yang, J., Gating Mechanism of Aquaporin Z in Synthetic Bilayers and Native Membranes Revealed by Solid-State NMR Spectroscopy, <i>J. Am. Chem. Soc.</i> , 140, 7885-7895 (2018)
Zhou, C.; Lin, H.; Worku, M.; Neu, J.; Zhou, Y.; Tian, Y.; Lee, S.; Djurovich, P.; Siegrist, T.; Ma, B., Blue Emitting Single Crystalline Assembly of Metal Halide Clusters, <i>J. Am. Chem. Soc.</i> , 140 (41), 13181-13184 (2018)
Zhu, Y.; Zhang, T.; Hu, J.; Kidd, J.; Graf, D.; Gui, X.; Xie, W.; Zhu, M.; Ke, X.; Cao, H.; Fang, Z.; Weng, H.; Mao, Z., Multiple topologically non-trivial bands in non-centrosymmetric YSn <sub>2</sub> , <i>Phys. Rev. B</i> , 98, 035117 (2018)
Zipfel, J.; Holler, J.; Mitioglu, A.; Ballottin, M.; Nagler, P.; Stier, A.V.; Taniguchi, T.; Watanabe, K.; Christianen, P.; Crooker, S.A.; Korn, T.; Chernikov, A., Spatial extent of the excited exciton states in WS <sub>2</sub> monolayers from diamagnetic shifts, <i>Phys. Rev. B</i> , 98, 075438 (2018)

#### d) All External Authors (28)

Asaba, T.; Wang, Y.; Li, G.; Xiang, Z.; Tinsman, C.; Chen, L.; Zhou, S.; Zhao, S.; Laleyan, D.; Li, Y.; Mi, Z.; Li, L., Magnetic Field Enhanced Superconductivity in Epitaxial Thin Film WTe <sub>2</sub> , <i>Scientific Report</i> , 8, 6520 (2018)
Chen, L.; Song, J.B.; Zhao, W.; Yi, G.J.; Zhou, Z.K.; Song, Y.; Wang, Z.; Ouyang, Z.W.; Yuan, A.H., A mononuclear five-coordinate Co(II) single molecule magnet with a spin crossover between the S = 1/2 and 3/2 states, <i>Dalton Trans. Chem.</i> , 47, 16596-16602 (2018)
Cleaves, H.; Butch, C.; Hongo, Y.; Giri, C.; Mamajanov, I.; Guttenberg, N.; Chandru, K., Simple prebiotic synthesis of high diversity dynamic combinatorial polyester libraries, <i>Nature Communications Chemistry</i> , 30 (1), 8 (2018)
Fataftah, M.S.; Freedman, D.E., Progress towards creating optically addressable Q2molecular qubits, <i>Chem. Commun.</i> , 54, 13773-13781 (2018)
Ferreira, T.; Carone, D.; Huon, A.; Herklotz, A.; Stoian, S.A.; Heald, S.M.; Morrison, G.; Smith, M.D.; Loye, H.C., Ba <sub>3</sub> Fe <sub>1.56</sub> Ir <sub>1.44</sub> O <sub>9</sub> : A Polar Semiconducting Triple Perovskite with Near Room Temperature Magnetic Ordering, <i>Inorg. Chem.</i> , 57 (12), 7362-7371 (2018)
Flores, J.A.; Andino, J.G.; Lord, R.L.; Wolfe, R.J.; Park, H.; Pink, M.; Telsler, J.; Caulton, K.G., Probing Redox Noninnocence of Copper and Zinc Bis-pyridylpyrrolides, <i>Eur. J. Inorg. Chem.</i> , 2018 (45), 4893-4904 (2018)
Hossain, M. S.; Mueed, M. A.; Ma, M. K.; Chung, Y. J.; Pfeiffer, L. N.; West, K. W.; Baldwin, K. W.; Shayegan, M., Anomalous coupling between magnetic and nematic orders in quantum Hall systems, <i>Phys. Rev. B</i> , 98, 081109(R) (2018)
Hossain, M.S.; Ma, M.K.; Mueed, M.K.; Pfeiffer, L.N.; West, K.W.; Baldwin, K.W.; Shayegan, M., Direct Observation of Composite Fermions and Their Fully-Spin-Polarized Fermi Sea near $\nu = 5/2$ , <i>Phys. Rev. Lett.</i> , 120, 256601 (2018)
Jarvis, J.M.; Albrecht, K.O.; Billing, J.M.; Schmidt, A.J.; Hallen, R.T.; Schaub, T.M., Assessment of Hydrotreatment for Hydrothermal Liquefaction Biocrudes from Sewage Sludge, Microalgae, and Pine Feedstocks, <i>Energy &amp; Fuels</i> , 32 (8), 8483-8493 (2018)
Kaniewska, K.; Dragulescu-Andrasi, A.; Ponikiewski, L.; Pikies, J.; Stoian, S.; Grubba, R., Syntheses, Structures and Reactivity of Terminal Phosphido Complexes of Iron(II) Supported by a $\beta$ -Diketiminato Ligand, <i>Eur. J. Inorg. Chem.</i> , 2018, 4298-4308 (2018)
Larentis, S.; Movva, H.C.P.; Fallahazad, B.; Kim, K.; Behroozi, A.; Taniguchi, T.; Watanabe, K.; Banerjee, S.K.; Tutuc, E., Large effective mass and interaction-enhanced Zeeman splitting of K-valley electrons in MoSe <sub>2</sub> , <i>Phys. Rev. B</i> , 97, 201407(R) (2018)
Leahy, I.A.; Lin, Y. P.; Siegfried, P.E.; Treglia, A.C.; Song, J.C.W.; Nandkishore, R.M.; Lee, M., Nonsaturating large magnetoresistance in semimetals, <i>P. Natl. Acad. Sci. U.S.A.</i> , 115 (42), 10570 (2018)
Li, J.; Tupikov, Y.; Watanabe, K.; Taniguchi, T.; Zhu, J., Effective Landau Level Diagram of Bilayer Graphene, <i>Phys. Rev. Lett.</i> , 120, 047701 (2018)
Li, J.; Wen, H.; Watanabe, K.; Taniguchi, T.; Zhu, J., Gate-Controlled Transmission of Quantum Hall Edge States in Bilayer Graphene, <i>Phys. Rev. Lett.</i> , 120, 057701 (2018)
Lusk, M.G.; Toor, G.S.; Inglett, P.W., Characterization of dissolved organic nitrogen in leachate from a newly established and fertilized turfgrass, <i>Water Research</i> , 131, 52-61 (2018)

Luzius, C.; Guillemette, F.; Podgorski, D.C.; Kellerman, A.M.; Spencer, G.M., Drivers of Dissolved Organic Matter in the Vent and Major Conduits of the World's Largest Freshwater Spring, <i>J. Geophys. Res. Biogeosci.</i> , 123 (9), 2775-2790 (2018)
Mazumder, S.; Dahal, S.R.; Chaudhary, B.P.; Mohanty, S., Structure and Function Studies of Asian Corn Borer <i>Ostrinia furnacalis</i> Pheromone Binding Protein2, <i>Sci. Rep.</i> , 8, 17105 (2018)
Movva, H.C.P.; Lovorn, T.; Fallahazad, B.; Larentis, S.; Kim, K.; Taniguchi, T.; Watanabe, K.; Banerjee, S.K.; MacDonald, A.H.; Tutuc, E., Tunable $\Gamma$ -K Valley Populations in Hole-Doped Trilayer WSe <sub>2</sub> , <i>Phys. Rev. Lett.</i> , 120, 107703 (2018)
O'Shea, D.M.; Langer, K.; Woods, A.J.; Porges, E.C.; Williamson, J.B.; O'Shea, A.; Cohen, R.A., Educational Attainment Moderates the Association Between Hippocampal Volumes and Memory Performances in Healthy Older Adults, <i>Frontiers in Aging Neurosci.</i> , 10, 361 (2018)
Romero, C.M.; Engel, R.E.; D'Andrilli, J.; Chen, C.; Zabinski, C.; Miller, P.R.; Wallander, R., Patterns of change in permanganate oxidizable soil organic matter from semiarid drylands reflected by absorbance spectroscopy and Fourier transform ion cyclotron resonance mass spectrometry, <i>Organic Geochemistry</i> , 120, 19-30 (2018)
Smith, H.J.; Tigges, M.; D'Andrilli, J.; Parker, A.; Bothner, B.; Foreman, C.M., Dynamic processing of DOM: Insights from exometabolomics, spectroscopy, and spectrometry, <i>Limnology and Oceanography Letters</i> , 3, 225-235 (2018)
Szymkowicz, S.M.; Woods, A.J.; Dotson, V.M.; Porges, E.C.; Nissim, N.R.; O'Shea, A.; Cohen, R.A.; Ebner, N.C., Associations between subclinical depressive symptoms and reduced brain volume in middle-aged to older adults, <i>Aging &amp; Mental Health</i> , n/a, 1-12 (2018)
Taen, T.; Uchida, K.; Osada, T.; Kang, W., Tunable magnetoresistance in thin-film graphite field-effect transistor by gate voltage, <i>Phys. Rev. B</i> , 98, 155136 (2018)
Textor, S.R.; Guillemette, F.; Zito, P.A.; Spencer, R.G.M., An Assessment of Dissolved Organic Carbon Biodegradability and Priming in Blackwater Systems, <i>J. Geophys. Res. Biogeosci.</i> , 123 (9), 2998-3015 (2018)
Vorobev, A.; Sharma, S.; Yu, M.; Lee, J.; Washington, B.J.; Whitman, W.B.; Ballantyne, F.; Medeiros, P.M.; Moran, M.A., Identifying Labile DOM Components in a Coastal Ocean Through Depleted Bacterial Transcripts and Chemical Signals, <i>Environmental Microbiology</i> , 20 (8), 3012-3030 (2018)
Wang, Y.; Spencer, R.G.M.; Podgorski, D.C.; Kellerman, A.M.; Rashid, H.; Zito, P.; Xiao, W.; Wei, D.; Yang, Y.; Xu, Y., Spatiotemporal Transformation of Dissolved Organic Matter Along an Alpine Stream Flow Path on the Qinghai-Tibet Plateau: Importance of Source and Permafrost Degradation, <i>Biogeosciences</i> , 15, 6637-6648 (2018)
Zhou, Y.; Xiao, Q.; Yao, X.; Zhang, Y.; Zhang, M.; Shi, K.; Lee, X.; Podgorski, D.C.; Qin, B.; Spencer, R.G.M.; Jeppesen, E., Accumulation of Terrestrial Dissolved Organic Matter Potentially Enhances Dissolved Methane Levels in Eutrophic Lake Taihu, China, <i>Environ. Sci. Technol.</i> , 52 (18), 10297-10306 (2018)
Zibrov, A.A.; Spanton, E.M.; Zhou, H.; Kometter, C.; Taniguchi, T.; Watanabe, K.; Young, A.F., Even-denominator fractional quantum Hall states at an isospin transition in monolayer graphene, <i>Nature Physics</i> , 14, 930-935 (2018)

## APPENDIX I: USER FACILITY STATISTICS

Seven user facilities — AMRIS (NMR-MRI@UF), DC Field, EMR, High B/T, ICR, NMR-MRI@FSU, and Pulsed Field — each with exceptional instrumentation and highly qualified staff scientists and staff, comprise the magnet lab's user program. In this appendix, each facility presents detailed information about its user demographics, operations statistics and requests for magnet time.

A user is an individual or a member of a research group that is allocated magnet time. The user does not have to be "on site" for the experiment. A researcher who sends samples for analysis; a scientist who uses new lab technologies to conduct experiments remotely; or a PI who sends students to the magnet lab, are all considered users. All user numbers reflect distinct individuals, i.e. if a user has multiple proposals (different scientific thrusts) or is allocated magnet time more than once during the year, he/she is counted only once. All user data in the user facility statistics is as of February 21, 2019.

### 1. Advanced Magnetic Resonance Imaging and Spectroscopy (AMRIS)

**Table 1a: User Demographics-NSF-Funded**

	Users <sup>1</sup>	Minority <sup>2</sup>	Non-Minority <sup>2</sup>	Prefer Not to Respond to Race <sup>3</sup>	Male	Female	Other	Prefer Not to Respond to Gender <sup>3</sup>
Senior Personnel, U.S.	47	4	30	13	25	12	0	10
Senior Personnel, non-U.S.	5	1	4	0	3	2	0	0
Postdocs, U.S.	13	3	5	5	5	4	0	4
Postdocs, non-U.S.	2	0	1	1	2	0	0	0
Students, U.S.	43	1	26	16	22	9	0	12
Students, non-U.S.	1	0	0	1	0	0	0	1
Technician, U.S.	9	0	5	4	2	4	0	3
Technician, non-U.S.	0	0	0	0	0	0	0	0
<b>Total</b>	<b>120</b>	<b>9</b>	<b>71</b>	<b>40</b>	<b>59</b>	<b>31</b>	<b>0</b>	<b>30</b>

<sup>1</sup> Users using multiple facilities are counted in each facility listed.

<sup>2</sup> NSF Minority status includes the following races: American Indian, Alaska Native, Black or African American, Hispanic, Native Hawaiian or other Pacific Islander. The definition also includes Hispanic Ethnicity as a minority group. Minority status excludes Asian and White-Not of Hispanic Origin.

<sup>3</sup> Includes pending user account activations.

**Table 1b: User Demographics-Non-NHMFL-Funded**

	Users <sup>1</sup>	Minority <sup>2</sup>	Non-Minority <sup>2</sup>	Prefer Not to Respond to Race <sup>3</sup>	Male	Female	Other	Prefer Not to Respond to Gender <sup>3</sup>
Senior Personnel, U.S.	94	4	46	44	39	16	0	39
Senior Personnel, non-U.S.	3	0	1	2	0	1	0	2
Postdocs, U.S.	45	7	27	11	17	18	0	10
Postdocs, non-U.S.	0	0	0	0	0	0	0	0
Students, U.S.	78	5	43	30	27	27	0	24
Students, non-U.S.	1	0	0	1	0	0	0	1
Technician, U.S.	36	3	14	19	7	11	0	18
Technician, non-U.S.	1	0	1	0	1	0	0	0
<b>Total</b>	<b>258</b>	<b>19</b>	<b>132</b>	<b>107</b>	<b>91</b>	<b>73</b>	<b>0</b>	<b>94</b>

<sup>1</sup> Users using multiple facilities are counted in each facility listed.

<sup>2</sup> NSF Minority status includes the following races: American Indian, Alaska Native, Black or African American, Hispanic, Native Hawaiian or other Pacific Islander. The definition also includes Hispanic Ethnicity as a minority group. Minority status excludes Asian and White-Not of Hispanic Origin.

<sup>3</sup> Includes pending user account activations.



**Table 1c: User Demographics Summary**

	Users <sup>1</sup>	Minority <sup>2</sup>	Non-Minority <sup>2</sup>	Prefer Not to Respond to Race <sup>3</sup>	Male	Female	Other	Prefer Not to Respond to Gender <sup>3</sup>
Total – NSF Funded	120	9	71	40	59	31	0	30
Total – Non-NHMFL Funded	258	19	132	107	91	73	0	94
<b>TOTAL</b>	<b>378</b>	<b>28</b>	<b>203</b>	<b>147</b>	<b>150</b>	<b>104</b>	<b>0</b>	<b>124</b>

<sup>1</sup> Users using multiple facilities are counted in each facility listed.

<sup>2</sup> NSF Minority status includes the following races: American Indian, Alaska Native, Black or African American, Hispanic, Native Hawaiian or other Pacific Islander. The definition also includes Hispanic Ethnicity as a minority group. Minority status excludes Asian and White-Not of Hispanic Origin.

<sup>3</sup> Includes pending user account activations.

**Table 2a: User by Participation-NSF-Funded**

	Users <sup>1</sup>	Users Present	Users Operating Remotely <sup>2</sup>	Users Sending Sample <sup>3</sup>	Off-Site Collaborators <sup>4</sup>
Senior Personnel, U.S.	47	25	0	3	19
Senior Personnel, non-U.S.	5	1	0	0	4
Postdocs, U.S.	13	8	0	1	4
Postdocs, non-U.S.	2	0	0	0	2
Students, U.S.	43	32	0	1	10
Students, non-U.S.	1	0	0	1	0
Technician, U.S.	9	8	0	0	1
Technician, non-U.S.	0	0	0	0	0
<b>Total</b>	<b>120</b>	<b>74</b>	<b>0</b>	<b>6</b>	<b>40</b>

<sup>1</sup> Users using multiple facilities are counted in each facility listed.

<sup>2</sup> "Users Operating Remotely" refers to users who operate the magnet system from a remote location. Remote operations are not currently available in all facilities.

<sup>3</sup> "Users Sending Sample" refers to users who send the sample to the facility and/or research group and the experiment is conducted by other collaborators on the experiment. Users at UF, FSU, and LANL cannot be "sample senders" for facilities located on their campuses.

<sup>4</sup> "Off-Site Collaborators" are scientific or technical participants on the experiment; who will not be present, sending sample, or operating the magnet system remotely; and who are not located on the campus of that facility (i.e., they are off-site).

**Table 2b: User by Participation-Non-NHMFL-Funded**

	Users <sup>1</sup>	Users Present	Users Operating Remotely <sup>2</sup>	Users Sending Sample <sup>3</sup>	Off-Site Collaborators <sup>4</sup>
Senior Personnel, U.S.	94	64	0	0	30
Senior Personnel, non-U.S.	3	0	0	0	3
Postdocs, U.S.	45	38	0	0	7
Postdocs, non-U.S.	0	0	0	0	0
Students, U.S.	78	75	0	0	3
Students, non-U.S.	1	0	0	0	1
Technician, U.S.	36	36	0	0	0
Technician, non-U.S.	1	1	0	0	0
<b>Total</b>	<b>258</b>	<b>214</b>	<b>0</b>	<b>0</b>	<b>44</b>

<sup>1</sup> Users using multiple facilities are counted in each facility listed.

<sup>2</sup> "Users Operating Remotely" refers to users who operate the magnet system from a remote location. Remote operations are not currently available in all facilities.

<sup>3</sup> "Users Sending Sample" refers to users who send the sample to the facility and/or research group and the experiment is conducted by other collaborators on the experiment. Users at UF, FSU, and LANL cannot be "sample senders" for facilities located on their campuses.

<sup>4</sup> "Off-Site Collaborators" are scientific or technical participants on the experiment; who will not be present, sending sample, or operating the magnet system remotely; and who are not located on the campus of that facility (i.e., they are off-site).

**Table 2c: User by Participation Summary**

	Users <sup>1</sup>	Users Present	Users Operating Remotely <sup>2</sup>	Users Sending Sample <sup>3</sup>	Off-Site Collaborators <sup>4</sup>
Total – NSF Funded	120	74	0	6	40
Total – Non-NHMFL Funded	258	214	0	0	44
<b>TOTAL</b>	<b>378</b>	<b>288</b>	<b>0</b>	<b>6</b>	<b>84</b>

<sup>1</sup> Users using multiple facilities are counted in each facility listed.

<sup>2</sup> "Users Operating Remotely" refers to users who operate the magnet system from a remote location. Remote operations are not currently available in all facilities.

<sup>3</sup> "Users Sending Sample" refers to users who send the sample to the facility and/or research group and the experiment is conducted by other collaborators on the experiment. Users at UF, FSU, and LANL cannot be "sample senders" for facilities located on their campuses.

<sup>4</sup> "Off-Site Collaborators" are scientific or technical participants on the experiment; who will not be present, sending sample, or operating the magnet system remotely; and who are not located on the campus of that facility (i.e., they are off-site).

**Table 3a: User Organization - NSF-Funded**

	Users <sup>1</sup>	NHMFL-Affiliated Users <sup>2, 3, 4</sup>	Local Users <sup>2</sup>	External Users	National			International		
					Lab <sup>3, 5</sup>	University <sup>4, 5</sup>	Industry <sup>5</sup>	Lab <sup>5</sup>	University <sup>5</sup>	Industry <sup>5</sup>
Senior Personnel, U.S.	47	15	6	26	2	43	2	0	0	0
Senior Personnel, non-U.S.	5	0	0	5	0	0	0	0	5	0
Postdocs, U.S.	13	2	2	9	1	11	1	0	0	0
Postdocs, non-U.S.	2	0	0	2	0	0	0	0	2	0
Students, U.S.	43	0	16	27	0	42	1	0	0	0
Students, non-U.S.	1	0	0	1	0	0	0	0	1	0
Technician, U.S.	9	3	2	4	0	9	0	0	0	0
Technician, non-U.S.	0	0	0	0	0	0	0	0	0	0
<b>Total</b>	<b>120</b>	<b>20</b>	<b>26</b>	<b>74</b>	<b>3</b>	<b>105</b>	<b>4</b>	<b>0</b>	<b>8</b>	<b>0</b>

<sup>1</sup> Users using multiple facilities are counted in each facility listed.

<sup>2</sup> NHMFL-Affiliated users are defined as anyone in the lab's personnel system (i.e. on our web site/directory), even if they travel to another site. Local users are defined as any non-NHMFL-Affiliated researchers originating at any of the institutions in proximity to the MagLab sites (i.e. researchers at FSU, UF, FAMU, or LANL), even if they travel to another site.

<sup>3</sup> Users with primary affiliations at NHMFL/LANL are reported in NHMFL-Affiliated Users and National Laboratory.

<sup>4</sup> Users with primary affiliations at FSU, UF, or FAMU are reported in NHMFL-Affiliated Users and National University.

<sup>5</sup> The total of university, industry, and national lab users will equal the total number of users.

**Table 3b: User Organization-Non-NHMFL-Funded**

	Users <sup>1</sup>	NHMFL-Affiliated Users <sup>2, 3, 4</sup>	Local Users <sup>2</sup>	External Users	National			International		
					Lab <sup>3, 5</sup>	University <sup>4, 5</sup>	Industry <sup>5</sup>	Lab <sup>5</sup>	University <sup>5</sup>	Industry <sup>5</sup>
Senior Personnel, U.S.	94	14	38	42	1	93	0	0	0	0
Senior Personnel, non-U.S.	3	0	0	3	0	0	0	0	3	0
Postdocs, U.S.	45	3	16	26	0	45	0	0	0	0
Postdocs, non-U.S.	0	0	0	0	0	0	0	0	0	0
Students, U.S.	78	0	34	44	0	78	0	0	0	0
Students, non-U.S.	1	0	0	1	0	0	0	0	1	0
Technician, U.S.	36	3	13	20	0	36	0	0	0	0
Technician, non-U.S.	1	0	0	1	0	0	0	0	0	1
<b>Total</b>	<b>258</b>	<b>20</b>	<b>101</b>	<b>137</b>	<b>1</b>	<b>252</b>	<b>0</b>	<b>0</b>	<b>4</b>	<b>1</b>

<sup>1</sup> Users using multiple facilities are counted in each facility listed.

<sup>2</sup> NHMFL-Affiliated users are defined as anyone in the lab's personnel system (i.e. on our web site/directory), even if they travel to another site. Local users are defined as any non-NHMFL-Affiliated researchers originating at any of the institutions in proximity to the MagLab sites (i.e. researchers at FSU, UF, FAMU, or LANL), even if they travel to another site.

<sup>3</sup> Users with primary affiliations at NHMFL/LANL are reported in NHMFL-Affiliated Users and National Laboratory.

<sup>4</sup> Users with primary affiliations at FSU, UF, or FAMU are reported in NHMFL-Affiliated Users and National University.

<sup>5</sup> The total of university, industry, and national lab users will equal the total number of users.

**Table 3c: User Organization - Summary**

					National			International		
	Users <sup>1</sup>	NHMFL-Affiliated Users <sup>2, 3, 4</sup>	Local Users <sup>2</sup>	External Users	Lab <sup>3, 5</sup>	Univer-sity <sup>4, 5</sup>	Indus-try <sup>5</sup>	Lab <sup>5</sup>	Univer-sity <sup>5</sup>	Industry <sup>5</sup>
Total – NSF Funded	120	20	26	74	3	105	4	0	8	0
Total – Non-NHMFL Funded	258	20	101	137	1	252	0	0	4	1
<b>TOTAL</b>	<b>378</b>	<b>40</b>	<b>127</b>	<b>211</b>	<b>4</b>	<b>357</b>	<b>4</b>	<b>0</b>	<b>12</b>	<b>1</b>

<sup>1</sup> Users using multiple facilities are counted in each facility listed.

<sup>2</sup> NHMFL-Affiliated users are defined as anyone in the lab's personnel system (i.e. on our web site/directory), even if they travel to another site. Local users are defined as any non-NHMFL-Affiliated researchers originating at any of the institutions in proximity to the MagLab sites (i.e. researchers at FSU, UF, FAMU, or LANL), even if they travel to another site.

<sup>3</sup> Users with primary affiliations at NHMFL/LANL are reported in NHMFL-Affiliated Users and National Laboratory.

<sup>4</sup> Users with primary affiliations at FSU, UF, or FAMU are reported in NHMFL-Affiliated Users and National University.

<sup>5</sup> The total of university, industry, and national lab users will equal the total number of users.

**Table 4a: User by Discipline-NSF-Funded**

	Users <sup>1</sup>	Condensed Matter Physics	Chemistry, Geochemistry	Engineering	Magnets, Materials, Testing, Instr.	Biology, Biochemistry, Biophysics
Senior Personnel, U.S.	47	1	8	7	1	30
Senior Personnel, non-U.S.	5	0	1	0	0	4
Postdocs, U.S.	13	0	2	0	1	10
Postdocs, non-U.S.	2	1	1	0	0	0
Students, U.S.	43	1	15	11	2	14
Students, non-U.S.	1	0	1	0	0	0
Technician, U.S.	9	0	0	3	1	5
Technician, non-U.S.	0	0	0	0	0	0
<b>Total</b>	<b>120</b>	<b>3</b>	<b>28</b>	<b>21</b>	<b>5</b>	<b>63</b>

<sup>1</sup> Users using multiple facilities are counted in each facility listed.

**Table 4b: User by Discipline-Non-NHMFL-Funded**

	Users <sup>1</sup>	Condensed Matter Physics	Chemistry, Geochemistry	Engineering	Magnets, Materials, Testing, Instr.	Biology, Biochemistry, Biophysics
Senior Personnel, U.S.	94	0	9	6	6	73
Senior Personnel, non-U.S.	3	0	0	0	0	3
Postdocs, U.S.	45	0	2	4	2	37
Postdocs, non-U.S.	0	0	0	0	0	0
Students, U.S.	78	1	9	10	11	47
Students, non-U.S.	1	0	0	0	0	1
Technician, U.S.	36	0	0	2	6	28
Technician, non-U.S.	1	0	0	0	0	1
<b>Total</b>	<b>258</b>	<b>1</b>	<b>20</b>	<b>22</b>	<b>25</b>	<b>190</b>

<sup>1</sup> Users using multiple facilities are counted in each facility listed.

**Table 4c: User by Discipline Summary**

	Users <sup>1</sup>	Condensed Matter Physics	Chemistry, Geochemistry	Engineering	Magnets, Materials, Testing, Instr.	Biology, Biochemistry, Biophysics
Total – NSF Funded	120	3	28	21	5	63
Total – Non-NHMFL Funded	258	1	20	22	25	190

	Users <sup>1</sup>	Condensed Matter Physics	Chemistry, Geochemistry	Engineering	Magnets, Materials, Testing, Instr.	Biology, Biochemistry, Biophysics
TOTAL	378	4	48	43	30	253

<sup>1</sup> Users using multiple facilities are counted in each facility listed.

**Table 5a: User Facility Operations by Magnet Systems-NSF-Funded**

	Total Days Used <sup>1</sup>	Percentage of Total Days Used	750 MHz	600 MHz Avance	600 MHz Avance II	600 MHz Agilent	500 MHz	4.7T	11T
NHMFL-Affiliated	107.2	9.4 %	8	6.5	14.3	6.3	13.6	54.2	4.3
Local	13	1.1 %	0	13	0	0	0	0	0
U.S. University	310.9	27.3 %	142	95	13	3.3	55.1	2.5	0
U.S. Govt. Lab.	4	0.4 %	0	0	0	0	0	4	0
U.S. Industry	19.8	1.7 %	0	0	0	0	0	0	19.8
Non-U.S.	35.8	3.1 %	0	0	4.6	9.2	13.9	0	8.2
Test, Calibration, Set-up, Maintenance, Inst. Dev.	650.2	57 %	56	70.5	150.1	109.2	80.5	80.3	103.7
Total	1,141	100 %	206	185	182	128	163	141	136

<sup>1</sup> User Units are defined as magnet days. One magnet day is defined as 24 hours in superconducting magnets.

**Table 5b: User Facility Operations by Magnet Systems-Non-NHMFL-Funded**

	Total Days Used <sup>1</sup>	Percentage of Total Days	750 MHz	600 MHz Avance	600 MHz Avance II	600 MHz Agilent	500 MHz	4.7T	11T	3T Siemens	3T Philips
NHMFL-Affiliated	348.3	26.5 %	32	18	31.2	1	76.5	37.5	72.5	66.7	12.9
Local	154.4	11.7 %	2	0	3.3	0	53.2	20	35.5	19.5	20.9
U.S. University	811.6	61.7 %	19	53	73.5	82	78.3	50.5	50	172.1	233.2
U.S. Govt. Lab.	0.7	0.1 %	0	0	0	0	0	0	0	0.7	0
U.S. Industry	0	0 %	0	0	0	0	0	0	0	0	0
Non-U.S.	0	0 %	0	0	0	0	0	0	0	0	0
Test, Calibration, Set-up, Maintenance, Inst. Dev.	0	0 %	0	0	0	0	0	0	0	0	0
Total	1,315	100 %	53	71	108	83	208	108	158	259	267

<sup>1</sup> User Units are defined as magnet days. One magnet day is defined as 24 hours in superconducting magnets.

**Table 5c: User Facility Operations by Magnet Systems-Summary**

	Total Days Used <sup>1</sup>	Percentage of Total Days	750 MHz	600 MHz Avance	600 MHz Avance II	600 MHz Agilent	500 MHz	4.7T	11T	3T Siemens	3T Philips
Total – NSF Funded	1,141	100 %	206	185	182	128	163	141	136	NA	NA
Total – Non-NHMFL Funded	1,315	100 %	53	71	108	83	208	108	158	259	267
TOTAL	2,456	2	259	256	290	211	371	249	294	259	267

<sup>1</sup> User Units are defined as magnet days. One magnet day is defined as 24 hours in superconducting magnets.

**Table 6a: Operations by Discipline-NSF-Funded**

	Total Days Used <sup>1</sup>	Condensed Matter Physics	Chemistry, Geochemistry	Engineering	Magnets, Materials	Biology, Biochemistry, Biophysics
NHMFL-Affiliated	107.2	0	4.5	0	0	102.7
Local	13	0	13	0	0	0



	Total Days Used <sup>1</sup>	Condensed Matter Physics	Chemistry, Geochemistry	Engineering	Magnets, Materials	Biology, Biochemistry, Biophysics
U.S. University	310.9	0	43.2	173.3	0	94.4
U.S. Govt. Lab.	4	0	0	0	0	4
U.S. Industry	19.8	0	0	0	0	19.8
Non-U.S.	35.8	0	0	0	0	35.8
Test, Calibration, Set-up, Maintenance, Inst. Dev.	650.2	0	0	0	385.9	264.3
<b>Total</b>	<b>1,141</b>	<b>0</b>	<b>60.7</b>	<b>173.3</b>	<b>385.9</b>	<b>521.1</b>

<sup>1</sup> User Units are defined as magnet days. One magnet day is defined as 24 hours in superconducting magnets.

**Table 6b: Operations by Discipline-Non-NHMFL-Funded**

	Total Days Used <sup>1</sup>	Condensed Matter Physics	Chemistry, Geochemistry	Engineering	Magnets, Materials	Biology, Biochemistry, Biophysics
NHMFL-Affiliated	348.3	0	0	0.2	0	348.1
Local	154.4	0	16.6	0	0	137.8
U.S. University	811.6	0	48	0	0	763.6
U.S. Govt. Lab.	0.7	0	0	0	0	0.7
U.S. Industry	0	0	0	0	0	0
Non-U.S.	0	0	0	0	0	0
Test, Calibration, Set-up, Maintenance, Inst. Dev.	0	0	0	0	0	0
<b>Total</b>	<b>1,315</b>	<b>0</b>	<b>64.6</b>	<b>0.2</b>	<b>0</b>	<b>1,250.2</b>

<sup>1</sup> User Units are defined as magnet days. One magnet day is defined as 24 hours in superconducting magnets.

**Table 6c: Operations by Discipline Summary**

	Total Days Used <sup>1</sup>	Condensed Matter Physics	Chemistry, Geochemistry	Engineering	Magnets, Materials	Biology, Biochemistry, Biophysics
Total – NSF Funded	1,141	0	60.7	173.3	385.9	521.1
Total – Non-NHMFL Funded	1,315	0	64.6	0.2	0	1,250.2
<b>TOTAL</b>	<b>2,456</b>	<b>0</b>	<b>125.3</b>	<b>173.5</b>	<b>385.9</b>	<b>1771.3</b>

<sup>1</sup> User Units are defined as magnet days. One magnet day is defined as 24 hours in superconducting magnets.

**Table 7: Subscription Rate-Summary**

	Experiments Submitted (Current year)	Experiments Submitted (Deferred from prev. year)	Experiments w/ Usage	Experiments Declined	Experiments Reviewed	Experiment Subscription (%) (Submitted / Used)
Total – NSF Funded	11	19	29 (96.67 %)	1 (3.33 %)	30	103.45 %
Total – Non-NHMFL Funded	23	87	109 (99.09 %)	1 (0.91 %)	110	100.92 %
<b>TOTAL</b>	<b>34</b>	<b>106</b>	<b>138</b>	<b>2</b>	<b>140</b>	<b>102.2 %</b>

**Table 8a: New<sup>1</sup> User PI's-NSF-Funded**

Name	Organization	Proposal	Year of Magnet Time	Is New To MagLab
Jeanine Brady	University of Florida	P17623	Received 2018	No
Samira Daroub	University of Florida	P17592	Received 2018	Yes
Jordi Diaz-Manera	University of Barcelona	P17648	Received 2018	Yes
Jeremy Flint	University of Florida	P17710	Received 2018	No
Catherine Kaczorowski	The Jackson Laboratory	P17323	Received 2018	Yes
Gerardo Morell	University of Puerto Rico, Rio Piedras	P17820	Received 2018	Yes

Name	Organization	Proposal	Year of Magnet Time	Is New To MagLab
Ahmad Mostafa	Al-Azhar University	P17558	Received 2018	Yes
Masteria Putra	Indonesian Institute of Sciences	P17457	Received 2018	Yes
QiQi Zhou	Malcom Randall VA Medical Center	P17580	Received 2018	Yes
<b>Total</b>	<b>9</b>			

<sup>1</sup> PIs who received magnet time for the first time.

**Table 8b: New<sup>1</sup> User PI's-Non-NHMFL-Funded**

Name	Organization	Proposal	Year of Magnet Time	Is New To MagLab
Jeff Boissoneault	University of Florida	P17959	Received 2018	Yes
Clifford Bowers	University of Florida	P17881	Received 2018	No
Eduardo Candelario-Jalil	University of Florida	P17809	Received 2018	Yes
James Collins	University of Florida	P17940	Received 2018	Yes
William Donahoo	University of Florida	P17953	Received 2018	Yes
Jianping Huang	University of Florida	P17930	Received 2018	Yes
Girdhar Kalamangalam	University of Florida	P17880	Received 2018	Yes
Ellen Keeley	University of Florida	P17883	Received 2018	Yes
Debra Lyon	University of Florida	P17939	Received 2018	Yes
Borna Mehrad	University of Florida	P17955	Received 2018	Yes
Karim Oweiss	University of Florida	P17956	Received 2018	Yes
Mark Segal	University of Florida	P17800	Received 2018	Yes
Rachael Seidler	University of Florida	P17960	Received 2018	Yes
Blanka Sharma	University of Florida	P17932	Received 2018	Yes
Aparna Wagle Shukla	University of Florida	P17799	Received 2018	Yes
Kevin Wang	University of Florida	P17837	Received 2018	Yes
<b>Total</b>	<b>16</b>			

<sup>1</sup> PIs who received magnet time for the first time.

**Table 9: Research Proposal<sup>1</sup> Profile with Magnet Time-Summary**

	Total Proposals <sup>1</sup>	Minority <sup>2</sup>	Non-Minority	Prefer Not to Respond to Race	Female <sup>3</sup>	Male	Other	Prefer Not to Respond to Gender	CM	Chem, Geochem	Engin	Magn, Mater, Testing, Instrum	Bio, Bio-chem Biophys
Total – NSF Funded	29	4	19	6	14	13	0	2	0	4	2	0	23
Total – Non-NHMFL Funded	75	3	43	29	19	33	0	23	0	0	0	0	75
<b>TOTAL</b>	<b>104</b>	<b>7</b>	<b>62</b>	<b>35</b>	<b>33</b>	<b>46</b>	<b>0</b>	<b>25</b>	<b>0</b>	<b>4</b>	<b>2</b>	<b>0</b>	<b>98</b>

<sup>1</sup> A "proposal" may have associated with it a single experiment or a group of closely related experiments. A PI may have more than one proposal.

<sup>2</sup> The number of proposals satisfying the following condition: The PI is a minority.

<sup>3</sup> The number of proposals satisfying the following condition: The PI is a female.

Find the list of AMRIS user proposals on our [website](#)

## 2. DC Field Facility

**Table 1: User Demographics**

	Users <sup>1</sup>	Minority <sup>2</sup>	Non-Minority <sup>2</sup>	Prefer Not to Respond to Race <sup>3</sup>	Male	Female	Other	Prefer Not to Respond to Gender <sup>3</sup>
Senior Personnel, U.S.	205	7	173	25	155	32	0	18

	Users <sup>1</sup>	Minority <sup>2</sup>	Non-Minority <sup>2</sup>	Prefer Not to Respond to Race <sup>3</sup>	Male	Female	Other	Prefer Not to Respond to Gender <sup>3</sup>
Senior Personnel, non-U.S.	91	1	69	21	68	8	0	15
Postdocs, U.S.	81	3	66	12	62	13	0	6
Postdocs, non-U.S.	24	0	16	8	17	2	0	5
Students, U.S.	212	9	165	38	154	36	0	22
Students, non-U.S.	47	3	36	8	38	7	0	2
Technician, U.S.	10	2	6	2	7	2	0	1
Technician, non-U.S.	0	0	0	0	0	0	0	0
<b>Total</b>	<b>670</b>	<b>25</b>	<b>531</b>	<b>114</b>	<b>501</b>	<b>100</b>	<b>0</b>	<b>69</b>

<sup>1</sup> Users using multiple facilities are counted in each facility listed.

<sup>2</sup> NSF Minority status includes the following races: American Indian, Alaska Native, Black or African American, Hispanic, Native Hawaiian or other Pacific Islander. The definition also includes Hispanic Ethnicity as a minority group. Minority status excludes Asian and White-Not of Hispanic Origin.

<sup>3</sup> Includes pending user account activations.

**Table 2: User by Participation**

	Users <sup>1</sup>	Users Present	Users Operating Remotely <sup>2</sup>	Users Sending Sample <sup>3</sup>	Off-Site Collaborators <sup>4</sup>
Senior Personnel, U.S.	205	109	0	21	75
Senior Personnel, non-U.S.	91	28	0	22	41
Postdocs, U.S.	81	56	0	2	23
Postdocs, non-U.S.	24	14	0	2	8
Students, U.S.	212	175	0	8	29
Students, non-U.S.	47	36	0	0	11
Technician, U.S.	10	10	0	0	0
Technician, non-U.S.	0	0	0	0	0
<b>Total</b>	<b>670</b>	<b>428</b>	<b>0</b>	<b>55</b>	<b>187</b>

<sup>1</sup> Users using multiple facilities are counted in each facility listed.

<sup>2</sup> "Users Operating Remotely" refers to users who operate the magnet system from a remote location. Remote operations are not currently available in all facilities.

<sup>3</sup> "Users Sending Sample" refers to users who send the sample to the facility and/or research group and the experiment is conducted by other collaborators on the experiment. Users at UF, FSU, and LANL cannot be "sample senders" for facilities located on their campuses.

<sup>4</sup> "Off-Site Collaborators" are scientific or technical participants on the experiment; who will not be present, sending sample, or operating the magnet system remotely; and who are not located on the campus of that facility (i.e., they are off-site).

**Table 3: User Organization**

					National			International		
	Users <sup>1</sup>	NHMFL-Affiliated Users <sup>2, 3, 4</sup>	Local Users <sup>2</sup>	External Users	Lab <sup>5</sup>	Univer-sity <sup>4, 5</sup>	Indus-try <sup>5</sup>	Lab <sup>5</sup>	Univer-sity <sup>5</sup>	Industry <sup>5</sup>
Senior Personnel, U.S.	205	60	11	134	23	175	7	0	0	0
Senior Personnel, non-U.S.	91	0	0	91	0	0	0	23	61	7
Postdocs, U.S.	81	16	3	62	9	68	4	0	0	0
Postdocs, non-U.S.	24	0	0	24	0	0	0	5	18	1
Students, U.S.	212	20	24	168	1	211	0	0	0	0
Students, non-U.S.	47	0	0	47	0	0	0	6	41	0
Technician, U.S.	10	8	1	1	0	10	0	0	0	0
Technician, non-U.S.	0	0	0	0	0	0	0	0	0	0
<b>Total</b>	<b>670</b>	<b>104</b>	<b>39</b>	<b>527</b>	<b>33</b>	<b>464</b>	<b>11</b>	<b>34</b>	<b>120</b>	<b>8</b>

<sup>1</sup> Users using multiple facilities are counted in each facility listed.

<sup>2</sup> NHMFL-Affiliated users are defined as anyone in the lab's personnel system (i.e. on our web site/directory), even if they travel to another site. Local users are defined as any non-NHMFL-Affiliated researchers originating at any of the institutions in proximity to the

MagLab sites (i.e. researchers at FSU, UF, FAMU, or LANL), even if they travel to another site.

<sup>3</sup> Users with primary affiliations at NHMFL/LANL are reported in NHMFL-Affiliated Users and National Laboratory.

<sup>4</sup> Users with primary affiliations at FSU, UF, or FAMU are reported in NHMFL-Affiliated Users and National University.

<sup>5</sup> The total of university, industry, and national lab users will equal the total number of users.

**Table 4: User by Discipline**

	Users <sup>1</sup>	Condensed Matter Physics	Chemistry, Geochemistry	Engineering	Magnets, Materials, Testing, Instr.	Biology, Biochemistry, Biophysics
Senior Personnel, U.S.	205	130	21	20	14	20
Senior Personnel, non-U.S.	91	63	16	2	5	5
Postdocs, U.S.	81	66	4	3	3	5
Postdocs, non-U.S.	24	19	3	0	2	0
Students, U.S.	212	153	26	19	10	4
Students, non-U.S.	47	45	1	0	1	0
Technician, U.S.	10	2	0	1	7	0
Technician, non-U.S.	0	0	0	0	0	0
<b>Total</b>	<b>670</b>	<b>478</b>	<b>71</b>	<b>45</b>	<b>42</b>	<b>34</b>

<sup>1</sup> Users using multiple facilities are counted in each facility listed.

**Table 5: User Facility Operations by Magnet System Groups**

	Total Days Used <sup>1</sup>	Percentage of Total Days Used	Super-conducting	SCH	Resistive	45T
NHMFL-Affiliated	405.7	22.8 %	228	14	128.7	35
Local	7	0.4 %	7	0	0	0
U.S. University	882.8	49.7 %	490	104	247.8	41
U.S. Govt. Lab.	62	3.5 %	29	0	33	0
U.S. Industry	0	0 %	0	0	0	0
Non-U.S.	330.8	18.6 %	149	43	93.8	45
Test, Calibration, Set-up, Maintenance, Inst. Dev.	87.8	4.9 %	68	4	15.8	0
<b>Total</b>	<b>1,776.1</b>	<b>100 %</b>	<b>971</b>	<b>165</b>	<b>519.1</b>	<b>121</b>

<sup>1</sup> Each 20 MW resistive magnet requires two power supplies to run, the 45T hybrid magnet requires three power supplies and the 36T Series Connected Hybrid requires one power supply. Thus there can be four resistive magnets + three superconducting magnets operating or the 45T hybrid, series connected hybrid, two resistive magnets and three superconducting magnets. User Units are defined as magnet days. Users of water-cooled resistive or hybrid magnets can typically expect to receive enough energy for 7 hours a day of magnet usage so a magnet day is defined as 7 hours. Superconducting magnets are scheduled typically 24 hours a day. There is an annual four week shutdown in fall of powered DC resistive and hybrid magnets for infrastructure maintenance and a two week shutdown period for the university mandated holiday break.

**Table 6: Operations by Discipline**

	Total Days Used <sup>1</sup>	Condensed Matter Physics	Chemistry, Geochemistry	Engineering	Magnets, Materials	Biology, Biochemistry, Biophysics
NHMFL-Affiliated	405.7	307	17	0	77.7	4
Local	7	0	7	0	0	0
U.S. University	882.8	757.7	37.6	28	14.5	45
U.S. Govt. Lab.	62	62	0	0	0	0
U.S. Industry	0	0	0	0	0	0
Non-U.S.	330.8	272.1	46	0	12.7	0
Test, Calibration, Set-up, Maintenance, Inst. Dev.	87.8	12.6	0	0	75.2	0
<b>Total</b>	<b>1,776.1</b>	<b>1,411.5</b>	<b>107.6</b>	<b>28</b>	<b>180.1</b>	<b>49</b>

<sup>1</sup> Each 20 MW resistive magnet requires two power supplies to run, the 45T hybrid magnet requires three power supplies and the 36T Series Connected Hybrid requires one power supply. Thus there can be four resistive magnets + three superconducting magnets



operating or the 45T hybrid, series connected hybrid, two resistive magnets and three superconducting magnets. User Units are defined as magnet days. Users of water-cooled resistive or hybrid magnets can typically expect to receive enough energy for 7 hours a day of magnet usage so a magnet day is defined as 7 hours. Superconducting magnets are scheduled typically 24 hours a day. There is an annual four week shutdown in fall of powered DC resistive and hybrid magnets for infrastructure maintenance and a two week shutdown period for the university mandated holiday break.

**Table 7: Subscription Rate**

Experiments Submitted (Current year)	Experiments Submitted (Deferred from prev. year)	Experiments w/ Usage	Experiments Declined	Experiments Reviewed	Experiment Subscription (%) (Submitted / Used)	Days Submitted	Days External Users Used	Days Local Users Used	Total Days Used	Subscription (%) (Days submitted / Days used)
418	45	288 (62.2 %)	175 (37.8 %)	463	160.76 %	3,570	1,275.6	7	1,776.1	201 %

**Table 8: New<sup>1</sup> User PI's**

Name	Organization	Proposal	Year of Magnet Time	Is New To MagLab
Henri Alloul	French National Center for Scientific Research	P17513	Received 2018	Yes
Boris Aronzon	Lebedev Physical Institute of the Russian Academy of Sciences	P16247	Received 2018	Yes
David Bryce	University of Ottawa	P17455	Received 2018	Yes
Eduard Chekmenev	Wayne State University	P17460	Received 2018	No
Suyeon Cho	Ewha Womans University	P17664	Received 2018	Yes
Jiun-Haw Chu	University of Washington	P17782	Received 2018	Yes
Myriam Cotten	College of William and Mary	P17425	Received 2018	No
John DiTusa	Louisiana State University	P17370	Received 2018	Yes
Cecil Dybowski	University of Delaware	P17354	Received 2018	No
Mikhail Eremets	Max Planck Institute for Chemistry, Mainz	P17644	Received 2018	Yes
Krzysztof Gofryk	Idaho National Laboratory	P17516	Received 2018	No
Robert Griffin	Massachusetts Institute of Technology	P17507	Received 2018	No
Oc Hee Han	Korea Basic Science Institute	P17424	Received 2018	No
Sophia Hayes	Washington University in St. Louis	P17330	Received 2018	No
Yining Huang	University of Western Ontario	P17504	Received 2018	Yes
Hans Jakobsen	Aarhus University	P14957	Received 2018	No
Bernhard Keimer	Max Planck Institute for Solid State Research, Stuttgart	P17679	Received 2018	Yes
Olivier Lafon	University of Lille	P17586	Received 2018	Yes
Danielle Laurencin	University of Montpellier	P17464	Received 2018	Yes
Daniel Lee	University of Grenoble Alpes	P17632	Received 2018	Yes
Ho Nyung Lee	Oak Ridge National Laboratory	P17777	Received 2018	Yes
Gang Li	Institute of Physics, Chinese Academy of Sciences	P16091	Received 2018	Yes
Chun Hung Lui	University of California, Riverside	P17665	Received 2018	Yes
Ariel Maniv	Israel Institute of Technology	P17509	Received 2018	Yes
Francesca Marassi	Sanford Burnham Prebys Medical Discovery Institute	P17471	Received 2018	Yes
Rachel Martin	University of California, Irvine	P17490	Received 2018	Yes
Alexander Molodyk	SuperOx	P17492	Received 2018	Yes
Leonard Mueller	University of California, Riverside	P17435	Received 2018	No
Yasuyuki Nakajima	University of Central Florida	P17651	Received 2018	Yes
Joscha Nehrkorn	Max Planck Institute for Chemical Energy Conversion	P17653	Received 2018	No
Ni Ni	University of California, Los Angeles	P17495	Received 2018	No
Hongkun Park	Harvard University	P17536	Received 2018	Yes

Name	Organization	Proposal	Year of Magnet Time	Is New To MagLab
Wan Kyu Park	National High Magnetic Field Laboratory (NHMFL)	P17666	Received 2018	Yes
Matej Pregelj	Jozef Stefan Institute	P17667	Received 2018	Yes
Ayyalusamy Ramamoorthy	University of Michigan	P17496	Received 2018	No
Arthur Ramirez	University of California, Santa Cruz	P17775	Received 2018	Yes
Robert Schurko	University of Windsor	P17514	Received 2018	No
Javad Shabani	New York University	P17680	Received 2018	Yes
Jie Shan	Pennsylvania State University	P17771	Received 2018	Yes
Julia Smith	National High Magnetic Field Laboratory (NHMFL)	P17594	Received 2018	Yes
oleksiy svitelskiy	Gordon College	P17487	Received 2018	Yes
Fazel Taffi	Boston College	P17387	Received 2018	Yes
Chiara Tarantini	National High Magnetic Field Laboratory (NHMFL)	P17643	Received 2018	Yes
Nikoleta Theodoropoulou	Texas State University	P17528	Received 2018	Yes
Komalavalli Thirunavukkuarasu	Florida Agricultural and Mechanical University	P17534	Received 2018	No
Nate Traaseth	New York University	P13593	Received 2018	No
John Tranquada	Brookhaven National Laboratory	P17369	Received 2018	Yes
Adam Tsen	University of Waterloo	P17757	Received 2018	Yes
Gianluigi Veglia	University of Minnesota, Twin Cities	P17438	Received 2018	No
Gang Wu	Queen's University at Kingston	P14705	Received 2018	No
<b>Total</b>	<b>50</b>			

<sup>1</sup> PIs who received magnet time for the first time.

**Table 9: Research Proposal<sup>1</sup> Profile with Magnet Time**

Total Proposals <sup>1</sup>	Minority <sup>2</sup>	Non-Minority	Prefer Not to Respond to Race	Female <sup>3</sup>	Male	Other	Prefer Not to Respond to Gender	Condensed Matter Physics	Chemistry, Geochemistry	Engineering	Magnets, Materials, Testing, Instr.	Biology, Biochem Biophys.
186	5	158	23	31	144	0	11	139	17	1	19	10

<sup>1</sup> A "proposal" may have associated with it a single experiment or a group of closely related experiments. A PI may have more than one proposal.

<sup>2</sup> The number of proposals satisfying the following condition: The PI is a minority.

<sup>3</sup> The number of proposals satisfying the following condition: The PI is a female.

Find the list of DC Field user proposals on our [website](#)

### 3. EMR Facility

**Table 1: User Demographics**

	Users <sup>1</sup>	Minority <sup>2</sup>	Non-Minority <sup>2</sup>	Prefer Not to Respond to Race <sup>3</sup>	Male	Female	Other	Prefer Not to Respond to Gender <sup>3</sup>
Senior Personnel, U.S.	60	3	50	7	46	9	0	5
Senior Personnel, non-U.S.	30	4	20	6	18	8	0	4
Postdocs, U.S.	13	0	11	2	10	2	0	1
Postdocs, non-U.S.	5	0	4	1	4	1	0	0
Students, U.S.	43	3	29	11	21	14	0	8
Students, non-U.S.	10	1	7	2	7	2	0	1
Technician, U.S.	0	0	0	0	0	0	0	0
Technician, non-U.S.	0	0	0	0	0	0	0	0
<b>Total</b>	<b>161</b>	<b>11</b>	<b>121</b>	<b>29</b>	<b>106</b>	<b>36</b>	<b>0</b>	<b>19</b>

<sup>1</sup> Users using multiple facilities are counted in each facility listed.

<sup>2</sup> NSF Minority status includes the following races: American Indian, Alaska Native, Black or African American, Hispanic, Native Hawaiian or other Pacific Islander. The definition also includes Hispanic Ethnicity as a minority group. Minority status excludes Asian and White-Not of Hispanic Origin.

<sup>3</sup> Includes pending user account activations.

**Table 2: User by Participation**

	Users <sup>1</sup>	Users Present	Users Operating Remotely <sup>2</sup>	Users Sending Sample <sup>3</sup>	Off-Site Collaborators <sup>4</sup>
Senior Personnel, U.S.	60	29	0	14	17
Senior Personnel, non-U.S.	30	4	0	15	11
Postdocs, U.S.	13	11	0	1	1
Postdocs, non-U.S.	5	3	0	0	2
Students, U.S.	43	29	0	5	9
Students, non-U.S.	10	5	0	2	3
Technician, U.S.	0	0	0	0	0
Technician, non-U.S.	0	0	0	0	0
<b>Total</b>	<b>161</b>	<b>81</b>	<b>0</b>	<b>37</b>	<b>43</b>

<sup>1</sup> Users using multiple facilities are counted in each facility listed.

<sup>2</sup> "Users Operating Remotely" refers to users who operate the magnet system from a remote location. Remote operations are not currently available in all facilities.

<sup>3</sup> "Users Sending Sample" refers to users who send the sample to the facility and/or research group and the experiment is conducted by other collaborators on the experiment. Users at UF, FSU, and LANL cannot be "sample senders" for facilities located on their campuses.

<sup>4</sup> "Off-Site Collaborators" are scientific or technical participants on the experiment; who will not be present, sending sample, or operating the magnet system remotely; and who are not located on the campus of that facility (i.e., they are off-site).

**Table 3: User Organization**

					National			International		
	Users <sup>1</sup>	NHMFL-Affiliated Users <sup>2, 3, 4</sup>	Local Users <sup>2</sup>	External Users	Lab <sup>3, 5</sup>	University <sup>4, 5</sup>	Industry <sup>5</sup>	Lab <sup>5</sup>	University <sup>5</sup>	Industry <sup>5</sup>
Senior Personnel, U.S.	60	19	3	38	1	59	0	0	0	0
Senior Personnel, non-U.S.	30	0	0	30	0	0	0	5	24	1
Postdocs, U.S.	13	3	6	4	3	9	1	0	0	0
Postdocs, non-U.S.	5	0	0	5	0	0	0	2	3	0
Students, U.S.	43	6	9	28	0	43	0	0	0	0
Students, non-U.S.	10	0	0	10	0	0	0	0	10	0
Technician, U.S.	0	0	0	0	0	0	0	0	0	0
Technician, non-U.S.	0	0	0	0	0	0	0	0	0	0
<b>Total</b>	<b>161</b>	<b>28</b>	<b>18</b>	<b>115</b>	<b>4</b>	<b>111</b>	<b>1</b>	<b>7</b>	<b>37</b>	<b>1</b>

<sup>1</sup> Users using multiple facilities are counted in each facility listed.

<sup>2</sup> NHMFL-Affiliated users are defined as anyone in the lab's personnel system (i.e. on our web site/directory), even if they travel to another site. Local users are defined as any non-NHMFL-Affiliated researchers originating at any of the institutions in proximity to the MagLab sites (i.e. researchers at FSU, UF, FAMU, or LANL), even if they travel to another site.

<sup>3</sup> Users with primary affiliations at NHMFL/LANL are reported in NHMFL-Affiliated Users and National Laboratory.

<sup>4</sup> Users with primary affiliations at FSU, UF, or FAMU are reported in NHMFL-Affiliated Users and National University.

<sup>5</sup> The total of university, industry, and national lab users will equal the total number of users.

**Table 4: User by Discipline**

	Users <sup>1</sup>	Condensed Matter Physics	Chemistry, Geochemistry	Engineering	Magnets, Materials, Testing, Instr.	Biology, Biochemistry, Biophysics
Senior Personnel, U.S.	60	21	26	1	0	12
Senior Personnel, non-U.S.	30	6	21	0	2	1
Postdocs, U.S.	13	8	3	1	0	1

	Users <sup>1</sup>	Condensed Matter Physics	Chemistry, Geochemistry	Engineering	Magnets, Materials, Testing, Instr.	Biology, Biochemistry, Biophysics
Postdocs, non-U.S.	5	2	3	0	0	0
Students, U.S.	43	11	25	0	0	7
Students, non-U.S.	10	2	7	0	0	1
Technician, U.S.	0	0	0	0	0	0
Technician, non-U.S.	0	0	0	0	0	0
<b>Total</b>	<b>161</b>	<b>50</b>	<b>85</b>	<b>2</b>	<b>2</b>	<b>22</b>

<sup>1</sup> Users using multiple facilities are counted in each facility listed.

**Table 5: User Facility Operations by Magnet Systems**

	Total Days Used <sup>1</sup>	Percentage of Total Days Used	HiPER	Bruker	12.5T	17T
NHMFL-Affiliated	186.5	19 %	56	76	25.5	29
Local	16	1.6 %	0	0	16	0
U.S. University	474.5	48.2 %	117	188.5	65	104
U.S. Govt. Lab.	10	1 %	0	0	0	10
U.S. Industry	0	0 %	0	0	0	0
Non-U.S.	236.5	24 %	59	23.5	54	100
Test, Calibration, Set-up, Maintenance, Inst. Dev.	60.5	6.1 %	26	0	22.5	12
<b>Total</b>	<b>984</b>	<b>100 %</b>	<b>258</b>	<b>288</b>	<b>183</b>	<b>255</b>

<sup>1</sup> User Units are defined as magnet days. One magnet day is defined as 24 hours in superconducting magnets.

**Table 6: Operations by Discipline**

	Total Days Used <sup>1</sup>	Condensed Matter Physics	Chemistry, Geochemistry	Engineering	Magnets, Materials	Biology, Biochemistry, Biophysics
NHMFL-Affiliated	186.5	18	33	0	2.5	133
Local	16	0	16	0	0	0
U.S. University	474.5	80.5	163.5	0	5	225.5
U.S. Govt. Lab.	10	10	0	0	0	0
U.S. Industry	0	0	0	0	0	0
Non-U.S.	236.5	90.5	102	0	7	37
Test, Calibration, Set-up, Maintenance, Inst. Dev.	60.5	0	0	0	60.5	0
<b>Total</b>	<b>984</b>	<b>199</b>	<b>314.5</b>	<b>0</b>	<b>75</b>	<b>395.5</b>

<sup>1</sup> User Units are defined as magnet days. One magnet day is defined as 24 hours in superconducting magnets.

**Table 7: Subscription Rate**

Experiments Submitted (Current year)	Experiments Submitted (Deferred from prev. year)	Experiments w/ Usage	Experiments Declined	Experiments Re-viewed	Experiment Subscription (%) (Submitted / Used)	Days Submitted	Days External Users Used	Days Local Users Used	Total Days Used	Subscription (%) (Days submitted / Days used)
114	46	141 (88.13 %)	19 (11.88 %)	160	113.48 %	1,007	721	16	984	102.34 %

**Table 8: New<sup>1</sup> User PI's**

Name	Organization	Proposal	Year of Magnet Time	Is New To MagLab
Alina Bienko	University of Wroclaw	P17642	Received 2018	Yes
Hailong Chen	Georgia Institute of Technology	P14967	Received 2018	No



Name	Organization	Proposal	Year of Magnet Time	Is New To MagLab
Steven Conradson	Washington State University	P17416	Received 2018	Yes
Natalia Drichko	Johns Hopkins University	P16105	Received 2018	No
David Graf	National High Magnetic Field Laboratory (NHMFL)	P16282	Received 2018	No
Kenneth Hanson	Florida State University (FSU)	P17610	Received 2018	Yes
Patrick Holland	Yale University	P17841	Received 2018	Yes
Zofia Janas	University of Wroclaw	P17629	Received 2018	Yes
Wei-Tsung Lee	Loyola University Chicago	P17840	Received 2018	Yes
Yi Lu	University of Illinois at Urbana-Champaign	P17805	Received 2018	Yes
Elzbieta Megiel	University of Warsaw	P17442	Received 2018	Yes
Grace Morgan	University College Dublin	P16285	Received 2018	No
Michael Nippe	Texas A&M University	P17842	Received 2018	Yes
Elizabeth Nolan	Massachusetts Institute of Technology	P17569	Received 2018	Yes
Valentin Novikov	Institute of Organoelement Compounds of Russian Academy of Sciences	P17639	Received 2018	Yes
Joshua Obaleye	University of Ilorin	P17620	Received 2018	Yes
Mykhaylo Ozerov	National High Magnetic Field Laboratory (NHMFL)	P17494	Received 2018	No
Lawrence Que	University of Minnesota, Twin Cities	P17897	Received 2018	Yes
Chandrasekhar Ramanathan	Dartmouth College	P17549	Received 2018	Yes
Joseph Zadrozny	Colorado State University	P17730	Received 2018	Yes
<b>Total</b>	<b>20</b>			

<sup>1</sup> PIs who received magnet time for the first time.

**Table 9: Research Proposal<sup>1</sup> Profile with Magnet Time**

Total Proposals <sup>1</sup>	Minority <sup>2</sup>	Non-Minority	Prefer Not to Respond to Race	Female <sup>3</sup>	Male	Other	Prefer Not to Respond to Gender	CM	Chemistry, Geochemistry	Engineering	Magnets, Materials, Testing, Instr.	Biology, Biochem Biophys
65	4	52	9	13	46	0	6	21	27	0	6	11

<sup>1</sup> A "proposal" may have associated with it a single experiment or a group of closely related experiments. A PI may have more than one proposal.

<sup>2</sup> The number of proposals satisfying the following condition: The PI is a minority.

<sup>3</sup> The number of proposals satisfying the following condition: The PI is a female.

Find the list of EMR user proposals on our [website](#)

#### 4. HBT Facility

**Table 1: User Demographics**

	Users <sup>1</sup>	Minority <sup>2</sup>	Non-Minority <sup>2</sup>	Prefer Not to Respond to Race <sup>3</sup>	Male	Female	Other	Prefer Not to Respond to Gender <sup>3</sup>
Senior Personnel, U.S.	7	0	5	2	6	0	0	1
Senior Personnel, non-U.S.	2	0	1	1	2	0	0	0
Postdocs, U.S.	4	0	3	1	3	0	0	1
Postdocs, non-U.S.	1	0	1	0	0	1	0	0
Students, U.S.	4	0	4	0	2	1	0	1
Students, non-U.S.	0	0	0	0	0	0	0	0
Technician, U.S.	0	0	0	0	0	0	0	0
Technician, non-U.S.	0	0	0	0	0	0	0	0
<b>Total</b>	<b>18</b>	<b>0</b>	<b>14</b>	<b>4</b>	<b>13</b>	<b>2</b>	<b>0</b>	<b>3</b>

<sup>1</sup> Users using multiple facilities are counted in each facility listed.

<sup>2</sup> NSF Minority status includes the following races: American Indian, Alaska Native, Black or African American, Hispanic, Native Hawaiian or other Pacific Islander. The definition also includes Hispanic Ethnicity as a minority group. Minority status excludes Asian and White-Not of Hispanic Origin.

<sup>3</sup> Includes pending user account activations.

**Table 2: User by Participation**

	Users <sup>1</sup>	Users Present	Users Operating Remotely <sup>2</sup>	Users Sending Sample <sup>3</sup>	Off-Site Collaborators <sup>4</sup>
Senior Personnel, U.S.	7	3	0	1	3
Senior Personnel, non-U.S.	2	1	0	0	1
Postdocs, U.S.	4	4	0	0	0
Postdocs, non-U.S.	1	1	0	0	0
Students, U.S.	4	4	0	0	0
Students, non-U.S.	0	0	0	0	0
Technician, U.S.	0	0	0	0	0
Technician, non-U.S.	0	0	0	0	0
<b>Total</b>	<b>18</b>	<b>13</b>	<b>0</b>	<b>1</b>	<b>4</b>

<sup>1</sup> Users using multiple facilities are counted in each facility listed.

<sup>2</sup> "Users Operating Remotely" refers to users who operate the magnet system from a remote location. Remote operations are not currently available in all facilities.

<sup>3</sup> "Users Sending Sample" refers to users who send the sample to the facility and/or research group and the experiment is conducted by other collaborators on the experiment. Users at UF, FSU, and LANL cannot be "sample senders" for facilities located on their campuses.

<sup>4</sup> "Off-Site Collaborators" are scientific or technical participants on the experiment; who will not be present, sending sample, or operating the magnet system remotely; and who are not located on the campus of that facility (i.e., they are off-site).

**Table 3: User Organization**

	Users <sup>1</sup>	NHMFL-Affiliated Users <sup>2, 3, 4</sup>	Local Users <sup>2</sup>	External Users	National			International		
					Lab <sup>3, 5</sup>	Univer- sity <sup>4, 5</sup>	Indus- try <sup>5</sup>	Lab <sup>5</sup>	Univer- sity <sup>5</sup>	Industry <sup>5</sup>
Senior Personnel, U.S.	7	2	1	4	0	7	0	0	0	0
Senior Personnel, non-U.S.	2	0	0	2	0	0	0	0	2	0
Postdocs, U.S.	4	1	1	2	0	4	0	0	0	0
Postdocs, non-U.S.	1	0	0	1	0	0	0	0	1	0
Students, U.S.	4	0	4	0	0	4	0	0	0	0
Students, non-U.S.	0	0	0	0	0	0	0	0	0	0
Technician, U.S.	0	0	0	0	0	0	0	0	0	0
Technician, non-U.S.	0	0	0	0	0	0	0	0	0	0
<b>Total</b>	<b>18</b>	<b>3</b>	<b>6</b>	<b>9</b>	<b>0</b>	<b>15</b>	<b>0</b>	<b>0</b>	<b>3</b>	<b>0</b>

<sup>1</sup> Users using multiple facilities are counted in each facility listed.

<sup>2</sup> NHMFL-Affiliated users are defined as anyone in the lab's personnel system (i.e. on our web site/directory), even if they travel to another site. Local users are defined as any non-NHMFL-Affiliated researchers originating at any of the institutions in proximity to the MagLab sites (i.e. researchers at FSU, UF, FAMU, or LANL), even if they travel to another site.

<sup>3</sup> Users with primary affiliations at NHMFL/LANL are reported in NHMFL-Affiliated Users and National Laboratory.

<sup>4</sup> Users with primary affiliations at FSU, UF, or FAMU are reported in NHMFL-Affiliated Users and National University.

<sup>5</sup> The total of university, industry, and national lab users will equal the total number of users.

**Table 4: User by Discipline**

	Users <sup>1</sup>	Condensed Matter Physics	Chemistry, Geochemistry	Engineering	Magnets, Materials, Testing, Instr.	Biology, Biochemistry, Biophysics
Senior Personnel, U.S.	7	4	0	2	0	1
Senior Personnel, non-U.S.	2	2	0	0	0	0
Postdocs, U.S.	4	4	0	0	0	0

	Users <sup>1</sup>	Condensed Matter Physics	Chemistry, Geochemistry	Engineering	Magnets, Materials, Testing, Instr.	Biology, Biochemistry, Biophysics
Postdocs, non-U.S.	1	1	0	0	0	0
Students, U.S.	4	4	0	0	0	0
Students, non-U.S.	0	0	0	0	0	0
Technician, U.S.	0	0	0	0	0	0
Technician, non-U.S.	0	0	0	0	0	0
<b>Total</b>	<b>18</b>	<b>15</b>	<b>0</b>	<b>2</b>	<b>0</b>	<b>1</b>

<sup>1</sup> Users using multiple facilities are counted in each facility listed.

**Table 5: User Facility Operations by Magnet Systems**

	Total Days Used <sup>1</sup>	Percentage of Total Days Used	Williamson Hall	Bay 2	Bay 3
NHMFL-Affiliated	0	0 %	0	0	0
Local	0	0 %	0	0	0
U.S. University	275	35 %	78	139	58
U.S. Govt. Lab.	0	0 %	0	0	0
U.S. Industry	0	0 %	0	0	0
Non-U.S.	308	39 %	75	0	233
Test, Calibration, Set-up, Maintenance, Inst. Dev.	201	26 %	27	174	0
<b>Total</b>	<b>784</b>	<b>100 %</b>	<b>180</b>	<b>313</b>	<b>291</b>

<sup>1</sup> User Units are defined as magnet days. One magnet day is defined as 24 hours in superconducting magnets.

**Table 6: Operations by Discipline**

	Total Days Used <sup>1</sup>	Condensed Matter Physics	Chemistry, Geochemistry	Engineering	Magnets, Materials	Biology, Biochemistry, Biophysics
NHMFL-Affiliated	0	0	0	0	0	0
Local	0	0	0	0	0	0
U.S. University	275	275	0	0	0	0
U.S. Govt. Lab.	0	0	0	0	0	0
U.S. Industry	0	0	0	0	0	0
Non-U.S.	308	308	0	0	0	0
Test, Calibration, Set-up, Maintenance, Inst. Dev.	201	201	0	0	0	0
<b>Total</b>	<b>784</b>	<b>784</b>	<b>0</b>	<b>0</b>	<b>0</b>	<b>0</b>

<sup>1</sup> User Units are defined as magnet days. One magnet day is defined as 24 hours in superconducting magnets.

**Table 7: Subscription Rate**

Experiments Submitted (Current year)	Experiments Submitted (Deferred from prev. year)	Experiments w/ Usage	Experiments Declined	Experiments Reviewed	Experiment Subscription (%) (Submitted / Used)	Days Submitted	Days External Users Used	Days Local Users Used	Total Days Used	Subscription (%) (Days submitted / Days used)
15	0	11 (73.33 %)	4 (26.67 %)	15	136.36 %	957	583	0	784	122.07 %

**Table 8: New<sup>1</sup> User PI's**

Name	Organization	Proposal	Year of Magnet Time	Is New To MagLab
Chao Huan	University of Florida	P17606	Received 2018	Yes
Ryuji Nomura	Tokyo Institute of Technology	P16308	Received 2018	Yes

Name	Organization	Proposal	Year of Magnet Time	Is New To MagLab
Total	2			

<sup>1</sup> PIs who received magnet time for the first time.

**Table 9: Research Proposal<sup>1</sup> Profile with Magnet Time**

Total Proposals <sup>1</sup>	Minority <sup>2</sup>	Non-Minority	Prefer Not to Respond to Race	Female <sup>3</sup>	Male	Other	Prefer Not to Respond to Gender	Condensed Matter Physics	Chemistry, Geochemistry	Engineering	Magnets, Materials, Testing, Instr.	Biology, Biochem Biophys.
4	0	2	2	0	4	0	0	4	0	0	0	0

<sup>1</sup> A "proposal" may have associated with it a single experiment or a group of closely related experiments. A PI may have more than one proposal.

<sup>2</sup> The number of proposals satisfying the following condition: The PI is a minority.

<sup>3</sup> The number of proposals satisfying the following condition: The PI is a female.

Find the list of HBT user proposals on our [website](#)

## 5. ICR Facility

**Table 1: User Demographics**

	Users <sup>1</sup>	Minority <sup>2</sup>	Non-Minority <sup>2</sup>	Prefer Not to Respond to Race <sup>3</sup>	Male	Female	Other	Prefer Not to Respond to Gender <sup>3</sup>
Senior Personnel, U.S.	157	6	100	51	76	37	0	44
Senior Personnel, non-U.S.	70	6	30	34	25	14	0	31
Postdocs, U.S.	26	2	19	5	12	12	0	2
Postdocs, non-U.S.	4	0	3	1	3	0	0	1
Students, U.S.	81	11	54	16	31	41	0	9
Students, non-U.S.	31	3	13	15	15	6	0	10
Technician, U.S.	5	0	5	0	5	0	0	0
Technician, non-U.S.	1	0	1	0	1	0	0	0
Total	375	28	225	122	168	110	0	97

<sup>1</sup> Users using multiple facilities are counted in each facility listed.

<sup>2</sup> NSF Minority status includes the following races: American Indian, Alaska Native, Black or African American, Hispanic, Native Hawaiian or other Pacific Islander. The definition also includes Hispanic Ethnicity as a minority group. Minority status excludes Asian and White-Not of Hispanic Origin.

<sup>3</sup> Includes pending user account activations.

**Table 2: User by Participation**

	Users <sup>1</sup>	Users Present	Users Operating Remotely <sup>2</sup>	Users Sending Sample <sup>3</sup>	Off-Site Collaborators <sup>4</sup>
Senior Personnel, U.S.	157	38	0	22	97
Senior Personnel, non-U.S.	70	8	0	10	52
Postdocs, U.S.	26	12	0	4	10
Postdocs, non-U.S.	4	0	0	0	4
Students, U.S.	81	48	0	6	27
Students, non-U.S.	31	8	0	5	18
Technician, U.S.	5	3	0	0	2
Technician, non-U.S.	1	1	0	0	0
Total	375	118	0	47	210

<sup>1</sup> Users using multiple facilities are counted in each facility listed.

<sup>2</sup> "Users Operating Remotely" refers to users who operate the magnet system from a remote location. Remote operations are not currently available in all facilities.

<sup>3</sup> "Users Sending Sample" refers to users who send the sample to the facility and/or research group and the experiment is conducted by other collaborators on the experiment. Users at UF, FSU, and LANL cannot be "sample senders" for facilities located on their campuses.



<sup>4</sup> "Off-Site Collaborators" are scientific or technical participants on the experiment; who will not be present, sending sample, or operating the magnet system remotely; and who are not located on the campus of that facility (i.e., they are off-site).

**Table 3: User Organization**

	Users <sup>1</sup>	NHMFL-Affiliated Users <sup>2, 3, 4</sup>	Local Users <sup>2</sup>	External Users	National			International		
					Lab <sup>3, 5</sup>	Univer-sity <sup>4, 5</sup>	Indus-try <sup>5</sup>	Lab <sup>5</sup>	Univer-sity <sup>5</sup>	Indus-try <sup>5</sup>
Senior Personnel, U.S.	157	14	11	132	21	123	13	0	0	0
Senior Personnel, non-U.S.	70	0	0	70	0	0	0	11	50	9
Postdocs, U.S.	26	4	7	15	1	25	0	0	0	0
Postdocs, non-U.S.	4	0	0	4	0	0	0	2	2	0
Students, U.S.	81	11	24	46	0	81	0	0	0	0
Students, non-U.S.	31	0	0	31	0	0	0	2	29	0
Technician, U.S.	5	2	1	2	0	5	0	0	0	0
Technician, non-U.S.	1	0	0	1	0	0	0	1	0	0
<b>Total</b>	<b>375</b>	<b>31</b>	<b>43</b>	<b>301</b>	<b>22</b>	<b>234</b>	<b>13</b>	<b>16</b>	<b>81</b>	<b>9</b>

<sup>1</sup> Users using multiple facilities are counted in each facility listed.

<sup>2</sup> NHMFL-Affiliated users are defined as anyone in the lab's personnel system (i.e. on our web site/directory), even if they travel to another site. Local users are defined as any non-NHMFL-Affiliated researchers originating at any of the institutions in proximity to the MagLab sites (i.e. researchers at FSU, UF, FAMU, or LANL), even if they travel to another site.

<sup>3</sup> Users with primary affiliations at NHMFL/LANL are reported in NHMFL-Affiliated Users and National Laboratory.

<sup>4</sup> Users with primary affiliations at FSU, UF, or FAMU are reported in NHMFL-Affiliated Users and National University.

<sup>5</sup> The total of university, industry, and national lab users will equal the total number of users.

**Table 4: User by Discipline**

	Users <sup>1</sup>	Condensed Matter Physics	Chemistry, Geochemistry	Engineering	Magnets, Materials, Testing, Instr.	Biology, Biochemistry, Biophysics
Senior Personnel, U.S.	157	0	93	9	3	52
Senior Personnel, non-U.S.	70	2	54	3	1	10
Postdocs, U.S.	26	0	12	2	0	12
Postdocs, non-U.S.	4	1	1	0	1	1
Students, U.S.	81	0	51	4	2	24
Students, non-U.S.	31	1	24	1	2	3
Technician, U.S.	5	0	2	1	1	1
Technician, non-U.S.	1	0	1	0	0	0
<b>Total</b>	<b>375</b>	<b>4</b>	<b>238</b>	<b>20</b>	<b>10</b>	<b>103</b>

<sup>1</sup> Users using multiple facilities are counted in each facility listed.

**Table 5: User Facility Operations by Magnet Systems**

	Total Days Used <sup>1</sup>	Percentage of Total Days Used	9.4T passive	9.4T active	14.5T Hybrid	21T Hybrid
NHMFL-Affiliated	146.4	16.9 %	68.2	2	36	40.3
Local	22.1	2.5 %	3.8	0	5	13.3
U.S. University	195.9	22.6 %	46.8	14.5	11.5	123.1
U.S. Govt. Lab.	9.1	1 %	6.3	1.5	0	1.3
U.S. Industry	13.6	1.6 %	2.5	0	0	11.1
Non-U.S.	116.2	13.4 %	15.1	37	0	64.1
Test, Calibration, Set-up, Maintenance, Inst. Dev.	364.7	42 %	55.3	108	152.5	48.9
<b>Total</b>	<b>868</b>	<b>100 %</b>	<b>198</b>	<b>163</b>	<b>205</b>	<b>302</b>

<sup>1</sup> User Units are defined as magnet days. One magnet day is defined as 24 hours in superconducting magnets.

**Table 6: Operations by Discipline**

	Total Days Used <sup>1</sup>	Condensed Matter Physics	Chemistry, Geochemistry	Engineering	Magnets, Materials	Biology, Biochemistry, Biophysics
NHMFL-Affiliated	146.4	0	108.3	0	31	7.1
Local	22.1	0	15.6	0	0	6.5
U.S. University	195.9	0	76	5.3	0	114.6
U.S. Govt. Lab.	9.1	0	9.1	0	0	0
U.S. Industry	13.6	0	8.6	0	0	5
Non-U.S.	116.2	0	110.2	3	0	3
Test, Calibration, Set-up, Maintenance, Inst. Dev.	364.7	0	13.6	0	343.7	7.5
<b>Total</b>	<b>868</b>	<b>0</b>	<b>341.3</b>	<b>8.3</b>	<b>374.7</b>	<b>143.7</b>

<sup>1</sup> User Units are defined as magnet days. One magnet day is defined as 24 hours in superconducting magnets.

**Table 7: Subscription Rate**

Experiments Submitted (Current year)	Experiments Submitted (Deferred from prev. year)	Experiments w/ Usage	Experiments Declined	Experiments Re-viewed	Experiment Subscription (%) (Submitted / Used)	Days Submitted	Days External Users Used	Days Local Users Used	Total Days Used	Subscription (%) (Days submitted / Days used)
134	16	136 (90.67 %)	14 (9.33 %)	150	110.29 %	2,246	334.7	22.1	868	258.76 %

**Table 8: New<sup>1</sup> User PI's**

Name	Organization	Proposal	Year of Magnet Time	Is New To MagLab
Jens Blotvogel	Colorado State University	P17688	Received 2018	Yes
Rene Boiteau	Oregon State University	P17788	Received 2018	Yes
Brian Bothner	Montana State University	P17821	Received 2018	Yes
Romy Chakraborty	Lawrence Berkeley National Laboratory	P17797	Received 2018	Yes
Ning Chen	Soochow University	P17484	Received 2018	Yes
Lisa DiPinto	NOAA	P17735	Received 2018	Yes
Huiyu Dong	University of South Carolina	P17868	Received 2018	Yes
Paul Dunk	National High Magnetic Field Laboratory (NHMFL)	P17734	Received 2018	Yes
Christopher Ewels	University of Nantes	P17732	Received 2018	Yes
Ron Heeren	Maastricht University	P17714	Received 2018	Yes
Nicole Heshka	Natural Resources Canada	P17711	Received 2018	Yes
Nathan Kaiser	Biodesix	P17715	Received 2018	Yes
Maria Maradei	Universidad Industrial de Santander	P17865	Received 2018	Yes
Robert Masserini	University of Tampa	P17696	Received 2018	Yes
James McClelland	University of Texas at Austin	P17617	Received 2018	Yes
Nga Nguyen	Infinium Corporation	P17636	Received 2018	Yes
Jeremy Owens	National High Magnetic Field Laboratory (NHMFL)	P17838	Received 2018	Yes
Jose Pinto	Florida State University (FSU)	P17808	Received 2018	No
Stephen Rappaport	University of California, Berkeley	P17700	Received 2018	Yes
Susan Richardson	University of South Carolina	P17855	Received 2018	Yes
Antonio Rodriguez-Fortea	The Public University of Tarragona	P17725	Received 2018	Yes
Christine Schaner Tooley	SUNY Buffalo	P17590	Received 2018	Yes
Joshua Schimel	University of California, Santa Barbara	P17745	Received 2018	Yes

Name	Organization	Proposal	Year of Magnet Time	Is New To MagLab
Lloyd Smith	University of Wisconsin, Madison	P17446	Received 2018	Yes
Patrick Tomco	University of Alaska Anchorage	P17796	Received 2018	Yes
Jemma Wadham	University of Bristol	P17562	Received 2018	Yes
Christopher Williamson	University of Bristol	P17565	Received 2018	Yes
Jianzhong Xu	Northwest Institute of Eco-Environment and Resources, Chinese Academy of Sciences	P17655	Received 2018	Yes
<b>Total</b>	<b>28</b>			

<sup>1</sup> Pls who received magnet time for the first time.

**Table 9: Research Proposal<sup>1</sup> Profile with Magnet Time**

Total Proposals <sup>1</sup>	Minority <sup>2</sup>	Non-Minority	Prefer Not to Respond to Race	Female <sup>3</sup>	Male	Other	Prefer Not to Respond to Gender	Condensed Matter Physics	Chemistry, Geochemistry	Engineering	Magnets, Materials, Testing, Instrum.	Biology, Biochem Biophys.
115	11	85	19	26	77	0	12	0	78	5	7	25

<sup>1</sup> A "proposal" may have associated with it a single experiment or a group of closely related experiments. A PI may have more than one proposal.

<sup>2</sup> The number of proposals satisfying the following condition: The PI is a minority.

<sup>3</sup> The number of proposals satisfying the following condition: The PI is a female.

Find the list of ICR user proposals on our [website](#)

## 6. NMR Facility

**Table 1: User Demographics**

	Users <sup>1</sup>	Minority <sup>2</sup>	Non-Minority <sup>2</sup>	Prefer Not to Respond to Race <sup>3</sup>	Male	Female	Other	Prefer Not to Respond to Gender <sup>3</sup>
Senior Personnel, U.S.	124	10	97	17	89	25	0	10
Senior Personnel, non-U.S.	51	1	36	14	29	12	0	10
Postdocs, U.S.	29	4	21	4	15	12	0	2
Postdocs, non-U.S.	8	0	5	3	5	0	0	3
Students, U.S.	78	5	61	12	46	23	0	9
Students, non-U.S.	19	1	9	9	7	6	0	6
Technician, U.S.	9	1	6	2	5	3	0	1
Technician, non-U.S.	2	0	2	0	2	0	0	0
<b>Total</b>	<b>320</b>	<b>22</b>	<b>237</b>	<b>61</b>	<b>198</b>	<b>81</b>	<b>0</b>	<b>41</b>

<sup>1</sup> Users using multiple facilities are counted in each facility listed.

<sup>2</sup> NSF Minority status includes the following races: American Indian, Alaska Native, Black or African American, Hispanic, Native Hawaiian or other Pacific Islander. The definition also includes Hispanic Ethnicity as a minority group. Minority status excludes Asian and White-Not of Hispanic Origin.

<sup>3</sup> Includes pending user account activations.

**Table 2: User by Participation**

	Users <sup>1</sup>	Users Present	Users Operating Remotely <sup>2</sup>	Users Sending Sample <sup>3</sup>	Off-Site Collaborators <sup>4</sup>
Senior Personnel, U.S.	124	51	3	27	43
Senior Personnel, non-U.S.	51	4	3	9	35
Postdocs, U.S.	29	18	1	2	8
Postdocs, non-U.S.	8	0	1	0	7
Students, U.S.	78	46	7	13	12
Students, non-U.S.	19	3	0	1	15
Technician, U.S.	9	7	0	0	2
Technician, non-U.S.	2	1	0	0	1

	Users <sup>1</sup>	Users Present	Users Operating Remotely <sup>2</sup>	Users Sending Sample <sup>3</sup>	Off-Site Collaborators <sup>4</sup>
<b>Total</b>	<b>320</b>	<b>130</b>	<b>15</b>	<b>52</b>	<b>123</b>

<sup>1</sup> Users using multiple facilities are counted in each facility listed.

<sup>2</sup> "Users Operating Remotely" refers to users who operate the magnet system from a remote location. Remote operations are not currently available in all facilities.

<sup>3</sup> "Users Sending Sample" refers to users who send the sample to the facility and/or research group and the experiment is conducted by other collaborators on the experiment. Users at UF, FSU, and LANL cannot be "sample senders" for facilities located on their campuses.

<sup>4</sup> "Off-Site Collaborators" are scientific or technical participants on the experiment; who will not be present, sending sample, or operating the magnet system remotely; and who are not located on the campus of that facility (i.e., they are off-site).

**Table 3: User Organization**

					National			International		
	Users <sup>1</sup>	NHMFL-Affiliated Users <sup>2, 3, 4</sup>	Local Users <sup>2</sup>	External Users	Lab <sup>3, 5</sup>	University <sup>4, 5</sup>	Industry <sup>5</sup>	Lab <sup>5</sup>	University <sup>5</sup>	Industry <sup>5</sup>
Senior Personnel, U.S.	124	23	14	87	2	114	8	0	0	0
Senior Personnel, non-U.S.	51	0	0	51	0	0	0	7	37	7
Postdocs, U.S.	29	8	6	15	0	27	2	0	0	0
Postdocs, non-U.S.	8	0	0	8	0	0	0	3	5	0
Students, U.S.	78	11	15	52	0	77	1	0	0	0
Students, non-U.S.	19	0	0	19	0	0	0	2	17	0
Technician, U.S.	9	5	1	3	0	8	1	0	0	0
Technician, non-U.S.	2	0	0	2	0	0	0	0	2	0
<b>Total</b>	<b>320</b>	<b>47</b>	<b>36</b>	<b>237</b>	<b>2</b>	<b>226</b>	<b>12</b>	<b>12</b>	<b>61</b>	<b>7</b>

<sup>1</sup> Users using multiple facilities are counted in each facility listed.

<sup>2</sup> NHMFL-Affiliated users are defined as anyone in the lab's personnel system (i.e. on our web site/directory), even if they travel to another site. Local users are defined as any non-NHMFL-Affiliated researchers originating at any of the institutions in proximity to the MagLab sites (i.e. researchers at FSU, UF, FAMU, or LANL), even if they travel to another site.

<sup>3</sup> Users with primary affiliations at NHMFL/LANL are reported in NHMFL-Affiliated Users and National Laboratory.

<sup>4</sup> Users with primary affiliations at FSU, UF, or FAMU are reported in NHMFL-Affiliated Users and National University.

<sup>5</sup> The total of university, industry, and national lab users will equal the total number of users.

**Table 4: User by Discipline**

	Users <sup>1</sup>	Condensed Matter Physics	Chemistry, Geochemistry	Engineering	Magnets, Materials, Testing, Instr.	Biology, Biochemistry, Biophysics
Senior Personnel, U.S.	124	5	36	21	7	55
Senior Personnel, non-U.S.	51	2	24	4	4	17
Postdocs, U.S.	29	1	6	1	3	18
Postdocs, non-U.S.	8	0	3	0	0	5
Students, U.S.	78	1	28	19	6	24
Students, non-U.S.	19	1	8	6	0	4
Technician, U.S.	9	0	1	1	1	6
Technician, non-U.S.	2	0	2	0	0	0
<b>Total</b>	<b>320</b>	<b>10</b>	<b>108</b>	<b>52</b>	<b>21</b>	<b>129</b>

<sup>1</sup> Users using multiple facilities are counted in each facility listed.

**Table 5: User Facility Operations by Magnet Systems**

	Total Days Used <sup>1</sup>	Percentage of Total Days Used	36T 40 mm SCH	900 MHz	830 MHz, 31 mm	800 MHz, 63 mm #1	800 MHz, 63 mm #2	800 MHz, 54 mm	600 MHz, 89 mm #1	600 MHz, 89 mm #2	600 MHz, 89 mm MAS DNP	500 MHz, 89 mm	500 MHz, 89 mm (E)
NHMFL-Affiliated	897.5	28 %	4	90	0	121	86.5	66	205	195	16	86	28
Local	134	4.2 %	0	18	0	0	0	5	4	13	0	39	55



	Total Days Used <sup>1</sup>	Percentage of Total Days Used	36T 40 mm SCH	900 MHz	830 MHz, 31 mm	800 MHz, 63 mm #1	800 MHz, 63 mm #2	800 MHz, 54 mm	600 MHz, 89 mm #1	600 MHz, 89 mm #2	600 MHz, 89 mm MAS DNP	500 MHz, 89 mm	500 MHz, 89 mm (E)
U.S. University	1,602.5	50 %	59	115	270	199	1.5	248	130	137	105.5	206	131.5
U.S. Govt. Lab.	19	0.6 %	0	8	0	0	0	0	0	0	0	0	11
U.S. Industry	48	1.5 %	0	47	0	0	0	0	0	0	1	0	0
Non-U.S.	308	9.6 %	39	59	55	25	0	0	6	18	63	22	21
Test, Calibration, Set-up, Maintenance, Inst. Dev.	193	6 %	0	8	27	15	0	46	7	0	66.5	0	23.5
<b>Total</b>	<b>3,202</b>	<b>100 %</b>	<b>102</b>	<b>345</b>	<b>352</b>	<b>360</b>	<b>88</b>	<b>365</b>	<b>352</b>	<b>363</b>	<b>252</b>	<b>353</b>	<b>270</b>

<sup>1</sup> User Units are defined as magnet days. One magnet day is defined as 24 hours in superconducting magnets and 7 hours for the hybrid magnet. 800 MHz 63 #2 magnet did not start operation until September 3rd, 2018.

**Table 6: Operations by Discipline**

	Total Days Used <sup>1</sup>	Condensed Matter Physics	Chemistry, Geochemistry	Engineering	Magnets, Materials	Biology, Biochemistry, Biophysics
NHMFL-Affiliated	897.5	7	5	0	6	879.5
Local	134	0	63	39	0	32
U.S. University	1,602.5	21	633	37.5	27.5	883.5
U.S. Govt. Lab.	19	0	0	0	0	19
U.S. Industry	48	0	1	0	0	47
Non-U.S.	308	0	231	0	0	77
Test, Calibration, Set-up, Maintenance, Inst. Dev.	193	0	2	0	66.5	124.5
<b>Total</b>	<b>3,202</b>	<b>28</b>	<b>935</b>	<b>76.5</b>	<b>100</b>	<b>2,062.5</b>

<sup>1</sup> User Units are defined as magnet days. One magnet day is defined as 24 hours in superconducting magnets and 7 hours for the hybrid magnet. 800 MHz 63 #2 magnet did not start operation until September 3rd, 2018.

**Table 7: Subscription Rate**

Experiments Submitted (Current year)	Experiments Submitted (Deferred from prev. year)	Experiments w/ Usage	Experiments Declined	Experiments Reviewed	Experiment Subscription (%) (Submitted / Used)	Days Submitted	Days External Users Used	Days Local Users Used	Total Days Used	Subscription (%) (Days submitted / Days used)
545	15	517 (92.32 %)	43 (7.68 %)	560	108.32 %	3,640	1,977.5	134	3,202	113.68 %

**Table 8: New<sup>1</sup> User PI's**

Name	Organization	Proposal	Year of Magnet Time	Is New To MagLab
Mavis Agbandje-McKenna	University of Florida	P17624	Received 2018	No
Alexander Barnes	Washington University in St. Louis	P17691	Received 2018	Yes
Jeanine Brady	University of Florida	P17623	Received 2018	No
David Bryce	University of Ottawa	P17455	Received 2018	Yes
William Dichtel	Northwestern University	P16036	Received 2018	Yes
Debra Fadool	Florida State University (FSU)	P17686	Received 2018	Yes
Robert Griffin	Massachusetts Institute of Technology	P17507	Received 2018	No
David Guilfoyle	Nathan Kline Institute for Psychiatric Research	P17721	Received 2018	Yes
Mei Hong	Massachusetts Institute of Technology	P17746	Received 2018	Yes
Yining Huang	University of Western Ontario	P17504	Received 2018	Yes

Name	Organization	Proposal	Year of Magnet Time	Is New To MagLab
Roger Koeppe	University of Arkansas	P17753	Received 2018	Yes
Olivier Lafon	University of Lille	P17586	Received 2018	Yes
Danielle Laurencin	University of Montpellier	P17464	Received 2018	Yes
Daniel Lee	University of Grenoble Alpes	P17632	Received 2018	Yes
Francesca Marassi	Sanford Burnham Prebys Medical Discovery Institute	P17471	Received 2018	Yes
Rachel Martin	University of California, Irvine	P17490	Received 2018	Yes
Michael McMahon	Johns Hopkins University	P17727	Received 2018	Yes
Luke O'Dell	Deakin University	P17626	Received 2018	Yes
Matteo Pasquali	Rice University	P17557	Received 2018	Yes
Jens Rosenberg	National High Magnetic Field Laboratory (NHMFL)	P17853	Received 2018	Yes
Aaron Rossini	Iowa State University	P17500	Received 2018	Yes
Joseph Schlenoff	Florida State University (FSU)	P17845	Received 2018	No
Bala Subramaniam	University of Kansas	P17566	Received 2018	Yes
Jeffery White	Oklahoma State University	P17925	Received 2018	Yes
Jim Zheng	Florida Agricultural and Mechanical University	P17813	Received 2018	Yes
<b>Total</b>	<b>25</b>			

<sup>1</sup> PIs who received magnet time for the first time.

**Table 9: Research Proposal<sup>1</sup> Profile with Magnet Time**

Total Proposals <sup>1</sup>	Minority <sup>2</sup>	Non-Minority	Prefer Not to Respond to Race	Female <sup>3</sup>	Male	Other	Prefer Not to Respond to Gender	Condensed Matter Physics	Chemistry, Geochemistry	Engineering	Magnets, Materials, Testing, Instrum.	Biology, Biochem Biophys.
108	6	92	10	23	82	0	3	3	32	5	7	61

<sup>1</sup> A "proposal" may have associated with it a single experiment or a group of closely related experiments. A PI may have more than one proposal.

<sup>2</sup> The number of proposals satisfying the following condition: The PI is a minority.

<sup>3</sup> The number of proposals satisfying the following condition: The PI is a female.

Find the list of NMR user proposals on our [website](#)

## 7. Pulsed Field Facility

**Table 1: User Demographics**

	Users <sup>1</sup>	Minority <sup>2</sup>	Non-Minority <sup>2</sup>	Prefer Not to Respond to Race <sup>3</sup>	Male	Female	Other	Prefer Not to Respond to Gender <sup>3</sup>
Senior Personnel, U.S.	46	1	40	5	38	5	0	3
Senior Personnel, non-U.S.	27	1	19	7	21	1	0	5
Postdocs, U.S.	29	1	26	2	20	8	0	1
Postdocs, non-U.S.	12	0	9	3	7	3	0	2
Students, U.S.	26	0	19	7	14	7	0	5
Students, non-U.S.	15	1	9	5	10	1	0	4
Technician, U.S.	0	0	0	0	0	0	0	0
Technician, non-U.S.	0	0	0	0	0	0	0	0
<b>Total</b>	<b>155</b>	<b>4</b>	<b>122</b>	<b>29</b>	<b>110</b>	<b>25</b>	<b>0</b>	<b>20</b>

<sup>1</sup> Users using multiple facilities are counted in each facility listed.

<sup>2</sup> NSF Minority status includes the following races: American Indian, Alaska Native, Black or African American, Hispanic, Native Hawaiian or other Pacific Islander. The definition also includes Hispanic Ethnicity as a minority group. Minority status excludes Asian and White-Not of Hispanic Origin.

<sup>3</sup> Includes pending user account activations.

**Table 2: User by Participation**

	Users <sup>1</sup>	Users Present	Users Operating Remotely <sup>2</sup>	Users Sending Sample <sup>3</sup>	Off-Site Collaborators <sup>4</sup>
Senior Personnel, U.S.	46	28	0	2	16
Senior Personnel, non-U.S.	27	10	0	3	14
Postdocs, U.S.	29	24	0	1	4
Postdocs, non-U.S.	12	6	0	2	4
Students, U.S.	26	24	0	1	1
Students, non-U.S.	15	11	0	0	4
Technician, U.S.	0	0	0	0	0
Technician, non-U.S.	0	0	0	0	0
<b>Total</b>	<b>155</b>	<b>103</b>	<b>0</b>	<b>9</b>	<b>43</b>

<sup>1</sup> Users using multiple facilities are counted in each facility listed.

<sup>2</sup> "Users Operating Remotely" refers to users who operate the magnet system from a remote location. Remote operations are not currently available in all facilities.

<sup>3</sup> "Users Sending Sample" refers to users who send the sample to the facility and/or research group and the experiment is conducted by other collaborators on the experiment. Users at UF, FSU, and LANL cannot be "sample senders" for facilities located on their campuses.

<sup>4</sup> "Off-Site Collaborators" are scientific or technical participants on the experiment; who will not be present, sending sample, or operating the magnet system remotely; and who are not located on the campus of that facility (i.e., they are off-site).

**Table 3: User Organization**

	Users <sup>1</sup>	NHMFL-Affiliated Users <sup>2,3,4</sup>	Local Users <sup>2</sup>	External Users	National			International		
					Lab <sup>3,5</sup>	Univer- sity <sup>4,5</sup>	Indus- try <sup>5</sup>	Lab <sup>5</sup>	Univer- sity <sup>5</sup>	Industry <sup>5</sup>
Senior Personnel, U.S.	46	16	6	24	16	26	4	0	0	0
Senior Personnel, non-U.S.	27	0	0	27	0	0	0	4	23	0
Postdocs, U.S.	29	8	6	15	12	13	4	0	0	0
Postdocs, non-U.S.	12	0	0	12	0	0	0	1	11	0
Students, U.S.	26	1	2	23	3	23	0	0	0	0
Students, non-U.S.	15	0	0	15	0	0	0	0	15	0
Technician, U.S.	0	0	0	0	0	0	0	0	0	0
Technician, non-U.S.	0	0	0	0	0	0	0	0	0	0
<b>Total</b>	<b>155</b>	<b>25</b>	<b>14</b>	<b>116</b>	<b>31</b>	<b>62</b>	<b>8</b>	<b>5</b>	<b>49</b>	<b>0</b>

<sup>1</sup> Users using multiple facilities are counted in each facility listed.

<sup>2</sup> NHMFL-Affiliated users are defined as anyone in the lab's personnel system (i.e. on our web site/directory), even if they travel to another site. Local users are defined as any non-NHMFL-Affiliated researchers originating at any of the institutions in proximity to the MagLab sites (i.e. researchers at FSU, UF, FAMU, or LANL), even if they travel to another site.

<sup>3</sup> Users with primary affiliations at NHMFL/LANL are reported in NHMFL-Affiliated Users and National Laboratory.

<sup>4</sup> Users with primary affiliations at FSU, UF, or FAMU are reported in NHMFL-Affiliated Users and National University.

<sup>5</sup> The total of university, industry, and national lab users will equal the total number of users.

**Table 4: User by Discipline**

	Users <sup>1</sup>	Condensed Matter Physics	Chemistry, Geochemistry	Engineering	Magnets, Materials, Testing, Instr.	Biology, Biochemistry, Biophysics
Senior Personnel, U.S.	46	39	2	2	0	3
Senior Personnel, non-U.S.	27	26	1	0	0	0
Postdocs, U.S.	29	27	1	0	1	0
Postdocs, non-U.S.	12	11	1	0	0	0
Students, U.S.	26	23	2	1	0	0
Students, non-U.S.	15	13	1	0	1	0
Technician, U.S.	0	0	0	0	0	0

	Users <sup>1</sup>	Condensed Matter Physics	Chemistry, Geochemistry	Engineering	Magnets, Materials, Testing, Instr.	Biology, Biochemistry, Biophysics
Technician, non-U.S.	0	0	0	0	0	0
<b>Total</b>	<b>155</b>	<b>139</b>	<b>8</b>	<b>3</b>	<b>2</b>	<b>3</b>

<sup>1</sup> Users using multiple facilities are counted in each facility listed.

**Table 5: User Facility Operations by Magnet System Groups**

	Total Days Used <sup>1</sup>	Percentage of Total Days Used	Single Turn	Short Pulse	100T
NHMFL-Affiliated	113	18.7 %	5	108	0
Local	95	15.7 %	0	95	0
U.S. University	145	24 %	0	136	9
U.S. Govt. Lab.	88	14.5 %	0	88	0
U.S. Industry	0	0 %	0	0	0
Non-U.S.	164	27.1 %	0	164	0
Test, Calibration, Set-up, Maintenance, Inst. Dev.	0	0 %	0	0	0
<b>Total</b>	<b>605</b>	<b>100 %</b>	<b>5</b>	<b>591</b>	<b>9</b>

<sup>1</sup> User Units are defined as magnet days. One magnet day is defined as 24 hours in superconducting magnets.

**Table 6: Operations by Discipline**

	Total Days Used <sup>1</sup>	Condensed Matter Physics	Chemistry, Geochemistry	Engineering	Magnets, Materials	Biology, Biochemistry, Biophysics
NHMFL-Affiliated	113	88	0	0	25	0
Local	95	95	0	0	0	0
U.S. University	145	135	10	0	0	0
U.S. Govt. Lab.	88	88	0	0	0	0
U.S. Industry	0	0	0	0	0	0
Non-U.S.	164	164	0	0	0	0
Test, Calibration, Set-up, Maintenance, Inst. Dev.	0	0	0	0	0	0
<b>Total</b>	<b>605</b>	<b>570</b>	<b>10</b>	<b>0</b>	<b>25</b>	<b>0</b>

<sup>1</sup> User Units are defined as magnet days. One magnet day is defined as 24 hours in superconducting magnets.

**Table 7: Subscription Rate**

Experiments Submitted (Current year)	Experiments Submitted (Deferred from prev. year)	Experiments w/ Usage	Experiments Declined	Experiments Re-viewed	Experiment Subscription (%) (Submitted / Used)	Days Submitted	Days External Users Used	Days Local Users Used	Total Days Used	Subscription (%) (Days submitted / Days used)
80	12	68 (73.91 %)	24 (26.09 %)	92	135.29 %	706	397	95	605	116.69 %

**Table 8: New<sup>1</sup> User PI's**

Name	Organization	Proposal	Year of Magnet Time	Is New To MagLab
Yisheng Chai	Chongqing University	P17501	Received 2018	Yes
Cory Dean	City College of New York	P16292	Received 2018	No
Mikhail Eremets	Max Planck Institute for Chemistry, Mainz	P17644	Received 2018	Yes
Priscila Ferrari Silveira Rosa	Los Alamos National Laboratory	P17682	Received 2018	Yes
Swee Goh	Hong Kong University of Science and Technology	P17646	Received 2018	Yes
Greg MacDougall	University of Illinois at Urbana-Champaign	P17656	Received 2018	Yes



Name	Organization	Proposal	Year of Magnet Time	Is New To MagLab
Yoon Seok Oh	Ulsan National Institute of Science and Technology	P17649	Received 2018	Yes
Kent Shirer	Max Planck Institute for Chemical Physics of Solids, Dresden	P17502	Received 2018	Yes
Dan Sun	Los Alamos National Laboratory	P17654	Received 2018	Yes
Alexander Vasiliev	Lomonosov Moscow State University	P17703	Received 2018	Yes
Ulrich Welp	Argonne National Laboratory	P17689	Received 2018	No
Dmitri Yakovlev	University of Dortmund	P17568	Received 2018	Yes
<b>Total</b>	<b>12</b>			

<sup>1</sup> PIs who received magnet time for the first time.

**Table 9: Research Proposal<sup>1</sup> Profile with Magnet Time**

Total Proposals <sup>1</sup>	Minority <sup>2</sup>	Non-Minority	Prefer Not to Respond to Race	Female <sup>3</sup>	Male	Other	Prefer Not to Respond to Gender	Condensed Matter Physics	Chemistry, Geochemistry	Engineering	Magnets, Materials, Testing, Instrum.	Biology, Biochem Biophys.
49	2	44	3	4	44	0	1	46	1	0	2	0

<sup>1</sup> A "proposal" may have associated with it a single experiment or a group of closely related experiments. A PI may have more than one proposal.

<sup>2</sup> The number of proposals satisfying the following condition: The PI is a minority.

<sup>3</sup> The number of proposals satisfying the following condition: The PI is a female.

Find the list of Pulsed Field user proposals on our [website](#)

## APPENDIX II: USER FACILITIES OVERVIEW

### Overall Statistics across All NHMFL User Facilities

**Table 1a: User Demographics of All Facilities**

	Users <sup>1</sup>	Minority <sup>2</sup>	Non-Minority <sup>2</sup>	Prefer Not to Respond to Race <sup>3</sup>	Male	Female	Other	Prefer Not to Respond to Gender <sup>3</sup>
Senior Personnel, U.S.	740	35	541	164	474	136	0	130
Senior Personnel, non-U.S.	279	14	180	85	166	46	0	67
Postdocs, U.S.	240	20	178	42	144	69	0	27
Postdocs, non-U.S.	56	0	39	17	38	7	0	11
Students, U.S.	565	34	401	130	317	158	0	90
Students, non-U.S.	124	9	74	41	77	22	0	25
Technician, U.S.	69	6	36	27	26	20	0	23
Technician, non-U.S.	4	0	4	0	4	0	0	0
<b>Total</b>	<b>2,077</b>	<b>118</b>	<b>1,453</b>	<b>506</b>	<b>1,246</b>	<b>458</b>	<b>0</b>	<b>373</b>

<sup>1</sup> Users using multiple facilities are counted in each facility listed.

<sup>2</sup> NSF Minority status includes the following races: American Indian, Alaska Native, Black or African American, Hispanic, Native Hawaiian or other Pacific Islander. The definition also includes Hispanic Ethnicity as a minority group. Minority status excludes Asian and White-Not of Hispanic Origin.

<sup>3</sup> Includes pending user account activations.

**Table 1b: User Demographics by Facilities**

	Users <sup>1</sup>	Minority <sup>2</sup>	Non-Minority <sup>2</sup>	Prefer Not to Respond to Race <sup>3</sup>	Male	Female	Other	Prefer Not to Respond to Gender <sup>3</sup>
AMRIS	120	9	71	40	59	31	0	30
AMRIS - Independently Funded	258	19	132	107	91	73	0	94
DC Field	670	25	531	114	501	100	0	69
EMR	161	11	121	29	106	36	0	19
High B/T	18	0	14	4	13	2	0	3
ICR	375	28	225	122	168	110	0	97
NMR	320	22	237	61	198	81	0	41
Pulsed Field	155	4	122	29	110	25	0	20
<b>Total</b>	<b>2,077</b>	<b>118</b>	<b>1,453</b>	<b>506</b>	<b>1,246</b>	<b>458</b>	<b>0</b>	<b>373</b>

<sup>1</sup> Users using multiple facilities are counted in each facility listed.

<sup>2</sup> NSF Minority status includes the following races: American Indian, Alaska Native, Black or African American, Hispanic, Native Hawaiian or other Pacific Islander. The definition also includes Hispanic Ethnicity as a minority group. Minority status excludes Asian and White-Not of Hispanic Origin.

<sup>3</sup> Includes pending user account activations.

**Table 2: New PI of all facilities who received magnet time in 2018**

Facility	New PI at MagLab	New PI at Facility
AMRIS (NSF Funded, non-NHMLF Funded)	7+15	9+16
DC Field	33	50
EMR	15	20
High BT	2	2
ICR	27	28
NMR	21	25
PFF	10	12
<b>Total</b>	<b>130</b>	<b>162</b>

**Table 3a: User by Participation of All Facilities**

	Users <sup>1</sup>	Users Present	Users Operating Remotely <sup>2</sup>	Users Sending Sample <sup>3</sup>	Off-Site Collaborators <sup>4</sup>
AMRIS	120	74	0	6	40
AMRIS - Independently Funded	258	214	0	0	44
DC Field	670	428	0	55	187
EMR	161	81	0	37	43
High B/T	18	13	0	1	4
ICR	375	118	0	47	210
NMR	320	130	15	52	123
Pulsed Field	155	103	0	9	43
<b>Total</b>	<b>2,077</b>	<b>1,161</b>	<b>15</b>	<b>207</b>	<b>694</b>

<sup>1</sup> Users using multiple facilities are counted in each facility listed.

<sup>2</sup> "Users Operating Remotely" refers to users who operate the magnet system from a remote location. Remote operations are not currently available in all facilities.

<sup>3</sup> "Users Sending Sample" refers to users who send the sample to the facility and/or research group and the experiment is conducted by other collaborators on the experiment. Users at UF, FSU, and LANL cannot be "sample senders" for facilities located on their campuses.

<sup>4</sup> "Off-Site Collaborators" are scientific or technical participants on the experiment; who will not be present, sending sample, or operating the magnet system remotely; and who are not located on the campus of that facility (i.e., they are off-site).

**Table 3b: User by Participation by Facilities**

	Users <sup>1</sup>	Users Present	Users Operating Remotely <sup>2</sup>	Users Sending Sample <sup>3</sup>	Off-Site Collaborators <sup>4</sup>
Senior Personnel, U.S.	740	347	3	90	300
Senior Personnel, non-U.S.	279	56	3	59	161
Postdocs, U.S.	240	171	1	11	57
Postdocs, non-U.S.	56	24	1	4	27
Students, U.S.	565	433	7	34	91
Students, non-U.S.	124	63	0	9	52
Technician, U.S.	69	64	0	0	5
Technician, non-U.S.	4	3	0	0	1
<b>Total</b>	<b>2,077</b>	<b>1,161</b>	<b>15</b>	<b>207</b>	<b>694</b>

<sup>1</sup> Users using multiple facilities are counted in each facility listed.

<sup>2</sup> "Users Operating Remotely" refers to users who operate the magnet system from a remote location. Remote operations are not currently available in all facilities.

<sup>3</sup> "Users Sending Sample" refers to users who send the sample to the facility and/or research group and the experiment is conducted by other collaborators on the experiment. Users at UF, FSU, and LANL cannot be "sample senders" for facilities located on their campuses.

<sup>4</sup> "Off-Site Collaborators" are scientific or technical participants on the experiment; who will not be present, sending sample, or operating the magnet system remotely; and who are not located on the campus of that facility (i.e., they are off-site).

**Table 4a: User Organization of All Facilities**

					National			International		
	Users <sup>1</sup>	NHMFL-Affiliated Users <sup>2, 3, 4</sup>	Local Users <sup>2</sup>	External Users	Lab <sup>3, 5</sup>	University <sup>4, 5</sup>	Industry <sup>5</sup>	Lab <sup>5</sup>	University <sup>5</sup>	Industry <sup>5</sup>
Senior Personnel, U.S.	740	163	90	487	66	640	34	0	0	0
Senior Personnel, non-U.S.	279	0	0	279	0	0	0	50	205	24
Postdocs, U.S.	240	45	47	148	26	202	12	0	0	0
Postdocs, non-U.S.	56	0	0	56	0	0	0	13	42	1
Students, U.S.	565	49	128	388	4	559	2	0	0	0
Students, non-U.S.	124	0	0	124	0	0	0	10	114	0
Technician, U.S.	69	21	18	30	0	68	1	0	0	0

					National			International		
	Users <sup>1</sup>	NHMFL-Affiliated Users <sup>2, 3, 4</sup>	Local Users <sup>2</sup>	External Users	Lab <sup>3, 5</sup>	Univer- sity <sup>4, 5</sup>	Indus- try <sup>5</sup>	Lab <sup>5</sup>	Univer- sity <sup>5</sup>	Indus- try <sup>5</sup>
Technician, non-U.S.	4	0	0	4	0	0	0	1	2	1
<b>Total</b>	<b>2,077</b>	<b>278</b>	<b>283</b>	<b>1,516</b>	<b>96</b>	<b>1,469</b>	<b>49</b>	<b>74</b>	<b>363</b>	<b>26</b>

<sup>1</sup> Users using multiple facilities are counted in each facility listed.

<sup>2</sup> NHMFL-Affiliated users are defined as anyone in the lab's personnel system (i.e. on our web site/directory), even if they travel to another site. Local users are defined as any non-NHMFL-Affiliated researchers originating at any of the institutions in proximity to the MagLab sites (i.e. researchers at FSU, UF, FAMU, or LANL), even if they travel to another site.

<sup>3</sup> Users with primary affiliations at NHMFL/LANL are reported in NHMFL-Affiliated Users and National Laboratory.

<sup>4</sup> Users with primary affiliations at FSU, UF, or FAMU are reported in NHMFL-Affiliated Users and National University.

<sup>5</sup> The total of university, industry, and national lab users will equal the total number of users.

**Table 4b: User Organization by Facilities**

					National			International		
	Users <sup>1</sup>	NHMFL-Affiliated Users <sup>2, 3, 4</sup>	Local Users <sup>2</sup>	External Users	Lab <sup>3, 5</sup>	Univer- sity <sup>4, 5</sup>	Indus- try <sup>5</sup>	Lab <sup>5</sup>	Univer- sity <sup>5</sup>	Indus- try <sup>5</sup>
AMRIS	120	20	26	74	3	105	4	0	8	0
AMRIS - Independently Funded	258	20	101	137	1	252	0	0	4	1
DC Field	670	104	39	527	33	464	11	34	120	8
EMR	161	28	18	115	4	111	1	7	37	1
High B/T	18	3	6	9	0	15	0	0	3	0
ICR	375	31	43	301	22	234	13	16	81	9
NMR	320	47	36	237	2	226	12	12	61	7
Pulsed Field	155	25	14	116	31	62	8	5	49	0
<b>Total</b>	<b>2,077</b>	<b>278</b>	<b>283</b>	<b>1,516</b>	<b>96</b>	<b>1,469</b>	<b>49</b>	<b>74</b>	<b>363</b>	<b>26</b>

<sup>1</sup> Users using multiple facilities are counted in each facility listed.

<sup>2</sup> NHMFL-Affiliated users are defined as anyone in the lab's personnel system (i.e. on our web site/directory), even if they travel to another site. Local users are defined as any non-NHMFL-Affiliated researchers originating at any of the institutions in proximity to the MagLab sites (i.e. researchers at FSU, UF, FAMU, or LANL), even if they travel to another site.

<sup>3</sup> Users with primary affiliations at NHMFL/LANL are reported in NHMFL-Affiliated Users and National Laboratory.

<sup>4</sup> Users with primary affiliations at FSU, UF, or FAMU are reported in NHMFL-Affiliated Users and National University.

<sup>5</sup> The total of university, industry, and national lab users will equal the total number of users.

**Table 5: Operations by Discipline of All Facilities**

	Total Days Used <sup>1</sup>	Condensed Matter Physics	Chemistry, Geochemistry	Engineering	Magnets, Materials	Biology, Biochemist, Biophysics
NHMFL-Affiliated	2,204.7	420	167.8	0.2	142.2	1,474.4
Local	441.5	95	131.2	39	0	176.3
U.S. University	4,698.2	1,269.2	1,011.2	244.2	47	2,126.6
U.S. Govt. Lab.	192.8	160	9.1	0	0	23.7
U.S. Industry	81.4	0	9.6	0	0	71.8
Non-U.S.	1,499.2	834.6	489.2	3	19.7	152.8
Test, Calibration, Set-up, Maintenance, Inst. Dev.	1,557.2	213.6	15.6	0	931.7	396.3
<b>Total</b>	<b>10,675</b>	<b>2,992.4</b>	<b>1,833.7</b>	<b>286.4</b>	<b>1,140.6</b>	<b>4,421.9</b>

<sup>1</sup> Each 20 MW resistive magnet requires two power supplies to run, the 45T hybrid magnet requires three power supplies and the 36T Series Connected Hybrid requires one power supply. Thus there can be four resistive magnets + three superconducting magnets operating or the 45T hybrid, series connected hybrid, two resistive magnets and three superconducting magnets. User Units are defined as magnet days. Users of water-cooled resistive or hybrid magnets can typically expect to receive enough energy for 7 hours a day of magnet usage so a magnet day is defined as 7 hours. Superconducting magnets are scheduled typically 24 hours a day. There is an annual four week shutdown in fall of powered DC resistive and hybrid magnets for infrastructure maintenance and a two week shutdown period for the university mandated holiday break.

**Table 6: Operations by User Type of All Facilities**

User Facility	Total Days Used	Days External Users Used <sup>8</sup>	Days NHMFL-Affiliated Users Used (In-house) <sup>9</sup>	Days for Inst. Dev., Test, and Maintenance (Combined) <sup>10</sup>	Days Local Users Used <sup>11</sup>
AMRIS <sup>1</sup>	1,141	370.6	107.2	650.2	13
AMRIS – Independently Funded <sup>1</sup>	1,315	812.2	348.3	0	154.4
DC Field <sup>2</sup>	1,776.1	1,275.6	405.7	87.8	7
EMR <sup>3</sup>	984	721	186.5	60.5	16
High B/T <sup>4</sup>	784	583	0	201	0
ICR <sup>5</sup>	868	334.7	146.4	364.7	22.1
NMR <sup>6</sup>	3,202	1,977.5	897.5	193	134
Pulsed Field <sup>7</sup>	605	397	113	0	95
<b>Total</b>	<b>10,675</b>	<b>6471.6</b>	<b>2204.6</b>	<b>1557.2</b>	<b>441.5</b>

<sup>1</sup> User Units are defined as magnet days; time utilized is recorded to the nearest 15 minutes. Magnet day definitions for AMRIS instruments: Verticals (500, 600s, & 750 MHz), 1 magnet day = 24 hours. Horizontals (4.7 and 11.1T), 1 magnet day = 8 hours. This accounts for the difficulty in running animal or human studies overnight. Magnet days were calculated by adding the total number of real used for each instrument and dividing by 24 (vertical) or 8 (horizontal). Note: Due to the nature of the 4.7 T and 11T studies, almost all studies with external users were collaborative with UF investigators.

<sup>2</sup> Each 20 MW resistive magnet requires two power supplies to run, the 45T hybrid magnet requires three power supplies and the 36 T Series Connected Hybrid requires one power supply. Thus there can be four resistive magnets + three superconducting magnets operating or the 45 T hybrid, series connected hybrid, two resistive magnets and three superconducting magnets. User Units are defined as magnet days. Users of water-cooled resistive or hybrid magnets can typically expect to receive enough energy for 7 hours a day of magnet usage so a magnet day is defined as 7 hours. Superconducting magnets are scheduled typically 24 hours a day. There is an annual four week shutdown in fall of powered DC resistive and hybrid magnets for infrastructure maintenance and a two week shutdown period for the university mandated holiday break.

<sup>3, 4, 5, 6</sup> User Units are defined as magnet days. One magnet day is defined as 24 hours in superconducting magnets.

<sup>7</sup> User Units are defined as magnet days. Magnets are scheduled typically 12 hours a day.

<sup>1, 2, 3, 4, 5, 6</sup> Shutdown due to Hurricane Michael on October 9-14, 2018.

<sup>8</sup> Days to external users at facility => all U.S. University, U.S. Govt. Lab., U.S. Industry, Non-U.S. excluding NHMFL Affiliated, Local, Test, Calibration, Set-up, Maintenance, Inst. Dev.

<sup>9</sup> Days to NHMFL-Affiliated (in-house) research => NHMFL-Affiliated only

<sup>10</sup> Days to instrument development and maintenance (combined) => test, calibration, set-up, maintenance, inst. Dev.

<sup>11</sup> Days to local => local only

**Table 7: User Program Proposal Pressure by User Facility**

User Facility	Experiments Submitted (Current year)	Experiments Submitted (Deferred from prev. year)	Experiments Re-viewed	Days Submitted	Days External Users Used	Days Local Users Used	Total Days Used	Subscription (%) (Days submitted / Days used)
AMRIS	11	19	30	1,141	370.6	13	1,141	100 %
AMRIS - Independently Funded	23	87	110	1,315	812.2	154.4	1,315	100 %
DC Field	418	45	463	3,570	1,275.6	7	1,776.1	201 %
EMR	114	46	160	1,007	721	16	984	102 %
High B/T	15	0	15	957	583	0	784	122 %
ICR	134	16	150	2,246	334.7	22.1	868	259 %
NMR	499	61	560	3,257	1,977.5	134	3,202	102 %
Pulsed Field	80	12	92	706	397	95	605	117 %
<b>Total</b>	<b>1,294</b>	<b>286</b>	<b>1,580</b>	<b>14,199</b>	<b>6,471.6</b>	<b>441.5</b>	<b>10,675.1</b>	<b>133 %</b>

**Table 8a: Funding Source of User's Research- Days Allotted (Counts)**

User Facility	Total Days Used	NSF <sup>1</sup>	NIH	DOE	DOD <sup>2</sup>	FFI	UF MBI	EPA	International	National	Industry <sup>3</sup>	Other
AMRIS	1,141	878.1	76.2	19.3	5.5	0	9.6	0	9.8	142.5	0	0
AMRIS - Independently Funded	1,315	30.7	683	0	4.3	0	15.7	0	13.8	524	35.5	6.8



User Facility	Total Days Used	NSF <sup>1</sup>	NIH	DOE	DOD <sup>2</sup>	FFI	UF MBI	EPA	International	National	Industry <sup>3</sup>	Other
DC Field	1,776.1	717.6	26	356.6	107.3	0	0	0	297.4	209.8	38.3	23.2
EMR	984	626.8	83	16.5	4.9	0	0	0	140.4	107.5	5	0
High B/T	784	449	0	0	0	0	0	0	335	0	0	0
ICR	868	587.1	95	0.5	2.5	4.2	0	0	113.7	37.2	27.4	0.3
NMR	3,202	1,422.7	1,285.1	12.5	7	0	0	10	219.3	222	10.5	13
Pulsed Field	605	229	0	169.3	0	0	0	0	108.5	98.2	0	0
<b>Total</b>	<b>10,675</b>	<b>4,942</b>	<b>2,248.3</b>	<b>574.7</b>	<b>131.5</b>	<b>4.2</b>	<b>25.3</b>	<b>10</b>	<b>1,237.9</b>	<b>1,341.2</b>	<b>116.7</b>	<b>43.3</b>

<sup>1</sup> Includes NSF, UCGP, and No other support.

<sup>2</sup> Includes NASA, US Army, US Navy, and US Air force.

<sup>3</sup> Includes US Industry and Non-US Industry.

**Table 8b: Funding Source of User's Research- Days Allotted (Percentage)**

User Facility	NSF <sup>1</sup>	NIH	DOE	DOD <sup>2</sup>	FFI	UF MBI	EPA	International	National	Industry <sup>3</sup>	Other
AMRIS	77	7	2	0	0	1	0	1	12	0	0
AMRIS - Independently Funded	2	52	0	0	0	1	0	1	40	3	1
DC Field	40	1	20	6	0	0	0	17	12	2	1
EMR	64	8	2	0	0	0	0	14	11	1	0
High B/T	57	0	0	0	0	0	0	43	0	0	0
ICR	68	11	0	0	0	0	0	13	4	3	0
NMR	44	40	0	0	0	0	0	7	7	0	0
Pulsed Field	38	0	28	0	0	0	0	18	16	0	0
<b>Total</b>	<b>46</b>	<b>21</b>	<b>5</b>	<b>1</b>	<b>0</b>	<b>0</b>	<b>0</b>	<b>12</b>	<b>13</b>	<b>1</b>	<b>0</b>

<sup>1</sup> Includes NSF, UCGP, and No other support.

<sup>2</sup> Includes NASA, US Army, US Navy, and US Air force.

<sup>3</sup> Includes US Industry and Non-US Industry.



2018

Florida State University | University of Florida | Los Alamos National Laboratory

Supported by the National Science Foundation and the State of Florida

